Physics Reports 954 (2022) 1–70

Contents lists available at ScienceDirect

Physics Reports

journal homepage: www.elsevier.com/locate/physrep

# Quantum collision models: Open system dynamics from repeated interactions

Francesco Ciccarello [a,b,*], Salvatore Lorenzo [a], Vittorio Giovannetti [c], G. Massimo Palma [a,b]

[a] Università degli Studi di Palermo, Dipartimento di Fisica e Chimica- Emilio Segrè, via Archirafi 36, I-90123 Palermo, Italy
[b] NEST, Istituto Nanoscienze-CNR, Piazza S. Silvestro 12, 56127 Pisa, Italy
[c] NEST, Scuola Normale Superiore and Istituto Nanoscienze, Consiglio Nazionale delle Ricerche, Piazza dei Cavalieri 7, IT-56126 Pisa, Italy

ARTICLE INFO

*Article history:*
Received 29 June 2021
Received in revised form 23 December 2021
Accepted 5 January 2022
Available online 12 February 2022
Editor: Andreas Buchleitner

*Keywords:*
Open quantum systems
Repeated interactions
Quantum thermodynamics
Quantum non-Markovian dynamics
Quantum trajectories
Quantum weak measurements
Quantum optics
Input–output formalism
Cascaded master equations

ABSTRACT

We present an extensive introduction to quantum collision models (CMs), also known as repeated interactions schemes: a class of microscopic system–bath models for investigating open quantum systems dynamics whose use is currently spreading in a number of research areas. Through dedicated sections and a pedagogical approach, we discuss the CMs definition and general properties, their use for the derivation of master equations, their connection with quantum trajectories, their application in non-equilibrium quantum thermodynamics, their non-Markovian generalizations, their emergence from conventional system–bath microscopic models and link to the input–output formalism. The state of the art of each involved research area is reviewed through dedicated sections. The article is supported by several complementary appendices, which review standard concepts/tools of open quantum systems used in the main text with the goal of making the material accessible even to readers possessing only a basic background in quantum mechanics.

The paper could also be seen itself as a friendly, physically intuitive, introduction to fundamentals of open quantum systems theory since most main concepts of this are treated such as quantum maps, Lindblad master equation, steady states, POVMs, quantum trajectories and stochastic Schrödinger equation.



**Contents**



* Corresponding author at: Università degli Studi di Palermo, Dipartimento di Fisica e Chimica- Emilio Segrè, via Archirafi 36, I-90123 Palermo, Italy.
*E-mail address:* francesco.ciccarello@unipa.it (F. Ciccarello).

https://doi.org/10.1016/j.physrep.2022.01.001
0370-1573/

## 1. Introduction and historical notes

The last two decades or so have seen the compelling emergence and subsequent consolidation of a set of research areas that today usually go under the joint name of *quantum technologies* [1]. This is the idea of taking advantage of some distinctive features of quantum mechanics – such as the superposition principle and entanglement – for devising a plethora of novel, potentially groundbreaking, applications. These include tasks such as quantum computing, quantum cryptography, quantum sensing, quantum metrology, quantum simulation, quantum imaging. As a paradigmatic instance (also in light of our goals here), harnessing "quantumness" in order to challenge longstanding thermodynamics bounds such as the Carnot efficiency so as to engineer more efficient thermal machines is a possibility that is being more and more investigated these days in the lively field of *quantum thermodynamics* [2–6].

The above scenario in particular gave momentum to the study of an old, but always topical, quantum mechanics problem: the dynamics of a system in contact with an external environment, namely a so called *open quantum system* [7–9]. In some respects, this problem arises from the hope to find an irreversible-dynamics analogue of the Schrödinger equation that governs quantum systems coupled to a large bath (*master equation*). No truly general master equation is known to date except for a restricted, although conceptually prominent, class of dynamics known as *Markovian dynamics*; and a very few others. It is likely that this formidable problem may even be unsolvable as in general the system's degrees of freedom can get entangled with the bath in such a way that one cannot give up keeping track of the environment dynamics, or at least a portion of it. In various contexts such as quantum thermodynamics, this may even be desirable e.g. in order to study energy or entropy exchange between system and bath, which requires describing the latter as well. In practice, especially when running experiments, "looking" at some environment is inevitable. A measurement on the system of interest, for instance, requires to make it interact with an external probe which is then analyzed [10,11].

On a methodological ground, tackling system–bath dynamics at a microscopic level is in general a very hard task, which necessarily demands for appropriate *models*. Traditionally, the standard scheme is to decompose the bath $B$ into a *continuum* of normal modes (defined by its free Hamiltonian) and let them interact with the system $S$ according to some physically-motivated coupling model [7,8].

The last few years have yet seen a growing use of a less conventional class of system–bath models known as quantum *collision models* (CMs) or *repeated interaction schemes*.[1] In its most basic formulation [see Fig. 1(a)], a CM model imagines the bath $B$ as a large collection of smaller subunits (*ancillas*) with which the open system $S$ interacts – one at a time – through a sequence of pairwise, short unitary interactions (*collisions*). Arguably inspired by the famous Boltzmann's *Stosszahlansatz* [13] and first adopted in the study of optical masers and weak continuous measurements, quantum CMs are currently spreading across research fields such as quantum non-Markovian dynamics, quantum optics and quantum thermodynamics (where they have become now a standard approach).

Compared to the conventional system–bath modeling mentioned before, CMs differ in many respects. Two hallmarks in particular stand out. First, they are intrinsically *discrete*: continuous time is effectively replaced by a step number (although the continuous-time limit is often taken in the end) and the bath is thought as a discrete collection of elementary subsystems instead of a continuum as usual. Second, as schematically pictured in Fig. 1, in contrast to standard models

[1] Many authors use the name "collision*al* models". Occasionally, it was used "refreshing models" [12].


**Fig. 1.** *Collision model versus conventional system–bath model.* In a collision model (a) the bath is made out of a large, discrete, collection of smaller units (ancillas) with which the open system $S$ interacts (collides) one at a time. In a conventional system–bath model (b), instead, the bath typically comprises a continuum of normal modes and $S$ interacts with (generally) all of them at any time.

where $S$ at each time interacts with (generally) all the normal modes, in CMs (at least memoryless ones) $S$ crosstalks with a single little portion of bath at a time. This in a way decomposes the extremely complex system–bath dynamics into simple elementary contributions, a traditionally effective strategy in Physics.

To our knowledge, the first appearance of a quantum CM in the literature dates back to the 60s through a paper by J. Rau [14]. Later on in the 80s, CMs appeared in seminal works on *weak measurements* by C. M. Caves and G. J. Milburn [15–17]. CMs are indeed a natural microscopic framework for introducing this important class of weak quantum measurements [10,11] because, taking a metrological viewpoint, ancillas can be seen as a large collection of "meters" each of which being measured after the collision. More or less in the same years, Javanainen and Meystre [18–20] developed the theory of *micromaser* whose basic setup features flying atoms that one at a time interact with a lossy cavity mode. This can be seen as a physically intuitive implementation of a CM with atoms embodying ancillas which undergo collisions with $S$ (the cavity mode).

A hallmark of the CM approach is viewing the system–bath dynamics as a sequence of *two-body* unitary collisions. This is very similar in spirit to a cornerstone of quantum information processing (and generally quantum technologies) [21], namely that two-qubit gates (assisted by one-qubit gates) are sufficient to carry out universal quantum computation, and was probably the reason why CMs gained renewed attention in the early 2000s. V. Scarani et al. in 2002 approached the thermalization of a qubit (two-level system) due to collisions with a bath of qubits as a quantum task whose goal is taking $S$ to a Gibbs state no matter what state it started from ("quantum thermalizing machine") [22,23]. At about the same time, A. Brun [24] used a CM made out of qubits and the language of quantum information to study basic concepts of quantum trajectories, including the stochastic Schrödinger equation, connecting as well to the aforementioned weak measurements.

Around the beginning of 2010s, a strong (still ongoing) interest arose in attacking quantum non-Markovian dynamics and defining on a firm basis the meaning of (non-)Markovian evolution in quantum mechanics [25–28]. CMs are an ideal playground in this respect as was shown by Rybar, Filippov, Ziman and Buzek [29], who demonstrated that CMs can simulate any indivisible dynamics of a qubit, and by Ciccarello, Palma and Giovannetti [30] who added ancilla–ancilla collisions to a basic CM to derive a completely-positive non-Markovian master equation.

In the same years, the field of quantum thermodynamics was emerging, prompted by a number of questions calling for manageable microscopic models. Due to their simplicity and the possibility to describe system–bath coupling non-perturbatively, CMs are a quite natural tool in this framework so that it is hard establishing when they were used for the first time. A comprehensive quantum thermodynamics theory of CMs (repeated interaction schemes) was presented in 2017 by Strasberg, Schaller, Brandes and Esposito [31]. In this context, CMs are actually seen mostly as a resource to harness in order to design machines with enhanced thermodynamic performances, possibly powered by genuinely quantum features. A paradigm in this respect came from an influential 2003 paper by Scully, Zubairy, Agarwal and Walther [32], which considered a single-bath thermal machine made out of a stream of three-level atoms flying through a cavity.

Having in mind a readership of physicists, even those armed with only a basic background in quantum mechanics, here we present a self-contained introduction to quantum CMs theory, including overviews of the state of the art and recent developments.

While to our knowledge this is the first, fully dedicated, comprehensive review on CMs, we note that there are some papers and PhD dissertations which introduce to certain aspects of CMs [24,33–39]. Dedicated sections on CMs can be found in the review on non-Markovian dynamics in Ref. [27] and the review on irreversible entropy production in Ref. [40]. We also quote a recent perspective on the topic [41].

Finally a disclaimer. The present review does not cover mathematical aspects, for which we point the interested reader to Ref. [42] and references therein.

## 2. Outline and structure of the paper

The body of the paper is organized into six big sections (each in turn structured in a number of subsections): *Basic collision model* (Section 4), *Equations of motion* (Section 5), *Quantum trajectories* 6, *Non-equilibrium quantum thermodynamics* 7, *Non-Markovian collision models* 8 and, finally, *Collision models from conventional models* 9. As sketched in Fig. 2, the paper's central Sections are 4 and 5 with which each of the other sections is directly connected.

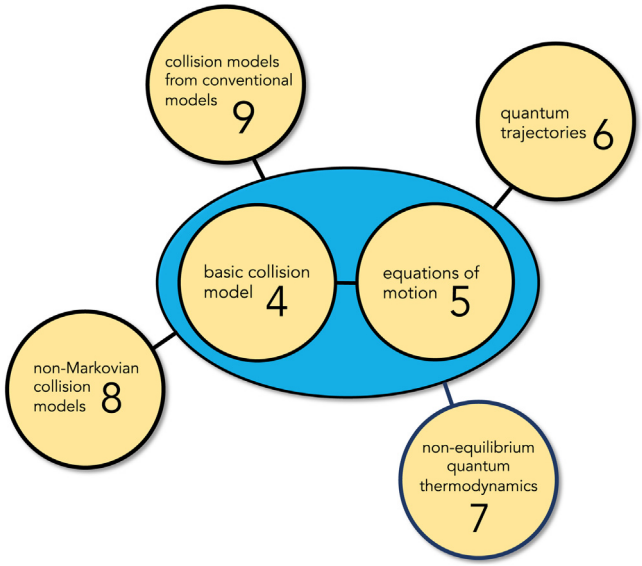


**Fig. 2.** *Structure of the paper*. The body of the paper comprises six big sections, numbered from 4 to 9. Sections 4 and 5 are the central ones, to which all the others are directly linked to.

Each of these six big sections is written with a quite pedagogical attitude. In particular, we note that – similarly to a textbook – there intentionally appear very *few references* in order not to distract the reader from the main line of discussion.[2] In the same spirit, in order not to interfere with the main discussion, references to previous equations or sections often appear between brackets like "(see Section xxx)" or "[see Eq. (xxx)]". Also, a large use of *footnotes* is made, which supply extra details, explanations, comments and disclaimers. Each big section, from 4 to 9, ends with a dedicated *State of the art* subsection, reviewing relevant literature related to the topic of the corresponding section.

We begin with a preliminary technical section (Section 3), which is intended to provide a sort of reading guide. The main conventions underpinning the notation we use are explained along with the (relatively few) acronyms appearing throughout the paper.

Section 4 defines the most basic CM 4.1 focusing first on the open dynamics of $S$4.2 and then also that of ancillas in 4.3. Next, in Section 4.4, we discuss Markovianity, a property of utmost importance for CMs and open quantum systems theory in general. Thereafter (Section 4.5) after introducing inhomogeneous CMs, we discuss a generalized notion of Markovian behavior called CP divisibility (where CP stands for "completely positive"). Some paradigmatic CMs are presented in Section 4.6 (all-qubit CM) and Section 4.8 (cascaded CMs). A major issue when dealing with open dynamics, i.e. the convergence to a steady state (if any), is discussed in Section 4.7. We close with Section 4.9 which studies the tensor-network structure of the joint system–bath state at each step.

Section 5 deals with the derivation of equations of motion for both states and expectation values of observables. The basis is the second-order expansion of the collision unitary operator with respect to the collision time (Section 5.1), resulting in finite-difference equations of motion having the structure of discrete Lindblad master equations and ensuing dynamical equations for expectation values (see Section 5.2). The Lindblad structure can be proven based on the spectral decomposition of the ancilla's initial state (see Section 5.3) or solely in terms of bath moments (see Section 5.4), the analogous of the latter being next worked out for expectation values as well in Section 5.5. We then show in Section 5.6 how the intrinsically discrete dynamics can be turned into a continuous-time one through coarse graining. The prominent example of micromaser is then discussed in the extensive Section 5.7. The possibility to define a strict continuous-time limit $\Delta t \to 0$ by introducing a diverging coupling strength is studied in (Section 5.8). We close with a section devoted to multiple baths (Section 5.9) and one deriving the master equation of cascaded CMs (Section 5.10).

Section 6 discusses quantum trajectories and weak measurements, these being important general topics that are naturally introduced in the CM language. The starting point (Section 6.1) is to view ancillas as probes and study how measurements of these condition the dynamics of $S$. This framework is used in the following Section 6.2 to introduce the important general concept of POVM (Positive Operator-Valued Measure). We then focus on a specific dynamics in the all-qubit CMs, which is used to introduce the concept of quantum jumps 6.3, the stochastic Schrödinger equation 6.4 and, finally, how averaging over all trajectories returns the Lindblad master equation 6.5. We conclude in Section 6.6 by deriving the stochastic Schrödinger equation for a general interaction Hamiltonian, at the same time highlighting the role of the bath's first and second moments.

[2] A general criterion is that a reference is given if a certain property is used in the main text but not proven (nor in the appendices).

Section 7 is dedicated to non-equilibrium quantum thermodynamics, beginning with the definition of quantum thermalization 7.1 and discussing next the important instance of a system thermalizing with a bath of quantum harmonic oscillators (Section 7.2) and the connection between thermalization and energy conservation (Section 7.3). There follow instances of non-equilibrium steady states with baths at different temperatures (Section 7.4). The intrinsic time dependence of the system–bath Hamiltonian, a major distinctive feature of CMs, is analyzed in Section 7.5. Following this, we present one by one the computation of relevant thermodynamic quantities like: the change of system free energy 7.6, that of ancillas or heat 7.7 and work 7.8. We then derive the non-equilibrium version of the 1st and 2nd law of thermodynamics (Sections 7.9 and 7.11, respectively) and discuss the Landauer's principle in Section 7.12. The energy balance of some of the previously introduced instances is studied in Section 7.10.

Section 8 deals with non-Markovian CMs. Three basic classes are introduced, where each arises from the introduction of a memory mechanism into the basic memoryless CM of Section 4: ancilla–ancilla collisions (Section 8.1), initially-correlated ancillas 8.3, multiple system–ancilla collisions 8.4. Section 8.2 shows the derivation of a fully CPT non-Markovian master equation based on the class in Section 8.1. A further class, the so called composite CMs, is presented in Section 8.5 and illustrated in a paradigmatic instance. We close with the demonstration that, so long as the open dynamics is concerned, ancilla–ancilla collisions can be mapped into a composite CM (Section 8.6).

The last Section 9 deals with the relationship between CMs and conventional system–bath models (see Fig. 1). The two descriptions are shown to be equivalent pictures in the case (recurrent in quantum optics) that $S$ is weakly coupled to a continuum of bosonic modes (field). All the steps of the mapping are illustrated in detail in Sections 9.1, 9.2, 9.3, 9.4 and 9.5. Occurrence of Markovian behavior depends on the field's initial state (see Section 9.6). This is then specifically illustrated for the vacuum state leading to spontaneous emission (see Section 9.7), thermal states yielding Einstein coefficients (Section 9.8), coherent states and optical Bloch equations 9.9. These are all special cases of a general master equation, fully defined by the field's first and second moments, which holds for Gaussian white-noise field states 9.10. Non-Markovian dynamics can occur for non-Gaussian initial states such as single-photon wavepackets 9.11. Finally, we explain the link to the input–output formalism that is broadly used in quantum optics 9.12. We conclude in Section 10 with a discussion of future prospects and open questions about quantum CMs.

In order to help the reader, in addition to the aforementioned reading guide in Section 3, there are a number of appendices. Those from A to F have a tutorial scope and recall basic notions: density matrices (Appendix A), various entropic quantities (Appendix B), quantum maps (Appendix C), the dynamical map (Appendix D), the Stinespring dilation theorem (Appendix E) and the Lindblad master equation (Appendix F). There follow technical sections featuring mostly proofs of properties used in the main text (Appendices G–L).

## 3. Reading guide

Hats are used throughout to identify all the operators, except density operators and the identity operator $\mathbb{I}$. When appearing, the identity operator is frequently used without subscripts, the (sub)system it refers to being often clear from the context. If an operator acts trivially on a subsystem, e.g. $\hat{O}_A \otimes \mathbb{I}_B$, then the identity operator is generally omitted.

Usually, *joint* states (generally represented by density operators) of the system plus bath are denoted with letter $\sigma$, while $\rho$ and $\eta$ are used for the *reduced* state of the open system $S$ and a single bath ancilla, respectively.

Letter $\sigma$ but with a hat is also used for spin operators such as $\hat{\sigma}_\pm$ and $\hat{\sigma}_z$.

The eigenstates of $\hat{\sigma}_z$ are denoted with $|0\rangle$ and $|1\rangle$, having respectively eigenvalues $-1$ and $+1$. We point out that this choice does *not* follow the usual convention in the quantum information literature, where $|0\rangle$ ($|1\rangle$) corresponds to eigenvalue $+1$ ($-1$). The rationale of this choice is that, in many cases, we deal with a ground and an excited state so that $|0\rangle$ and $|1\rangle$ are understood as the state with zero and one excitations, respectively.

Superoperators, including quantum maps, are denoted with capital (usually calligraphic) letters and the argument is shown between square brackets, e.g. $\mathcal{M}[\varrho]$. The symbol of composition of quantum maps is most of the times omitted, thus

$$\mathcal{M}\mathcal{M}'[\varrho] = (\mathcal{M} \circ \mathcal{M}')[\varrho] = \mathcal{M}[\mathcal{M}'[\varrho]].$$

Arguments of partial traces are shown between curly brackets.

Anti-commutators are denoted as $[\hat{A}, \hat{B}]_+ = \hat{A}\hat{B} + \hat{B}\hat{A}$.

We use units such that $\hbar = 1$ throughout.

In some contexts such as Section 9, in order to avoid making the notation cumbersome, dependencies on a continuous variable are shown through a subscript (as is usually done with discrete time variables), thus e.g. $f_t = f(t)$.

The tensor product symbol $\otimes$ is often omitted.

The ancilla index usually appears as a subscript, e.g. $\eta_n$ stands for a state of ancilla $n$.

Time dependencies, where time is often embodied by the (discrete) number of steps, can appear as subscripts or superscripts, which generally depends on the quantity or subsystem they refer to or on the considered context.

We generally do not use the same symbol for different purposes depending on the context/section. Some exceptions are yet unavoidable (given the considerable size of the paper), e.g. "$M$" stands for the number of baths in Section 5.9 while in Section 8.5 it denotes the memory coupled to $S$.

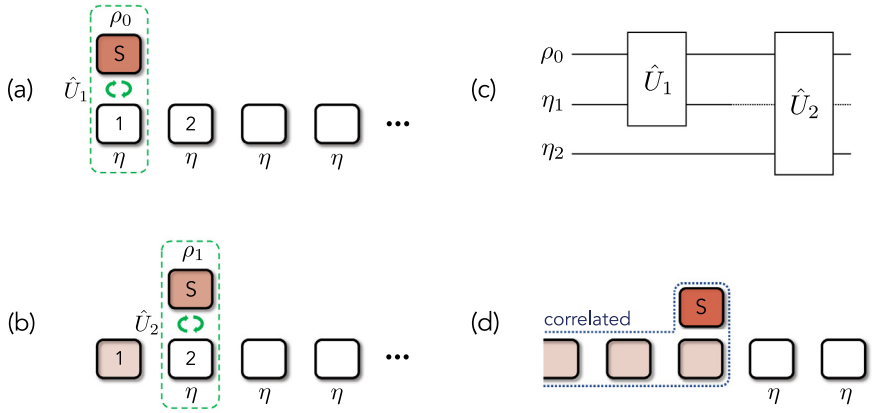


**Fig. 3.** *Basic collision model.* (a): First collision: the pairwise unitary $\hat{U}_1$ is applied on $S$ and ancilla 1 (initially in state $\rho_0$ and $\eta$, respectively). At the end of the collision, $S$ is in state $\rho_1$. (b): Second collision: unitary $\hat{U}_2$ is applied on $S$ and ancilla 2 (initially in state $\rho_1$ and $\eta$, respectively). (c): Quantum circuit representation of the first two CM steps. Each wire represents a subsystem ($S$ or an ancilla), while each rectangular box is a two-body quantum gate (collision unitary). (d): Correlations: $S$ and all of the ancillas it already collided with are jointly correlated, while each ancilla which still has to collide with $S$ is yet in the initial state $\eta$ (hence uncorrelated with $S$ and all the remaining ancillas).

### 3.1. Acronyms and some terminology

CM = "Collision model"
ME = "Master equation"
CPT = "Completely positive and trace-preserving"
NM = "Non-Markovian"
"Qubit" = Two-level system (quantum bit), formally equivalent to a spin-1/2 particle.

## 4. Basic collision model

### 4.1. Definition

Consider a quantum system with unspecified Hilbert-space dimension called $S$ (*open system*) coupled to a quantum *bath* $B$. By hypothesis, the bath is made out of a large collection of smaller identical subunits (*ancillas*) labeled by an integer number $n$. It is assumed that $S$ and $B$ start in the joint state

$$\sigma_0 = \rho_0 \otimes \eta \otimes \eta \otimes \cdots \tag{1}$$

with $\rho_0$ the initial state of $S$ and $\eta$ the initial state common to all ancillas [see Fig. 3(a)]. Here, $\sigma_0$, $\rho_0$ and $\eta$ are (generally mixed) density matrices (see Appendix A). Note that $\sigma_0$ is a *product* state: neither correlations between $S$ and $B$ nor between ancillas are present.

By hypothesis, as sketched in Figs. 3(a) and (b), the entire dynamics takes place through successive collisions, namely pairwise short interactions each involving $S$ and one ancilla of $B$. Collision $S$-1 (i.e., between $S$ and ancilla 1) occurs at step $n = 1$, then $S$-2 at step $n = 2$, then $S$-3 and so on. Importantly, each ancilla $n$ collides with $S$ only *once* (at the corresponding step $n$).

The dynamics of an elementary collision is described by the time evolution unitary operator

$$\hat{U}_n = e^{-i\left(\hat{H}_S + \hat{H}_n + \hat{V}_n\right)\Delta t}, \tag{2}$$

with $\Delta t$ the collision duration, $\hat{H}_S$ ($\hat{H}_n$) the free Hamiltonian of $S$ ($n$th ancilla) and $\hat{V}_n$ the $S$-$n$ interaction Hamiltonian. Note that, although only the ancilla subscript appears, $\hat{V}_n$ acts on *both* $S$ and $n$, and so does $\hat{U}_n$.

#### 4.1.1. Conditions for Markovian behavior

Among the series of assumptions introduced so far that define the CM, three in particular stand out:

(1) Ancillas do not interact with each other;
(2) Ancillas are initially uncorrelated;
(3) Each ancilla collides with $S$ only once.

Hypotheses (1)–(3) crucially underpin many major properties of CMs, in particular those related to Markovian behavior. Is worth pointing out that the essential meaning of (3) is to rule out sequences of collisions such as $S$-1, $S$-2, $S$-3, $S$-1, $S$-2, … , while dynamics like $S$-1, $S$-1, $S$-2, $S$-2, … can be seen as not violating (3) provided that one simply redefines the collision as a double collision with the same ancilla.

### 4.2. Open dynamics and collision map

After $n$ collisions, i.e. at step $n$, the joint system–bath state reads

$$\sigma_n = \hat{U}_n \cdots \hat{U}_1 \, \sigma_0 \, \hat{U}_1^\dagger \cdots \hat{U}_n^\dagger \, . \tag{3}$$

In passing, we note that this dynamics can be represented [see Fig. 3(c)] as a quantum circuit [21] where each wire stands for a subsystem ($S$ or an ancilla) while each rectangular box is a two-body quantum gate (collision unitary $\hat{U}_n$).

By replacing $\sigma_0$ with the uncorrelated state (1), Eq. (3) can be expressed as[3]

$$\sigma_n = \hat{U}_n \cdots \hat{U}_1 \, \rho_0 \, \eta_1 \cdots \eta_n \, \hat{U}_1^\dagger \cdots \hat{U}_n^\dagger \, \eta_{n+1}\eta_{n+2} \cdots = \left(\hat{U}_n \cdots \left(\hat{U}_2 \left(\hat{U}_1 \rho_0 \, \eta_1 \hat{U}_1^\dagger\right) \eta_2 \hat{U}_2^\dagger\right) \, \ldots \, \eta_n \hat{U}_n^\dagger\right) \eta_{n+1} \cdots \, .$$

In the last identity we used that $\hat{U}_n$ acts on $S$ and $n$, hence it commutes with any $\eta_m$ with $m \neq n$. We see that, up to step $n$, ancillas $\eta_m$ with $m > n$ play no role and we will thus ignore them in the following.

Tracing off the bath, the corresponding state of the open system $S$ is

$$\rho_n = \mathrm{Tr}_B\{\sigma_n\} = \mathrm{Tr}_n \cdots \mathrm{Tr}_1\{\sigma_n\} = \mathrm{Tr}_n \left\{\hat{U}_n \cdots \mathrm{Tr}_2 \left\{\hat{U}_2 \, \mathrm{Tr}_1 \left\{\hat{U}_1 \rho_0 \, \eta_1 \hat{U}_1^\dagger\right\} \eta_2 \hat{U}_2^\dagger\right\} \, \ldots \eta_n \hat{U}_n^\dagger\right\} \, , \tag{4}$$

with $\mathrm{Tr}_m$ the partial trace [see Eq. (A.2)] over the $m$th ancilla and where we used that $\mathrm{Tr}_n$ and $\hat{U}_n$ do not involve ancillas different from $n$. We next express (4) in the compact form

$$\rho_n = \mathcal{E}\left[\cdots\left[\mathcal{E}\left[\mathcal{E}\left[\rho_0\right]\right]\right]\right] = \mathcal{E}^n[\rho_0] \, , \tag{5}$$

where we defined the quantum map (see Appendix C) on $S$

$$\rho' = \mathcal{E}[\rho] = \mathrm{Tr}_n \left\{\hat{U}_n \left(\rho \otimes \eta_n\right) \hat{U}_n^\dagger\right\} \qquad \text{(collision map)} \, . \tag{6}$$

We will henceforth refer to (6) as the *collision map*[4] : the knowledge of map $\mathcal{E}$ allows to determine the state of $S$ at the end of a collision, $\rho'$, for any state $\rho$ prior to the collision. Note that map $\mathcal{E}$ depends on the unitary (2) describing each collision (in turn depending on $H_S$, $H_n$ and $\hat{V}_n$) as well as on the ancilla's initial state $\eta$. As a property of utmost importance in CMs theory, the form of (6) ensures that $\mathcal{E}$ is a *completely positive and trace-preserving* (CPT) map (see Appendix C). The essential reason behind this property is that, *before* the $S$-$n$ collision starts, $S$ is still uncorrelated with ancilla $n$ [see Figs. 3(a), (b) and (d)] this being a consequence of assumptions (1)–(3) in Section 4.1.1. The breaking of even only one of these generally brings about that the initial and final states of $S$ in a collision are no longer connected to one another by a CPT map as we will discuss extensively in Section 8.

Thus Eq. (5) states that, when looking only at the open system $S$, $n$ collisions correspond to $n$ applications of collision map $\mathcal{E}$ on $\rho_0$ (initial state of $S$). We immediately see that Eq. (5) entails[5]

$$\rho_n = \mathcal{E}[\rho_{n-1}] \, . \tag{7}$$

Eq. (7) in fact governs the entire open dynamics and, as will become clearer in Section 5, it can be regarded as the discrete analogue of a time-local master equation (see Appendix F). In particular, it shows that the state of $S$ at the current step depends only on that at the previous step. This means that the dynamics keeps *no memory* of past history: if we are given state $\rho_{n-1}$ but we do not know what happened to $S$ up to step $n-1$, the entire future evolution at any step $m \geq n$ can be predicted from (7). This property no more holds for non-Markovian CMs to be discussed in Section 8. Yet, the Markovian nature of a basic CM has a tremendous conceptual relevance for all CMs, including non-Markovian ones, as will become clear in the development of this paper.

### 4.3. Ancilla dynamics

While, as shown above, the open dynamics of $S$ is relatively easy to work out, deriving the full bath dynamics is generally far more challenging (see however Section 4.9). Although not directly coupled, indeed, ancillas that *already* collided with $S$ get correlated with each other [see Fig. 3(d)]. However, if one is concerned only with the *single* ancilla

[3] Note that subscript $n$ is used here with different although related meanings. For $S-B$ and $S$ states, such as $\sigma_n$ and $\rho_n$, it refers to the time step. For single-ancilla states, such as $\eta_n$, it indicates which ancilla the state refers to.

[4] Map $\mathcal{E}$ does not depend on $n$ since we are assuming a fully homogeneous model (same initial state for all ancillas and same collision unitary $\hat{U}_n$). This assumption will be relaxed in Section 4.5.

[5] The converse holds as well, i.e., Eq. (7) implies $\rho_n = \mathcal{E}^n[\rho_0]$. Eqs. (5) and (7) are thus equivalent.

dynamics (as is often the case) this is simply obtained from Eq. (3) by tracing off $S$ and all the remaining ancillas. The result is similar to the collision map (6) except that the partial trace is now over $S$ (instead of $n$)

$$\eta_n' = \mathrm{Tr}_S\{\hat{U}_n \rho_{n-1} \eta_n \hat{U}_n^\dagger\}\,, \tag{8}$$

Thereby, the collision with $S$ transforms the ancilla state as

$$\eta_n' = \mathcal{A}_{\rho_{n-1}}[\eta_n] \tag{9}$$

with

$$\eta' = \mathcal{A}_\rho[\eta] = \mathrm{Tr}_S\left\{\hat{U}_n\,(\rho\otimes\eta)\;\hat{U}_n^\dagger\right\}\,. \tag{10}$$

Eq. (10) defines a CPT map on the ancilla, showing that this evolves at each collision somewhat similarly to $S$. Yet, at variance with (7) which can be determined once for all given $\hat{U}_n$ and $\eta$, map (10) does depend parametrically on the current state of $S$. Thereby, to work out $\eta_n'$ we need to keep track of the open dynamics of $S$ (i.e. $\rho_n$).[6] Note that after colliding with $S$ the ancilla's state no longer changes [due to conditions (1)–(3) in Section 4.1.1], hence (9) fully specifies the single-ancilla dynamics. At the next steps, however, the correlations between the ancilla and the rest of the system (both $S$ and other ancillas) generally change [see Fig. 3(d)].

### 4.4. Markovianity

It is convenient to introduce the *dynamical map* (see Appendix D))

$$\rho_n = \Lambda_n[\rho_0]\,, \tag{11}$$

which, given the initial state $\rho_0$, returns the state of $S$ at any step $n$. The dynamical map (in fact the propagator of the open dynamics) depends on the collision unitary (2) and the initial state of ancillas. It is ensured to be CPT since $S$ shares no initial correlations with the bath.

In terms of the dynamical map $\Lambda_n$, Eq. (5) is simply expressed as

$$\Lambda_n = \mathcal{E}^n\,, \tag{12}$$

showing the exponential dependence of $\Lambda_n$ on the collision map $\mathcal{E}$. It immediately follows that, for any integer $m$ between 0 and $n$,

$$\Lambda_n = \Lambda_{n-m}\,\Lambda_m\,. \tag{13}$$

This is the discrete-dynamics version of the so called *semigroup property* (see Appendix F). It states that, like for any group (in the mathematical sense), the composition of dynamical maps produces another legitimate dynamical map. Here, the prefix "semi" comes from the fact that dynamical maps are generally non-unitary and thus cannot be inverted [see Appendix C)] (physically this means that they describe irreversible dynamics).

The semi-group property is another equivalent way to express the memoryless nature of the dynamics [already stressed below Eq. (7)]: if we know the state at an intermediate step $m$, $\rho_m$, no matter what happened at previous steps, we can determine the following evolution up to a final time $n$.

### 4.5. Inhomogeneous collision model and CP divisibility

So far we assumed that the entire model is homogeneous: the ancilla's initial state $\eta$ was assumed to be the same for all ancillas [cf. Eq. (1)] and so was the collision unitary (2). Accordingly, the open dynamics resulted from repeated applications of the same map (6) [recall Eqs. (5) and (12)]. This homogeneity assumption, made mostly for the sake of argument to better highlight general properties, can be relaxed straightforwardly. By still maintaining the assumption of initially uncorrelated ancillas (a constraint which we will relax in Sections 8.3 and 9.11), the initial state (1) can be generalized as

$$\sigma_0 = \rho_0 \bigotimes_n \eta_n \tag{14}$$

with $\eta_n$ not necessarily the same state for all ancillas, while in the collision unitary (2) $\hat{H}_S$, $\hat{H}_n$, $\hat{V}_n$ can be different for different values of $n$. Accordingly, the system's collision map (6) is generally step-dependent and we thus rename it $\mathcal{E}^{(n)}$.[7] Correspondingly, the dynamical map (12) is generalized as

$$\Lambda_n = \mathcal{E}^{(n)}\mathcal{E}^{(n-1)}\cdots\,\mathcal{E}^{(0)}\,. \tag{15}$$

[6] The ancilla's reduced dynamics (9) can be equivalently described as a CPT map connecting *different* Hilbert spaces in that its input is a state of $S$ while its output is the final state of the $n$th ancilla after colliding with $S$. This shows even more directly that recording the whole dynamics of $S$ is required in order to determine the ancilla evolution.

[7] This kind of integer subscript between brackets will usually denote the step number (discrete time).

The semigroup property (13) is replaced by the more general

$$\Lambda_n = \Phi_{n,m}\,\Phi_{m,0}\,, \tag{16}$$

holding for any integer $0 \leq m \leq n$. Here, we defined map

$$\Phi_{n_2,n_1} = \mathcal{E}^{(n_2)}\mathcal{E}^{(n_2-1)}\dots\,\mathcal{E}^{(n_1)} \qquad (n_2 \geq n_1)\,, \tag{17}$$

which, being a composition of CPT maps, is also CPT (this can be easily shown).

Eq. (16) is the discrete version of a property called "CP divisibility" [9]. This is in fact the statement that the open dynamics can be divided into a sequence of elementary CPT maps which generally need not be the same. In the special case that they are the same, we recover the semigroup property (13). Fulfillment of CP divisibility has been proposed as a quantitative definition of Markovian behavior that is more general than the traditional Markovianity associated with the semigroup property [26,43]. In this sense, the inhomogeneous CM defined above can still be considered to be Markovian, an assessment in agreement with the fact that conditions (1)–(3) of Section 4.1.1 are still matched.

### 4.6. All-qubit collision model

To illustrate more concretely some of the concepts introduced so far, we next present one the simplest instances of CM which we will refer to repeatedly in this paper as the "all-qubit CM". The open system $S$ is a *"qubit"* (two-level system), whose Hilbert space is spanned by the orthonormal basis $\{|0\rangle, |1\rangle\}$ with $\hat{\sigma}_z|0\rangle = -|0\rangle$ and $\hat{\sigma}_z|1\rangle = |1\rangle$, where $\hat{\sigma}_\alpha$ ($\alpha = x, y, z$) are the usual Pauli spin operators. Ancillas are also qubits, each with orthonormal basis $\{|0\rangle_n, |1\rangle_n\}$ (eigenstates of $\hat{\sigma}_{nz}$, i.e. the $z$-component of the $n$th ancilla spin operator). We assume for simplicity no free Hamiltonian for both $S$ and ancillas, i.e. $\hat{H}_S = \hat{H}_n = 0$, and consider the (homogeneous) system–ancilla coupling Hamiltonian

$$\hat{V}_n = g\left(\hat{\sigma}_+ \otimes \hat{\sigma}_- + \hat{\sigma}_- \otimes \hat{\sigma}_+\right) + g_z\,\hat{\sigma}_z \otimes \hat{\sigma}_z\,, \tag{18}$$

where in each term the first (second) operator acts on $S$ ($n$th ancilla) and with

$$\hat{\sigma}_- = \hat{\sigma}_+^\dagger = \tfrac{1}{\sqrt{2}}\left(\hat{\sigma}_x + i\hat{\sigma}_y\right) = |0\rangle\langle 1|\,, \tag{19}$$

the usual spin ladder operators. The eigenstates of $\hat{V}_n$ are $|00\rangle$, $|11\rangle$ and

$$|\Psi^\pm\rangle = \tfrac{1}{\sqrt{2}}\left(|10\rangle \pm |01\rangle\right) \tag{20}$$

with eigenvalues $g_z$, $g_z$ and $\pm g - g_z$, respectively (we use the short notation $|ab\rangle = |a\rangle_S|b\rangle_n$).

Hence, the collision unitary (2) for this class of CMs explicitly reads[8]

$$\hat{U}_n = e^{-i2g_z\Delta t}\left(|00\rangle\langle 00| + |11\rangle\langle 11|\right) + \cos(g\Delta t)\left(|10\rangle\langle 10| + |01\rangle\langle 01|\right) - i\sin(g\Delta t)\left(\hat{\sigma}_+\hat{\sigma}_- + \hat{\sigma}_-\hat{\sigma}_+\right)\,, \tag{21}$$

where we omitted an irrelevant phase factor $e^{ig_z\Delta t}$ and all tensor product symbols.

Although the all-qubit CM at first may appear somewhat artificial, there are realistic physical scenarios (see Section 9) where it provides an accurate description of the dynamics (especially in the case $g_z = 0$).

#### 4.6.1. Partial swap unitary collision

An important special case is when $\hat{U}_n$ reduces to a *partial swap*, this being a recurrent collision unitary in the CM literature.

Let us first define the SWAP unitary operator $\hat{S}_n$ as the operator such that

$$\hat{S}_n|\psi\rangle_S|\chi\rangle_n = |\chi\rangle_S|\psi\rangle_n \tag{22}$$

for any pair of states $|\psi\rangle$ and $|\chi\rangle$. In line with the notation used for $\hat{V}_n$ and $\hat{U}_n$, only the ancilla index appears in the subscript of $\hat{S}_n$ (yet recall that it acts on both $S$ and ancilla). Note that

$$\hat{S}_n\,\hat{S}_n = \mathbb{I}\,. \tag{23}$$

Thus operator $\hat{S}_n$ is both Hermitian and unitary.

Operator $\hat{S}_n$ thus swaps the states of $S$ and the ancilla. Note that definition (22) applies even if $S$ and ancilla $n$ are not qubits, the essential requirement being that they have the same Hilbert space dimension.

A partial swap is a generalization of the SWAP defined as[9]

$$\hat{U}_n = e^{-i\theta\hat{S}_n} = \cos\theta\,\mathbb{I} - i\sin\theta\hat{S}_n\,, \tag{24}$$

where angle $\theta$ (such that $0 \leq \theta \leq \pi/2$) measures the amount of swapping. For $\theta = 0$, $\hat{U}_n$ reduces to the identity corresponding to a fully ineffective collision. For $\theta = \pi/2$, instead, the collision has the maximum effect, swapping the states of the interacting systems.

---

[8] Using eigenstates and eigenvalues of $\hat{V}_n$, $\hat{U}_n$ is spectrally decomposed as $\hat{U}_n = e^{-ig_z\Delta t}\left(|00\rangle\langle 00| + |11\rangle\langle 11|\right) + e^{-i(g-g_z)\Delta t}|\Psi^+\rangle\langle\Psi^+| + e^{i(g+g_z)\Delta t}|\Psi^-\rangle\langle\Psi^-|$. We next expand $|\Psi^\pm\rangle$ and then use that $\hat{\sigma}_+ \otimes \hat{\sigma}_- = |10\rangle\langle 01|$

[9] The conversion from the exponential to the trigonometric form straightforwardly follows from $\hat{S}_n^2 = \mathbb{I}$ (the analogous property holds for any spin-1/2 operator).

*4.6.2. Partial swap in the all-qubit CM*

In the case of the all-qubit CM ($S$ and ancilla $n$ are both qubits), $\hat{S}_n$ leaves $|00\rangle$ and $|11\rangle$ unchanged while $|01\rangle$ and $|10\rangle$ are turned into one another. It is then easily shown that the SWAP operator can be expressed in terms of the identity and Pauli operators as

$$\hat{S}_n = \tfrac{1}{2}\left(\mathbb{I} + \hat{\boldsymbol{\sigma}}\cdot\hat{\boldsymbol{\sigma}}_n\right) . \tag{25}$$

The partial swap unitary (24) occurs in the all-qubit model for $g_z = g/2$ [cf. Eq. (18)], corresponding to the *Heisenberg exchange* interaction Hamiltonian

$$\hat{V}_n = \frac{g}{2}\,\hat{\boldsymbol{\sigma}}\cdot\hat{\boldsymbol{\sigma}}_n . \tag{26}$$

Indeed, up to an irrelevant phase factor, the corresponding unitary (21) has the form (24) with $\hat{S}_n$ given by (25) and $\theta = g\Delta t$.[10]

*4.6.3. Reduced dynamics of S and ancilla*

Take all ancillas initially in the same state $\eta_n = |0\rangle_n\langle 0|$ [cf. Eq. (1)]. Using basis $\{|0\rangle_n, |1\rangle_n\}$ to carry out the partial trace over each ancilla, the collision map (6) is worked out from (21) as

$$\rho' = \mathcal{E}[\rho] = \hat{K}_0\rho\hat{K}_0^\dagger + \hat{K}_1\rho\hat{K}_1^\dagger , \tag{27}$$

where the Kraus operators $\hat{K}_k = {}_n\langle k|\hat{U}_n|0\rangle_n$ (see Appendix C) explicitly read[11]

$$\hat{K}_0 = e^{-ig_z\Delta t}|0\rangle_S\langle 0| + e^{ig_z\Delta t}\cos(g\Delta t)|1\rangle_S\langle 1| , \qquad \hat{K}_1 = -i\,e^{ig_z\Delta t}\sin(g\Delta t)\,\hat{\sigma}_- . \tag{28}$$

Any qubit state has the general form

$$\rho = \begin{pmatrix} \langle 1|\rho|1\rangle & \langle 0|\rho|1\rangle \\ \langle 1|\rho|0\rangle & \langle 0|\rho|0\rangle \end{pmatrix} = \begin{pmatrix} p & c \\ c^* & 1-p \end{pmatrix} \tag{29}$$

with $0 \le p \le 1$ and $(1-2p)^2 + 4|c|^2 \le 1$ (to ensure that eigenvalues of $\rho$ are positive). Entries $c$ and $p$ are routinely called "coherences" and "populations", respectively.

Plugging (29) into (27) yields

$$\rho' = \mathcal{E}[\rho] = \begin{pmatrix} \cos^2(g\Delta t)\,p & e^{2ig_z\Delta t}\cos(g\Delta t)\,c \\ e^{-2ig_z\Delta t}\cos(g\Delta t)\,c^* & (1-p) + \sin^2(g\Delta t)\,p \end{pmatrix} , \tag{30}$$

which is an alternative way to represent the collision map (27). The effect of the map, as can be seen, is to multiply the coherences $c$ by a factor $e^{2ig_z\Delta t}\cos(g\Delta t)$ and populations $p$ by $\cos^2(g\Delta t)$. In light of Eq. (5), the state of $S$ at step $n$ is thus given by

$$\rho_n = \mathcal{E}^n[\rho] = \begin{pmatrix} p_n & c_n \\ c_n^* & 1-p_n \end{pmatrix} \tag{31}$$

with

$$p_n = \cos^{2n}(g\Delta t)\,p , \quad c_n = e^{2ig_z n\Delta t}\cos^n(g\Delta t)\,c . \tag{32}$$

This entails the following: provided that $|\cos(g\Delta t)| < 1$, no matter what state $S$ started from (i.e. regardless of $c$ and $p$), the coherences and populations vanish for $n \to \infty$ meaning that $S$ asymptotically ends up in state $|0\rangle_S$. This is a rather extreme example of non-unitary, i.e. irreversible, open dynamics, which can be pictured as a transformation mapping the entire Hilbert space of $S$ into a single point representing the asymptotic states $|0\rangle_S$.

By replacing (21) and (31) into Eq. (9) for $\eta_n = |0\rangle_n\langle 0|$, we get that the state of ancilla $n$ after colliding with $S$ is given by

$$\eta_n' = \begin{pmatrix} \pi_n & d_n \\ d_n^* & 1-\pi_n \end{pmatrix} . \tag{33}$$

with

$$\pi_n = \sin^2(g\Delta t)\cos^{2(n-1)}(g\Delta t)\,p , \quad d_n = -i\sin(g\Delta t)\cos^{n-1}(g\Delta t)e^{2ig_z n\Delta t}\,c . \tag{34}$$

Note that, as $n$ grows up and for $|\cos(g\Delta t)| < 1$, $\eta_n' \to |0\rangle_n\langle 0| = \eta_n$, Namely, after a sufficient number of steps, ancillas basically no longer change their state after colliding with $S$. This is consistent with the convergence of $S$ to $|0\rangle_S$ since the collision leaves state $|0\rangle_S|0\rangle_n$ unaffected, i.e. $\hat{U}_n|00\rangle_{Sn}\langle 00|\hat{U}_n^\dagger = |00\rangle_{Sn}\langle 00|$.

[10] Replacing $\hat{S}_n = 1/2\,(\mathbb{I} + \hat{\boldsymbol{\sigma}}\cdot\hat{\boldsymbol{\sigma}}_n)$, we get $\hat{U}_n = e^{-ig/2\hat{\boldsymbol{\sigma}}\cdot\hat{\boldsymbol{\sigma}}_n\Delta t} = e^{i\frac{g}{2}\Delta t}e^{-ig\hat{S}_n\Delta t}$. Thus, $\theta = g\Delta t$ up to phase factor $e^{i\frac{g}{2}\Delta t}$.

[11] For $g_z = 0$, the collision map reduces to a so called amplitude damping channel [21].

### 4.7. Steady states

As discussed, Eq. (31) shows that for, $|\cos(g\Delta t)| < 1$, $S$ eventually ends up in state $|0\rangle_S$,[12] i.e. $\rho_n \to \rho^* = |0\rangle_S\langle 0|$. Once $S$ reaches this state, this will be not be affected by collisions with ancillas. In these cases, we say that $\rho^*$ is a *steady* or *stationary* state for $S$.

In the language of quantum maps (see Appendix C), a steady state $\rho^*$ is a *fixed point* of the collision map, i.e.

$$\mathcal{E}[\rho^*] = \rho^* \quad \text{(steady state)}. \tag{35}$$

This expresses the fact that $\rho^*$ is unchanged by the collisions, no matter how many (since we also have $\mathcal{E}^n[\rho^*] = \rho^*$ for any $n$). Note that, in general, map $\mathcal{E}$ could admit more than one fixed point, i.e. many steady states can exist. When only one steady state is possible (as in the previous instance), i.e. there is a *unique* fixed point, we say that the collision map is *ergodic*.[13]

Actually, the instance in the previous subsection fulfills a stronger property in that $\rho_n \to \rho^*$ for *any* initial state $\rho_0$. In the language of quantum maps, in such cases map $\mathcal{E}$ is said to be *mixing*. A paradigm of mixing processes is thermalization (which will be discussed in Section 7.1), enforcing $S$ to end up in the Gibbs state at the reservoir temperature no matter what state it started from. Importantly, note that a necessary – but not sufficient – condition for a map to be mixing with respect to a steady state $\rho^*$ is that this be a fixed point i.e. fulfill (35)]. A more stringent necessary condition, although still insufficient, is that $\rho^*$ be the *only* fixed point, namely (see above) the collision map must be ergodic (if there were two or more fixed points, mixingness clearly could not occur).

A simple paradigmatic instance where ergodicity, hence mixingness, does not take place is the all-qubit CM for $g\Delta t = \pi$ and $g_z = 0$. The corresponding collision map (30) then is

$$\rho' = \mathcal{E}[\rho] = \begin{pmatrix} p & -c \\ -c^* & 1-p \end{pmatrix}. \tag{36}$$

This leaves populations unaffected, while coherences change sign. Clearly, any mixture of $|0\rangle_S\langle 0|$ and $|1\rangle_S\langle 1|$ (zero coherences) is a fixed point of map $\mathcal{E}$ [cf. Eq. (35)]. Notably, there exist initial states giving rise to a dynamics where $S$ never reaches a steady state. For instance, observing that $\mathcal{E}[|\pm\rangle\langle\pm|] = |\mp\rangle\langle\mp|$ with $|\pm\rangle = \frac{1}{\sqrt{2}}(|0\rangle \pm |1\rangle)$ (eigenstates of $\hat{\sigma}_x$), we see that if $\rho_0 = |+\rangle\langle +|$ then $S$ will indefinitely oscillate between states $|+\rangle$ ($n$ even) and $|-\rangle$ ($n$ odd).

We finally mention a special type of mixing dynamics called *quantum homogenization*, which occurs when $\mathcal{E}$ is mixing with steady state $\rho^*$ such that $\rho^* = \eta$ for any initial state $\eta$ of ancillas. Note how this definition poses the constraint that $S$ and each ancilla have the same Hilbert space dimension (and moreover that all ancillas start in the same state). Physically, the intuitive idea behind quantum homogenization is that, since the bath is made out of a huge number of identical subsystems, if $S$ "talks" long enough with them then its state will more and more look like that of ancillas until becoming homogeneous with these. It can be shown [22] that in the all-qubit CM quantum homogenization occurs when the collision unitary $\hat{U}_n$ is a partial swap [cf. Eq. (24)] corresponding to the Heisenberg exchange interaction (26).

### 4.8. Cascaded collision model

The basic CM of Fig. 3 comes with an intrinsic *unidirectionality*: $S$ explores the bath along a specific direction (say from left to right as in Fig. 3). Remarkably, if we let $S$ be *multipartite* in such a way that each ancilla collides with one subsystem of $S$ at a time, then the above unidirectionality yields an interesting effect.

To see this, let $S$ comprise a pair of subsystems, $S_1$ and $S_2$. By hypothesis, the collision with each ancilla consists of two *cascaded* sub-collisions (see Fig. 4): $n$ collides *first* with $S_1$ and only *afterward* with $S_2$. Accordingly, the collision unitary reads

$$\hat{U}_n = \hat{U}_{2,n}\hat{U}_{1,n}\,. \tag{37}$$

The remaining hypotheses of the basic CM in Section 4.1 are unchanged. Already at this stage, it is clear that there exists an asymmetry between $S_1$ and $S_2$ since $\hat{U}_n$ does change if 1 and 2 are swapped (as $\hat{U}_{1,n}$ and $\hat{U}_{2,n}$ generally do not commute). The open dynamics of $S_1$ is indeed quite different from that of $S_2$, as we show next.

We first note that, just like in the basic collision model, the *joint* system $S$ undergoes a fully Markovian dynamics according to [cf. Eq. (6)]

$$\rho_n = \mathcal{E}[\rho_{n-1}] = \mathrm{Tr}_n\left\{\hat{U}_{2,n}\hat{U}_{1,n}\,\rho_{n-1}\eta_n\,\hat{U}_{1,n}^\dagger\hat{U}_{2,n}^\dagger\right\}. \tag{38}$$

[12] The rigorous mathematical statement is that, for any $\varepsilon > 0$, there exists $n_\varepsilon$ such that $\|\rho_n - |0\rangle_S\langle 0|\| < \varepsilon$ for any $n > n_\varepsilon$, where $\|\ldots\|$ is some distance measure between quantum states (e.g. trace distance).

[13] More formally, since a fixed point is an eigenstate of $\mathcal{E}$ with eigenvalue 1 [cf. Eq. (35)], the map is ergodic when 1 is a non-degenerate eigenvalue of $\mathcal{E}$.

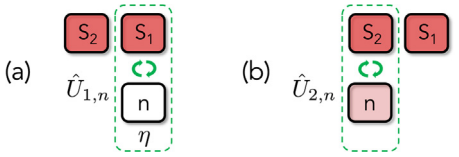


**Fig. 4.** *Cascaded collision model.* The open system $S$ is made out of two subsystems, $S_1$ and $S_2$. At each collision, the ancilla interacts *first* with $S_1$ (unitary $\hat{U}_{1,n}$) and only *afterward* with $S_2$ (unitary $\hat{U}_{2,n}$). Thus the collision consists of two time-ordered sub-collisions according to the collision unitary $\hat{U}_n = \hat{U}_{2,n}\hat{U}_{1,n}$. Subsystem $S_1$ always collides with "fresh" ancillas (still in the initial state $\eta$), while $S_2$ collides with "recycled" ancillas that already interacted (and got correlated) with $S_1$.

We next ask whether or not the same statement holds for the reduced dynamics of $S_1$ and $S_2$ (whose reduced states will be respectively denoted as $\rho_{1,n}$ and $\rho_{2,n}$). Let us start with $S_1$: tracing off $S_2$ in (38) yields[14]

$$\rho_{1,n} = \mathrm{Tr}_2\{\rho_n\} = \mathrm{Tr}_2\mathrm{Tr}_n\left\{\hat{U}_{2,n}\hat{U}_{1,n}\,\rho_{n-1}\eta_n\,\hat{U}_{1,n}^\dagger\hat{U}_{2,n}^\dagger\right\} = \mathrm{Tr}_2\mathrm{Tr}_n\left\{\hat{U}_{1,n}\,\rho_{n-1}\eta_n\,\hat{U}_{1,n}^\dagger\right\}. \tag{39}$$

Since $\mathrm{Tr}_2\{\ldots\}$ does not act on either $S_1$ or ancilla $n$, it can be moved to the right of $\hat{U}_{1,n}$

$$\rho_{1,n} = \mathrm{Tr}_n\left\{\hat{U}_{1,n}\,\mathrm{Tr}_2\{\rho_{n-1}\}\eta_n\,\hat{U}_{1,n}^\dagger\right\} = \mathrm{Tr}_n\left\{\hat{U}_{1,n}\,\rho_{1,n-1}\eta_n\hat{U}_{1,n}^\dagger\right\} \equiv \mathcal{E}[\rho_{1,n-1}]\,,$$

where we introduced the usual collision map (6). Thus $S_1$ evolves exactly as if $S_2$ were absent, entailing in particular that its dynamics is Markovian. This occurs because $S_1$ always collides with "fresh" ancillas that are still in the initial state $\eta$ [see Fig. 4(a)]. Once the ancilla has collided with $S_1$, the following collision with $S_2$ cannot affect the reduced state of $S_1$.

In contrast, since it collides with "recycled" ancillas that already collided with $S_1$, the dynamics of $S_2$ does depend on that of $S_1$. Indeed, if we now trace off subsystem $S_1$ from Eq. (38) we get

$$\rho_{2,n} = \mathrm{Tr}_1\mathrm{Tr}_n\left\{\hat{U}_{2,n}\hat{U}_{1,n}\,\rho_{n-1}\eta_n\,\hat{U}_{1,n}^\dagger\hat{U}_{2,n}^\dagger\right\} = \mathrm{Tr}_n\left\{\hat{U}_{2,n}\,\mathrm{Tr}_1\left\{\hat{U}_{1,n}\,\rho_{n-1}\eta_n\,\hat{U}_{1,n}^\dagger\right\}\hat{U}_{2,n}^\dagger\right\}. \tag{40}$$

At least two features stand out. First, the state of $S_2$ is affected by the previous subcollision (the one involving $S_1$). Second, upon comparison with $\rho_{1,n}$, we see that $\rho_{2,n}$ does *not* evolve according to a CPT map. This is because, after the first sub-collision but before the second one starts, $S_2$ is in general already correlated with ancilla $n$. Indeed, even if $S_1$ and $S_2$ start in a product state, very soon they will get correlated during the collisional dynamics due to their interaction with the common bath of ancillas. Thus, as soon as ancilla $n$ has finished colliding with $S_1$, it establishes correlations with both $S_1$ and $S_2$.

To summarize, in a cascaded CM, the two subsystems jointly undergo a Markovian evolution. The reduced dynamics of $S_1$ is Markovian as well and completely insensitive to the presence of $S_2$. Instead, the reduced dynamics of $S_2$ depends on that of $S_1$ and is generally *non*-Markovian since it cannot be divided into a sequence of CPT maps. This *asymmetry* in the mutual dependence of the two reduced dynamics reflects the intrinsic CM unidirectionality (causal order) that we discussed above.

The next subsection (connecting CMs with matrix product states theory) is not indispensable to access the remainder of the paper. As such, it could be skipped by the uninterested reader.

### 4.9. Collision models and matrix product states

We have previously focused on the reduced dynamics of either $S$ or an ancilla. Here, we will consider the joint dynamics of $S$ and all ancillas showing that it enjoys interesting properties.

Starting from state (1), as the collisional dynamics proceeds, multipartite correlations are established so that the joint system evolves at step $n$ into a generally *entangled* state[15] having the generic form

$$|\Psi_n\rangle = \sum_{\alpha,k_1,\ldots,k_n} c_{\alpha,k_1,k_2,\ldots,k_n}|\alpha, k_1, k_2, \ldots, k_n\rangle \tag{41}$$

with $\{|\alpha\rangle\}$ denoting a basis of $S$ and $\{|k_n\rangle\}$ a basis of the $n$th ancilla.[16]

[14] We use that $\mathrm{Tr}_2\mathrm{Tr}_n\left\{\hat{U}_{2,n}\sigma\hat{U}_{2,n}^\dagger\right\} \equiv \mathrm{Tr}_2\mathrm{Tr}_n\{\sigma\}$ since if $\{|k_2, k_n\rangle\}$ is an orthonormal basis of system 2-$n$ used to compute $\mathrm{Tr}_2\mathrm{Tr}_n\{\ldots\}$ another legitimate basis to perform the trace is $\{\hat{U}_{2,n}^\dagger|k_2, k_n\rangle\}$ (recall that the trace can be carried out in any basis).

[15] An entangled state is a state which is not separable, i.e. such that the corresponding density matrix cannot be expressed as a mixture of product states. For bipartite systems, a separable state reads $\sigma_{12} = \sum_j p_j\rho_1^{(j)} \otimes \rho_2^{(j)}$ with $\sum_j p_j = 1$ (this naturally generalizes to $N$ systems).

[16] Here, $|\alpha\rangle$ and $|k_n\rangle$ respectively stand for $|\alpha\rangle_S$ and $|k_n\rangle_n$, a light notation that will be used again later on in the paper.

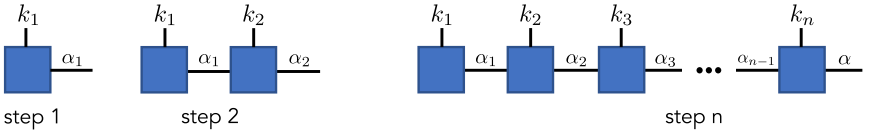


**Fig. 5.** *Tensor-network representation of the joint CM dynamics.* The joint state at step $n$ is generally defined by the rank-$(n+1)$ tensor $c_{\alpha,k_1,\ldots,k_n}$ [cf. Eq. (41)]. This can be decomposed into one rank-2 tensor of dimension $d_S \times d_A$ (leftmost square) and $n-1$ rank-3 tensors each of dimension $d_S \times d_S \times d_A$ (squares with three legs) with $d_S$ ($d_A$) the Hilbert space dimension of $S$ (ancilla). A joined leg (each link between nearest-neighbor squares) represents an index contraction. The steps $n=1$ and $n=2$ are also shown for comparison.

We will show next that state (41) can be expressed in a computationally advantageous form. The basic idea is to view the expansion coefficients $c_{\alpha,k_1,k_2,\ldots,k_n}$ (each labeled by $n+1$ indexes) as a rank-$(n+1)$ tensor and decompose it into $n$ tensors each with the smallest possible rank.

For the sake of argument, we will refer to the basic CM of Section 4.1 and assume that $\alpha = 1, 2, \ldots, d_S$ with $d_S$ the Hilbert space dimension of $S$, while $k_n$ takes integer values from 1 to $d_A$ with $d_A$ the dimension of each ancilla. We consider an initial pure state $\sigma_0 = |\Psi_0\rangle\langle\Psi_0|$, which without loss of generality can be written as

$$|\Psi_0\rangle = |1, 1_1, 1_2, \ldots\rangle. \tag{42}$$

At the end of the first collision, the joint state reads

$$|\Psi_1\rangle = \hat{U}_1|\Psi_0\rangle = \sum_{\alpha,k_1} |\alpha, k_1\rangle\langle\alpha, k_1|\hat{U}_1|1, 1_1\rangle \otimes |1_2, 1_3, \ldots\rangle = \sum_{\alpha,k_1} \mathrm{U}^{(k_1)}_{1\alpha}\, |\alpha, k_1, 1_2, 1_3, \ldots\rangle\,, \tag{43}$$

where we plugged in the identity operator $\mathbb{I}_S \otimes \mathbb{I}_1$ expressed in terms of basis $|\alpha, k_1\rangle$ and defined

$$\mathrm{U}^{(k_1)}_{\alpha\alpha'} = \langle\alpha', k_1|\hat{U}_1|\alpha, 1_1\rangle\,. \tag{44}$$

This is a rank-3 tensor of dimension $d_S \times d_S \times d_A$ due to dependence on the three indexes $\alpha$, $\alpha'$ and $k$.

Using this, the joint state at the end of the second collision, $|\Psi_2\rangle = \hat{U}_2|\Psi_1\rangle$, can be worked out as

$$\begin{aligned}|\Psi_2\rangle &= \sum_{\alpha,k_1} \mathrm{U}^{(k_1)}_{1\alpha}\, \hat{U}_2|\alpha, k_1, 1_2, \ldots\rangle = \sum_{\alpha,k_1} \mathrm{U}^{(k_1)}_{1\alpha} \sum_{\alpha',k_2} |\alpha', k_2\rangle\langle\alpha', k_2|\hat{U}_2|\alpha, 1_2\rangle \otimes |k_1\rangle \otimes |1_3, \ldots\rangle \\ &= \sum_{\alpha,k_1}\sum_{\alpha',k_2} \mathrm{U}^{(k_1)}_{1\alpha}\, \mathrm{U}^{(k_2)}_{\alpha\alpha'} |\alpha', k_1, k_2, 1_3, \ldots\rangle = \sum_{\alpha',k_1,k_2} \left(\sum_{\alpha} \mathrm{U}^{(k_1)}_{1\alpha}\, \mathrm{U}^{(k_2)}_{\alpha\alpha'}\right) |\alpha', k_1, k_2, 1_3, \ldots\rangle\,.\end{aligned}$$

For $n=3$, analogous steps lead to

$$|\Psi_3\rangle = \sum_{\alpha'',k_1,k_2,k_3} \left(\sum_{\alpha\alpha'} \mathrm{U}^{(k_1)}_{1,\alpha}\, \mathrm{U}^{(k_2)}_{\alpha\alpha'} \mathrm{U}^{(k_3)}_{\alpha',\alpha''}\right) |\alpha'', k_1, k_2, k_3, 1_4, \ldots\rangle\,. \tag{45}$$

Finally, at the $n$th step, we get (41) with each coefficient given by

$$c_{\alpha,k_1,\ldots,k_n} = \sum_{\alpha_1,\ldots,\alpha_{n-1}} \mathrm{U}^{(k_1)}_{1\alpha_1}\, \mathrm{U}^{(k_2)}_{\alpha_1\alpha_2} \ldots \mathrm{U}^{(k_n)}_{\alpha_{n-1}\alpha}\,. \tag{46}$$

Thus, as schematically sketched in Fig. 5, we get that the rank-$(n+1)$ tensor $c_{\alpha,k_1,\ldots,k_n}$ can be decomposed in terms of $n-1$ rank-3 tensors of dimension $d_S \times d_S \times d_A$ and one rank-2 tensor of dimensions $d_S \times d_A$.[17] Interestingly, each of these low-rank tensors [cf. Eq. (44)] corresponds to a single collision: Eq. (46) thus reflects the decomposition of the overall complex system–bath dynamics in terms of elementary two-body unitaries. This way of expressing the multipartite $S$-bath state is very close to the so called *matrix product states* decomposition [44–46]. The idea is that reducing to low-rank tensors with *small* enough dimension (if possible) allows to limit the computational complexity of the problem (with clear advantages for numerical simulations of the dynamics). A collisional dynamics typically has such features in that, as shown, the dimension of each rank-three tensor is bounded in terms of the Hilbert space dimensions of the open system $S$ and a single ancilla these being often small.

### 4.10. Basic collision model: state of the art

Throughout we considered each collision to be described by a well-defined unitary. One can yet consider *random unitary collisions*. These were investigated in Ref. [47], where it was shown that $S$ reaches the same asymptotic state which would be attained for repeated random collisions with a single effective ancilla of suitable dimension.

[17] The rank-2 tensor is $\mathrm{U}^{(k_1)}_{1\alpha_1}$, which derives from the rank-3 tensor (44) by fixing one $\alpha$ index.

A more general and formal treatment than Section 4.3 of the ancilla dynamics was carried out in the context of so called *non-anticipatory quantum channels with memory* [48]. Similarly to cascaded CMs (see Section 4.8), this dynamics features an explicit causal ordering of the ancillas, which reflects the different times at which these interact with $S$.

The Markovianity notion based on divisibility discussed in Section 4.5 is featured in the review paper Ref. [49], where CMs are used as an effective way to visualize the memoryless properties characteristic of quantum Markovian processes.

A thorough treatment of mixing channels and fixed points mentioned in Section 4.7 can be found in Ref. [50]. Note that the properties of mixing CPT maps which we referred to are directly connected with the concept of *forgetful channels* introduced in 2005 by Kretschmann and Werner [51] within the general framework of memory quantum communication lines (reviewed in Ref. [48]). These models describe the evolution of an ordered collection of quantum information carriers, which sequentially interact with a common reservoir. In this context, if the reservoir asymptotically loses track of its initial state for a growing number of carriers then the resulting transformation is said to be “forgetful". Accordingly, from the point of view of the bath ancillas, any CM featuring a collision map $\mathcal{E}$ that is mixing can be seen as a special instance of forgetful channel.

*Quantum homogenization* (see Section 4.7) was first considered by Ziman, Stelmachovic, Buzek, Scarani and Gisin in Ref. [22], where they introduced a so called “universal quantum homogenizer" this being in fact an all-qubit CM such that $\rho_n \to \eta$ for any $\rho_0$ and $\eta$. A related paper [52] carried out a detailed analysis of the nature of correlations (in the form of entanglement) between $S$ and the bath of ancillas that are established during the collisional dynamics [cf. Fig. 3(d)]. We also note that quantum homogenization was studied also in the more general case that $S$ is a composite system (spin chain) colliding locally with a bath of ancillas [53].

*Cascaded CMs* (Section 4.8) were first introduced in 2012 by Giovannetti and Palma [54,55] mostly with the goal of defining a simple microscopic framework underpinning cascaded master equations (which will be discussed in detail in Section 5.10).

Connections between CMs and *matrix product states* (for a friendly introduction see e.g. Refs. [45,46]) can be found in papers dealing with the more general framework of non-Markovian dynamics, see e.g. Ref. [56,57] (which we will discuss in Section 8.7) and Ref. [58].

## 5. Equations of motion

A hallmark of CMs is their *discrete* nature, which is indeed a major reason why these models are useful. Yet, most dynamics in Physics are intrinsically continuous or, better to say, conveniently approached through a continuous-time description, allowing to write down an associated differential equation of motion.

When it comes to open quantum systems, a relevant equation of motion is the so called *master equation* (ME) governing the time evolution of the open system state $\rho$ (much like the Schrödinger equation does for closed systems). In some applications, such as quantum thermodynamics (see Section 7, it is yet often convenient working with a specific dynamical equation for the expectation value of an observable of concern (e.g. energy). Accordingly, in this section we will introduce both kinds of equations of motion (although they are tightly connected to one another of course).

In the last part of the present section, we will in particular revisit the instances of CMs introduced in the previous section with the aim of providing the corresponding ME for each.

### 5.1. Equations of motion for small collision time: states

In light of an eventual conversion of the discrete collisional dynamics into a continuous-time one, such that $t_n = n\Delta t$ is turned into the continuous time variable $t$, the collision duration $\Delta t$ must approach zero.

With this in mind, we are interested in the approximated expression of the collision unitary in the regime of *small collision time*. We thus consider the basic CM in Section 4.1 and replace $\hat{U}_n$ with the small-$\Delta t$ approximation[18]

$$\hat{U}_n \simeq \hat{\mathbb{I}} - i(\hat{H}_0 + \hat{V}_n)\Delta t - \tfrac{1}{2}\hat{V}_n^2 \Delta t^2 \,, \tag{47}$$

where $\hat{H}_0$ is the total system–ancilla free Hamiltonian

$$\hat{H}_0 = \hat{H}_S + \hat{H}_n \,. \tag{48}$$

Note that (47) is of the 2nd-order in $\hat{V}_n$ but of the 1st order in $\hat{H}_S$ and $\hat{H}_n$. This is in fact due to a hypothesis of the CM that we are making: *second-order terms in $\Delta t$ that are not quadratic in $\hat{V}_n$ are negligible*.[19] The rationale of this assumption, requiring in fact that $\hat{H}_S$ and $\hat{H}_n$ be much weaker than $\hat{V}_n$, will become clear later on.

Accordingly, at each collision, the joint $S$-bath state $\sigma_n$ evolves according to

$$\Delta\sigma_n = -i\,[\hat{H}_0 + \hat{V}_n, \sigma_n]\,\Delta t + \left(\hat{V}_n\,\sigma_n\,\hat{V}_n - \tfrac{1}{2}[\hat{V}_n^2, \sigma_n]_+\right)\Delta t^2 \tag{49}$$

[18] Note that this lowest-order expansion relies on treating the $S$-ancilla Hamiltonian as time-independent. If not, an additional 2nd-order term would appear in the expansion as is the case of Eq. (259) in Section 9 (see also Ref. [36]).

[19] This hypothesis will be partially relaxed in Section 7.8.

with $\Delta\sigma_n = \sigma_n - \sigma_{n-1}$ and $[\ ,\ ]_+$ the anti-commutator. We dropped third-order terms in $\Delta t$ and, in line with the aforementioned hypothesis, all second-order terms but those having a quadratic dependence on $\hat{V}_n$. Eq. (49) has a central role in CM theory.[20]

Eq. (49) can be equivalently arranged solely in terms of commutators as

$$\Delta\sigma_n = -i\,[\hat{H}_0 + \hat{V}_n, \sigma_n]\,\Delta t - \tfrac{1}{2}\,[\hat{V}_n, [\hat{V}_n, \sigma_n]]\Delta t^2\,, \tag{50}$$

an alternative expression which is useful in some contexts.

We next focus on $S$ and the $n$th ancilla. Before colliding, they are in the *product* state $\rho_{n-1}\otimes\eta_n$ (see Section 4.1). The collision changes their joint state according to

$$\frac{\Delta\varrho_{Sn}}{\Delta t} = -i\,[\hat{H}_0 + \hat{V}_n, \rho_{n-1}\,\eta_n] + \Delta t\,(\hat{V}_n\,\rho_{n-1}\,\eta_n\,\hat{V}_n - \tfrac{1}{2}[\hat{V}_n^2, \rho_{n-1}\,\eta_n]_+)\,, \tag{51}$$

with $\Delta\varrho_{Sn} = \varrho_{Sn} - \rho_{n-1}\,\eta_n$. This equation, which simply follows from (49) by tracing off all ancillas not involved in the collision and dividing either side by $\Delta t$, underpins memoryless CMs.

Note that Eqs. (49) and (51) also hold for the general inhomogeneous CM in Section 4.5, in which case $\hat{H}_S$, $\hat{H}_n$, $\hat{V}_n$ and $\eta_n$ are understood as generally dependent on step $n$.

To get a closed equation for the reduced dynamics of $S$ we trace off the $n$th ancilla in (51), obtaining

$$\frac{\Delta\rho_n}{\Delta t} = -i\,[\hat{H}_S + \mathrm{Tr}_n\{\hat{V}_n\,\eta_n\}, \rho_{n-1}] + \Delta t\,\mathrm{Tr}_n\{\hat{V}_n\,\rho_{n-1}\eta_n\,\hat{V}_n - \tfrac{1}{2}[\hat{V}_n^2, \rho_{n-1}\eta_n]_+\} \tag{52}$$

with $\Delta\rho_n = \rho_n - \rho_{n-1} = \mathrm{Tr}_n\{\Delta\varrho_{Sn}\}$. Note that, since $\Delta\rho_n = (\mathcal{E} - \mathcal{I})\,[\rho_{n-1}]$ with $\mathcal{I}$ the identity map on $S$, Eq. (52) in fact represents the short-time expression of the collision map $\mathcal{E}$ [cf. Eq. (6)].

By tracing off $S$ (instead of ancilla $n$) in Eq. (51), a similar discrete-time equation of motion can be obtained for the change of ancilla's state $\Delta\eta_n = \eta_n' - \eta_n$ due to the collision with $S$ (see Section 4.3). This reads

$$\frac{\Delta\eta_n}{\Delta t} = -i\,[\hat{H}_n + \mathrm{Tr}_S\{\hat{V}_n\,\rho_{n-1}\}, \eta_n] + \Delta t\,\mathrm{Tr}_S\{\hat{V}_n\rho_{n-1}\eta_n\,\hat{V}_n - \tfrac{1}{2}[\hat{V}_n^2, \rho_{n-1}\eta]_+\}\,. \tag{53}$$

Eq. (52) (discrete-time *master equation*) and Eq. (53) are finite-difference equations that govern the reduced dynamics of $S$ and ancilla $n$, respectively, at the discrete times $t_n = n\Delta t$.[21] We will show shortly (Section 5.3) that these equations are in the so called Lindblad form (see Appendix F).

### 5.2. Equations of motion for small collision time: expectation values

While all the above equations of motion describe the evolution of states, one may be interested in the evolution of the expectation value of a given observable $\hat{O}$, denoted as $\langle\hat{O}\rangle_n = \mathrm{Tr}_{SB}\{\hat{O}\sigma_n\}$ (at this stage we allow $\hat{O}$ to generally act on the joined system, i.e. $S$ plus all the ancillas). The general change of the expectation value $\Delta\langle\hat{O}\rangle_n = \langle\hat{O}\rangle_n - \langle\hat{O}\rangle_{n-1}$ at each time step reads

$$\Delta\langle\hat{O}\rangle_n = \mathrm{Tr}_{SB}\{\Delta\hat{O}_n\,\sigma_{n-1}\} + \mathrm{Tr}_{SB}\{\hat{O}_n\,\Delta\sigma_n\} \tag{54}$$

with $\Delta\hat{O}_n = \hat{O}_n - \hat{O}_{n-1}$. The former and latter terms respectively describe the contribution due to an intrinsic time dependence of operator $\hat{O}$ (if any) and that due to the evolution of state $\sigma_n$. For a time-independent observable, only the second term can contribute.

Plugging Eq. (49) in (54) and exploiting the cyclic property of trace, we find that the rate of change of $\langle\hat{O}\rangle_n$ is given by

$$\frac{\Delta\langle\hat{O}\rangle_n}{\Delta t} = \left\langle\frac{\Delta\hat{O}_n}{\Delta t}\right\rangle + i\,\langle[\hat{H}_0 + \hat{V}_n, \hat{O}]\rangle + \Delta t\,\langle\hat{V}_n\,\hat{O}\,\hat{V}_n - \tfrac{1}{2}[\hat{V}_n^2, \hat{O}]_+\rangle\,, \tag{55}$$

where on the right hand side $\langle\ldots\rangle = \mathrm{Tr}_{SB}\{\ldots\,\sigma_{n-1}\}$.

Alternatively, expressing $\Delta\sigma_n$ in the form (50), we get

$$\frac{\Delta\langle\hat{O}\rangle_n}{\Delta t} = \left\langle\frac{\Delta\hat{O}_n}{\Delta t}\right\rangle + i\,\langle[\hat{H}_0 + \hat{V}_n, \hat{O}]\rangle - \tfrac{1}{2}\Delta t\,\langle[\hat{V}_n, [\hat{V}_n, \hat{O}]]\rangle\,. \tag{56}$$

[20] Note that Eq. (49) is not restricted to the memoryless CMs specified by assumptions (1)–(3) in Section 4.1.1 (i.e. the CM which we refer to in the present section). In particular, it remains valid for initially correlated ancillas (see Section 8.3).

[21] This is sometimes called "stroboscopic evolution" in that we are not interested in the dynamics at any possible instant but only at regular intervals of duration $\Delta t$.

### 5.3. Lindblad form

The initial ancilla's density operator state $\eta_n$ can be spectrally decomposed (see Appendix A) as

$$\eta_n = \sum_k p_k \, |k\rangle_n\langle k| \, . \tag{57}$$

with $\sum_k p_k = 1$. Replacing this in (52) yields

$$\frac{\Delta\rho_n}{\Delta t} = -i\,[\hat{H}_S + \mathrm{Tr}_n\{\hat{V}_n\,\eta_n\},\,\rho_{n-1}] + \sum_{kk'}\left(\hat{L}_{kk'}\rho_{n-1}\hat{L}_{kk'}^\dagger - \tfrac{1}{2}[\hat{L}_{kk'}^\dagger\hat{L}_{kk'},\,\rho_{n-1}]_+\right) \tag{58}$$

with jump operators $\hat{L}_{kk'}$ given by

$$\hat{L}_{kk'} = \sqrt{p_k}\;{}_n\langle k'|\hat{V}_n|k\rangle_n\,\sqrt{\Delta t}\;. \tag{59}$$

Here, $|k\rangle$ and $|k'\rangle$ are eigenstates of $\eta$ [cf. Eq. (A.1)]. Note that operator $\mathrm{Tr}_n\{\hat{V}_n\,\eta_n\}$ appearing in the commutator is Hermitian.

Eq. (58) has the form of a discrete Lindblad master equation (see Appendix F). An analogous reasoning, this time based on the spectral decomposition of $\rho_{n-1}$, shows that Eq. (53) is also in Lindblad form.

The Lindblad form essentially arises because both $S$ and the ancilla evolve at each step according to a CPT map that can be expanded in Kraus operators [see Eqs. (6) and (9)]. We stress that this crucially relies on the fact that $S$ and each ancilla are uncorrelated before colliding (their initial state $\rho_{n-1}\,\eta_n$ is factorized), which is guaranteed by assumptions (1)–(3) in Section 4.1.1.

### 5.4. Reduced equations of motion in terms of moments

Eq. (58) relies on the spectral decomposition (A.1) of the ancilla's state, whose calculation could be impractical in some cases. We derive next an alternative form of Eqs. (52) and (53) in terms of first and second moments of the bath/system operator entering the coupling Hamiltonian $\hat{V}_n$, which is both technically advantageous and conceptually important in that it pinpoints the essential quantities controlling the reduced dynamics of either subsystem.

The system–ancilla coupling Hamiltonian can be always decomposed as

$$\hat{V}_n = \sum_\nu g_\nu \hat{A}_\nu\hat{B}_\nu\,, \tag{60}$$

with $g_\nu$ generally complex coefficients and $\hat{A}_\nu(\hat{B}_\nu)$ a set of (generally non-Hermitian) operators on $S$ (ancilla) subject to the constraint $\hat{V}_n = \hat{V}_n^\dagger$ (index $n$ is omitted in ancilla operators).[22]

Let us define first and second moments of $S$ and ancilla as

$$\langle\hat{A}_\nu\rangle = \mathrm{Tr}_n\{\hat{A}_\nu\rho_{n-1}\},\;\langle\hat{A}_\nu\hat{A}_\mu\rangle = \mathrm{Tr}_n\{\hat{A}_\nu\hat{A}_\mu\rho_{n-1}\},\;\langle\hat{B}_\nu\rangle = \mathrm{Tr}_n\{\hat{B}_\nu\eta_n\},\;\langle\hat{B}_\nu\hat{B}_\mu\rangle = \mathrm{Tr}_n\{\hat{B}_\nu\hat{B}_\mu\eta_n\}\,. \tag{61}$$

Note that the moments of $\hat{A}_\nu$ are calculated on the current state of $S$, $\rho_{n-1}$, to be updated after each collision. Regardless, both moments of $S$ and ancilla have an intrinsic dependence on step $n$ when the CM is inhomogeneous (see Section 4.5; e.g. when ancillas are prepared in different states).

In terms of the moments just defined, the contributions to the discrete ME (52) can be decomposed as

$$\mathrm{Tr}_n\{\hat{V}_n\,\eta_n\} = \sum_\nu g_\nu\langle\hat{B}_\nu\rangle\hat{A}_\nu\,,\quad \mathrm{Tr}_n\{\hat{V}_n\rho_n\eta_n\hat{V}_n\} = \sum_{\nu\mu} g_\nu g_\mu\,\langle\hat{B}_\mu\hat{B}_\nu\rangle\,\hat{A}_\nu\rho_n\hat{A}_\mu\,, \tag{62}$$

$$\mathrm{Tr}_n\{[\hat{V}_n^2,\,\rho_{n-1}\,\eta_n]_+\} = \sum_{\nu\mu} g_\nu g_\mu\,\langle\hat{B}_\nu\hat{B}_\mu\rangle\,[\hat{A}_\nu A_\mu\,\rho_{n-1}]_+\,. \tag{63}$$

Analogous expressions are worked out for Eq. (53) in terms of moments of $\hat{A}_\nu$'s calculated on state $\rho_{n-1}$.

To summarize, Eq. (52) can be written as

$$\frac{\Delta\rho_n}{\Delta t} = -i\,[\hat{H}_S + \hat{H}'_S,\,\rho_{n-1}] + \mathcal{D}_S[\rho_{n-1}] \tag{64}$$

with

$$\hat{H}'_S = \mathrm{Tr}_n\{\hat{V}_n\eta_n\} = \sum_\nu g_\nu\,\langle\hat{B}_\nu\rangle\hat{A}_\nu\,,\quad \mathcal{D}_S[\rho_{n-1}] = \sum_{\nu\mu}\gamma_{\nu\mu}\langle\hat{B}_\mu\hat{B}_\nu\rangle(\hat{A}_\nu\rho_{n-1}\hat{A}_\mu - \tfrac{1}{2}[\hat{A}_\mu\hat{A}_\nu,\,\rho_{n-1}]_+)\,, \tag{65}$$

[22] It can be shown that there always exists a decomposition such that $\hat{A}_\nu = \hat{A}_\nu^\dagger$, $\hat{B}_\nu = \hat{B}_\nu^\dagger$ and $g_\nu = g_\nu^*$. Yet, we prefer allowing for generally non-Hermitian operators since this is the natural form of many usual interactions (e.g. atom-field interactions, in which case $\hat{A}_\nu$ and $\hat{B}_\nu$ are ladder operators).

while Eq. (53) as

$$\frac{\Delta\eta_n}{\Delta t} = -i\,[\hat{H}_n + \hat{H}'_n, \eta_n] + \mathcal{D}_n[\eta_n] \tag{66}$$

with

$$\hat{H}'_n = \mathrm{Tr}_S\{\hat{V}_n\rho_{n-1}\} = \sum_\nu g_\nu\,\langle\hat{A}_\nu\rangle\hat{B}_\nu\,, \quad \mathcal{D}_n[\eta_n] = \sum_{\nu\mu}\gamma_{\nu\mu}\langle\hat{A}_\mu\hat{A}_\nu\rangle(\hat{B}_\nu\rho_n\hat{B}_\mu - \tfrac{1}{2}[\hat{B}_\mu\hat{B}_\nu, \rho_n]_+)\,, \tag{67}$$

and where the rates appearing in the dissipators $\mathcal{D}_S$ and $\mathcal{D}_n$ are given by

$$\gamma_{\nu\mu} = g_\nu g_\mu\,\Delta t\ . \tag{68}$$

We see that the $S$-bath interaction brings about two main effects on the reduced dynamics. One is the appearance of an extra Hamiltonian term ($\hat{H}'_S$ and $\hat{H}'_n$) that adds to the free Hamiltonian ($\hat{H}_S$ and $\hat{H}_n$, respectively). Hamiltonian $\hat{H}'_S$, taken alone, would change the reduced dynamics of $S$ without yet affecting its *unitary* nature, despite the $S$-bath coupling (and similarly $\hat{H}'_n$ with respect to ancilla $n$). The other effect, embodied by dissipator $\mathcal{D}_S$ ($\mathcal{D}_n$), instead causes *non-unitary* dynamics.

Finally, note the explicit appearance of a $\Delta t$ factor in the rates (68), which will be shown later to have consequences on the passage to the continuous-time limit.

### 5.5. Equations of motion for expectation values in terms of moments

In the (frequent) case of observables acting only on $S$ or ancilla, also the equations of motion in Section 5.2 can be simply decomposed in terms of simple moments.

For an operator on $S$, in Eq. (54) $\sigma$ can be replaced with $\rho$ so that, in light of Eqs. (64) and (65), we get

$$\frac{\Delta\langle\hat{O}_S\rangle}{\Delta t} = \left\langle\frac{\Delta\hat{O}_S}{\Delta t}\right\rangle + i\,\langle[\hat{H}_S, \hat{O}_S]\rangle + i\sum_\nu g_\nu\langle\hat{B}_\nu\rangle\,\langle[\hat{A}_\nu, \hat{O}_S]\rangle + \sum_{\nu\mu}\gamma_{\nu\mu}\langle\hat{B}_\mu\hat{B}_\nu\rangle\langle\hat{A}_\mu\hat{O}_S\hat{A}_\nu - \tfrac{1}{2}\,[\hat{A}_\mu\hat{A}_\nu, \hat{O}_S]_+\rangle. \tag{69}$$

Likewise, in light of Eqs. (66) and (67), the expectation value of an operator on ancilla $n$ evolves at the $n$th step as[23]

$$\frac{\Delta\langle\hat{O}_n\rangle}{\Delta t} = \left\langle\frac{\Delta\hat{O}_n}{\Delta t}\right\rangle + i\,\langle[\hat{H}_n, \hat{O}_n]\rangle + i\sum_\nu g_\nu\langle\hat{A}_\nu\rangle\langle[\hat{B}_\nu, \hat{O}_n]\rangle + \sum_{\nu\mu}\gamma_{\nu\mu}\langle\hat{A}_\mu\hat{A}_\nu\rangle\langle\hat{B}_\mu\hat{O}_n\hat{B}_\nu - \tfrac{1}{2}\,[\hat{B}_\mu\hat{B}_\nu, \hat{O}_n]_+\rangle\,. \tag{70}$$

On the right hand sides of Eqs. (69) and (70), expectation values of operators on $S$ are computed on state $\rho_{n-1}$ and those on the ancilla on $\eta_n$. Note that here subscript $n$ must be intended as the ancilla index, not the time step. Accordingly, the changes are understood as $\Delta\hat{O}_n = \hat{O}_n^{(n)} - \hat{O}_n^{(n-1)}$ and likewise for $\Delta\langle\hat{O}_n\rangle$, where each subscript denotes the time step.

### 5.6. Continuous-time limit via coarse graining

So far we have considered finite-difference equations of motion, which reflects a stroboscopic description of the dynamics at the discrete times $t_n = n\Delta t$ with $\Delta t$ *short* enough that $\hat{U}_n$ can be replaced with its 2nd-order expansion in $\Delta t$. Clearly, if one observes the system evolution on a time scale much larger than $\Delta t$, then the dynamics will look like effectively time-continuous.

This is illustrated in a simple case study in Fig. 6, where the open dynamics of the all-qubit CM of Section 4.6 is considered for $g_z = 0$ with $S$ initially in state $\frac{1}{\sqrt{2}}(|0\rangle_S + |1\rangle_S)$ and each ancilla prepared in $|0\rangle_n$. Making $\Delta t$ too large (compared to $g^{-1}$) results in a generally abrupt change of the state of $S$ after each time step, which rules out a continuous interpolation [see Fig. 6(a)]. This change is instead negligible by setting a small collision time $\Delta t$ in a way that, for evolution times much longer than $\Delta t$, the dynamics will appear effectively continuous [see Fig. 6(b)].

Accordingly, if the collision time is small and for evolution times much larger than $\Delta t$, one can replace the elapsed time (after $n$ collisions) $t_n = n\Delta t$ with a continuous time variable, i.e. $t_n \to t$, substituting at the same time the incremental ratio in Eq. (64) with a continuous derivative,

$$t_n = n\Delta t \to t\,, \quad \frac{\Delta\rho_n}{\Delta t} \to \frac{d\rho}{dt} \quad \text{(coarse graining)}\,. \tag{71}$$

Of course, all the discrete functions depending on the step number $n$ (such as $\rho_{n-1}$) become now continuous functions of time $t$. This procedure is carried out after choosing a short enough but finite collision time $\Delta t$ (coarse graining time) which is then kept always fixed [which sets rates (68)]. This coarse graining procedure turns the finite-difference ME into a continuous-time ME. A prominent instance is the micromaser dynamics, which we will discuss in the next subsection.

[23] This holds only at the $n$th step. At any other step, since ancilla $n$ does not change its state, $\Delta\langle\hat{O}_n\rangle/\Delta t = \langle\Delta\hat{O}_n/\Delta t\rangle$.

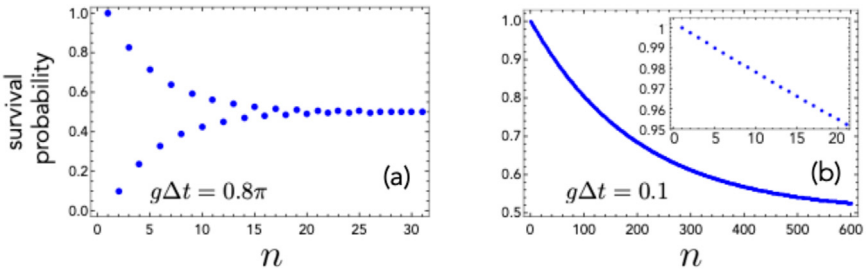


**Fig. 6.** *Continuous-time limit of the collisional dynamics.* We consider the all-qubit CM in Section 4.6 for $g_z = 0$ with the ancillas prepared in $\eta_n = |0\rangle_n\langle 0|$ and $S$ initially in $|\psi_0\rangle = \frac{1}{\sqrt{2}}(|0\rangle_S + |1\rangle_S)$ [thus $p = c = 1/2$ according to Eq. (29)]. The probability to find $S$ still in the initial state (survival probability) at the $n$th step is given by $\langle\psi_0|\rho_n|\psi_0\rangle = \frac{1}{2}(1 + \cos^n(g\Delta t))$ [cf. Eq. (32)]. This is plotted in panel (a) for $g\Delta t = 0.8\pi$, while in panel (b) we set $g\Delta t = 10^{-1}$ (the inset shows the first 20 steps). Clearly, the dynamics cannot be approximated as continuous in the case (a) due to the generally non-negligible change of $\rho_n$ at each step, $\Delta\rho_n = \rho_n - \rho_{n-1}$. Note that setting an ultra-short collision time, e.g. $g\Delta t = 10^{-3}$ (not shown here), and keeping the same total simulated time $n_{\max}\Delta t$ as (a) or (b) would yield $\langle\psi_0|\rho_n|\psi_0\rangle \simeq 1$.

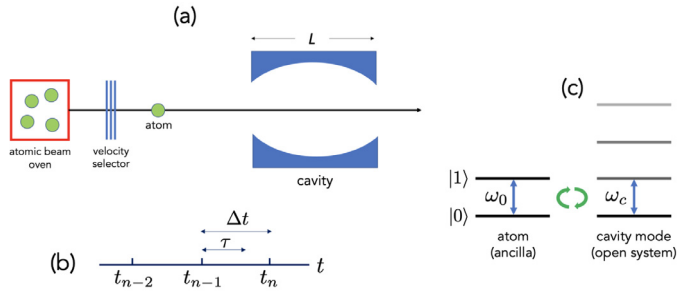


**Fig. 7.** *Micromaser.* (a): Basic micromaser setup. Atoms are heated in an oven (on the left). As atoms are ejected from the oven, a velocity selector filters only those of desired velocity $v$. Each selected atom then travels at speed $v$ towards the cavity (of length $L$) until it crosses it. (b): Characteristic times. If $L$ is the cavity length, each atom interacts with the cavity mode for a time $\tau = v/L$. Since $\tau \leq \Delta t$, where $\Delta t$ is the time between two consecutive atomic injections, there are never two atoms in the cavity at the same time meaning that the dynamics is naturally described by a basic CM (atoms interact with the cavity mode one at a time). In the interaction picture, during the interval $[t_{n-1} + \tau, t_n]$ when the $n$th atom is out of the cavity, the system does not change its state. (c): Atomic and cavity-mode levels involved the interaction.

In physical terms, the coarse-graining procedure means that we give up keeping track of the dynamics in fine detail (i.e. on a time scale shorter than $\Delta t$) and are happy with a coarse description on a small but *finite* time scale $\Delta t$. We point out that different choices of $\Delta t$ (but still small) will result in generally *different* rates (68), hence the coarse-grained ME and associated dynamics are $\Delta t$-dependent. Notably, as rates (68) are proportional to $\Delta t$, if this is very short then the dissipator $\mathcal{D}_S$ will become in fact negligible with the only effect of the bath reducing to Hamiltonian $\hat{H}'_S$ [cf. Eqs. (64) and (65)]. In this extreme regime of ultra-short collision times, the open dynamics is thus unitary.

### 5.7. Micromaser

The micromaser [59] is a system of utmost importance in CMs theory as it is an experimental setup whose dynamics is, in fact by definition, described by a CM. The paradigm of micromaser features a lossy cavity pumped by a beam of atoms which drive the cavity field into a lasing-like state.[24] More specifically, as sketched in Fig. 7(a), a flux of Rydberg atoms ejected from an oven is directed through a velocity selector toward a high-finesse cavity where the atoms interact resonantly with a single normal mode of the cavity (the interaction with the other modes is off-resonant and thus can be neglected). In the ideal model, the atomic beam is monochromatic (fixed velocity) and the rate of injection $r$ is low enough that the atoms cross the cavity one by one (i.e. there are never two atoms in the cavity at the same time).

We have therefore a CM dynamics with $S$ embodied by the cavity mode and ancillas by the flying atoms. In realistic conditions, atoms can be assumed as non-interacting and initially uncorrelated with each other, hence assumptions (1)–(3) in Section 4.1.1 are all satisfied meaning that the dynamics is described by a basic Markovian CM. For simplicity, we will neglect the cavity loss so that the atomic beam is the only environment driving the cavity open dynamics.

The interaction between the $n$th atom and the cavity mode is well-described by the Jaynes and Cummings (JC) model [59] in which a two-level atom (qubit) with ground state $|0\rangle_n$, excited state $|1\rangle_n$ and energy spacing $\omega_0$ [see Fig. 7(c)]

[24] This is the reason for the name "micromaser", where "maser" is intended as "microwave laser" since the cavity frequency is in the range of microwaves.

couples to a cavity mode of frequency $\omega_c$. On resonance ($\omega_a = \omega_c$), the JC Hamiltonian reads $\hat{H}_{\rm JC} = \hat{H}_S + \hat{H}_n + \hat{V}_n$ with

$$\hat{H}_S = \omega_c \hat{a}^\dagger \hat{a}\,, \qquad \hat{H}_n = \omega_c \hat{\sigma}_{n+}\hat{\sigma}_{n-}\,, \qquad \hat{V}_n = g\left(\hat{a}\hat{\sigma}_{n+} + \hat{a}^\dagger \hat{\sigma}_{n-}\right)\,, \tag{72}$$

where $\hat{a}$ and $\hat{a}^\dagger$ are bosonic annihilation and creation operators of the mode such that $[\hat{a}, \hat{a}^\dagger] = 1$ while (as usual) $\hat{\sigma}_{n-} = \hat{\sigma}_{n+}^\dagger = |0\rangle_n\langle 1|$ are pseudo-spin operators of the $n$th atom.

It is convenient to move to the *interaction picture* with respect to the free Hamiltonian $\hat{H}_0 = \hat{H}_S + \hat{H}_n$. Accordingly, the field and atomic operators are transformed as $\hat{a} \to \hat{a}e^{-i\omega_c t}$, $\hat{\sigma}_{n\pm} \to \hat{\sigma}_{n\pm}e^{\pm i\omega_c t}$ in a way that the coupling Hamiltonian $\hat{V}_n$ is unaffected. We note that expansion (47) trivially holds here simply because the free Hamiltonians of $S$ and $n$ are zero in the interaction picture.

For the sake of argument, let us assume a constant atomic injection rate $r = 1/\Delta t$. Here, $\Delta t$ is the time elapsed between two consecutive injections in terms of which we discretize time as $t_n = n\Delta t$, hence $\Delta t$ embodies the CM time step [see Fig. 7(b)].

It can be shown that the collision unitary at each step [cf. Eq. (2)] takes the form [60]

$$\hat{U}_n = \exp\left[-ig\tau\left(\hat{a}\,\hat{\sigma}_{n+} + \hat{a}^\dagger\hat{\sigma}_{n-}\right)\right] = \hat{\mathcal{C}}|1\rangle_n\langle 1| + \hat{\mathcal{C}}'|0\rangle_n\langle 0| - i(\hat{\mathcal{S}}\hat{a}\,\hat{\sigma}_{n+} + \hat{a}^\dagger\hat{\mathcal{S}}\,\hat{\sigma}_{n-}) \tag{73}$$

where for convenience we defined the nonlinear field operators

$$\hat{\mathcal{C}} = \cos\left(g\tau\sqrt{\hat{n}+1}\right)\,, \qquad \hat{\mathcal{C}}' = \cos\left(g\tau\sqrt{\hat{n}}\right)\,, \qquad \hat{\mathcal{S}} = \frac{\sin\left(g\tau\sqrt{\hat{n}+1}\right)}{\sqrt{\hat{n}+1}}\,. \tag{74}$$

Here, $\tau$ is the time spent by each atom inside the cavity which is generally shorter than the injection time $\Delta t$ [see Fig. 7(b)].

Let the atoms be prepared each in the same incoherent superposition of ground and excited states

$$\eta_n = (1-p)\,|0\rangle_n\langle 0| + p\,|1\rangle_n\langle 1| \tag{75}$$

with $p$ a probability. Then the collision map, which fully describes the cavity open dynamics [cf. Eqs. (6) and (7)], is given by

$$\rho_n = \mathcal{E}[\rho_{n-1}] = {\rm Tr}_n\{\hat{U}_n\,\rho_{n-1}\,\eta\,\hat{U}_n^\dagger\} = (1-p)(\hat{\mathcal{C}}'\rho_{n-1}\,\hat{\mathcal{C}}' + \hat{\mathcal{S}}\,\hat{a}\,\rho_{n-1}\,\hat{a}^\dagger\hat{\mathcal{S}}) + p\,(\hat{\mathcal{C}}\,\rho_{n-1}\,\hat{\mathcal{C}} + \hat{a}^\dagger\hat{\mathcal{S}}\rho_{n-1}\,\hat{\mathcal{S}}\,\hat{a}) \tag{76}$$

with ${\rm Tr}_n$ the trace over the $n$th flying atom.

#### 5.7.1. Master equation of micromaser

We note that, in the interaction picture, $\hat{H}_S = \hat{H}_n = 0$ while $\hat{V}_n$ is just the same as in the Schrödinger picture (thus time-independent).

Using Eq. (72), index $\nu$ in the expansion (60) here takes values $\nu = \pm$ while $\hat{A}_- = \hat{A}_+^\dagger = \hat{a}$, $\hat{B}_- = \hat{B}_+^\dagger = \hat{\sigma}_{n-}$ and $g_\pm = g$. In light of Eq. (65) and given the initial state (75), the only non-zero moments of ancilla (i.e. atomic) operators entering the finite-difference ME (64) are $\langle\hat{0}|\hat{\sigma}_-\hat{\sigma}_+|0\rangle = \langle\hat{1}|\hat{\sigma}_+\hat{\sigma}_-|1\rangle = 1$ (the first-order Hamiltonian $\hat{H}'_S$ is zero since first moments vanish). Taking next the *coarse-grained* continuous-time limit [cf. Eq. (71)], one finds the ME [cf. Eq. (64)]

$$\dot{\rho} = (1-p)\,\Gamma\,\left(\hat{a}\rho\hat{a}^\dagger - \tfrac{1}{2}[\hat{a}^\dagger\hat{a},\rho]\right) + p\,\Gamma\,\left(\hat{a}^\dagger\rho\hat{a} - \tfrac{1}{2}[\hat{a}\hat{a}^\dagger,\rho]\right)\,, \tag{77}$$

where we defined the rate[25] $\Gamma = g^2\frac{\tau^2}{\Delta t}$. For $\tau = \Delta t$, this reduces to the simpler expression $\Gamma = g^2\Delta t$.

Eq. (77) shows that atoms in the excited state $|1\rangle$ act as an incoherent pump (gain) on the cavity mode (corresponding to jump operator $\hat{a}^\dagger$), while atoms in the ground state (jump operator $\hat{a}$) deplete the cavity (loss).

We note that a full micromaser description must account for fluctuations affecting the injection rate and, notably, cavity damping between atomic transits (neglected above). In such a case, we have an interesting example of a quantum system (cavity mode) in contact with *two* baths, namely the atomic beam plus the external environment into which the cavity leaks out. Indeed, the cavity field steady state depends crucially on the balance between gain (due to the atomic pumping) and losses (due to cavity leakage). This leads to an extremely rich physics in the nonlinear strong-coupling regime $g\tau \gg 1$,[26] where trapping states can arise. In general, the micromaser can produce non-classical light.

### 5.8. Continuous-time limit by introducing a diverging coupling strength

As discussed in Section 5.6, the coarse-graining procedure returns a continuous-time ME with $\Delta t$-dependent rates [cf. Eq. (68)], where $\Delta t$ is small but finite.

In some contexts, one may want to define a rigorous mathematical limit $\Delta t \to 0$ yielding a continuous-time ME where any dependence on $\Delta t$ is lost. Clearly, in order for this ME to feature a non-vanishing dissipator $\mathcal{D}_S$ (see final remarks of Section 5.6), the price to pay is introducing $\Delta t$-dependent coupling strength(s) $g_\nu$. These must *diverge* in such a way

[25] To achieve this, a slight generalization of Section 5.1 is required since the injection time $\Delta t$ (time step) here can be generally larger than the collision time $\tau$. This leads to (65) but with rates $\gamma_{\nu\mu}$ redefined as $\gamma_{\nu\mu} = g_\nu g_\mu\,\tau^2/\Delta t$.

[26] In this regime, operators (74) entering $\hat{U}_n$ cannot be approximated as linear as done above.

that rates $\gamma_{\mu\nu}$ (hence $\mathcal{D}_S$) keep finite [cf. Eq. (68)]. Yet, this may still be insufficient to get a well-defined continuous-time limit as illustrated by the next example.

Consider the all-qubit CM (cf. Section 4.6) with $g_z = g$. Using Eq. (18), index $\nu$ in the expansion (60) here takes values $\nu = \pm, z$ while $\hat{A}_- = \hat{A}_+^\dagger = \sigma_-$, $\hat{A}_z = \hat{\sigma}_z$, $\hat{B}_- = \hat{B}_+^\dagger = \hat{\sigma}_{n-}$, $\hat{B}_z = \hat{\sigma}_{nz}$ and $g_\pm = g_z = g$ [cf. Eqs. (64) and (65)]. Since $\eta_n = |0\rangle_n\langle 0|$, the only non-zero moments of ancilla operators entering the finite-difference ME (64) are $\langle 0|\hat{\sigma}_{nz}|0\rangle = -1$ and $\langle \hat{0}|\hat{\sigma}_{n-}\hat{\sigma}_{n+}|0\rangle = 1$. Hence, the first-order Hamiltonian and dissipator [cf. Eq. (65)] explicitly read

$$\hat{H}'_S = -g\,\hat{\sigma}_z\,, \quad \mathcal{D}_S[\rho_n] = \gamma\left(\hat{\sigma}_-\,\rho_{n-1}\,\hat{\sigma}_+ - \tfrac{1}{2}[\hat{\sigma}_+\hat{\sigma}_-,\rho_{n-1}]_+\right) + \gamma\left(\hat{\sigma}_z\,\rho_{n-1}\,\hat{\sigma}_z - \rho_{n-1}\right)\,, \tag{78}$$

where we set [cf. Eq. (68)]

$$\gamma = g^2\Delta t\,. \tag{79}$$

In order for the dissipator to survive the $\Delta t \to 0$ limit one can define a diverging coupling strength as

$$g = \sqrt{\frac{\gamma}{\Delta t}} \quad \text{(diverging coupling strength)}\,. \tag{80}$$

Such a scaling $\sim 1/\sqrt{\Delta t}$ of the coupling rate is a distinctive feature of many quantum CMs.

However, while Eq. (80) fixes the issue of the vanishing dissipator, it has a potential drawback. Indeed, as the coupling strength is also the characteristic rate of the 1st-order Hamiltonian $\hat{H}'_S$ [cf. Eq. (78)], its divergence may cause $\hat{H}'_S$ to diverge as well for $\Delta t \to 0$.

Thereby, in general, in cases such as the present instance the introduction of a diverging coupling strength does not allow to perform a well-defined continuous-time limit fulfilling the double constraint that the dissipator *and* $\hat{H}'_S$ must remain finite. Whether or not such a problem arises depends on the system–ancilla coupling Hamiltonian $\hat{V}_n$ as well as the initial ancilla's state. For instance, if in the considered example we set $g_z = 0$ and $g = \sqrt{\gamma/\Delta t}$ [cf. Eq. (18)] then of course $\hat{H}'_S = 0$ for any $\Delta t$. Thus, in the limit $\Delta t \to 0$, the finite-difference Eq. (64) is turned into the well-defined continuous-time Lindblad ME

$$\dot{\rho} = \gamma\left(\hat{\sigma}_-\,\rho\,\hat{\sigma}_+ - \tfrac{1}{2}\,[\hat{\sigma}_+\hat{\sigma}_-,\rho]_+\right)\,, \tag{81}$$

which is identical to the well-known ME describing *spontaneous emission* of a two-level atom.[27] This is not accidental: in Section 9, we will show that the all-qubit CM with the diverging coupling strength (80) (leading to this ME) can be directly derived from a microscopic atom-field model (see in particular Section 9.7 discussing the field vacuum state).

#### 5.8.1. $\Delta t$-dependent ancilla state

As anticipated, however, also the initial state of ancillas matters. For instance, considering the above example for $g = \sqrt{\gamma/\Delta t}$ and $g_z = 0$ but with the ancillas now initially in $\eta_n = |+\rangle_n\langle +|$ will result again (for $\Delta t \to 0$) in a diverging Hamiltonian in this case given by $\hat{H}'_S = \sqrt{\gamma/\Delta t}\,\hat{\sigma}_x$.

It is natural to ask whether ensuring that $\hat{H}'_S = 0$ is the only way for $\hat{H}'_S$ not to diverge (for $\Delta t \to 0$) due to (80). We show next that both $\hat{H}'_S$ and the dissipator can remain finite if one allows for the ancilla's state itself to depend on $\Delta t$. As a representative example in the all-qubit CM, consider the initial ancilla's state $\eta_n = |\chi\rangle_n\langle\chi|$ with

$$|\chi\rangle_n = \frac{1}{1+|\alpha_n|^2\Delta t}\left(|0\rangle_n + \alpha_n\sqrt{\Delta t}\,|1\rangle_n\right)\,, \tag{82}$$

where $\alpha_n$ is generally complex. Setting again $g = \sqrt{\gamma/\Delta t}$ and $g_z = 0$, the only non-zero ancilla moments [cf. Eq. (61)] in this case are $\langle\hat{\sigma}_{n-}\rangle = \langle\hat{\sigma}_{n+}\rangle^* = \alpha_n\sqrt{\Delta t}$ and $\langle\hat{\sigma}_{n-}\hat{\sigma}_{n+}\rangle = 1$, where we neglected terms of order $\Delta t$ or higher. These entail the 1st-order Hamiltonian and dissipator

$$\hat{H}'_S = g\,(\alpha_n\hat{\sigma}_- + \alpha_n^*\hat{\sigma}_+)\,, \quad \mathcal{D}_S[\rho_n] = \gamma\left(\hat{\sigma}_-\,\rho_{n-1}\,\hat{\sigma}_+ - \tfrac{1}{2}[\hat{\sigma}_+\hat{\sigma}_-,\rho_{n-1}]_+\right)\,. \tag{83}$$

Neither $\hat{H}'_S$ nor $\mathcal{D}_S$ depends on $\Delta t$, hence both remain finite for $\Delta t \to 0$. This happens because the $\sqrt{\Delta t}$ on the denominator of the coupling strength is canceled by that coming from the initial state with the latter not affecting the dissipator to leading order.

In the case $\alpha_n = A\,e^{-i\omega_L t_n}$ with $A > 0$, by taking the continuous-time limit of (83) we get the ME

$$\dot{\rho} = -i\left[g\,A\,(e^{-i\omega_L t}\hat{\sigma}_- + e^{i\omega_L t}\hat{\sigma}_+),\rho\right] + \gamma\left(\hat{\sigma}_-\,\rho\,\hat{\sigma}_+ - \tfrac{1}{2}\,[\hat{\sigma}_+\hat{\sigma}_-,\rho]_+\right)\,. \tag{84}$$

This generalizes (81) to the case where a driving Hamiltonian is added. This ME is equivalent to the well-known optical Bloch equations describing the evolution of an atom driven by a classical oscillating field while undergoing spontaneous emission at the same time [61].

[27] Indeed, it is easily checked that, if $p = 1$ and $c = 0$ [cf. Eq. (29)], then Eq. (81) entails $p(t) = e^{-\gamma t}$, $c(t) = 0$ namely the (initially excited) atom decays to the ground state with emission rate $\gamma$.

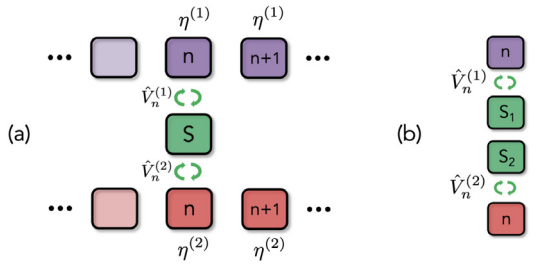


**Fig. 8.** *Collision model with two baths of ancillas.* (a): System $S$ collides with two baths of ancillas, labeled with 1 and 2. This CM can be formally seen as basic CM [see Fig. 3] where each ancilla is bipartite and initially in state $\eta^{(1)}\otimes\eta^{(2)}+\chi^{(\mathrm{corr})}$ (in the panel $\chi^{(\mathrm{corr})}=0$). (b): Same as (a) except that now system $S$ is itself bipartite, comprising subsystems $S_1$ and $S_2$. Collisions with ancillas of bath $i$ involve only subsystem $S_i$.

The assumption that we made of having a $\Delta t$-dependent ancilla state may appear somewhat artificial. In Section 9, we will show in detail that state (82) arises from an initial *coherent* state of the electromagnetic field.

Before concluding the discussion on the continuous-time limit, it is worth noting that a diverging coupling strength [cf. Eq. (80)] allows the condition underlying expansion (47) (i.e. $\hat{H}_S$, $\hat{H}_n$ much weaker than $\hat{V}_n$) to be satisfied for $\Delta t$ short enough.

In the following subsections, we will consider equations of motion for two important collisional dynamics: multiple baths and cascaded CMs.

### 5.9. Multiple baths

In many realistic problems, the open system is in contact with many baths at once. Accordingly, it is useful to define CMs where $S$ collides with $M\geq 1$ baths of ancillas, as shown in Fig. 8(a) for the case of two baths ($M=2$). At each step, $S$ collides with $M$ ancillas, one for each bath $i=1,\ldots,M$. To make contact with previous theory, it is convenient to view the CM as featuring a single bath of $M$-*partite* ancillas, each initially in state

$$\eta_n=\eta_n^{(1)}\otimes\eta_n^{(2)}\otimes\cdots\otimes\eta_n^{(M)}+\chi_n^{(\mathrm{corr})}\,. \tag{85}$$

Here, $\eta_n^{(i)}$ is the reduced state of ancilla of bath $i=1,\ldots,M$. Note we allowed ancillas of different baths to share initial correlations described by term $\chi_n^{(\mathrm{corr})}$. Thus when the $M$ baths are uncorrelated, $\chi_n^{(\mathrm{corr})}=0$. The interaction Hamiltonian reads

$$\hat{V}_n=\hat{V}_n^{(1)}+\hat{V}_n^{(2)}+\cdots+\hat{V}_n^{(M)}\quad\text{with}\quad\hat{V}_n^{(i)}=\sum_\nu g_{\nu i}\hat{A}_{\nu i}\hat{B}_{\nu i}\,, \tag{86}$$

where as usual we expanded each $\hat{V}_n^{(i)}$ (coupling Hamiltonian between $S$ and an ancilla of bath $i$) in the form (60). Here, $\hat{B}_{\nu i}$ is an operator acting on the ancilla of bath $i$ while $\hat{A}_{\nu i}$ is an operator of $S$ which we allow to be generally $i$-dependent. Note that $\hat{V}_n$ can be written as

$$\hat{V}_n=\sum_{i,\nu}g_{\nu i}\hat{A}_{\nu i}\hat{B}_{\nu i}\,. \tag{87}$$

This is still of the form (60) with the role of index $\nu$ now embodied by the double index $(\nu,i)$, hence all the theory in Sections 5.4 and 5.5 applies with the replacements $\nu\to(\nu,i)$, $\mu\to(\mu,j)$.

For *uncorrelated* baths, i.e. $\chi_n^{(\mathrm{corr})}=0$ [cf. Eq. (85)], all crossed second moments of the bath factorize as

$$\langle\hat{B}_{\mu j}\hat{B}_{\nu i}\rangle=\langle\hat{B}_{\mu j}\rangle\langle\hat{B}_{\nu i}\rangle\qquad\text{for }\ i\neq j \tag{88}$$

with $\langle\hat{B}_{\nu i}\rangle=\mathrm{Tr}_i\{\hat{B}_{\nu i}\eta_i\}$. This implies that when all the first moments vanish, i.e. $\langle\hat{B}_{\nu i}\rangle=0$ for any $\mu$ and $i$, so do all the crossed second moments. In this case, based on Eqs. (64) and (65), we get that

$$\frac{\Delta\rho_n}{\Delta t}=\sum_{i=1}^{M}\mathcal{D}_S^{(i)}[\rho_{n-1}] \tag{89}$$

with $\mathcal{D}_S^{(i)}$ the dissipator that would arise if $S$ were in contact only with bath $i$. We can thus say that the dissipative effects of uncorrelated baths are *additive*. We point out that this holds as well (for $\Delta t$ short enough) when $\langle\hat{B}_{\nu i}\rangle\propto\sqrt{\Delta t}$ since in such a case (88) can be neglected. This can happen with states like (82) as we discussed in Section 5.8.

For *correlated* baths, namely $\chi^{(\mathrm{corr})}\neq 0$ [cf. Eq. (85)], crossed second moments are generally non-zero. An interesting consequence of this occurs when $S$ itself is made out of $M$ subsystems $S_1,\ldots,S_M$ such that the collisions with ancillas of

the $i$th bath involve only subsystem $S_i$ [see Fig. 8(b)]. In this case, therefore, operator $\hat{A}_{\nu i}$ in Eq. (87) acts only on $S_i$. Then, based on (65), we see that the dissipator entering the ME will in particular contain terms of the form

$$\propto \langle \hat{B}_{\mu j}\hat{B}_{\nu i}\rangle(\hat{A}_{\nu i}\rho_{n-1}\hat{A}_{\mu j} - \tfrac{1}{2}[\hat{A}_{\mu j}\hat{A}_{\nu i},\rho_{n-1}]_+) \quad \text{for } i\neq j\,. \tag{90}$$

These represent incoherent interactions between subsystems $S_i$ and $S_j$ mediated by the baths. Thus, correlations between the baths enable the establishment of correlations between the subsystems of $S$ even if these are not directly coupled.

### 5.10. Cascaded master equation

As another important instance, we next derive the ME of the cascaded CM of Section 4.8. Recall that the collision unitary is given by [cf. Eq. (37)] $\hat{U}_n = \hat{U}_{2,n}\hat{U}_{1,n}$ with $\hat{U}_{j,n}$ describing the sub-collision with subsystem $S_j$ (see Fig. 4). Equivalently, one can think of a single collision with a *time-dependent* interaction that reads

$$\hat{V}_n(t) = \begin{cases} \hat{V}_{1,n} & t\in[t_{n-1},\, t_{n-1}+\Delta t/2[ \\ \hat{V}_{2,n} & t\in[t_{n-1}+\Delta t/2,\, t_n[ \end{cases}\,. \tag{91}$$

with $\hat{V}_{j,n}$ the interaction Hamiltonian between $n$ and $S_j$ such that $\hat{U}_{j,n} = e^{-i\hat{V}_{j,n}\frac{\Delta t}{2}}$. Thus $\hat{V}_n$ suddenly switches from $\hat{V}_{1n}$ to $\hat{V}_{2n}$ after the first subcollision.

The framework that we developed previously (in particular Sections 5.1 and 5.4) holds for a time-independent $\hat{V}_n$, hence it cannot be directly applied for deriving the ME. We thus start over by expanding each subcollision unitary $\hat{U}_{jn}$ to the second order in $\Delta t/2$, eventually discarding terms of order higher than $\sim \Delta t^2$. This yields the overall collision unitary

$$\hat{U}_n = \hat{U}_{2n}\hat{U}_{1n} \simeq \hat{\mathbb{I}} - i(\hat{V}_{1n}+\hat{V}_{2n})\,\Delta t' - (\tfrac{1}{2}\hat{V}_{1n}^2 + \tfrac{1}{2}\hat{V}_{2n}^2 + \hat{V}_{2n}\hat{V}_{1n})\,\Delta t'^2 \quad \text{with } \Delta t' = \tfrac{\Delta t}{2}. \tag{92}$$

Note that this is not invariant under the swap $1\leftrightarrow 2$, which is due to the intrinsic CM unidirectionality discussed in Section 4.8. To gain a better physical insight, we note that (92) can be equivalently arranged as

$$\hat{U}_n \simeq \hat{\mathbb{I}} - i(\hat{V}_{1n}+\hat{V}_{2n}+\hat{\mathcal{H}}_{Sn})\,\Delta t' - \tfrac{1}{2}(\hat{V}_{1n}+\hat{V}_{2n})^2\,\Delta t'^2 \quad \text{with } \hat{\mathcal{H}}_{Sn} = i\tfrac{\Delta t'}{2}\left[\hat{V}_{1n},\hat{V}_{2n}\right]. \tag{93}$$

Now observe that, if each ancilla collided with $S_1$ and $S_2$ *at once* during the time $\Delta t'$, then one would get the usual collision unitary (47) (for $\Delta t \to \Delta t'$) with the natural replacement $\hat{V}_n \to \hat{V}_{1n}+\hat{V}_{2n}$. This matches all the terms in (93) but the *unitary* contribution coming from the effective Hamiltonian $\hat{\mathcal{H}}_{Sn}$. Hence, the intrinsic system's unidirectionality, due to the fact that ancillas collide *first* with $S_1$ and *then* with $S_2$, is fully condensed in the appearance of the effective Hamiltonian $\hat{\mathcal{H}}_{Sn}$.[28] To work out the ensuing ME of $S$, let us expand $\hat{V}_{j,n}$ as $\hat{V}_{j,n} = \sum_\nu g_\nu \hat{A}_{j\nu}\hat{B}_\nu$ [cf. Eq. (60)]. Plugging this into (93) and proceeding analogously to Sections 5.1 and 5.4, we get the discrete ME

$$\frac{\Delta\rho_n}{\Delta t} = -i[\hat{H}'_S + \hat{H}''_S,\rho_{n-1}] + \mathcal{D}_S[\rho_{n-1}] \tag{94}$$

with

$$\hat{H}'_S = \sum_\nu g'_\nu\langle\hat{B}_\nu\rangle\hat{A}_\nu\,,\quad \hat{H}''_S = \mathrm{Tr}_n\{\hat{\mathcal{H}}_{Sn}\eta_n\} = i\tfrac{\Delta t}{2}\sum_{\nu\mu} g'_\nu g'_\mu\left\langle[\hat{B}_\nu,\hat{B}_\mu]\right\rangle\hat{A}_{2\mu}\hat{A}_{1\nu}\,, \tag{95}$$

$$\mathcal{D}_S[\rho_{n-1}] = \sum_{\nu\mu}\gamma_{\nu\mu}\langle\hat{B}_\mu\hat{B}_\nu\rangle\left(\hat{A}_\nu\rho_{n-1}\hat{A}_\mu - \tfrac{1}{2}\left[\hat{A}_\mu\hat{A}_\nu,\rho_{n-1}\right]_+\right) \quad \text{with } \gamma_{\nu\mu} = g'_\nu g'_\mu\,\Delta t\,, \tag{96}$$

where we set $g'_\nu = g_\nu/2$ and defined the collective operators $\hat{A}_\nu = \hat{A}_{1\nu}+\hat{A}_{2\nu}$. Here, $\hat{H}'_S$ and $\mathcal{D}_S$ have the same form as Eq. (65) with $\hat{A}_\nu$ now intended as collective operators. Notably, the second-order Hamiltonian $\hat{\mathcal{H}}_{Sn}$ upon partial trace results in an effective *coherent* coupling between $S_1$ and $S_2$ (mediated by the ancillas) described by Hamiltonian $\hat{H}''_S$. We point out that this is an effective *second-order* Hamiltonian of $S$, in contrast to $\hat{H}'_S$ [this being the analogue of the Hamiltonian in Eq. (65)], which in particular explains the notation we adopted.

As a significant example, let each ancilla be a qubit initially in state $|0\rangle_n$ with $\hat{V}_{j,n}$ of the form

$$\hat{V}_{j,n} = \sqrt{\tfrac{2\gamma}{\Delta t}}\left(\hat{A}_j\,\hat{\sigma}_{n+} + \hat{A}_j^\dagger\,\hat{\sigma}_{n-}\right). \tag{97}$$

Then the only non-vanishing ancilla moments entering the ME are $\langle\hat{\sigma}_{n-}\hat{\sigma}_{n+}\rangle = 1$. This yields

$$\hat{H}'_S = 0\,,\quad \hat{H}''_S = \tfrac{\gamma}{2}(i\hat{A}_2\hat{A}_1^\dagger - i\hat{A}_1\hat{A}_2^\dagger)\,,\quad \mathcal{D}_S[\rho_{n-1}] = \gamma\left(\hat{A}\,\rho_{n-1}\,\hat{A}^\dagger - \tfrac{1}{2}\,[\hat{A}^\dagger\hat{A},\rho_{n-1}]_+\right) \tag{98}$$

with $\hat{A} = \hat{A}_1+\hat{A}_2$, hence in the CTL we end up with the ME

$$\dot{\rho} = -i\left[\tfrac{\gamma}{2}(i\hat{A}_2\hat{A}_1^\dagger - i\hat{A}_1\hat{A}_2^\dagger),\rho\right] + \gamma\left(\hat{A}\,\rho\,\hat{A}^\dagger - \tfrac{1}{2}\left[\hat{A}^\dagger\hat{A},\rho\right]_+\right). \tag{99}$$

[28] Note that this is indeed the only term in (93) which is not invariant under the exchange $S_1\leftrightarrow S_2$. Instead, it transforms as $\hat{\mathcal{H}}_{Sn}\to-\hat{\mathcal{H}}_{Sn}$

### 5.11. Equations of motion: state of the art

Explicit derivations of the Lindblad master equation through the continuous-time limit of a CM were given in Ref. [24,62]. See also Ref. [63] by the same authors of Ref. [62], which includes a general characterization of decoherence channels of a qubit and their implementation via suitably defined CMs.

The dynamics most intuitively associated with a CM is arguably the dissipative interaction of a system with a dilute *gas* of particles (ancillas). In such a case, the time between two next system–ancilla collisions is random, at variance with the assumption of time-periodic collisions (one for each $\Delta t$) made in our discussion. Yet, as shown in Ref. [64], a Lindblad ME can be worked out in this case as well even with strong collisions,[29] the associated rate $\gamma$ (entering the dissipator) being now the number of collisions per unit time (similar CM and ME appeared in Ref. [65]). Note that, if the gas particles are quantum then a CM description relies on approximating their motion as semiclassical. Ref. [66] showed that this is equivalent to the low-density, fast-particle limit of a fully quantum treatment.

The *micromaser* theory (cf. Section 5.7) was first introduced by Javanainen and Meystre [18–20]. Works that use explicitly the CM approach in particular for deriving the cavity field's master equation are e.g. Refs. [67,68]. An introduction to micromaser can be found in the textbook by Meystre and Sargent [61]. See also Ref. [60], which includes the master equation. Basics of cavity QED and JC model, which we referred to in Section 5.7, can be found e.g. in the textbook by Haroche [59]. Issues closely related to the continuous-time limit via diverging coupling strength (see Section 5.8) were carefully investigated in Refs. [36,69] (see also a previous paper by Milburn [70]). Particular attention was given to the regime of ultra-short collision times yielding a unitary dynamics (as we discussed). This paradigm of unitary CM was proposed to carry out indirect quantum control [71] and universal two-qubit quantum gates in spintronics systems [72].

Cascaded master equations like (99) were independently introduced in 1993 by Carmichael [73] and Gardiner [74] using the input–output formalism [61]. They were later derived through a CM in Refs. [54,55] (introducing an internal bath dynamics as well) although with a treatment somewhat different than the one in Section 5.10. Note that, for the sake of argument, we considered only a bipartite system $S$. The generalization to more than two subsystems is straightforward, leading to an interesting many-body Hamiltonian $\hat{H}''_S$. Multipartite cascaded CMs can be advantageously applied to work out MEs of complex cascaded networks where interference effects can occur [75,76]. From a more general perspective, cascaded systems are currently receiving large attention in quantum optics also due to recent experimental realizations of chiral emission (e.g. in photonic crystals or fibers) [77].

## 6. Quantum trajectories

The possibility of interpreting the Lindblad master equation as the result of an ensemble average of different stochastic quantum trajectories, each corresponding to a particular sequence of measurement outcomes on the environment, is a pillar of open quantum systems dynamics with important applications in various fields such as quantum optics and quantum transport [7,10,11,59,78].

Quantum trajectories emerge very naturally from a CM as soon as one imagines to measure each ancilla right after its collision with $S$. This and related concepts are the subject of the present section.

### 6.1. Collision model unraveling

Let us come back to the basic CM in Section 4.1 and assume for the sake or argument that $S$ and ancillas are initially in the pure states $|\psi_0\rangle$ and $\{|\chi_n\rangle\}$, respectively (thus $\eta_n = |\chi_n\rangle\langle\chi_n|$). Accordingly, the initial joint state is $\sigma_0 = |\Psi_0\rangle\langle\Psi_0|$ with $|\Psi_0\rangle = |\psi_0\rangle \otimes_n |\chi_n\rangle$.[30] At step $n$, this is turned into

$$|\Psi_n\rangle = \hat{U}_n \cdots \hat{U}_1 |\psi_0\rangle|\chi_1\rangle \cdots |\chi_n\rangle \,. \tag{100}$$

Let now $\{|k_n\rangle\}$ be a single-ancilla orthonormal basis. Using the basis completeness, Eq. (100) can be equivalently arranged by putting $\sum_{k_m} |k_m\rangle\langle k_m|$ in front of each collision unitary $\hat{U}_m$ as

$$\begin{aligned} |\Psi_n\rangle &= \left(\sum_{k_n} |k_n\rangle\langle k_n|\right) \hat{U}_n \left(\sum_{k_{n-1}} |k_{n-1}\rangle\langle k_{n-1}|\right) \hat{U}_{n-1} \ \ldots \left(\sum_{k_1} |k_1\rangle\langle k_1|\right) \hat{U}_1 |\psi_0\rangle|\chi_1\rangle \cdots |\chi_n\rangle \\ &= \sum_{k_n} \sum_{k_{n-1}} \cdots \sum_{k_1} \left(|k_n\rangle\langle k_n|\hat{U}_n\right) \left(|k_{n-1}\rangle\langle k_{n-1}|\hat{U}_{n-1}\right) \ldots \left(|k_1\rangle\langle k_1|\hat{U}_1\right) |\psi_0\rangle|\chi_1\rangle \cdots |\chi_n\rangle \,. \end{aligned} \tag{101}$$

[29] For a strong collision, the collision unitary $\hat{U}_n$ cannot be approximated to the lowest orders.

[30] In the present section, we use a compact notation such that $|\chi_n\rangle = |\chi_n\rangle_n$ (and similarly for bras). This convention simplifies the formalism without affecting clarity.

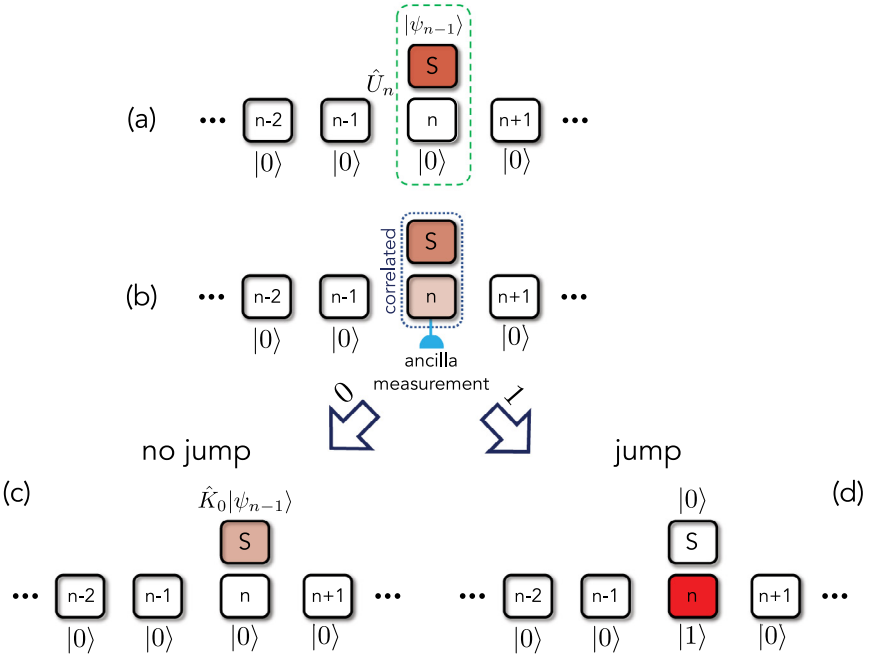


**Fig. 9.** *Quantum trajectories in the all-qubit collision model.* Like the basic CM of Fig. 3, ancillas are prepared in $\otimes_n|0_n\rangle$ (thus uncorrelated) and $S$, initially in state $|+\rangle$, collides with each sequentially. After the collision [shown in panel (a)], the ancilla gets correlated with $S$ and (prior to the next collision) is measured in the basis $\{|0_n\rangle, |1_n\rangle\}$ (b). If outcome 0 is recorded (c) no jump takes place and the state of $S$ is only slightly affected. Instead, if outcome 1 is recorded (d) then $S$ abruptly jumps to state $|0\rangle$. Note that, in either case, the ancilla is eventually uncorrelated with $S$, this being left in a pure state. We assumed that ancillas from 1 to $n-1$ were all measured in $|0\rangle$.

Each ancilla state $|\chi_m\rangle$ can now be moved to the left and placed to the immediate right of the corresponding unitary $\hat{U}_m$, while kets $|k_1\rangle, \ldots, |k_n\rangle$ can be moved to the right of $|\psi_0\rangle$. This allows to arrange $|\Psi_n\rangle$ as

$$|\Psi_n\rangle = \sum_{k_n}\sum_{k_{n-1}}\cdots\sum_{k_1} \langle k_n|\hat{U}_n|\chi_n\rangle\,\langle k_{n-1}|\hat{U}_{n-1}|\chi_{n-1}\rangle\,\ldots\,\langle k_1|\hat{U}_1|\chi_1\rangle\;|\psi_0\rangle\,|k_1\rangle\cdots|k_n\rangle\,. \tag{102}$$

Each sandwich on the left of $|\psi_0\rangle$ is effectively an operator on $S$

$$\hat{K}_{k_m} = \langle k_m|\hat{U}_m|\chi_m\rangle\,, \tag{103}$$

in terms of which (102) is compactly expressed as

$$|\Psi_n\rangle = \sum_{k_n}\sum_{k_{n-1}}\cdots\sum_{k_1} \left(\hat{K}_{k_n}\cdots\hat{K}_{k_1}|\psi_0\rangle\right)\,|k_1\rangle\cdots|k_n\rangle\,. \tag{104}$$

Note that operators (103) are generally non-unitary. Thereby, the state of $S$ between brackets $(\ldots)$ is not normalized. We thus rearrange (104) in the equivalent form

$$|\Psi_n\rangle = \sum_{k_n}\sum_{k_{n-1}}\cdots\sum_{k_1} \sqrt{p_{k_1\cdots k_n}}\;\left(\frac{\hat{K}_{k_n}\cdots\hat{K}_{k_1}|\psi_0\rangle}{\sqrt{p_{k_1\cdots k_n}}}\right)\,|k_1\rangle\cdots|k_n\rangle\,. \tag{105}$$

with

$$p_{k_1\cdots k_n} = \|\,\hat{K}_{k_n}\cdots\hat{K}_{k_1}|\psi_0\rangle\|^2 = \langle\psi_0|\hat{K}_{k_1}^\dagger\cdots\hat{K}_{k_n}^\dagger\,\hat{K}_{k_n}\cdots\hat{K}_{k_1}|\psi_0\rangle\;, \tag{106}$$

where $\sum_{k_n}\cdots\sum_{k_1}\,p_{k_1\cdots k_n} = 1$. Here, we used that Eq. (103) defines a set of Kraus operators (see Appendix C) which thus fulfill $\sum_{k_m}\hat{K}_{k_m}^\dagger\hat{K}_{k_m} = \mathbb{I}$.

The above shows that the CM dynamics can be seen as an average over a (very large) ensemble of "histories" that result from projective measurements on the ancillas.

Right after colliding with $S$ [see Fig. 9(a)], each ancilla is measured in the basis $\{|k_m\rangle\}$ [cf. Eq. (101)] and the measurement outcome recorded, as sketched in Fig. 9(b). If this takes the specific value $k_m$, then operator $\hat{K}_{k_m}$ is applied on $S$. A *specific* sequence of measurements results $\{k_1, \ldots, k_n\}$ thus determines a particular history (realization), at the end of which $S$ is in state $\hat{K}_{k_n}\cdots\hat{K}_{k_1}|\psi_0\rangle$ (up to a normalization factor), this history occurring with probability $p_{k_1\cdots k_n}$. Remarkably, in each history, the state of $S$ remains pure at each step.

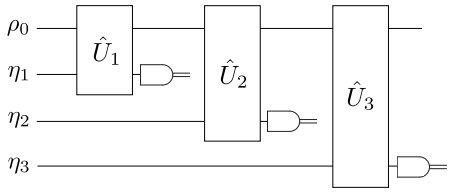


**Fig. 10.** *Quantum circuit representation of a CM conditional dynamics.* Compared to a basic CM (unconditional) dynamics [see Fig. 3(c)], each ancilla undergoes a projective measurement right after it collided with $S$. The double wire indicates that the measurement outcome can be encoded as classical information [21]. The usual CM (unconditional) dynamics can be equivalently seen as an ensemble average over all possible conditional evolutions, each corresponding to a possible sequence of measurement outcomes.

Note that the dynamics of histories does depend on the measurement basis $\{|k_m\rangle\}$. Different choices of this basis will result in different *unravelings* of the same average dynamics (using a common jargon). What we called histories so far usually go under the name of *quantum trajectories*. The way the system evolves in a specific quantum trajectory is said *conditional dynamics*: which Kraus operator (103) is to be applied on $S$ at each step is conditioned to the specific outcome of the measurement on the ancilla (recall that in quantum mechanics measurement is an intrinsically *stochastic* process). A quantum circuit representation of the conditional CM dynamics is shown in Fig. 10.

### 6.2. POVM and weak measurements

The above framework, when the interaction of $S$ with each ancilla is very weak, in fact defines the concept of *weak measurements* in quantum mechanics.

Introductory textbooks to quantum mechanics usually describe measurements on a quantum system in terms of an orthonormal basis $\{|k\rangle\}$, each being the eigenstate of a certain observable with associated eigenvalue $k$ (assume for now that these are non-degenerate). According to the wavefunction collapse axiom, a measurement with outcome $k$ projects $S$ (initially in state $|\psi\rangle$) in the eigenstate $|k\rangle$ with probability $p_k = |\langle k|\psi\rangle|^2$. In the density–matrix language, this is expressed (and generalized at the same time) by saying that the act of measurement forces the state of $S$ to transform as

$$\rho \to \frac{\hat{\Pi}_k \rho \hat{\Pi}_k}{p_k} \quad \text{with} \quad \sum_k \hat{\Pi}_k = \mathbb{I}\,, \tag{107}$$

whose associated probability is given by

$$p_k = \mathrm{Tr}_S\{\hat{\Pi}_k \rho\}\,. \tag{108}$$

Here, $\hat{\Pi}_k$ is the projector onto the eigenspace of eigenvalue $k$.[31] The $\hat{\Pi}_k$'s are a set of *orthogonal* projectors, i.e. $\hat{\Pi}_k \hat{\Pi}_{k'} = \delta_{k,k'} \hat{\Pi}_k$. Measurements of this kind are called Von Neumann measurements.

One can now define a generalized quantum measurement as

$$\rho \to \frac{\hat{K}_k \rho \hat{K}_k^\dagger}{p_k} \quad \text{with} \quad \sum_k \hat{\Pi}_k = \mathbb{I}\,, \quad \text{where} \quad \hat{\Pi}_k = \hat{K}_k^\dagger \hat{K}_k\,, \tag{109}$$

the associated probability being $p_k = \mathrm{Tr}_S\{\hat{\Pi}_k \rho\}$. Here, the $\hat{\Pi}_k$'s are a set of positive operators (due to the constraint $p_k \geq 0$), which are not constrained to be orthogonal (at variance with Von Neumann measurements discussed before). Such a generalized quantum measure is usually referred to as *positive operator-valued measure* (POVM).

Upon comparison of (109) with the framework discussed in the last section, it should be clear that measuring each ancilla after the collision effectively performs a sequence of POVMs on $S$, one at each step. In this sense, the collisional dynamics is like continuously "watching" the system. More specifically, when the system–ancilla coupling is weak [as we assumed in Section 5, cf. Eq. (47)] one talks about *weak measurements*. The essential idea is that, instead of abruptly interrupting the dynamics through an instantaneous Von-Neumann measurement, one performs a gentle measurement that is yet diluted in time. Nevertheless, occasionally, this may still result in sudden changes of state (quantum jumps), as shown in the next section.

### 6.3. Quantum trajectories in the all-qubit collision model and quantum jumps

To illustrate the framework in a concrete case, consider the (by now usual) all-qubit model of Section 4.6 for $g_z = 0$ and $g = \sqrt{\gamma/\Delta t}$. There, we had already computed the Kraus operators (103) in the ancilla basis $\{|0_n\rangle, |1_n\rangle\}$ [see Eq. (28)].

[31] If $k$ is non-degenerate, $\hat{P}_k = |k\rangle\langle k|$. Also, note that the expression of $p_k$ was obtained from $\mathrm{Tr}\{\hat{\Pi}_k \rho \hat{\Pi}_k\}$ by using the cyclic property of trace and $\hat{\Pi}_k^2 = \hat{\Pi}_k$ (as $\hat{\Pi}_k$ is a projector).

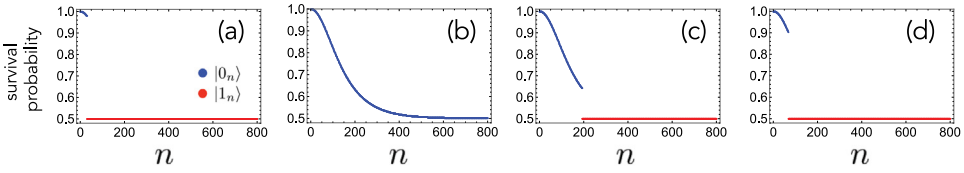


**Fig. 11.** Four sampled quantum trajectories in the all-qubit collision model of Section 4.6 for $g_z = 0$ and $g = \sqrt{\gamma/\Delta t}$ [cf. Eq. (18)] when $S$ starts in state $|+\rangle_S$ and ancillas are all prepared in $|0_n\rangle$, each being measured in the basis $\{|0_n\rangle, |1_n\rangle\}$ right after the collision with $S$. We plot the survival probability $|\langle+|\psi_n\rangle|^2$ against the step number $n$, where each blue (red) dot stands for the measurement outcome $|0_n\rangle$ ($|1_n\rangle$). In each case, the survival probability tends to $|\langle+|0\rangle|^2 = 1/2$ witnessing that $S$ eventually converges to $|0\rangle$. Throughout we set $g\Delta t = \sqrt{\gamma\Delta t} = 0.2$. The plots were obtained through a simple Monte Carlo simulation, where probabilities (112) are updated at each step and used to randomly select a measurement outcome and hence the corresponding state in Eq. (113). No jump occurs in trajectory (b), which exhibits a smooth exponential decay.

Assume that, right before a collision, qubit $S$ is in a superposition state $|\psi\rangle = c_0|0\rangle + c_1|1\rangle$ with $|c_0|^2 + |c_1|^2 = 1$ (we omit the step index $n$ for a while). The collision with ancilla $n$ and a subsequent measurement on $n$ in the basis $\{|0_n\rangle, |1_n\rangle\}$ with outcome $|0_n\rangle$ projects $S$ into the (unnormalized) state

$$\hat{K}_0|\psi\rangle = \left(|0\rangle\langle 0| + \cos\sqrt{\gamma\Delta t}\,|1\rangle\langle 1|\right)|\psi\rangle = c_0|0\rangle + \cos\sqrt{\gamma\Delta t}\;c_1|1\rangle\,, \tag{110}$$

and, if the measurement outcome is $|1_n\rangle$, into the (unnormalized) state

$$\hat{K}_1|\psi\rangle = \left(-i\,\sin\sqrt{\gamma\Delta t}\,|0\rangle\langle 1|\right)|\psi\rangle = -i\,\sin\sqrt{\gamma\Delta t}\;c_1|0\rangle\;. \tag{111}$$

These outcomes occur with probabilities $p_k = \langle\psi|\hat{K}_k^\dagger\hat{K}_k|\psi\rangle$, which are explicitly worked out as

$$p_0 = |c_0|^2 + \cos^2\sqrt{\gamma\Delta t}\;|c_1|^2\,, \quad p_1 = \sin^2\sqrt{\gamma\Delta t}\;|c_1|^2 \tag{112}$$

(note that we correctly get $p_0 + p_1 = 1$). Accordingly, the normalized version of (110) and (111) reads

$$\frac{\hat{K}_0|\psi\rangle}{\|\hat{K}_0|\psi\rangle\|} = \frac{c_0|0\rangle + \cos\sqrt{\gamma\Delta t}\,c_1|1\rangle}{\sqrt{p_0}}\,, \quad \frac{\hat{K}_1|\psi\rangle}{\|\hat{K}_1|\psi\rangle\|} = \frac{-i\,\sin\sqrt{\gamma\Delta t}\,c_1|0\rangle}{\sqrt{p_1}} \equiv |0\rangle \tag{113}$$

up to an irrelevant phase factor in the last identity. Thus both $\hat{K}_0$ and $\hat{K}_1$ have the effect of enhancing the $|0\rangle$'s component of $|\psi\rangle$. This entails that $|\psi_n\rangle$ asymptotically converges to $|0\rangle$. Therefore, we get that $S$ eventually ends up in $|0\rangle_S$ (cf. Section 4.7) even along single trajectories.

Eqs. (112) and (113) can be used to simulate quantum trajectories through a random number generator. Some samples are shown in Fig. 11, where we plot the survival probability $\langle+|\psi_n\rangle\langle\psi_n|+\rangle$ for $g\Delta t = \sqrt{\gamma\Delta t} = 0.2$ when $S$ starts in state $|+\rangle$. Trajectories typically exhibit a continuous evolution, corresponding to repeated measurement outcomes $|0_n\rangle$ [recall sketch in Fig. 9(c)] interrupted by a sudden *jump* when outcome $|1_n\rangle$ is recorded [recall sketch in Fig. 9(d)]. In the latter case, $S$ abruptly collapses to $|0\rangle$ in agreement with (111) (signaled by the survival probability which jumps to 1/2) and then no longer changes its state. The precise step at which a jump occurs is unpredictable [e.g. compare jumps in Figs. 11(a), (c) and (d)]. Note that jumps may even not occur at all, as in Fig. 11(b) where no ancilla is detected in $|1_n\rangle$.[32]

The reason why in the considered example only outcome $|1_n\rangle$ produces a sudden jump is that we set a relatively short collision time such that $g\Delta t \ll 1$.[33] Indeed, in this limit, Eqs. (110) and (111) reduce to

$$\hat{K}_0|\psi\rangle \simeq c_0|0\rangle + \left(1 - \tfrac{1}{2}\gamma\Delta t\right)c_1|1\rangle\,, \quad \hat{K}_1|\psi\rangle \simeq -i\sqrt{\gamma}\,\sqrt{\Delta t}\,c_1|0\rangle\,, \tag{114}$$

the associated probabilities being

$$p_0 \simeq 1 - \gamma\Delta t\,|c_1|^2\,, \quad p_1 \simeq \gamma\Delta t\,|c_1|^2\,. \tag{115}$$

We see that outcome $|0_n\rangle$ is very likely and, when occurring, it causes a tiny shrinking of the $|1\rangle$'s component. In contrast, outcome $|1_n\rangle$ is rather unlikely. However, *if* occurring, it causes a *dramatic* change of the state of $S$ which is projected to $|0\rangle$ altogether in one shot.

### 6.4. Stochastic schrödinger equation

As seen thus far, during the conditional dynamics the state of $S$ remains pure all the time. However, its evolution is generally non-deterministic due to the occurrence of quantum jumps. In the previous instance, we saw that outcome $|1_n\rangle$ causes a sudden jump, in contrast to $|0_n\rangle$ producing only a small change in the state of $S$. We would like now both

[32] All no-jump trajectories have just the same evolution as that in Fig. 11(b).

[33] If $\Delta t \sim g^{-1}$ both outcomes will generally produce a sudden change in the state of $S$ as is clear from Eqs. (110) and (111).

these behaviors to be incorporated into a *single equation* that governs the *stochastic* time evolution of state $|\psi\rangle$, like the usual Schrödinger equation does for conventional unitary (deterministic) dynamics. We next show how to achieve this for the CM and associated coupling Hamiltonian $\hat{V}_n$ considered in the previous section when $S$ starts in a pure state (a generalization will be presented in Section 6.6).

To this aim, we first express the low-order expansion of the Kraus operators [scf. Eqs. (110)–(111)] in the more compact form

$$\hat{K}_0|\psi\rangle = \left(\mathbb{I} - \tfrac{1}{2}\gamma\Delta t\,\hat{\sigma}_+\hat{\sigma}_-\right)|\psi\rangle\,, \quad \hat{K}_1|\psi\rangle = -i\sqrt{\gamma}\sqrt{\Delta t}\;\hat{\sigma}_-|\psi\rangle\,, \tag{116}$$

(we used that $\hat{\sigma}_+\hat{\sigma}_-|\psi\rangle = c_1|1\rangle$ and $\hat{\sigma}_-|\psi\rangle = c_1|0\rangle$), the associated probabilities being

$$p_1 = 1 - p_0 = \gamma\,\langle\hat{\sigma}_+\hat{\sigma}_-\rangle\,\Delta t\,, \tag{117}$$

where $\langle\hat{\sigma}_+\hat{\sigma}_-\rangle = \langle\psi|\,\hat{\sigma}_+\hat{\sigma}_-|\psi\rangle$.

The normalized state of $S$ for each measurement outcome is thus[34]

$$|\psi_{n+1}\rangle = \Big(\mathbb{I} - \tfrac{1}{2}\gamma\Delta t\,(\hat{\sigma}_+\hat{\sigma}_- - \langle\hat{\sigma}_+\hat{\sigma}_-\rangle)\Big)|\psi_n\rangle \quad (\text{for } 0_n)\,, \qquad |\psi_{n+1}\rangle = \frac{\hat{\sigma}_-|\psi_n\rangle}{\sqrt{\langle\hat{\sigma}_+\hat{\sigma}_-\rangle}} \quad (\text{for } 1_n)\,. \tag{118}$$

The corresponding changes in the state of $S$, $\Delta|\psi_n\rangle = |\psi_{n+1}\rangle - |\psi_n\rangle$, read

$$\Delta|\psi_n\rangle = -\tfrac{1}{2}\gamma\Delta t\,(\hat{\sigma}_+\hat{\sigma}_- - \langle\hat{\sigma}_+\hat{\sigma}_-\rangle)|\psi_n\rangle \quad (\text{for } 0_n)\,, \qquad \Delta|\psi_n\rangle = \left(\frac{\hat{\sigma}_-}{\sqrt{\langle\hat{\sigma}_+\hat{\sigma}_-\rangle}} - \mathbb{I}\right)|\psi_n\rangle \quad (\text{for } 1_n)\,. \tag{119}$$

We next define a binary *random variable* $\Delta N$, which can take on values 0 or 1 with probabilities $p_0$ and $p_1$, respectively. Clearly, $(\Delta N)^2 \equiv \Delta N$ and $\overline{\Delta N} = 0\cdot p_0 + 1\cdot p_1 = p_1$. Hence, in light of Eq. (117),

$$\overline{\Delta N} = \overline{(\Delta N)^2} = p_1 = \gamma\,\langle\hat{\sigma}_+\hat{\sigma}_-\rangle\,\Delta t\,. \tag{120}$$

The meaning of $\Delta N$ should be clear: $\Delta N = 1$ when outcome $1_n$ is recorded and $S$ thereby evolves as in the second identity (119). Now, we combine together the two increments (119) as

$$\Delta|\psi_n\rangle = -\tfrac{1}{2}\gamma\Delta t\,(\hat{\sigma}_+\hat{\sigma}_- - \langle\hat{\sigma}_+\hat{\sigma}_-\rangle)|\psi_n\rangle + \left(\frac{\hat{\sigma}_-}{\sqrt{\langle\hat{\sigma}_+\hat{\sigma}_-\rangle}} - \mathbb{I}\right)|\psi_n\rangle\,\Delta N\,. \tag{121}$$

When $\Delta N = 0$, $\Delta|\psi_n\rangle$ reduces to that for outcome $0_n$. When $\Delta N = 1$, instead, we would get the sum of the two possible increments. However, for $\Delta t$ short enough (as we are assuming), the term $\sim \Delta N$ dominates [plots such as those in Fig. 11 could have been generated using Eq. (121)]. Now, we naturally take the continuous-time limit $\Delta t \to 0$,[35] obtaining

$$d|\psi\rangle = -\tfrac{1}{2}\gamma\,(\hat{\sigma}_+\hat{\sigma}_- - \langle\hat{\sigma}_+\hat{\sigma}_-\rangle)|\psi\rangle dt + \left(\frac{\hat{\sigma}_-}{\sqrt{\langle\hat{\sigma}_+\hat{\sigma}_-\rangle}} - \mathbb{I}\right)|\psi\rangle\,dN\,, \tag{122}$$

where

$$\overline{dN} = \overline{(dN)^2} = \gamma\,\langle\hat{\sigma}_+\hat{\sigma}_-\rangle\,dt\,. \tag{123}$$

Eq. (122) fully describes the stochastic evolution of $S$ and indeed usually goes under the name of *stochastic Schrödinger equation*. Note that, in contrast to the usual (deterministic) Schrödinger equation, this is highly *nonlinear*. An equivalent way to write it is

$$d|\psi\rangle = -i\hat{H}_{\text{eff}}\,|\psi\rangle dt + i\tfrac{\gamma}{2}\,\langle\hat{\sigma}_+\hat{\sigma}_-\rangle|\psi\rangle dt + \left(\frac{\hat{\sigma}_-}{\sqrt{\langle\hat{\sigma}_+\hat{\sigma}_-\rangle}} - \mathbb{I}\right)|\psi\rangle\,dN\,, \tag{124}$$

where

$$\hat{H}_{\text{eff}} = -i\tfrac{\gamma}{2}\,\hat{\sigma}_+\hat{\sigma}_- \tag{125}$$

is an effective non-Hermitian Hamiltonian.

[34] Using $1/\sqrt{1-x} \simeq 1 + x/2$, the normalization factor of $\hat{K}_0|\psi\rangle$ [cf. Eqs. (116) and (117)] is $1/\sqrt{p_0} \simeq 1 + \frac{\gamma}{2}\langle\hat{\sigma}_+\hat{\sigma}_-\rangle\Delta t$. Neglecting terms in $\Delta t^2$, we thus get the first identity in (118). Also, note that, in the $1_n$ case, we could simply write $|\psi_{n+1}\rangle = |0\rangle$.

[35] This continuous-time limit corresponds to the one discussed in Section 5.8 [indeed the coupling strength was chosen here in agreement with Eq. (80)].

### 6.5. Unconditional dynamics: recovering the master equation

Based on the discussion in Section 6.1, the ensemble average of (122), namely the average over all possible outcomes of the random variable $dN$, must return the Lindblad ME (recall Sections 5.3, 5.4 and 5.8). To prove this, we first work out the density–matrix version of Eq. (122). The differential increment of $\rho = |\psi\rangle\langle\psi|$ is

$$d\rho = d\left(|\psi\rangle\langle\psi|\right) = \left(d|\psi\rangle\right)\langle\psi| + |\psi\rangle d\langle\psi| + d|\psi\rangle d\langle\psi| \,. \tag{126}$$

As a point of utmost importance, note that, although of second order with respect to $d\psi$, the last term must be retained since $(dN)^2$ is in fact of *first* order in $dt$ [cf. Eq. (123)]. After plugging (122) and its bra in $d|\psi\rangle$ and $d\langle\psi|$, respectively, we replace $dN$ and $(dN)^2$ with their common average (123). To first order in $dt$, this yields as expected the Lindblad ME (see Appendix G for details)

$$d\rho = \gamma\,\left(\hat{\sigma}_-\rho\,\hat{\sigma}_+ - \tfrac{1}{2}\left[\hat{\sigma}_+\hat{\sigma}_-,\,\rho\right]_+\right)dt \,,$$

which we formerly derived in a different way in Section 5.8.

Consistently with the previous terminology (see end of Section 6.1), any reduced dynamics discussed in Sections 4 and 5 – in particular that of $S$ – is referred to as *unconditional dynamics*. In real experiments, unconditional dynamics are usually not directly measurable but rather inferred by averaging over a large enough number of quantum trajectories. In this sense, although inherently stochastic, quantum trajectories reflect more closely the experimental reality. In contrast, the unconditional dynamics has a somewhat more indirect relationship with experiments but is fully deterministic.

We mention that the connection with the Lindblad master equation just discussed has major computational applications in that it provides the basis for the widely used *quantum jump method* or *Monte Carlo wave function* [59,78–80]. This allows to work out the dynamics of open quantum systems, especially of large dimension, by keeping track of their *wavefunction* over simulated quantum trajectories (and then averaging), thus bypassing the computationally demanding use of the density matrix.

### 6.6. A more general stochastic schrödinger equation

Consider again the general (Markovian) CM in Section 5.4 with coupling Hamiltonian (60) [which we assumed in the derivation Eqs. (64) and (66)]. The low-order collision unitary (47) then explicitly reads

$$\hat{U}_n \simeq \mathbb{I} - i\sum_\nu g_\nu \hat{A}_\nu\hat{B}_\nu\Delta t - \tfrac{1}{2}\sum_{\nu\mu} g_\nu g_\mu \hat{A}_\nu\hat{A}_\mu\hat{B}_\nu\hat{B}_\mu\,\Delta t^2 \,. \tag{127}$$

For simplicity we do not consider free Hamiltonian terms, which would simply result in an additional term $\sim \Delta t$ (we come back to this point at the end).

We will restrict to qubit ancillas (initially uncorrelated as usual), each prepared in state $|\chi_n\rangle$.[36] We also assume that first moments of the bath vanish [recall Eq. (61)], i.e. $\langle\hat{B}_\nu\rangle = \langle\chi_n|\hat{B}_\nu|\chi_n\rangle = 0$ for all $\nu$ and $n$.

Based on Section 6.1 [see in particular Eqs. (103) and (104)], the $n$th collision transforms the state of $S$ and ancilla $n$ as

$$\hat{U}_n|\psi_{n-1}\rangle|\chi_n\rangle = \hat{K}_0|\psi_{n-1}\rangle\,|0_n\rangle + \hat{K}_1|\psi_{n-1}\rangle\,|1_n\rangle \,, \tag{128}$$

where, combining Eqs. (103) and (127), operators $\hat{K}_k$ are given by

$$\hat{K}_k = \langle k|\chi_n\rangle\,\mathbb{I} + \hat{K}_k^{(1)}\Delta t + \hat{K}_k^{(2)}\Delta t^2 \,, \tag{129}$$

with

$$\hat{K}_k^{(1)} = -i\sum_\nu g_\nu\langle k|\hat{B}_\nu|\chi_n\rangle\,\hat{A}_\nu \,, \quad \hat{K}_k^{(2)} = -\tfrac{1}{2}\sum_{\nu\mu} g_\nu g_\mu\,\langle k|\hat{B}_\nu\hat{B}_\mu|\chi_n\rangle\,\hat{A}_\nu\hat{A}_\mu \,. \tag{130}$$

From now on, we drop index $n$. We consider next the case that $k = 0, 1$ with $|\chi\rangle = |0\rangle$, i.e. we measure the ancilla in a basis whose an element is just the initial state $|\chi\rangle$. This together with our initial assumption $\langle\hat{B}_\nu\rangle = 0$ in particular yield

$$\langle k|\chi\rangle = \delta_{k,0}\,\mathbb{I} \,, \quad \hat{K}_0^{(1)} = 0 \,, \quad \langle 0|\hat{B}_\nu\hat{B}_\mu|\chi\rangle = \langle 0|\hat{B}_\nu|1\rangle\langle 1|\hat{B}_\mu|0\rangle \,, \quad \langle 1|\hat{B}_\nu\hat{B}_\mu|\chi\rangle = 0 \,, \tag{131}$$

where to compute the second moments we inserted $|0\rangle\langle 0| + |1\rangle\langle 1| = \mathbb{I}$ between $\hat{B}_\nu$ and $\hat{B}_\mu$. Thereby

[36] For the sake of argument and to better highlight the physics, as done throughout this Section, we will keep assuming that both the system and ancilla initial states are pure. The extension to mixed states is straightforward.

$$\hat{K}_0^{(2)} = -\tfrac{1}{2}\underbrace{\sum_\nu g_\nu \langle 0|\hat{B}_\nu|1\rangle \hat{A}_\nu}_{=\hat{J}^\dagger}\underbrace{\sum_\mu g_\mu \langle 1|\hat{B}_\mu|0\rangle \hat{A}_\mu}_{=\hat{J}}\,, \quad \hat{K}_1^{(2)} = 0\,, \tag{132}$$

where we suitably defined an operator $\hat{J}$ on $S$.[37]

Putting together all the above and setting $g_\nu = \sqrt{\gamma_\nu/\Delta t}$, we conclude that

$$\hat{K}_0 = \mathbb{I} - \tfrac{1}{2}\hat{L}^\dagger\hat{L}\,\Delta t\,, \quad \hat{K}_1 = -i\hat{L}\sqrt{\Delta t} \tag{133}$$

with associated probabilities

$$p_1 = 1 - p_0 = \langle \hat{L}^\dagger\hat{L}\rangle\,\Delta t\,, \tag{134}$$

where the jump operator $\hat{L}$ is given by

$$\hat{L} = \sqrt{\Delta t}\,\hat{J} = \sum_\nu \sqrt{\gamma_\nu}\,\langle 1|\hat{B}_\nu|0\rangle\hat{A}_\nu\,. \tag{135}$$

In the example of Section 6.4 [see in particular Eqs. (116) and (134)], $\hat{L} = \sqrt{\gamma}\,\sigma_-$.

Since the structure of Kraus operators (133) is identical to (116), the reasoning followed in Section 6.4 can be formally repeated leading to the general stochastic Schrödinger equation [cf. Eqs. (122) and (123)]

$$d|\psi\rangle = -\tfrac{1}{2}(\hat{L}_+\hat{L}_- - \langle\hat{L}_+\hat{L}_-\rangle)|\psi\rangle dt + \left(\frac{\hat{\sigma}_-}{\sqrt{\langle\hat{L}^\dagger\hat{L}\rangle}} - \mathbb{I}\right)|\psi\rangle\, dN\,, \tag{136}$$

where $\overline{dN} = \overline{(dN)^2} = \langle\hat{L}_+\hat{L}_-\rangle\, dt$. In the common case where an external drive or local field is applied on $S$ one simply needs to add the extra term $-i\hat{H}_S|\psi\rangle dt$, where Hamiltonian $\hat{H}_S$ could generally be time-dependent.

### 6.7. Quantum trajectories: state of the art

We already mentioned in the Introduction the seminal works by Caves and Milburn (see in particular Ref. [17]). Therein, each ancilla is modeled as a quantum harmonic oscillator which gets displaced due to the interaction with $S$. Measuring the resulting displacement implements a POVM. The corresponding unconditional dynamics is described by a characteristic ME, whose dissipator (when $S$ is a harmonic oscillator itself) has the form $\mathcal{D}_S[\rho] = -K[\hat{x},[\hat{x},\rho]]$ with $K > 0$ and $\hat{x}$ the position operator [17]. A bipartite generalization of this collision model (with additional feedback) has been used more recently in some gravitational decoherence theories to construct a classical channel that accounts for Newtonian interaction [81,82]. These are critically reviewed in Ref. [36], which encompasses as well a general presentation of metrological aspects of CMs (another one can be found in an introductory section of Ref. [38]).

A significant part of the discussion we developed relies on the seminal paper by Brun [24] already mentioned in the Introduction. At variance with Caves and Milburn, Brun employs qubit ancillas taking advantage of the quantum information approach [21].

It is important to note that in the considered instances we always measured the ancillas in a basis containing the initial state $|\chi_n\rangle$. If this is not the case, then two different outcomes could have comparable probabilities [unlike e.g. Eq. (134) where $p_0 \ll p_1$]. The treatment in Section 6.6 up to Eq. (130) would still apply, but the stochastic Schrödinger equation would be different. A case of this kind is presented in the Brun's paper and shown to lead to a quantum state diffusion equation [24].

We point out that micromaser (see Section 5.7) is a setup enabling direct measurement of the state of each ancilla (embodied by a flying atom). The related statistics of detections thus supplies informations on the cavity field and has been extensively studied, see e.g. Refs. [83].

Finally, we mention that the collisional picture of quantum trajectories can be profitably applied to quantum steering [84] and engineering of quantum jump statistics [85]. Important applications to stochastic quantum thermodynamics and quantum optics will be discussed in Sections 7.13 and 9.13, respectively.

## 7. Non-equilibrium quantum thermodynamics

We now address the thermodynamics of quantum CMs in non-equilibrium transformations, this being arguably the area in which CMs (also known in this context as *repeated interaction* schemes) occur most frequently. As the field is growing fast, the related body of literature is already considerable enough that several relevant topics cannot be covered here. Thus, given the pedagogical attitude of our paper, the present section aims to provide the reader with some basic tools for applying CMs in quantum thermodynamics problems. A number of topics that we do not discuss, e.g. exploiting

[37] The two quantities between brackets are easily shown to be mutually adjoint by recalling that $\sum_\nu g_\nu\hat{A}_\nu\hat{B}_\nu$ is Hermitian.

CMs as a resource for improving thermodynamic performances, are mentioned in the state of the art Section 7.13 and related references supplied therein.

Before formulating general definitions and laws, we discuss a specific but quite paradigmatic non-equilibrium process: the relaxation to an equilibrium state.

### 7.1. Relaxation to thermal equilibrium

In Section 4.7, we introduced *mixing* collision maps, namely those dynamics such that $S$ reaches a state $\rho^*$ no matter what initial state it started from (i.e. $\rho_n \to \rho^*$ for any $\rho_0$) . If so, then $\rho^*$ is necessarily the only possible steady state, i.e. the unique fixed point of the collision map ($\mathcal{E}[\rho^*] = \rho^*$). It is natural to ask whether, by converging to $\rho^*$, $S$ inherits some intensive property of the bath. The most natural one is *temperature*: if the bath is in an equilibrium state at a given temperature, will $S$ asymptotically end up in a Gibbs state at the same temperature? In other words, we wonder whether $S$ will *thermalize* with the ancillas.

We can formally define thermalization in terms of a basic CM (cf. Section 4.1) where each ancilla is initially in the Gibbs state (henceforth referred to as thermal state)

$$\eta_{\rm th} = \frac{e^{-\beta H_n}}{Z_n} \tag{137}$$

with $\beta = 1/(KT)$ the inverse temperature and $Z_n = {\rm Tr}_n\left\{e^{-\beta H_n}\right\}$ the partition function. We say that thermalization occurs when $\rho_n \to \rho^*$ for any $\rho_0$ such that the asymptotic state $\rho^*$ is a thermal state of $S$ at the same temperature as each ancilla, i.e.

$$\rho^* = \frac{e^{-\beta H_S}}{Z_S}\,. \tag{138}$$

This definition can be generalized in many ways. For instance, one can conceive a generalized thermalization whose steady state is given by (138) but $\beta$ generally differs from the bath's one. If so then equilibrium is never reached. Another possibility is that $S$ ends up in a thermal state like (138) even though the bath is not in a thermal state (this would again entail lack of equilibrium).

### 7.2. System thermalizing with a bath of quantum harmonic oscillators

A typical instance to illustrate thermalization is the basic CM in Section 4.1 in the case that ancillas are quantum harmonic oscillators (with associated bosonic ladder operators $\hat{b}_n$ and $\hat{b}_n^\dagger$ such that $[\hat{b}_n, \hat{b}_{n'}^\dagger] = \delta_{n,n'}$). The free Hamiltonian of $S$ (ancilla $n$) is $\hat{H}_S = \omega_0 \hat{A}_+\hat{A}_-$ ($\hat{H}_n = \omega_0\, \hat{b}_n^\dagger \hat{b}_n$), while for the interaction Hamiltonian we take $\hat{V}_n = \sqrt{\gamma/\Delta t}\,(\hat{A}_+\hat{b}_n + {\rm H.c.})$. The nature of $\hat{A}_\pm$, which are ladder operators of $S$ fulfilling $[\hat{H}_S, \hat{A}_\pm] = \pm\omega_0\hat{A}_\pm$, will be left unspecified for a while.

Each ancilla is initially in the Gibbs state [cf. Eq. (137)]

$$\eta_{\rm th} = \frac{e^{-\beta H_n}}{Z_n} = \sum_k \frac{e^{-\beta\omega_0 k}}{Z_n}\, |k\rangle_n\langle k|\,, \tag{139}$$

with $\{|k\rangle_n\}$ the basis of Fock states.[38] Recalling Eqs. (64) and (65), we see that $\hat{H}'_S = 0$ while the dissipator is given by

$$\mathcal{D}_S[\rho_{n-1}] = \gamma\,\langle \hat{b}_n\hat{b}_n^\dagger\rangle(\hat{A}_-\rho_{n-1}\hat{A}_+ - \tfrac{1}{2}\,[\hat{A}_+\hat{A}_-, \rho_{n-1}]_+) + \gamma\,\langle \hat{b}_n^\dagger\hat{b}_n\rangle(\hat{A}_+\rho_{n-1}\hat{A}_- - \tfrac{1}{2}\,[\hat{A}_-\hat{A}_+, \rho_{n-1}]_+)\,. \tag{140}$$

Replacing $\hat{b}_n\hat{b}_n^\dagger = \hat{b}_n^\dagger\hat{b}_n + 1$ and introducing the thermal number of excitations

$$\bar{n}_{\omega_0} = \langle \hat{b}_n^\dagger\hat{b}_n\rangle = {\rm Tr}_n\{\hat{b}_n^\dagger\hat{b}_n\,\eta_n\} = \frac{1}{e^{\beta\omega_0} - 1}\,, \tag{141}$$

the dissipator is written as

$$\mathcal{D}_S[\rho_{n-1}] = \gamma_-(\,\hat{A}_-\rho_{n-1}\hat{A}_+ - \tfrac{1}{2}\,[\hat{A}_+\hat{A}_-, \rho_{n-1}]_+) + \gamma_+(\hat{A}_+\rho_{n-1}\hat{A}_- - \tfrac{1}{2}\,[\hat{A}_-\hat{A}_+, \rho_{n-1}]_+)\,, \tag{142}$$

where we defined the emission and absorption rates

$$\gamma_- = \gamma\,(\bar{n}_{\omega_0} + 1)\,, \quad \gamma_+ = \gamma\,\bar{n}_{\omega_0}\,. \tag{143}$$

This is a well-known master equation describing a system in contact with a thermal bath, where we can recognize the *Einstein coefficients* [86] $A_E = \gamma$ (spontaneous emission rate) and $B_{\rm E} = \gamma\,\bar{n}_{\omega_0}$ (stimulated emission/absorption rate). These are related to rates (143) according to $\gamma_- = A_{\rm E} + B_{\rm E}$ and $\gamma_+ = B_{\rm E}$. Note that Eqs. (141) and (143) entail

$$\frac{\gamma_+}{\gamma_-} = e^{-\beta\omega_0}\,. \tag{144}$$

[38] A Fock or number state $|k\rangle_n$ (for $k = 0, 1, 2, \ldots$) fulfills $\hat{H}_n|k\rangle_n = \omega_0 k|k\rangle_n$. Hence, $e^{-\beta\hat{H}_n} = \sum_k e^{-\beta\omega_0 k}|k\rangle_n\langle k|$.

This identity connects rates (associated with relaxation, thus a non-equilibrium process) to temperature (defined for equilibrium states).

Similar conclusions hold when ancillas are qubits (instead of harmonic oscillators), i.e. $\hat{H}_n = \omega_0 \hat{\sigma}_{n+}\hat{\sigma}_{n-}$ and $\hat{V}_n = \sqrt{\gamma/\Delta t}\left(\hat{A}_+\hat{\sigma}_{n-} + \text{H.c.}\right)$. The resulting ME dissipator is identical to (142) except that the thermal number of excitations of each ancilla is now given by $\bar{n}_{\omega_0} = 1/(e^{\beta\omega_0}+1)$ [instead of (141)]. This is just ME (77) which we encountered in Section 5.7, describing the cavity dynamics of a micromaser with the atomic population given by $p = \bar{n}_{\omega_0}$ and for $\tau = \Delta t$, $g = \sqrt{\gamma/\Delta t}$ (where in that case $S$ is a harmonic oscillator such that $\hat{A}_- = \hat{A}_+^\dagger = \hat{a}$). Note that this rules out atomic initial states such that $p > 1/2$, i.e. that cannot be regarded as thermal states at any temperature (unless one defines a negative temperature such that $\beta < 0$).

Mostly for the sake of argument, in all the forthcoming instances we will refer to the case that $S$ is a qubit (ancillas being still harmonic oscillators), thus we will set $\hat{A}_\pm = \hat{\sigma}_\pm$.

In the basis $\{|0\rangle, |1\rangle\}$ of $S$, ME (142) translates into a pair of differential equations for the excited-state population $p$ and coherences $c$ [recall Eq. (29)], which read

$$\dot{p} = \gamma_+(1-p) - \gamma_- p\,, \quad \dot{c} = -\tfrac{1}{2}(\gamma_+ + \gamma_-)c\,. \tag{145}$$

Under stationary conditions the derivatives vanish, yielding $c = 0$ and

$$p = \frac{1}{1+(\gamma_+/\gamma_-)^{-1}}\,. \tag{146}$$

Using (144) this means that, regardless of the initial state, $S$ eventually ends up in

$$\rho_{\text{th}} = \frac{e^{-\beta H_S}}{\text{Tr}_S\left\{e^{-\beta H_S}\right\}} = \frac{1}{1+e^{-\beta\omega_0}}|0\rangle_S\langle 0| + \frac{e^{-\beta\omega_0}}{1+e^{-\beta\omega_0}}|1\rangle_S\langle 1|\,, \tag{147}$$

namely the thermal state at the same temperature of ancillas (defined by $\beta$). Thus thermalization occurs.

Although very common, the thermalization process considered here regards a specific class of systems. In the next section, we consider a general situation where $S$ and ancillas are unspecified, shedding some light at the same time on the reason why thermalization may take place.

### 7.3. Thermalization and energy conservation

Occurrence of thermalization depends, in particular, on the form of system–ancilla Hamiltonian. For example, let us consider the last instance of the previous section and simply add a detuning to $S$ such that $\hat{H}_S = (\omega_0+\delta)\hat{\sigma}_+\hat{\sigma}_-$. The ancilla thermal state $\eta_n$ and rates (143) are unaffected by $\delta$ and thus ME (142) continues to hold unchanged, hence $S$ still asymptotically converges to (147). Yet, this is *not* the thermal state of $S$ at the ancilla temperature, thus thermalization now does not take place.[39]

An important necessary (although generally not sufficient) condition for thermalization to occur is that collisions be *energy-conserving*. This means that $\hat{H}_S + \hat{H}_n$ (total free Hamiltonian of $S$ and $n$th ancilla) is a constant of motion in the $n$th collision, i.e. it commutes with the collision unitary

$$[\hat{U}_n, \hat{H}_S + \hat{H}_n] = 0\,. \tag{148}$$

This is because if this is true then the $S$-ancilla state

$$\frac{e^{-\beta H_S}}{Z_S} \otimes \frac{e^{-\beta H_n}}{Z_n} \propto e^{-\beta(\hat{H}_S+\hat{H}_n)} \tag{149}$$

is clearly unaffected by the $n$th collision. It follows that state (138) is a fixed point of the collision map (i.e. a steady state), this being a necessary condition for thermalization as we discussed in Sections 4.7 and 7.1.

Based on the form of the collision unitary [cf. Eqs. (2) and (47)], energy conservation can be equivalently expressed as

$$[\hat{V}_n, \hat{H}_S + \hat{H}_n] = 0\,. \tag{150}$$

In the example mentioned at the beginning of this subsection, when $\delta \neq 0$ (150) does not hold thus thermalization cannot occur.

Physically, conservation of $\hat{H}_S + \hat{H}_n$ means that if the free energy of $S$ decreases then that of the colliding ancilla grows by exactly the same amount (and viceversa). This intuition can be made formally rigorous as follows.

Let us first define an eigenoperator $\hat{A}_\nu$ of $\hat{H}_S$ with eigenvalue $\omega_\nu$ as an operators on $S$ fulfilling

$$[\hat{H}_S, \hat{A}_\nu] = -\omega_\nu \hat{A}_\nu\,. \tag{151}$$

[39] The state can still be arranged as a thermal state but at an effective temperature different from the ancilla's one.

Likewise, eigenoperators of $\hat{H}_n$ are defined as

$$[\hat{H}_n, \hat{B}_\nu] = -w_\nu \hat{B}_\nu \tag{152}$$

with $w_\nu$ the associated eigenvalues. Here, $\hat{A}_\nu$ and $\hat{B}_\nu$ are defined as dimensionless operators. Note that the values taken by index $\nu$ in (151) and (152) are generally different.

Now, for given $\hat{H}_S$ and $\hat{H}_n$, it can be shown (see Appendix H) that the most general class of interaction Hamiltonians $\hat{V}_n$ satisfying (150) has the form

$$\hat{V}_n = \sum_\nu g_\nu \left(\hat{A}_\nu^\dagger \hat{B}_\nu + \hat{A}_\nu \hat{B}_\nu^\dagger\right) \quad \text{with} \quad \omega_\nu = w_\nu \ . \tag{153}$$

It can be immediately checked that (153) fulfills (150).

Many coupling Hamiltonians appearing throughout this paper can be recognized as falling within this class. Note that $\hat{V}_n \neq 0$ only provided that there exist eigenvalues common to both $\hat{H}_S$ ad $\hat{H}_n$. To make clear the physical meaning of (153), it suffices to consider a generic eigenstate $|E\rangle$ of $\hat{H}_S$ with energy $E$ and note that $\hat{A}_\nu|E\rangle$ is another eigenstate but with energy $E-\omega$, while $\hat{A}_\nu^\dagger|E\rangle$ is an eigenstate with eigenvalue $E+\omega$.[40] Analogous properties hold for $\hat{B}_\nu$. Thereby, according to $\hat{V}_n$, if $S$ undergoes a transition $|E_i\rangle \to |E_f\rangle$ changing its energy by the amount $\omega = E_f - E_i$ then the ancilla will make a simultaneous transition with energy change $-\omega$. For instance, in Section 7.1, if $S$ is a qubit making the transition $|0\rangle \to |1\rangle$ with energy gain $\omega_0$ then a harmonic-oscillator ancilla can only decay from a Fock state $|k\rangle$ to $|k-1\rangle$ losing the same amount of energy $\omega_0$.

The general ME corresponding to interaction (153) can be calculated in terms of the ancilla's moments [see Section 5.4 and Eq. (64)]. Since $\eta_n$ is a thermal state (mixture of eigenstates of $\hat{H}_n$), each $\hat{\hat{B}}_\nu$ (in light of the aforementioned properties) has vanishing expectation value. Thus $\hat{H}'_S = 0$ [cf. Eq. (65)]. Regarding the dissipator $\mathcal{D}_S$, we note that $\langle \hat{B}_{\nu'} \hat{B}_\nu \rangle = \langle \hat{B}_{\nu'}^\dagger \hat{B}_\nu^\dagger \rangle = 0$ for all $\nu$ and $\nu'$. Therefore,

$$\mathcal{D}_S[\rho_{n-1}] = \sum_{\nu,\nu'} \gamma_{\nu,\nu'} \langle \hat{B}_{\nu'} \hat{B}_\nu^\dagger \rangle (\hat{A}_\nu \rho_{n-1} \hat{A}_{\nu'}^\dagger - \tfrac{1}{2}[\hat{A}_{\nu'}^\dagger \hat{A}_\nu, \rho_{n-1}]_+) + \sum_{\nu,\nu'} \gamma_{\nu,\nu'} \langle \hat{B}_{\nu'}^\dagger \hat{B}_\nu \rangle (\hat{A}_\nu^\dagger \rho_{n-1} \hat{A}_{\nu'} - \tfrac{1}{2}[\hat{A}_{\nu'} \hat{A}_\nu^\dagger, \rho_{n-1}]_+) . \tag{154}$$

### 7.4. Non-equilibrium steady states with baths at different temperatures

We have dealt so far with a non-equilibrium process where however $S$ eventually ends up in an equilibrium state. We next consider a dynamics where $S$ never attains equilibrium although it reaches a (non-equilibrium) steady state. This is the simultaneous interaction with *many* thermal baths at different temperatures, which is a paradigmatic dynamics to illustrate e.g. thermal conduction, where it is known that $S$ can reach an effective thermal state at a temperature which is a weighted average of those of the reservoirs. CMs are very effective in handling multiple baths as discussed in Section 5.9.

We thus focus on a CM comprising $M = 2$ baths of ancillas labeled with 1 and 2 as shown in Fig. 8(a). Ancillas of bath $i = 1, 2$ are in a thermal state $\eta^{(i)} = \eta_{\rm th}^{(i)}$ with inverse temperature $\beta_i$ [cf. Eq. (85) for $\chi_n^{(\rm corr)} = 0$] where in general $\beta_1 \neq \beta_2$. The coupling Hamiltonian ruling each collision has the form (87). As in the instance in Section 7.1, we assume that first moments vanish for each bath, i.e. $\langle \hat{B}_{\nu i} \rangle = 0$. Hence, $\dot{\rho} = \mathcal{D}_S[\rho]$ with [cf. Eq. (89)]

$$\mathcal{D}_S[\rho] = \mathcal{D}_S^{(1)}[\rho] + \mathcal{D}_S^{(2)}[\rho] \, , \tag{155}$$

where $\mathcal{D}_S^{(i)}$ is the dissipator that would arise if $S$ collided only with ancillas of bath $i$.

As an illustrative instance, fully in line with Section 7.1, we model each ancilla of bath $i$ as a harmonic oscillator of frequency $\omega_0$ initially in a thermal state like (139) with inverse temperature $\beta_i$. The coupling with $S$ has the same form as in Section 7.1 with coupling strength $\sqrt{\gamma_i/\Delta t}$. Note that $S$ and all ancillas. have the same frequency $\omega_0$ in a way that, if $\gamma_2$ were zero (meaning that bath 2 is decoupled from $S$), then $S$ would reach thermal equilibrium with bath 1 (and viceversa).

Due to (155) we see that the dissipator is analogous to (142) under the replacements $\gamma_\pm \to \gamma'_\pm$ with the effective emission and absorption rates given by

$$\gamma'_\pm = \gamma_\pm^{(1)} + \gamma_\pm^{(2)} \, , \tag{156}$$

where

$$\gamma_-^{(i)} = \gamma_i (\bar{n}^{(i)} + 1) \, , \quad \gamma_+^{(i)} = \gamma_i \, \bar{n}^{(i)} \quad \text{with} \quad \bar{n}_i = (e^{\beta_i \omega_0} - 1)^{-1} \ . \tag{157}$$

[40] From Eq. (151), $\hat{H}_S \hat{A}_\nu = \hat{A}_\nu \hat{H}_S - \omega_\nu \hat{A}_\nu$. Hence, $\hat{H}_S \hat{A}_\nu |E\rangle = \hat{A}_\nu \hat{H}_S |E\rangle - \omega_\nu \hat{A}_\nu |E\rangle = E \hat{A}_\nu |E\rangle - \omega_\nu \hat{A}_\nu |E\rangle = (E - \omega_\nu) \hat{A}_\nu |E\rangle$, showing that $\hat{A}_\nu |E\rangle$ is eigenstate of $\hat{H}_S$. The property for $\hat{A}_\nu^\dagger$ is proven likewise by noting that $[\hat{H}_S, \hat{A}_\nu^\dagger] = \omega_\nu \hat{A}_\nu^\dagger$. Note that $\hat{A}_\nu |E\rangle$ (or $\hat{A}_\nu^\dagger |E\rangle$) could be zero: e.g. for a qubit of Hamiltonian $\omega_0 |1\rangle\langle 1|$ we have $\hat{\sigma}_- |0\rangle = \hat{\sigma}_+ |1\rangle = 0$.

As the ME is formally identical to that in Section 7.1, $S$ asymptotically converges to an effective thermal state of the form (147) with inverse temperature $\beta_{\rm eff}$ given by[41]

$$\beta_{\rm eff} = \frac{1}{\omega_0}\log\frac{\gamma'_-}{\gamma'_+} = \frac{1}{\omega_0}\log\frac{(\gamma_1+\gamma_2)e^{(\beta_1+\beta_2)\omega_0} - \gamma_1 e^{\beta_1\omega_0} - \gamma_2 e^{\beta_2\omega_0}}{\gamma_2\left(e^{\beta_1\omega_0}-1\right)+\gamma_1\left(e^{\beta_2\omega_0}-1\right)}\,. \tag{158}$$

This entails that $\beta_{\rm eff}$ is generally different from both $\beta_1$ and $\beta_2$ (confirming that a non-equilibrium steady state is reached), reducing to $\beta_1$ for $\gamma_2 = 0$ and to $\beta_2$ for $\gamma_1 = 0$. Thermal equilibrium is retrieved when the two baths have the same temperature, in which case (158) predicts (as expected) $\beta_{\rm eff} = \beta_1 = \beta_2$ regardless of $\gamma_1$ and $\gamma_2$.

Since CMs can keep track of the bath dynamics in a relatively straightforward way, they are an advantageous tool for calculating the rate of change (or flux) of thermodynamic quantities in non-equilibrium transformations (such as thermalization) even beyond the weak coupling regime [i.e. when the collision unitary cannot be approximated with the lowest-order expansion (47)]. The general definition and calculation of these, as well as the basic laws governing them, will be a main subject of the following subsections.

### 7.5. Time dependence of the total system–bath hamiltonian and equations of motion

We allow the free Hamiltonian of the open system $S$ to be generally *time-dependent*. This allows to encompass situations where $S$ is subject to an external classical drive such that one or more parameters of $\hat{H}_S$ can be deterministically modulated in time according to an assigned protocol. For instance, in the CM considered in Section 7.1, we could have $\hat{H}_S(t) = \omega_0(\lambda_t)\,|e\rangle\langle e|$, describing a time-modulated detuning with $\lambda_t$ some smooth function of time defining the protocol. We also assume that the characteristic time over which $\hat{H}_S(t)$ changes is much larger than $\Delta t$, hence during the $n$th collision we can approximate $\hat{H}_S(t) \simeq \hat{H}_S^{(n)}$ so that $\hat{H}_S$ becomes step-dependent.[42]

Accordingly, the total $S$-bath Hamiltonian at an arbitrary time $t$ has the general expression

$$\hat{H}_{SB}(t) = \hat{H}_S(t) + \hat{H}_B + \hat{V}(t)\,, \tag{159}$$

with the (time-independent) bath Hamiltonian given by

$$\hat{H}_B = \sum_n \hat{H}_n \tag{160}$$

and the $S$-$B$ coupling Hamiltonian by

$$\hat{V}(t) = \sum_n \Theta_n(t)\,\hat{V}_n\,, \tag{161}$$

where $\Theta_n(t) = 1$ for $t_{n-1} \le t < t_n$ and zero otherwise.

Notably, besides the possible time dependence coming from $H_S(t)$, the total Hamiltonian has an *intrinsic* time dependence due to the sudden replacement of the bath ancilla interacting with $S$ at times $t = t_n$. This time dependence, due to the periodic *switching* (on and off) of the interaction with ancillas, is a distinctive feature of CMs not present in conventional microscopic system–bath models. This generally introduces a contribution to the work as we will see in Section 7.8.

### 7.6. Rate of change of energy of S

We generally define the internal energy (or simply energy) of $S$ as the quantum expectation value $E_S = \langle\hat{H}_S\rangle = {\rm Tr}_S\{\hat{H}_S\rho\}$. Since in general both the operator $\hat{H}_S$ itself and the state of $S$ evolve in time, the change of $E_S$ at each step has two contributions

$$\Delta E_S = {\rm Tr}_S\{\Delta\hat{H}_S\,\rho_{n-1}\} + {\rm Tr}_S\{\hat{H}_S\,\Delta\rho_n\} \tag{162}$$

with $\Delta\hat{H}_S = \hat{H}_S^{(n)} - \hat{H}_S^{(n-1)}$ (subscripts between brackets denote the step number). Using Eq. (69), in terms of the usual decomposition (60) of $\hat{V}_n$, the rate of change of $E_S$ at each collision (i.e. during the time interval $t_{n-1} \le t < t_n$) is generally given by

$$\frac{\Delta E_S}{\Delta t} = \left\langle\frac{\Delta\hat{H}_S}{\Delta t}\right\rangle + i\sum_\nu g_\nu\langle\hat{B}_\nu\rangle\,\langle[\hat{A}_\nu,\hat{H}_S]\rangle + \sum_{\nu\mu}\gamma_{\nu\mu}\langle\hat{B}_\mu\hat{B}_\nu\rangle\langle\hat{A}_\mu\hat{H}_S\hat{A}_\nu - \tfrac{1}{2}\,[\hat{A}_\mu\hat{A}_\nu,\hat{H}_S]_+\rangle. \tag{163}$$

41 We write down the analogue of (144) under the replacements $\beta \to \beta_{\rm eff}$ and $\gamma_\pm \to \gamma'_\pm$ and then solve for $\beta_{\rm eff}$.

42 More in detail, $\hat{H}_S^{(n)}$ can e.g. be defined as the time average of $\hat{H}_S(t)$ during the $n$th time interval.

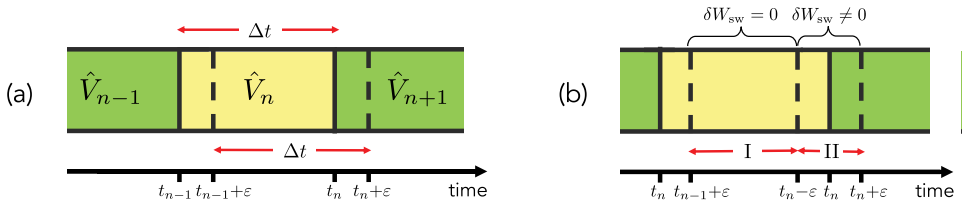


**Fig. 12.** *Redefinition of the time step.* (a): The interaction with ancilla $n$ (yellow area) is switched on at time $t_{n-1}$ and then turned off at $t_n = t_{n-1}+\Delta t$, at which time interaction $V_{n+1}$ is switched on (green). To correctly take into account the work required for the switching (if any), we redefine the time interval as $[t_{n-1}, t_n[ \to [t_{n-1}+\varepsilon, t_n+\varepsilon[$ with $\varepsilon \to 0^+$. (b): The redefined time step in turn can be split into a pair of consecutive intervals: $[t_{n-1}+\varepsilon, t_n-\varepsilon[$ (interval I) and $[t_n-\varepsilon, t_n+\varepsilon[$ (interval II). In I, $\hat{V}(t)=\hat{V}_n$ (constant). During II, instead, $\hat{V}(t)$ jumps as $\hat{V}_n \to \hat{V}_{n+1}$ at $t=t_n$.

### 7.7. Heat flux

Analogously to $S$, the energy of the $n$th-ancilla is defined as $E_n = \langle \hat{H}_n \rangle$. As ancillas are uncoupled to one another, $E_n$ can change only during the $n$th collision. Accordingly, $\Delta E_n$ at the $n$th step is also the change of energy of the entire bath $B$, i.e. $\Delta E_n = \Delta E_B^{(n)}$. This in fact gives the exchanged *heat* whose definition reads

$$\delta Q = -\Delta E_B^{(n)} = -\Delta E_n \,. \tag{164}$$

Therefore, using Eq. (70), the heat flux (exchanged heat per unit time) is given by

$$\frac{\delta Q}{\Delta t} = -i \sum_\nu g_\nu \langle \hat{A}_\nu \rangle \langle [\hat{B}_\nu, \hat{H}_n] \rangle - \sum_{\nu\mu} \gamma_{\nu\mu} \langle \hat{A}_\mu \hat{A}_\nu \rangle \langle \hat{B}_\mu \hat{H}_n \hat{B}_\nu - \tfrac{1}{2} [\hat{B}_\mu \hat{B}_\nu, \hat{H}_n]_+ \rangle \tag{165}$$

(note that, unlike $\hat{H}_S$, $\hat{H}_n$ is time-independent).

### 7.8. Work rate

Work is the contribution to the change of total energy $E_{SB} = \langle \hat{H}_{SB} \rangle$ due to the time dependence of the total Hamiltonian operator $\hat{H}_{SB}(t)$ [cf. Eq. (159)]. Thus a natural definition of the work performed in each time step $t_{n-1} \le t < t_n$ reads

$$\delta W = \mathrm{Tr}_{SB} \{ \Delta \hat{H}_{SB}\, \sigma_{n-1} \} \tag{166}$$

with $\Delta \hat{H}_{SB}$ the change of operator $\hat{H}_{SB}$ in the considered time interval. Since the only time-dependent terms in $\hat{H}_{SB}(t)$ are (in general) $\hat{H}_S(t)$ and $\hat{V}(t)$, we can split $\delta W$ into a pair of corresponding terms

$$\delta W = \delta W_d + \delta W_{\rm sw} \tag{167}$$

with

$$\delta W_d = \mathrm{Tr}_S \{ \Delta \hat{H}_S\, \rho_{n-1} \} \,, \quad \delta W_{\rm sw} = \mathrm{Tr}_{SB} \{ \Delta \hat{V}\, \sigma_{n-1} \} \,, \tag{168}$$

where subscript $d$ stands for "drive" (we used that $\hat{H}_S$ acts only on $S$). Here, $\delta W_{\rm sw}$ is the contribution due to the time dependence of $\hat{V}(t)$. We call it *switching work* since, physically, it is the work (generally) required for replacing an ancilla which completed its collision with a fresh one.

Now a subtle but relevant issue arises since the time derivative of $\Theta_n(t)$ [cf. Eq. (161)] is singular at times $t=t_n$ (for any $n$). At these times, $\hat{V}(t)$ undergoes the instantaneous switch $\hat{V}_n \to \hat{V}_{n+1}$. To take this switch into due account, all the changes throughout must be intended as computed over the time interval $[t_{n-1}+\varepsilon, t_n+\varepsilon[$ as sketched in Fig. 12(a) with the understanding that $\varepsilon \to 0^+$. As the singularity of (159) at time $t=t_n$ comes only from $\hat{V}(t)$, this slight change of time interval does not affect all the thermodynamic quantities other than $\delta W_{\rm sw}$ (in particular $\delta W_d$) with the only exception of $E'_S = \langle \hat{H}'_S \rangle$ which will be analyzed in Section 7.9.

Now, the redefined time step $[t_{n-1}+\varepsilon, t_n+\varepsilon[$ can be conveniently decomposed into a pair of consecutive intervals [see Fig. 12(b)]: $[t_{n-1}+\varepsilon, t_n-\varepsilon[$ (interval I) and $[t_n-\varepsilon, t_n+\varepsilon[$ (interval II). As $\hat{V}(t)$ is constant all over interval I, the switching work $\delta W_{\rm sw}$ is performed only in the very short time interval II [within which $\hat{V}(t)$ undergoes the sudden jump $\hat{V}_n \to \hat{V}_{n+1}$]. Accordingly, the switching work is correctly worked out as $\delta W_{\rm sw} = \mathrm{Tr}_{SB}\{(\hat{V}_{n+1}-\hat{V}_n)\hat{\sigma}(t_n-\varepsilon)\}$. More explicitly, using that $\hat{V}_{n+1}$ and $\hat{V}_n$ respectively involve ancillas $n$ and $n+1$, we get

$$\delta W_{\rm sw} = \mathrm{Tr}_{S,n+1} \{ \hat{V}_{n+1}\, \rho_n \eta_{n+1} \} - \mathrm{Tr}_{S,n} \{ \hat{V}_n\, \varrho_{Sn} \} \,, \tag{169}$$

where $\varrho_{Sn}$ (cf. Section 5.1) is the joint state of $S$ and ancilla $n$ *right after* they collided with one another.[43]

[43] Note that states must be continuous functions of time, hence in particular $\sigma(t_n-\varepsilon) = \sigma(t_n) = \sigma_n$.

### 7.9. First law of thermodynamics

During a *single* collision, the dynamics of $S$ and the involved ancilla is governed by the total Hamiltonian

$$\hat{H}_{\rm coll} = \hat{H}_S + \hat{H}_n + \hat{V}_n \,. \tag{170}$$

Since operators $\hat{H}_n$ and $\hat{V}_n$ are time-independent, $\Delta\hat{H}_{\rm coll} = \Delta\hat{H}_S$. Making now the replacements $\langle\Delta\hat{H}_{\rm coll}\rangle = \Delta E_S + \Delta E_n + {\rm Tr}_{S,n}\{\hat{V}_n\,\Delta\varrho_{S,n}\}$ and [cf. Eq. (168)] $\langle\Delta\hat{H}_S\rangle = W_d$, we get

$$\Delta E_S - \delta Q + {\rm Tr}_{S,n}\{\hat{V}_n\,\Delta\varrho_{Sn}\} = \delta W_d \,, \tag{171}$$

where we used $\langle\Delta\hat{H}_{\rm coll}\rangle = \langle\Delta\hat{H}_S\rangle = W_d$ and $\Delta E_n = -\delta Q$ [cf. Eq. (164)].

To connect the last identity with the switching work, in Eq. (169) we replace $\varrho_{Sn} = \rho_{n-1}\eta_n + \Delta\varrho_{Sn}$ obtaining

$$\delta W_{\rm sw} = {\rm Tr}_{S,n+1}\{\hat{V}_{n+1}\,\rho_n\eta_{n+1}\} - {\rm Tr}_{Sn}\{\hat{V}_n\,\rho_{n-1}\eta_n\} - {\rm Tr}_{S,n}\{\hat{V}_n\,\Delta\varrho_{Sn}\} \,. \tag{172}$$

Combining this with (171) and recalling the definition of $\hat{H}'_S$ [cf. Eq. (65)] and total work (167), we finally end up with the *1st law* of thermodynamics

$$\Delta E_S + \Delta E'_S = \delta Q + \delta W \,, \tag{173}$$

where $\Delta E_S + \Delta E'_S$ can be identified as the total energy change of $S$ when also the bath-induced Hamiltonian $\hat{H}'_S$ is accounted for.

The analogous law for instantaneous rates/fluxes (in the continuous-time limit) reads $\dot{E}_S + \dot{E}'_S = \dot{Q} + \dot{W}$.

An important case occurs for energy-conserving interactions [see Section 7.3 and Eqs. (150), (170)]. In this case, in the absence of drive i.e. for $\delta W_d = 0$, we get $[\hat{H}_S, \hat{H}_{\rm coll}] = -[\hat{H}_n, \hat{H}_{\rm coll}]$. Hence,

$$\Delta E_S = \delta Q \,. \tag{174}$$

This formalizes energy conservation in thermodynamic terms: energy lost (gained) by $S$ is absorbed from (released to) the bath of ancillas in the form of heat. Note that (173) in this case reduces to $\Delta E'_S = \Delta W_{\rm sw}$, namely the work (done by some external agent) for switching on and off the interaction with ancillas is entirely converted into extra energy of $S$ which adds to $E_S$.[44] This work yet vanishes for interaction Hamiltonians and ancilla states such that ${\rm Tr}_n\{\hat{V}_n\,\eta_n\} = 0$, as in Section 7.1.

### 7.10. Qubit coupled to baths of harmonic oscillators: energy balance per unit time and heat current

To illustrate the thermodynamic quantities introduced so far and the 1st law, let us reconsider the CM of Section 7.1 when $S$ is a qubit and each ancilla a quantum harmonic oscillator. Since the interaction is energy conserving, Eq. (174) holds. Moreover, $\delta W_d = 0$ (no drive) and ${\rm Tr}_n\{\hat{V}_n\,\eta_n\} = 0$, hence $\Delta E'_S = 0$. Consistently, the switching work vanishes since, using Eq. (173), $W_{\rm sw} = \Delta E_S - \Delta Q = 0$. Thus overall no work is performed. Hence, in this thermalization process, Eq. (174) coincides with the 1st law.

Using Eq. (165) or the opposite of (163), after simple calculations we get that in the continuous-time limit the heat flux is given by[45]

$$\frac{dQ}{dt} = \omega_0\,[\gamma_+(1-p) - \gamma_- p\,] \,. \tag{175}$$

where the introduced the excited-state probability $p = \langle\hat{\sigma}_+\hat{\sigma}_-\rangle = 1 - \langle\hat{\sigma}_-\hat{\sigma}_+\rangle$ and the previously defined rates (143). Using Eq. (145), we get as expected that $\dot{Q} = \omega_0\dot{p} = \dot{E}_S$. We see that the heat flux undergoes an exponential decay (in magnitude) until it stops when $S$ reaches thermal equilibrium.

Next, as in the beginning of Section 7.3, we add a detuning to $S$ such that $\hat{H}_S = (\omega_0 + \delta)\hat{\sigma}_+\hat{\sigma}_-$. As the evolution of $p$ is just the same, heat flux (175) is identical. However, since now $[\hat{H}_S, \hat{H}_n] \neq 0$, $\dot{Q}$ no longer matches $\dot{E}_S$. Indeed, applying Eq. (163) in the continuous-time limit yields

$$\frac{dE_S}{dt} = (\omega_0 + \delta)\,[\gamma_+(1-p) - \gamma_- p] \,. \tag{176}$$

Upon comparison with (175), this shows that $\dot{E}_S$ differs from $\dot{Q}$ whenever $\delta \neq 0$. Their difference, using the 1st law (173) and $\hat{H}'_S = 0$, is the switching work per unit time

$$\dot{W}_{\rm sw} = \dot{E}_S - \dot{Q} = \delta\,[\gamma_+(1-p) - \gamma_- p] \,. \tag{177}$$

---

[44] This is reasonable since $\delta W_{\rm sw}$ is in fact the contribution to the change of $\langle\hat{H}'_S\rangle$ coming from a step dependence of operator $\hat{H}'_S$ [cf. Eqs. (65) and (168)].

[45] First-order terms vanish since in this case $[\hat{B}_\nu, \hat{H}_n] \propto \hat{b}_n, \hat{b}_n^\dagger$ whose expectation value on $\eta_n$ is zero. We also used $|0\rangle_S\langle 0| = \hat{\sigma}_-\hat{\sigma}_+ = \mathbb{I}_S - \hat{\sigma}_+\hat{\sigma}_-$ and $[\hat{b}_n, \hat{b}_n^\dagger] = 1$.

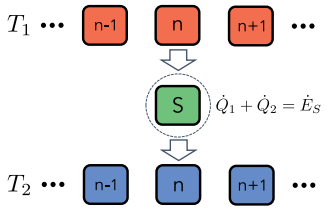


**Fig. 13.** *Stationary heat flux in a CM with two baths.* System $S$ collides with two baths of thermal ancillas, one at temperature $T_1$ one at $T_2$ with $T_1 \neq T_2$. In general, the continuity equation for heat current reads $\dot{Q}_1 + \dot{Q}_2 = \dot{E}_S$, meaning that the net energy entering/exiting from the dashed region must balance the change of energy of $S$. As stationary conditions are reached, the energy of $S$ no longer changes and a permanent heat current $\dot{Q}_1 = -\dot{Q}_2$ flows from the hot to the cold bath.

This provides the complete energy balance at each instant, showing that in order for $S$ to reach the asymptotic state work must be performed by an external agent.

Note that, in the situation just analyzed, $\dot{p} = 0$ entails $\dot{Q} = \dot{E}_S = \dot{W}_{\rm sw} = 0$, meaning that no energy flux occurs throughout the system once the steady state is reached. This is true regardless of $\delta$ since $\gamma_+(1-p) - \gamma_- p = \dot{p}$.

Differently from the case just seen, let us now illustrate an instance featuring an uninterrupted heat flux. This is the dynamics of Section 7.4 featuring system $S$ is contact with two baths at different temperatures, in which case (as explained at that time) the open dynamics of $S$ is formally the same (so that $S$ reaches a steady state) except that the absorption and emission rates are replaced by $\gamma_\pm \to \gamma'_\pm$ [cf. Eqs. (156) and (157)]. Thus in particular

$$\dot{p} = \gamma'_+(1-p) - \gamma'_- p\,, \tag{178}$$

Accordingly,

$$\frac{dE_S}{dt} = \omega_0 \left[\gamma'_+(1-p) - \gamma'_- p\right]\,. \tag{179}$$

Instead, the heat flux of bath $i$ [cf. Eq. (165)] is given by

$$\frac{dQ_i}{dt} = \omega_0 \left[\gamma^{(i)}_+(1-p) - \gamma^{(i)}_- p\right]\,. \tag{180}$$

Since $\gamma'_\pm = \gamma^{(1)}_\pm \pm \gamma^{(2)}_\pm$ we get the energy balance

$$\frac{dQ_1}{dt} + \frac{dQ_2}{dt} = \frac{dE_S}{dt} \tag{181}$$

(the switching work vanishes). This embodies a continuity equation for heat [see Fig. 13].

Asymptotically, $\dot{E}_S = 0$ so that

$$\frac{dQ_1}{dt} = -\frac{dQ_2}{dt}\,, \tag{182}$$

showing that stationary heat current flows from one bath to the other. In these conditions, by deducing from (178) the steady value of $p$ and using (156)–(157), we get the heat current

$$\frac{dQ_1}{dt} = -\frac{dQ_2}{dt} = \frac{\gamma_1\gamma_2(\bar{n}_1 - \bar{n}_2)}{\gamma_1 + \gamma_2 + 2(\gamma_1\bar{n}_1 + \gamma_2\bar{n}_2)}\,. \tag{183}$$

As expected, for $\bar{n}_1 > \bar{n}_2$ that is $T_1 > T_2$, $\dot{Q}_1 > 0$ meaning that heat flows from bath 1 towards bath 2.

### 7.11. Second law of thermodynamics

Each collision changes the joint state of $S$ and the involved ancilla, which evolves from $\rho_{n-1}\eta_n$ (uncorrelated) to $\varrho_{Sn}$ (generally correlated). The relative entropy of these two states, which we call *entropy production* $\Sigma$ for reasons that will be clear shortly, fulfills

$$\Sigma = \mathcal{S}(\varrho_{Sn} \parallel \rho_{n-1}\eta_n) \geq 0\,, \tag{184}$$

which simply follows from the property that relative entropy is always non-negative (see Appendix B). If, due to the interaction during the collision, $\varrho_{Sn}$ is a correlated state then it must be different from the initial state $\rho_{n-1}\otimes\eta_n$, entailing $\Sigma > 0$. Thus the strict positivity of $\Sigma$ witnesses establishment of system–ancilla correlations at each collision.

It can be shown[46] that $\Sigma$ can be split into the two contributions

$$\Sigma = \mathcal{I}_{Sn} + \mathcal{S}(\eta_n' \parallel \eta_n) \geq 0\,, \tag{185}$$

where $\mathcal{I}_{Sn}$ stands for the mutual information (see Appendix B) of $S$ and ancilla $n$ at the end of the collision, while $\mathcal{S}(\eta_n' \parallel \eta_n)$ is the relative entropy (see Appendix B) between the final and initial states of the ancilla. Now, since $S$ and $n$ are initially uncorrelated (mutual information zero), we have

$$\mathcal{I}_{Sn} = \Delta\mathcal{S}_S + \Delta\mathcal{S}_n \tag{186}$$

with $\Delta\mathcal{S}_S = \mathcal{S}(\rho_n) - \mathcal{S}(\rho_{n-1})$ and $\Delta\mathcal{S}_n = \mathcal{S}(\eta_n') - \mathcal{S}(\eta_n)$ the change of entropy of $S$ and ancilla, respectively. Here, we used that the $S$-$n$ dynamics during the collision is globally unitary, hence it cannot change the entropy of the joint state, i.e. $\Delta\mathcal{S}_{Sn} = \mathcal{S}(\varrho_{Sn}) - \mathcal{S}(\rho_{n-1}\eta_n) = 0$.

While the above holds for any ancilla state $\eta_n$, we now focus on a thermal bath of ancillas, i.e. we take $\eta_n = \eta_{\rm th}$ [cf. Eq. (139)]. In this case, recalling Eq. (B.4), the second term of (185) is given by,[47]

$$\mathcal{S}(\eta_n' \parallel \eta_{\rm th}) = -{\rm Tr}\{\eta_n' \log \eta_{\rm th} - \eta_n' \log \eta_n'\} = -\Delta\mathcal{S}_n - \beta\delta Q\,. \tag{187}$$

Replacing (186) and (187) in Eq. (185), we end up with the 2nd law in the form

$$\Delta\mathcal{S}_S \geq \beta\,\delta Q\,, \tag{188}$$

which in terms of instantaneous rates (in the continuous-time limit) reads $\dot{\mathcal{S}}_S \geq \beta\,\dot{Q}$.

In particular, note that we get an identity connecting a thermodynamic quantity to an information-theoretical one. Hence, production of entropy in (the thermodynamics sense) results from creation of system–ancilla correlations as well as perturbation of the ancilla thermal state (caused by the interaction with $S$).

We point out that the above derivation of the 2nd law for each time *step* relies crucially on having used a CM, this allowing to decompose the bath into distinct uncorrelated units which $S$ interacts with one at a time. In particular, we exploited that $S$ at each step is initially uncorrelated with the involved ancilla and this is still in the respective thermal state. The analogue of Eq. (185) for the entire bath $B$ holds only if it is referred to the entire evolution up to the considered step (i.e. replacing $t_{n-1} \to t_0$). This is because $S$ is uncorrelated with all the ancillas and these are all in a thermal state only at the initial time $t = t_0$ [see Figs. 3(a) and (d)]. From this viewpoint, it is remarkable that we got inequality (188) connecting the entropy change of system $S$ with the heat exchanged with the full bath $B$. This highlights particularly well a major advantage of employing a collisional description of non-equilibrium processes.

### 7.12. Landauer's principle

Let us define $\tilde{\mathcal{S}} = -\mathcal{S}$ and $\tilde{Q} = -Q$ in a way that $\Delta\tilde{\mathcal{S}}$ represents the decrease of entropy while $\tilde{Q} > 0$ is positive when heat flows from $S$ to $B$. Then (188) yields

$$\beta\,\delta\tilde{Q} \geq \Delta\tilde{\mathcal{S}}\,. \tag{189}$$

This is the quantum version of the so called Landauer's principle [87], stating that the heat dissipated into the bath is lower-bounded by the entropy decrease of system $S$. It entails that, in order to decrease the entropy of the open system so as to gain more information about it (see Appendix B), a finite amount of heat must be dissipated into the reservoir. In the continuous-time limit, the corresponding statement in terms of heat flux and instantaneous entropy decrease per unit time reads $\beta\dot{Q} \geq \dot{\tilde{\mathcal{S}}}$.

As an illustration, consider once again the CM analyzed at the beginning of Section 7.11. The dissipated heat per unit time is given by the opposite of (175). The entropy instead reads $S_S = -(1-p)\log p - p\log p$ (we assume zero coherences $c$ for simplicity). Hence, $\dot{\tilde{S}}_S = -\dot{p}\log\left(\frac{1-p}{p}\right)$ and we get

$$\beta\,\dot{\tilde{Q}} - \dot{\tilde{S}} = \gamma\left(\beta\omega_0 + \log\frac{p}{1-p}\right)\left((1+e^{\beta\omega_0})p - 1\right)\,. \tag{190}$$

Both factors between brackets on the right hand side change their sign when $p$ becomes greater than $1/(1+e^{\beta\omega_0})$, meaning that the product is indeed non-negative at any time $t$.

---

46 This is worked out as

$$\mathcal{S}(\varrho_{Sn} \parallel \rho_n \otimes \eta_n) = {\rm Tr}\{\varrho_{Sn}\log\varrho_{Sn}\} - {\rm Tr}\{\varrho_{Sn}\log\rho_n\otimes\eta_n\} = {\rm Tr}\{\varrho_{Sn}\log\varrho_{Sn}\} - {\rm Tr}\{\rho_n\log\rho_n\} - {\rm Tr}\{\eta_n'\log\eta_n\} =$$
$${\rm Tr}\{\varrho_{Sn}\log\varrho_{Sn}\} - {\rm Tr}\{\rho_n\log\rho_n\} - {\rm Tr}\{\eta_n'\log\eta_n\}\,.$$

Now, adding and subtracting ${\rm Tr}\{\eta_n'\log\eta_n'\}$ yields $\mathcal{S}(\varrho_{Sn} \parallel \rho_n\otimes\eta_n) = \mathcal{I}\{\varrho_{Sn}\} - {\rm Tr}\{\eta_n'\log\eta_n\} + {\rm Tr}\{\eta_n'\log\eta_n'\} = \mathcal{I}\{\varrho_{Sn}\} + \mathcal{S}(\eta_n' \parallel \eta_n) \geq 0$.

47 Inside the trace, we added and subtracted a term $\eta_{\rm th}\log\eta_{\rm th}$ and used ${\rm Tr}_n\{\Delta\eta_n\} = 0$ (since the state of ancilla of course remains normalized). We finally used $\delta Q = -{\rm Tr}_n\{\hat{H}_n(\eta_n' - \eta_{\rm th})\}$.

### 7.13. Non-equilibrium quantum thermodynamics: state of the art

The definition of thermodynamic quantities and derivation of thermodynamics laws are largely based on Refs. [31,88,89] (see also Ref. [90] where some aspects concerning the use of CMs in quantum thermodynamics are discussed). Note that Eq. (185) was first derived for bath thermal states in Ref. [91] and then generalized in Refs. [31,92].

We present next an overview of the quantum thermodynamics literature focusing on works that make explicit use of a collisional approach (our concern being mostly the methodological relevance for CMs theory).

The use of a CM to gain insight into the thermalization of a quantum system (see Sections Section 7.1, 7.2,7.3) appeared in a seminal work published in 2002 [23] (related to Ref. [22] mentioned in Section 4.10). This linked together dissipation, fluctuations (by deriving a CM-based version of the fluctuation–dissipation theorem [93]) and maximal system–ancilla entangling power. Notably, the CM approach allowed the authors to explicitly show how, due to entanglement, a dissipative (thus irreversible) process can result from a jointly unitary system–bath dynamics (see also Ref. [94]). Roughly in the same period, a similar CM was used by Diosi, Feldmann and Kosloff [95], where however the joint dynamics is made irreversible by randomizing identities of the ancillas.

Deviations from thermalization, in particular because of lack of energy-conserving interactions (see Section 7.3), were investigated in Refs. [96–98].

In the context of resource theories, Ref. [99] introduced a resource theory called "elementary thermalization operations" (ETOs) and showed that Markovian ETOs are closely linked to memoryless CMs. Ref. [100] instead studied almost thermal operations by relaxing the constraint of having identical ancillas all in the same thermal state.

Since only the reduced state of $S$ is involved in the definition of thermalization, an interesting question is whether or not $S$ can share correlations with the ancillas even after reaching thermalization. Strong evidence that $S$ gets asymptotically uncorrelated with the bath was provided in Ref. [101].

Note that not only a CM can model thermal baths, but can even implement an effective thermometer as proposed in Refs. [102,103] showing that collective measurements on the ancillas can provide quantum metrological advantages (an extension to stochastic collisions has been recently put forward in Ref. [104]) .

A class of problems where the collisional approach is very helpful are non-equilibrium dynamics in the presence of multiple, usually thermal, baths (see Sections 5.9 and 7.4). A standard case typically features a multipartite open system $S$ [cf. Fig. 8(b)] comprising a generally large number of subsystems $\{S_1, \ldots, S_N\}$ which are coupled to one another (modeled e.g. as a spin chain) [88,89,105–109]. Note that switching work (see Section 7.8) was first identified in a system of this kind by Barra in Ref. [88] and then further investigated in Refs. [31,89].

As seen in Section 5.9, uncorrelated multiple baths typically result in MEs of the form (89) featuring only local dissipators. The thermodynamic consistency of such *local MEs* (regardless of the way they are derived) was disputed [110]. In this context, Ref. [89] considered a CM with multiple baths and coupled subsystems yielding a local ME. By highlighting the key role of switching work (see Section 7.8), full consistency with both laws of thermodynamics (see Sections 7.9 and 7.11) was demonstrated.

Note that, while the baths are commonly assumed to be uncorrelated, Ref. [111] studied how inter-bath correlations affect thermal machine performances. This corresponds to a CM with multiple baths where in Eq. (85) $\chi_n^{\rm corr} \neq 0$, resulting in ME terms that couple the subsystems to one another [cf. Eq. (90)]. The corresponding ME can then be arranged in terms of collective jump operators as first demonstrated in Ref. [112]. The effect of correlated ancillas was also recently studied in the derivation of quantum Onsager relations via a collision model [113].

Multiple baths naturally enter thermal machines (see next) as these usually operate between reservoirs at different temperatures.

In 2003, Scully, Zubairy, Agarwal and Walther [32] proposed a heat engine based on the micromaser setup of Sections Section 5.7 with the difference that each thermal atom is a three-level system featuring a nearly two-fold-degenerate ground state (doublet). They showed that coherences stored in the doublet can work as an added control parameter to extract work from a single heat bath with some features unattainable by classical engines [32]. This established a paradigm of proposed engines/thermal machines whose working principle exploits some genuine quantum property (such as entanglement) [114–121].

CMs have become a routine description tool to investigate thermal machines, mostly in the quest for quantum-enhanced performances [122–127] and/or with the aim to explore quantum non-Markovian effects (see Section 8.7). Note in particular the possibility of using CMs to model processes with *partial* thermalization, which was investigated in Refs. [128–130].

A topical research line is investigating thermodynamics laws in the presence of *non-thermal* reservoirs, mostly motivated by the hope that bath in non-classical states could enable improved thermodynamic performances. Ref. [131] considered a CM with each ancilla prepared in a thermal state with added *coherences* of the order of $\sim \sqrt{\Delta t}$ quite like state (82) in Section 5.1. A bound was derived demonstrating explicitly that the consumption of bath quantum coherences can convert heat into work on $S$. Ref. [132] showed that coherences in the energy basis can both enhance (or deteriorate in some cases) the performance of thermal machines and let them operate in otherwise forbidden regimes. Ref. [133] showed that coherences in the bath can cause a thermalization to an apparent temperature which could be spectroscopically inferred [133].

A major class of bath quantum states with promising thermodynamic advantages are *squeezed states*. A broadband (white-noise) squeezed reservoir can be simulated via a CM featuring identical harmonic oscillator ancillas each prepared

in the same one-mode squeezed state, which could be implemented through an array of beam splitters as proposed in the 90s in Ref. [134] (see also Section 9.10). Such scheme can be generalized by considering non-identical ancillas each initially in a squeezed-thermal state (so as to encompass a thermal reservoir as a special case). Baths of ancillas prepared in squeezed-thermal states were used in Refs. [135–137].

The collisional approach to the Landauer's bound for fluxes (see Section 7.12) was introduced in Ref. [138], where a major focus was exploring the bound when $S$ is part of a larger multipartite system which causes deviations from the Markovian behavior. One of the considered case studies was the cascaded configuration of Sections 4.8 and 5.10, where the dependence of heat fluxes in the transient regime on intra-system correlations was formerly studied in Ref. [139]. We also note that, although not explicitly connected with CMs, a pertinent basic reference on the Landauer's principle adopting the language of quantum maps is a 2014 paper by Reeb and Wolf [140].

An intensively investigated topic in quantum thermodynamics is the possibility to define thermodynamic quantities and non-equilibrium laws at the level of single *quantum trajectories* (instead of unconditional dynamics as assumed throughout the present section) in a way that the resulting thermodynamics acquires an intrinsically stochastic nature (see the recent review in Ref. [141]). As discussed in Section 6, CMs are the natural microscopic framework for describing quantum trajectories, which explains their use as an advantageous tool in studies of *stochastic quantum thermodynamics* [92,142–148].

A major appeal of CMs in quantum thermodynamics (and beyond) is that they allow relaxing the standard weak-coupling assumption and thus exploring the "ultra-strong" coupling regime where counter-rotating terms cannot be neglected as done e.g. in Refs. [89,149–151].

CMs can be used to introduce decoherence for extending *fluctuations theorems* to quantum *non-unitary* transformations [152].

Although not discussed in Section 7.8, the work on $S$ can be seen as resulting from collisions with a bath of ancillas in the case that the unitary collision is approximated to first order, resulting only in $\hat{H}'_S$ [cf. Eqs. (64) and (65)]. This was used for proposing a definition of work independent of the $S$ free Hamiltonian [153]

## 8. Non-Markovian collision models

So far we have been focusing on memoryless (i.e. Markovian) CMs. Yet, an important application of CMs is the description of *non-Markovian* (NM) dynamics. This will be the subject of the present section.

Corresponding to assumptions (1)–(3) (cf. Section 4.1.1) underpinning the basic, Markovian, CM (see Section 4.1.1), one can identify three main classes of NM extensions of CMs:

(i) CMs with added ancilla–ancilla collisions;
(ii) CMs with initially-correlated ancillas;
(iii) CMs with multiple collisions.

It is understood that each class relaxes the corresponding hypothesis in Section 4.1 without breaking the other two. Of course mixed cases relaxing two or all of the hypotheses are also possible, an instance being the so called *composite* CMs (which will be introduced in Section 8.5) which have connections with both classes (1) and (3).

In the following, we introduce each of the above three classes discussing some related basic properties.

### 8.1. Ancilla–ancilla collisions

Introducing ancilla–ancilla collisions is physically motivated since it natural to think that ancillas can generally interact with one another. In its (arguably) simplest formulation (see Fig. 14), such a CM is obtained from the basic CM of Section 4.1 by adding extra pairwise ancilla–ancilla (AA) collisions between system–ancilla (SA) collisions. As sketched in Fig. 14, the CM dynamics starts with a standard collision between $S$ and ancilla 1 (unitary $\hat{U}_1$). Then ancillas 1 and 2 collide together (unitary $\hat{W}_{12}$). This is followed by an SA collision between $S$ and ancilla 2 (unitary $\hat{U}_2$), then an AA collision 2–3, then $S$-3 and so on. As a key feature, AA collisions are interspersed with SA collisions: for instance, *prior to* the collision with $S$, ancilla 2 interacts with ancilla 1 (with which $S$ is correlated due to the previous collision). As a result of this AA collision, $S$ and ancilla 2 are thus already correlated *before* collision $S$-2 starts. Hence, regarding the open dynamics of $S$, the second step (ending with $S$-2 collision) cannot be described by a CPT map and so cannot all the remaining steps. The CP-divisibility condition [cf. Eq. (15)] thereby does not hold, making the dynamics non-Markovian.

Calling $\hat{W}_{n,n-1}$ the unitary describing the AA collision between ancillas $n-1$ and $n$, the joint $S$-$B$ dynamics is given by

$$\sigma_n = \hat{U}'_n \cdots \hat{U}'_2 \, \hat{U}'_1 \, \sigma_0 \, (\hat{U}'_1)^\dagger \, (\hat{U}'_2)^\dagger \cdots , (\hat{U}'_n)^\dagger \tag{191}$$

with the step unitary $\hat{U}'_n$ defined as

$$\hat{U}'_n = \hat{U}_n \hat{W}_{n,n-1} \ \ (\text{for } \ n \geq 2) , \quad \hat{U}'_1 = \hat{U}_1 , \tag{192}$$

hence (except for $n = 1$) $\hat{U}'_n$ describes an AA collision followed by a SA one. This can be contrasted with Eq. (3) holding for a basic CM. As usual, we take as initial state $\sigma_0 = \rho_0 \otimes_n \eta_n$ featuring no correlations.

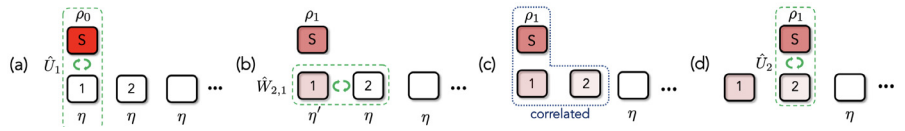


**Fig. 14.** *Non-Markovian collision model with ancilla–ancilla collisions*. Just like the basic CM of Fig. 3, all ancillas are initially uncorrelated and in the first step $S$ collides with ancilla 1 (a), getting correlated with it (not shown here). Yet, before $S$ collides with $n = 2$, ancillas 1 and 2 collide together (b). As a result of this AA collision, $S$, ancilla 1 and ancilla 2 are jointly correlated (c). Now, $S$ collides with 2 (d) with which it is however correlated already *before* collision $S$-2 starts. Collisions with ancillas $m > 3$ are obtained by iteration.

To understand the main features of the open dynamics entailed by this CM, it is helpful to take each AA collision unitary in the form of a partial SWAP [cf. Eq. (24)]

$$\hat{W}_{n,n-1} = \sqrt{q}\,\mathbb{I} + \sqrt{p}\,\hat{S}_{n,n-1} \tag{193}$$

with $q = 1 - p$, where we recall that unitary $\hat{S}_{n,n-1} \equiv \hat{S}^{\dagger}_{n,n-1}$ [cf. Eq. (22)] swaps the states of ancillas $n-1$ and $n$. Here, the swap probability $p$ can be regarded as a measure of the effectiveness of AA collisions.

For $p = 0$, $\hat{W}_{n,n-1} = \mathbb{I}$, thus AA collisions are fully ineffective. We retrieve in this case the standard memoryless CM [cf. Section 4.1] where $S$ undergoes the usual Markovian dynamics given by

$$\rho_n = \mathcal{E}^n[\rho_0] \tag{194}$$

with $\mathcal{E}$ the usual collision (CPT) map [cf. Eq. (6)].

Let us now study the other extreme case $p = 1$, when $\hat{W}_{n,n-1}$ is just a swap and AA collisions have the maximum effect. First note that the unitary transformation defined by $\hat{S}_{n,n-1}$ turns an operator acting on $S$ and $n$ into its analogue on $S$ an ancilla $n-1$

$$\hat{O}_{S,n-1} = \hat{S}_{n,n-1}\hat{O}_{S,n}\hat{S}_{n,n-1}\,. \tag{195}$$

Using this and $\hat{S}_{2,1}\hat{S}_{2,1} = \mathbb{I}$, the overall unitary at step $n = 2$ can be arranged as

$$\hat{U}'_2\hat{U}'_1 = \hat{U}_2\hat{S}_{2,1}\hat{U}_1 = (\hat{S}_{2,1}\hat{S}_{2,1})\,\hat{U}_2\hat{S}_{2,1}\hat{U}_1 = \hat{S}_{2,1}(\hat{S}_{2,1}\hat{U}_2\hat{S}_{2,1})\hat{U}_1 = \hat{S}_{2,1}\hat{U}_1^2\,, \tag{196}$$

where we used that $\hat{S}_{2,1}\hat{U}_2\hat{S}_{2,1} = \hat{U}_{S,1}$ [due to Eq. (195)].

Upon iteration,[48] at step $n$

$$\hat{U}'_n\cdots\hat{U}'_1 = \hat{S}_{2,1}\cdots\hat{S}_{n-1,n-2}\hat{S}_{n,n-1}\,\hat{U}_1^n\,. \tag{197}$$

Thereby, we get that the CM dynamics can be equivalently seen as the usual collision between $S$ and ancilla 1 yet repeated $n$ times, followed by a sequence of AA swaps. This property, along with the assumption that ancillas start all in the *same* state $\eta_n$, allows to work out the evolution of $S$ as (see Appendix I)

$$\rho_n = \mathcal{F}_n[\rho_0] = \mathrm{Tr}_1\{\hat{U}_1^n\rho_0\,\eta_1\hat{U}_1^{\dagger n}\}\,. \tag{198}$$

This can be contrasted with the case $p = 0$ [see Eq. (194)] which, since $\eta_n$ is the same for all ancillas, can be written as

$$\rho_n = \mathcal{E}^n[\rho_0] \quad \text{with} \quad \mathcal{E}[\rho] = \mathrm{Tr}_1\{\hat{U}_1\,\rho\,\eta_1\,\hat{U}_1^{\dagger}\} \equiv \mathcal{F}_1[\rho]\,. \tag{199}$$

Interestingly, from a formal viewpoint, maps (198) and (199) differ for the fact that, while in (198) the exponentiation to power $n$ involves the collision *unitary*, in (199) the exponentiation is instead over the collision *map* (i.e. the exponentiation is carried out after the partial trace).

Physically, Eq. (198) describes just the same open dynamics which $S$ would undergo if it were interacting all the time with the *same* ancilla.[49] Notably, adopting such a viewpoint, even Eq. (199) could be seen as resulting from an everlasting interaction with the same ancilla, yet with the crucial difference that the ancilla state is *periodically reset* to $\eta_1$ at each time step $\Delta t$.

The reason why, when $p = 1$, the open dynamics effectively results from a non-stop interaction always with the same ancilla [cf. (198)] is easily grasped. As pictured in Fig. 15, at the end of collision $S$-1 [see Fig. 15(a)], $S$ and ancillas 1–2 are in state $\varrho_{S,1}\otimes\eta_2$ with $\varrho_{S,1}$ a correlated state. Swap $\hat{S}_{2,1}$ is now applied [see Fig. 15(b)], yielding

$$\hat{S}_{2,1}\varrho_{S,1}\otimes\eta_2\hat{S}_{2,1} = \eta_1\otimes\varrho_{S,2}\,, \tag{200}$$

[48] In the case $n = 3$, we get $\hat{U}'_3\hat{U}'_2\hat{U}'_1 = \hat{U}_3\hat{S}_{3,2}\hat{U}_2\hat{S}_{2,1}\hat{U}_1 = \hat{U}_3\hat{S}_{3,2}(\hat{S}_{2,1}\hat{U}_1^2) = \hat{S}_{2,1}\hat{S}_{3,2}\,\hat{U}_1^3$, where we used that $(\hat{S}_{2,1}\hat{S}_{3,2})\hat{U}_3(\hat{S}_{3,2}\hat{S}_{2,1}) = \hat{S}_{2,1}\hat{U}_2\hat{S}_{2,1} = \hat{U}_1$ and $(\hat{S}_{2,1}\hat{S}_{3,2})^2 = \mathbb{I}$.

[49] Indeed, $(\hat{U}_n)^n = (e^{-i\hat{H}_{\rm coll}\Delta t})^n = e^{-i\hat{H}_{\rm coll}t_n}$ (with $t_n = n\Delta t$ as usual).

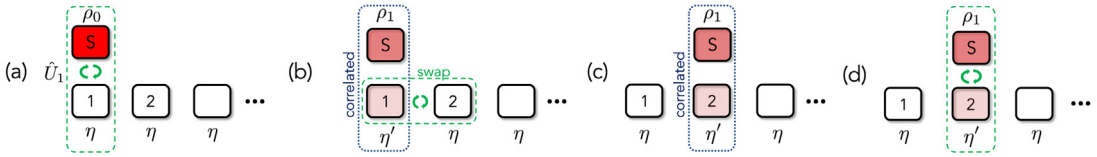


**Fig. 15.** *Fully swapping ancilla–ancilla collisions*. The unitary describing each AA collision is a full swap, $\hat{W}_{n,n-1} = \hat{S}_{n,n-1}$. At the end of the first SA collision (a), a swap is applied on ancillas 1 and 2 (b). Thereby, in particular, state $\eta'$, is transferred to ancilla 2 with 1 thus returning to the initial state $\eta$ (c). Actually, it is the joint (correlated) state of $S$ and 1 which is transferred altogether to $S$ and 2 (c). Thus, in terms of *open* dynamics, it is just as if the first SA collision resumed with the same ancilla, lasting a further time $\Delta t$ until $t = t_2$ (d).

which transfers altogether the *joint* $S$-1 state to $S$ and ancilla 2, while 1 returns to state $\eta$ uncorrelated with $S$ and 2 [see Fig. 15(c)]. This entails that the $S$-2 collision [see Fig. 15(d)] is seen by $S$ (open dynamics) just as if the collision with ancilla 1 resumed and then continued up to time $t = t_2$. We point out that, while the above *in particular* implies that 1 and 2 swap their respective reduced states (during the AA collision), this alone would not be sufficient for Eq. (198) to hold. The transfer of system–ancilla correlations from $S$-1 to $S$-2 brought about by (200) is thus essential. Analogous considerations apply at any step with $S$-$n$ correlations transferred to $S$ and ancilla $n+1$.

It is worth stressing that the mapping into a continuous interaction with the same ancilla does not hold for the *joint* dynamics. A major appeal of the CMs with ancilla–ancillas collisions as defined here is that the open dynamics can be analytically described, as will be shown in Section 8.5 by connecting these models with composite CMs. Moreover, under an appropriate redefinition of AA collisions, one can even work out a closed ME for $S$ as discussed next.

### 8.2. Non-Markovian master equation in the presence of ancilla–ancilla collisions

In the previous CM when AA collisions are full swaps ($p = 1$), the dynamics is strongly *non-Markovian*. Formally, this is because there is no way of decomposing map (198) into a sequence of CPT maps, one for each step, thus the CP divisibility condition (15) is not satisfied. To understand the physical reason behind NM behavior, think of a continuous coherent interaction between $S$ and another system $A$. If this dynamics were memoryless, the knowledge of the reduced state $\rho(t')$ at an intermediate time $t'$, such that $t_0 < t' < t$, would be sufficient for determining the evolution of $\rho$ between $t'$ and $t$ (if the Hamiltonian is known). This cannot be the case as during the evolution the two systems are generally in a *correlated* state $\varrho_{SA}(t)$ such that $\rho(t) = \mathrm{Tr}_A\{\varrho_{SA}(t)\}$: knowing only $\rho(t)$ does not allow reconstructing the joint state $\varrho_{SA}(t)$.[50]

To sum up, if $p = 0$, to get $\rho_n$ it is enough knowing the state of $S$ at the previous step and apply map $\mathcal{E} = \mathcal{F}_1$, i.e. $\rho_n = \mathcal{F}_1[\rho_{n-1}]$. In contrast, if $p = 1$, we need to know in which state $S$ ultimately started at $t = t_0$ and apply map $\mathcal{F}_n$, i.e. $\rho_n = \mathcal{F}_n[\rho_0]$. We might expect these two evolutions to be special cases of a recurrence rule, valid for any swap probability $p$, expressing $\rho_n$ generally in terms of $\rho_0$, $\rho_1$, …, $\rho_{n-1}$ in a way that, as $p$ tends to 1, the number of previous steps which $\rho_n$ in fact depends on grows up. Unfortunately, it is not possible to work out such a closed relationship unless one introduces a little *modification* in the CM, as shown next.

First of all, it is convenient to introduce a compact formalism for unitary operators and partial traces expressing them as quantum maps[51]

$$\mathcal{U}[\sigma] = \hat{U}\sigma\hat{U}^\dagger\,, \quad \mathcal{T}_i[\sigma] = \mathrm{Tr}_i[\sigma]\,, \tag{201}$$

where $i$ can be any subsystem of the joint system which state $\sigma$ generically refers to (here $\hat{U}$ is intended as a generic unitary). For instance, in terms of (201), the usual open dynamics of a basic CM of Section [cf. Section 4.1] could be expressed as

$$\rho_n = \mathcal{T}_n \cdots \mathcal{T}_1 \mathcal{U}_n \ldots \mathcal{U}_1[\sigma_0] = \mathcal{T}_n \mathcal{U}_n \cdots \mathcal{T}_1 \mathcal{U}_1[\sigma_0] \tag{202}$$

(any $\mathcal{T}_n$ commutes with $\mathcal{U}_{n'\neq n}$). When AA collisions are added, each $\mathcal{U}_m$ is replaced by $\mathcal{U}_m\mathcal{W}_{m,m-1}$.

It is immediate to check that an AA collision in the form of a partial swap [cf. Eq. (193)] is described by the map

$$\mathcal{W}_{n,n-1}[\sigma] = q\sigma + p\hat{S}_{n,n-1}\sigma\hat{S}_{n,n-1} + \sqrt{qp}\,[\sigma, \hat{S}_{n.n-1}]_+\,. \tag{203}$$

The aforementioned modification of the CM with partial swaps consists in removing terms $\sim \sqrt{qp}$, namely we replace (203) with the new map

$$\mathcal{W}_{n,n-1} = q\,\mathcal{I} + p\,\mathcal{S}_{n,n-1}\,. \tag{204}$$

[50] Note that the same statement applies to the dynamics of each single collision even for a basic memoryless CM. Yet, this lasts only a short time $\Delta t$, so that on a time scale far larger than $\Delta t$ the dynamics is Markovian.

[51] Despite we use the same symbol, map $\mathcal{T}_i$ here is different from map $\mathcal{T}_n$ introduced in Section 4.3.

This is a well-defined CPT map, having $\sqrt{q}\,\mathbb{I}$ and $\sqrt{p}\,\hat{S}_{n,n-1}$ as Kraus operators (see Appendix C). Note that, while the removal of such terms affects the collisional dynamics, all the salient features discussed so far hold. In particular, map $\mathcal{W}_{n,n-1}$ swaps the states of ancillas with probability $p$ or leave them unchanged.

To get a closed ME for $\rho_n$, we note that the joint state at each step evolves as

$$\sigma_n = \mathcal{U}_n\,(q\,\mathcal{I} + p\,\mathcal{S}_{n,n-1})\,[\sigma_{n-1}] = q\;\mathcal{U}_n[\sigma_{n-1}] + p\;\mathcal{U}_n\mathcal{S}_{n,n-1}[\sigma_{n-1}] \tag{205}$$

for $n \geq 2$ and $\sigma_1 = \mathcal{U}_1[\sigma_0]$.

For $n = 2$, we explicitly get $\sigma_2 = q\,\mathcal{U}_2\,[\sigma_1] + p\;\mathcal{U}_2\,\mathcal{S}_{2,1}[\sigma_1]$. Replacing next $\sigma_1 = \mathcal{U}_1[\sigma_0]$ only in the second term yields

$$\sigma_2 = q\,\mathcal{U}_2\,[\sigma_1] + p\;\mathcal{U}_2\,\mathcal{S}_{2,1}\,\mathcal{U}_1[\sigma_0] = q\,\mathcal{U}_2\,[\sigma_1] + p\,\mathcal{U}_2^2[\sigma_0]\,, \tag{206}$$

where we used the identity $\mathcal{S}_{n,n-1}\,\mathcal{U}_{n-1} = \mathcal{U}_n\mathcal{S}_{n,n-1}$[52] along with the invariance of the initial state $\sigma_0$ under any swap of ancillas (see Section 8.1). Notably, Eq. (206) is now arranged so as to feature only powers of $\mathcal{U}_2$. We can accomplish an analogous task at step $n = 3$ starting from $\sigma_3 = q\,\mathcal{U}_2\,[\sigma_2] + p\;\mathcal{U}_2\,\mathcal{S}_{2,1}[\sigma_2]$. Similarly to what done in the previous step, we replace $\sigma_2$ with (206) only in the second term, obtaining

$$\sigma_3 = q\,\mathcal{U}_3[\sigma_2] + qp\,\mathcal{U}_3\mathcal{S}_{3,2}\mathcal{U}_2[\sigma_1] + p^2\mathcal{U}_3\mathcal{S}_{3,2}\mathcal{U}_2^2[\sigma_0] = q\left(\mathcal{U}_3[\sigma_2] + p\,\mathcal{U}_3^2[\sigma_1]\right) + p^2\mathcal{U}_3^3[\sigma_0],$$

which now features only powers of $\mathcal{U}_3$.

Upon induction, at the $n$th step we get

$$\sigma_n = q\sum_{j=1}^{n-1} p^{j-1}\mathcal{U}_n^j\,[\sigma_{n-j}] \;+\; p^{n-1}\mathcal{U}_n{}^n[\sigma_0]\;, \tag{207}$$

containing only powers of $\mathcal{U}_n$ (collision unitary corresponding to the last SA collision). Note that the larger the power of $\mathcal{U}_n$ the older is the state it acts on. This property is remarkable since, given that $\mathcal{U}_n$ does not act on ancillas different from the $n$th one, the trace over all ancillas yields an equation formally analogous to (207) with $\sigma_n$ replaced by $\rho_n$ and each power $\mathcal{U}_n^j$ by map $\mathcal{F}_j$ [cf. Eq. (198)]

$$\rho_n = q\sum_{j=1}^{n-1} p^{j-1}\mathcal{F}_j\,[\rho_{n-j}] \;+\; p^{n-1}\mathcal{F}_n[\rho_0]\,. \tag{208}$$

As promised, we thus end up with a closed equation for the reduced state of $S$, which holds for arbitrary swap probability $p$. The corresponding dynamics interpolates between the memoryless case for $p = 0$ and the strongly NM dynamics for $p = 1$ [cf. Eq. (198)]. For arbitrary $p$, note that, due to the exponential weights $p^{j-1}$ and $p^{n-1}$, the current state is more affected by the latest steps. This formalizes the property that the system keeps *memory* of its past evolution, whose memory length ranges from 1 (Markovian case occurring for $p = 0$) to $n$ (strongly NM case occurring for $p = 1$).

Most remarkably, by defining a memory rate $\Gamma$ through $p = e^{-\Gamma\Delta t}$ in a way that, for $\Delta t \ll \Gamma^{-1}$, $p \simeq 1 - \Gamma\Delta t$, one can convert Eq. (208) into a corresponding ME in the continuous-time limit (see Appendix J) which reads

$$\dot{\rho} = \Gamma\int_0^t dt' e^{-\Gamma t'}\;\mathcal{F}(t')\left[\dot{\rho}(t-t')\right] + e^{-\Gamma t}\;\dot{\mathcal{F}}(t)[\rho_0]\;. \tag{209}$$

Here, $\mathcal{F}(t)$ is the continuous-time version of map (198).[53]

This kind of integro-differential non-Markovian MEs are called memory-kernel MEs. Independently of its derivation as the continuous-time limit of an intrinsically CPT discrete dynamics, it can be shown that Eq. (209) correctly entails a continuous-time CPT dynamics for any $\Gamma > 0$ [30].

### 8.3. Initially-correlated ancillas

Consider the basic CM of Section 4.1 where the initial state of the ancillas is generalized as

$$\rho_B = \sum_{m=1}^{M} p_m\,\chi_m\,, \tag{210}$$

where probabilities $\{p_m\}$ fulfill $\sum_{m=1}^{M} p_m = 1$ while

$$\chi_m = \eta_{m1}\otimes\eta_{m2}\otimes\;\ldots\;. \tag{211}$$

[52] Using Eq. (195), we get $\hat{S}_{n,n-1}\hat{U}_n\,\ldots\,\hat{U}_n^\dagger\hat{S}_{n,n-1} = \hat{S}_{n,n-1}\hat{U}_n\hat{S}_{n,n-1}^2\,\ldots\,\hat{S}_{n,n-1}^2\hat{U}_n^\dagger\hat{S}_{n,n-1} = \hat{U}_{n-1}\hat{S}_{n,n-1}\,\ldots\,\hat{S}_{n,n-1}\hat{U}_{n-1}^\dagger$, proving the identity.

[53] This is obtained by replacing in the definition [cf. Eq. (198)] $\hat{U}_n = (e^{-i\hat{H}_{\rm coll}\Delta t})^n = e^{-i\hat{H}_{\rm coll}t_n}$ with $\hat{U}(t) = e^{-i\hat{H}_{\rm coll}t}$ (with $t_n \to t$).

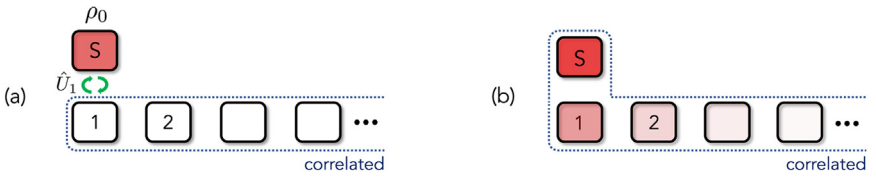


**Fig. 16.** *Non-Markovian collision model with initially-correlated ancillas.* Before interacting with $S$, ancillas are initially correlated with one other (a). Thereby, after colliding with ancilla 1, $S$ gets correlated with all the bath ancillas. Thus each collision (starting from the second one) is generally not described by a CPT map on $S$, making the dynamics non-Markovian.

Here, $\{\eta_{mn}\}$ are an arbitrary set of $M$ states of ancilla $n$. When all the $p_m$'s but one are zero, we recover the memoryless CM [cf. Eq. (1)]. In the general case, however, (210) is a not a product state and thus describe initially *correlated* ancillas [see panel (a) of Fig. 16]. After $n$ collisions, the joint initial state $\sigma_0 = \rho_0 \otimes \rho_B$ evolves into (cf. Eq. (3))

$$\sigma_n = \sum_{m=1}^{M} p_m \, \hat{U}_n \cdots \hat{U}_1 \, \rho_0 \otimes \chi_m \, \hat{U}_1^\dagger \cdots \hat{U}_n^\dagger \, . \tag{212}$$

The corresponding open dynamics of $S$ is given by

$$\rho_n = \sum_{m=1}^{M} p_m \, \mathrm{Tr}_B \left\{ \hat{U}_n \cdots \hat{U}_1 \, \rho_0 \otimes \chi_m \, \hat{U}_1^\dagger \cdots \hat{U}_n^\dagger \right\} = \sum_{m=1}^{M} p_m \, \Lambda_{mn}[\rho_0] \, , \tag{213}$$

where

$$\Lambda_{mn} = (\mathcal{E}_m)^n \tag{214}$$

with the CPT map $\mathcal{E}_m$ defined by

$$\rho' = \mathcal{E}_m[\rho] = \mathrm{Tr}_n \left\{ \hat{U}_n \rho \, \eta_{mn} \, \hat{U}_n^\dagger \right\} \, . \tag{215}$$

The evolution is thus a *mixture* of $M$ dynamics, each described by a dynamical map $\Lambda_{mn}$ (cf. Section 4.4) with associated collision map $\mathcal{E}_m$. As shown by (214), each $\Lambda_{mn}$ alone describes a fully Markovian collisional dynamics [cf. Eq. (12)].

According to (213), the dynamical map of the present collision model reads

$$\Lambda_n = \sum_{m=1}^{M} p_m \, \Lambda_{mn} \, . \tag{216}$$

Remarkably, while each $\Lambda_{mn}$ can be divided into elementary CPT collision maps [cf. Eq. (214)] thus being Markovian [cf. Section 4.4] this is generally *not* possible for $\Lambda_n$ despite it results from a seemingly innocent mixture of $\Lambda_{mn}$'s. This is best illustrated with a simple counterexample, which is discussed next.

Consider the all-qubit CM [see Section 4.6] with the ancillas starting in the correlated state

$$\rho_B = p|00\cdots\rangle_B\langle 00\cdots| + q|11\cdots\rangle_B\langle 11\cdots| \, , \tag{217}$$

where $|ii\cdots\rangle = \otimes_n |i\rangle_n$ with $i = 0, 1$ and with $p = 1 - q$ a probability. Assuming that $S$ starts in state $|1\rangle_S$, at the end of the first collision the joint state reads

$$\sigma_1 = p \, \left( \hat{U}_1 |10\rangle_{S1}\langle 01| \hat{U}_1^\dagger \right) \, |00\cdots\rangle_{23\ldots}\langle 00\cdots| + q \, \left( \hat{U}_1 |11\rangle_{S1}\langle 11| \hat{U}_1^\dagger \right) \, |11\cdots\rangle_{23\ldots}\langle 11\cdots| \, . \tag{218}$$

Taking for simplicity $g_z = 0$ [cf. Eq. (18)] and based on (21), we have

$$\hat{U}_1|10\rangle_{S1} = \cos(g\Delta t)|1\rangle_S|0\rangle_1 - i\sin(g\Delta t)|0\rangle_S|1\rangle_1 \, , \quad \hat{U}_1|11\rangle_{S1} = |1\rangle_S|1\rangle_1 \, . \tag{219}$$

By replacing these in (218) and tracing over ancilla 1, we get the reduced state of $S$ and ancillas 2,3, …

$$\mathrm{Tr}_1\{\sigma_1\} = p \left( c^2 |1\rangle_S\langle 1| + s^2 |0\rangle_S\langle 0| \right) \otimes |00\cdots\rangle_{23\ldots}\langle 00\cdots| + q|1\rangle_S\langle 1| \otimes |11\cdots\rangle_{23\ldots}\langle 11\cdots| \, , \tag{220}$$

where we set $c = \cos(g\Delta t)$ and $s = \sin(g\Delta t)$.

For $0 < p < 1$, this is a correlated state between $S$ and all ancillas 2,3, … . This means that each collision starting from the second one is generally not described a CPT map. It follows that the overall dynamical map $\Lambda_n$ does not satisfy the CP-divisibility condition (15), which witnesses the non-Markovian nature of the dynamics.

We note that, since a dynamics like (215) is a mixture of Markovian dynamics, if each of these admits a continuous-time limit then one can work out as many Lindblad master equations $\dot{\rho}_m = \mathcal{L}_m[\rho]$ having a form like Eq. (64). Solving these, the overall dynamics then results from the mixture of the respective solutions $\rho(t) = \sum_m p_m \rho_m(t)$. Due to non-Markovianity, however, $\rho(t)$ generally cannot be expressed as the solution of a well-defined Lindblad master equation.

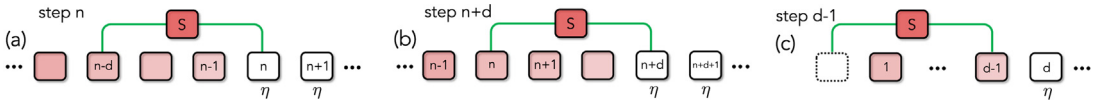


**Fig. 17.** *Non-Markovian collision model with non-local collisions.* Like in a basic CM, ancillas are non-interacting and initially uncorrelated. Yet, system $S$ interacts with the bath *non-locally* in the following sense: at the $n$th step, $S$ collides at once with ancillas $n-d$ and $n$ (bi-local collision). As a major consequence, ancilla $n$ collides with the system *twice*: the first time at step $n$ (a) and then again at step $n+d$ (b). Thus $d$ is the delay between the two collisions with the same ancilla. Before the second collision starts, ancilla $n$ and $S$ are already correlated so that the CP-divisibility condition (16) does not hold, making the dynamics NM. Notice that, until step $n=d-1$ (c), no memory effect can occur as each ancilla underwent at most one collision with $S$ [the dotted square in (c) is a phantom ancilla].

It is worth pointing out that, while state (210) is not entangled as it is a mixture of product states,[54] the essential conclusions on the non-Markovian nature of the dynamics apply to entangled states as well as is for instance the case of single-photon wavepackets to be discussed in Section 9.11.

### 8.4. Multiple collisions

Another mechanism for introducing memory in a CM is allowing each ancilla to collide with $S$ at many distinct, non-consecutive, steps, instead of only one [as in the basic CM of Section 4.1]]. A simple instance is a CM featuring a sequence of collisions like $\hat{U}_1, \hat{U}_2, \hat{U}_3, \hat{U}_1, \hat{U}_4, \hat{U}_5, \hat{U}_1, \ldots$ such that $S$-1 collision takes places every three steps.

While several possible multiple-collision schemes can be conceived (see also Section 8.7), here we focus on CMs with *non-local* collisions that naturally arise in quantum optics dynamics where delay times (light retardation) are non-negligible. The paradigm of such dynamics is shown in Fig. 17: at each step, $S$ simultaneously collides with *many* ancillas (two in the simplest case, as in the figure). More in detail, at the $n$th step, $S$ collides with ancillas $n-d$ and $d$, where $d$ is an integer such that $d \geq 1$ [see Fig. 17(a)]. Accordingly, at step $n+d$, the collision will involve ancillas $n$ and $n+d$ [see Fig. 17(b)]. It follows that a generic ancilla labeled with $n$ collides with $S$ *twice*: the first time at step $n$ and then again at step $n+d$. The resulting collisional dynamics is evidently non-Markovian: before the second collision starts (step $n+d$), $S$ is already correlated with ancilla $n$ due to the first collision (step $n$), hence the dynamical map will generally not fulfill the CP divisibility condition [cf. Eq. (16)]. As a paradigmatic, analytically solvable, instance consider the usual all-qubit model of Section 4.6 with $\hat{H}_S = \hat{H}_n = 0$ and the interaction Hamiltonian describing the $n$th collision now replaced by

$$\hat{V}^{(n)} = \sqrt{\tfrac{\gamma}{\Delta t}}\ \hat{\sigma}_+ (\hat{\sigma}_{n,-} + e^{i\phi}\hat{\sigma}_{n-d,-}) + \text{H.c.} \tag{221}$$

Here and throughout the present subsection, superscript "$(n)$" refers to the time step.[55] For completeness, we allowed for a phase shift $\phi$ between the couplings to the two ancillas. As initial state, we take $S$ in state $|1\rangle$ and each ancilla in state $|0\rangle$. Thus the joint initial state is $|\Psi^{(0)}\rangle = |1\rangle_S \otimes_m |0\rangle_m$.

Defining the total number of excitations as $\hat{N} = |1\rangle_S\langle 1| + \sum_m |1\rangle_m\langle 1|$, we note that this is conserved at all steps since $[\hat{V}^{(n)}, \hat{N}] = 0$. The eigenspace of $\hat{N}$ with eigenvalue $N=1$ (single-excitation sector) is spanned by $|e_S\rangle = |1\rangle_S \otimes_m |0\rangle_m$ (excitation on $S$) and $|e_{m'}\rangle = |0_S\rangle \otimes_{m\neq m'} |0\rangle_m \otimes |1\rangle_{m'}$ (excitation on ancilla $m'$). Thereby, since $|\Psi^{(0)}\rangle = |e_S\rangle$, the joint dynamics remains at all steps within the single-excitation sector. Accordingly, the joint state at step $n$ can be expanded as

$$|\Psi^{(n)}\rangle = \alpha^{(n)}|e_S\rangle + \sum_m \lambda_m^{(n)}|e_m\rangle\,. \tag{222}$$

In terms of excitation amplitudes $\alpha^{(n)}$ and $\lambda_m^{(n)}$, the initial state $|\Psi^{(0)}\rangle$ reads $\alpha^{(0)}=1$ and $\lambda_m^{(n)}=0$ for any $m$. For formal convenience, we will assume that the excitation amplitudes are defined also for negative values of the step index $n$, taking values $\alpha^{(n\leq 0)}=1$, $\lambda_m^{(n\leq 0)}=0$ (for any $m$). The evolution of the joint state at each step reads $|\Psi^{(n+1)}\rangle = \hat{U}_{n+1}|\Psi^{(n)}\rangle$[56] where the collision unitary is defined by $\hat{U}_n = \exp[-i\hat{V}^{(n)}\Delta t]$ with $\hat{V}_n$ having the form (221).

At short enough $\Delta t$ (we limit the analysis to this regime only), we expand $\hat{U}_{n+1}$ to the 2nd order in $\hat{V}^{(n)}$ and then apply it to (222). Projecting the resulting state on $|e_S\rangle$ yields a recurrence relation for amplitudes $\alpha^{(n)}$ and $\lambda_m^{(n)}$, which reads

$$\alpha^{(n+1)} = \alpha^{(n)} - \gamma\,\Delta t\,\alpha^{(n)} - i\sqrt{\gamma\,\Delta t}\,e^{i\phi}\lambda_{n-d}^{(n)}\,. \tag{223}$$

Here, we used that $\lambda_n^{(n)} = 0$ since, at step $n$, the $n$th ancilla is still in the initial state $|0\rangle_n$ [see Fig. 17(a)]. Our goal is expressing $\lambda_{n-d}^{(n)}$ in terms of $\{\alpha^{(n)}\}$ so as to end up with a closed equation for $\{\alpha^{(n)}\}$ (which fully describes the open dynamics).

54 Yet, one such state can still feature non-classical correlations in the form of so called quantum discord [154].

55 Since more than one ancilla collides with the system at each step, we can longer use a common index for labeling the colliding ancilla and time step.

56 Due to the specific type of calculations involved, in this subsection we define the generic step as the time interval between times $t_n$ and $t_{n+1}$, instead of $t_{n-1}$ and $t_n$ as usually done throughout the paper. This helps keeping notation relatively light.

Considering first the case $n \geq d$, note that ancilla $n-d$ collides with $S$ the first time at step $n-d$ and then at step $n$. Thus the corresponding amplitude at step $n-d+1$ cannot change any more until step $n$

$$\lambda_{n-d}^{(n)} = \lambda_{n-d}^{(n-1)} = \cdots = \lambda_{n-d}^{(n-d+1)} \,. \tag{224}$$

Amplitude $\lambda_{n-d}^{(n-d+1)}$ can be worked out, similarly to $\alpha^{(n+1)}$ in Eq. (223), by applying the collision unitary $\hat{U}_{n-d+1}$ to $|\Psi^{(n-d)}\rangle$ and projecting next to $|1_{n-d}\rangle$. This yields

$$\lambda_{n-d}^{(n-d+1)} = -i\sqrt{\gamma\,\Delta t}\,\alpha^{(n-d)} + \tfrac{1}{2}\gamma\,\Delta t\,\lambda_{n-2d}^{(n-d)} \,. \tag{225}$$

Due to Eq. (224), this coincides with $\lambda_{n-d}^{(n)}$ so that Eq. (223) becomes

$$\alpha^{(n+1)} - \alpha^{(n)} = -\gamma\,\Delta t\,\alpha^{(n)} - \gamma\,\Delta t\,e^{i\phi}\,\alpha^{(n-d)} \,,$$

where the term $\sim \lambda_{n-2d}^{(n-d)}$ was neglected being of order $\sim \Delta t^{3/2}$. We thus get

$$\frac{\Delta\alpha^{(n)}}{\Delta t} = -\gamma\alpha^{(n)} - \gamma e^{i\phi}\alpha^{(n-d)} \quad \text{for} \;\; n \geq d \,. \tag{226}$$

where $\Delta\alpha^{(n)} = \alpha^{(n+1)} - \alpha^{(n)}$.

We are left with the case $0 \leq n < d$. For these values of $n$, Eq. (223) misses the last term because of the initial conditions [see below Eq. (222)], thus reducing to $\Delta\alpha^{(n)}/\Delta t = -\gamma\alpha^{(n)}$.

To sum up, we thus conclude that the dynamics of $S$ is governed by the finite-difference equation

$$\frac{\Delta\alpha^{(n)}}{\Delta t} = \begin{cases} -\gamma\,\alpha^{(n)} & \text{for} \quad n < d \\ -\gamma\,\alpha^{(n)} - \gamma e^{i\phi}\alpha^{(n-d)} & \text{for} \quad n \geq d \end{cases} \,. \tag{227}$$

We can understand this equation as follows. Until step $n = d-1$ [see Fig. 17(c)], each ancilla undergoes at most one collision with $S$: in this initial stage, the dynamics is identical to a memoryless basic CM with $\alpha^{(n)}$ undergoing a standard exponential decay just like for spontaneous emission [cf. Eq. (81)]. Step $n = d$ is the first featuring an ancilla undergoing a second collision with $S$ (this is ancilla $m = 1$). From this step on, thereby, memory effects come into play as witnessed by the presence of term $\alpha^{(n-d)}$.

In the continuous-time limit, such that $t_n \to t$ and $d\Delta t \to \tau$ with $\tau$ a characteristic *delay time*, Eq. (227) is turned into[57]

$$\dot{\alpha} = -\gamma\alpha(t) - \gamma e^{i\phi}\alpha(t-\tau)\theta(t-\tau) \,, \tag{228}$$

which is a so called delay differential equation [here $\theta(x) = 1$ for $x > 0$ and $\theta(x) = 0$ otherwise].

### 8.5. Composite collision models

Besides the three non-Markovian generalizations of CM discussed so far, each constructed so as to directly break one of the assumptions (1)–(3) in Section 4.1.1, there is a further natural scheme to endow a CM with memory.

Consider a memoryless CM where $S$ is bipartite as sketched in Fig. 18(a). Its two susbsytems are $\mathcal{S}$ and $M$, the latter referred to as the "memory". The former, namely $\mathcal{S}$, is the *open system* we are concerned with. By hypothesis, ancillas collide only with memory $M$ [see Figs. 18(a) and (c)] through unitaries $\hat{U}_{Mn}$. Between two next collisions, however, $\mathcal{S}$ undergoes a collision with $M$ described by unitary $\hat{U}_{\mathcal{S}M}$ [see Fig. 18(b)]. Now, while the reduced dynamics of $S$ is of course fully Markovian, so is not that of $\mathcal{S}$ which will be generally correlated with $M$ before each internal collision $\hat{U}_{\mathcal{S}M}$. More explicitly, if $\varrho_{\mathcal{S}M}^{(n-1)}$ is the (generally correlated) state of $\mathcal{S}$ and $M$ at the end of collision $\hat{U}_{M,n-1}$, the state of $\mathcal{S}$ at step $n$ is given by[58]

$$\rho_n = \mathrm{Tr}_M \mathrm{Tr}_n\{\hat{U}_{Mn}\hat{U}_{\mathcal{S}M}\,\varrho_{\mathcal{S}M}^{(n-1)} \otimes \eta_n\,\hat{U}_{\mathcal{S}M}^\dagger \hat{U}_{Mn}^\dagger\} \,. \tag{229}$$

This is not a CPT map on $\mathcal{S}$ because unitary $\hat{U}_{Mn}\hat{U}_{\mathcal{S}M}$ acts on a state featuring correlations between $\mathcal{S}$ and $M$-$n$ (since $\varrho_{\mathcal{S}M}^{(n-1)}$ is not a product state).

We see that in this dynamics the effective environment in contact with $\mathcal{S}$ in fact comprises the ancillas *plus* $M$. Only the former are still "fresh" when colliding with $S$. In contrast, $M$ is continuously recycled, thus keeping memory of the evolution at previous steps. Note that, in contrast to $\mathcal{S}$, the reduced dynamics of $S$ is always fully memoryless (in this specific respect similarly to the cascaded CM of Section 4.8). One can thus describe the non-Markovian system $\mathcal{S}$ as "embedded" into the Markovian system $S$, in line with a common jargon in the open quantum systems literature. Indeed, this way of endowing a dynamics with memory ultimately is a typical one in the theory of open quantum systems. We also note that, as anticipated, a composite CM does not originate from breaking a single hypothesis among (1)–(3) (see

[57] This equation usually appears in the literature with phase $\phi \to \phi + \pi$, i.e. without the minus sign in the second term.

[58] In the present subsection, $\rho_n$ denotes the state of $\mathcal{S}$ not $S$

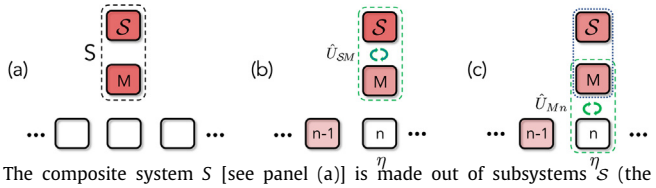


**Fig. 18.** *Composite collision model.* The composite system $S$ [see panel (a)] is made out of subsystems $\mathcal{S}$ (the open system under study) and $M$ ("memory"). System $S$ undergoes collisions with the ancillas (just like in a memoryless CM) which however involve only subsystem $M$. Before each $M$-ancilla collision [see panel (c)], $\mathcal{S}$ and $M$ collide with one another [see (b)] through unitary $\hat{U}_{\mathcal{S}M}$, hence they are generally correlated. Due to these correlations, the open dynamics of $\mathcal{S}$ cannot be divided into a sequence of CPT maps, one for each step, and is thus non-Markovian. In contrast, the dynamics of $S$ (i.e, $\mathcal{S}$ plus $M$) is fully Markovian since no correlations with ancilla $n$ exists prior to the $\hat{U}_{Mn}$ collision.

beginning of the section). Indeed, as the effective bath seen by $\mathcal{S}$ comprises in fact both $M$ and ancillas in a way that $M$ could be seen itself as an additional ancilla, we could say that both hypotheses (1) and (3) do not hold (since $M$ keeps interacting with the other ancillas and because $S$ collides with $M$ more than once). We will yet see in the next subsection that, so long as only the open dynamics is concerned, one can establish a precise mapping between CMs with ancilla–ancilla collisions and composite CMs.

In order to express the open dynamics in terms of the compact notation for unitaries and partial traces defined in Eq. (201), let us define the collision map on $M$ (corresponding to the $M$-$n$ collision) as[59]

$$\mathcal{M}[\ldots] = \mathrm{Tr}_n\{\hat{U}_{Mn}\ldots\otimes\eta_n\hat{U}_{Mn}^\dagger\} = \mathcal{T}_n\,\mathcal{U}_{Mn}[\ldots\otimes\eta_n]\,. \tag{230}$$

Accordingly, the initial state of $S$ after $n$ steps turns into

$$\rho_n = \mathcal{T}_M\,(\mathcal{M}\,\mathcal{U}_{\mathcal{S}M})^n\,[\rho_0\otimes\eta_M]\ \ , \tag{231}$$

where the leftmost partial trace returns the final reduced state of $\mathcal{S}$ (we assumed that the system starts in state $\sigma_0 = \rho_0\otimes\rho_M\otimes_n\eta_n$).

As an illustrative instance, consider a qubit $\mathcal{S}$, a memory qubit $M$ and a bath of qubit ancillas, whose pseudo-spin ladder operators are respectively denoted as $\hat{\sigma}_\pm$, $\hat{\sigma}_{M\pm}$ and $\{\hat{\sigma}_{n\pm}\}$. The $\mathcal{S}$-$M$ and $M$-ancilla collisions are described by unitaries[60]

$$\hat{U}_{\mathcal{S}M} = \exp\,[-i\hat{V}_{\mathcal{S}M}\,\Delta t]\,,\qquad \hat{U}_{Mn} = \exp\,[-i\hat{V}_{Mn}\Delta t] \tag{232}$$

with

$$\hat{V}_{\mathcal{S}M} = G\,(\hat{\sigma}_+\hat{\sigma}_{M-} + \hat{\sigma}_-\hat{\sigma}_{M+})\,,\qquad \hat{V}_{Mn} = g\,(\hat{\sigma}_{M+}\hat{\sigma}_{n-} + \hat{\sigma}_{M-}\hat{\sigma}_{n+})\,. \tag{233}$$

Both unitaries (232) conserve the total number of excitations $\hat{N} = |1\rangle_S\langle 1| + |1\rangle_M\langle 1| + \sum_n|1\rangle_n\langle 1|$. Accordingly, if all ancillas and $M$ are initially in state $|0\rangle$ and $\mathcal{S}$ is in state $|1\rangle$, a reasoning analogous to that in Section 8.4 [around Eq. (222)] entails that the joint state at each step necessarily has the form

$$|\Psi^{(n)}\rangle = \alpha^{(n)}|e_{\mathcal{S}}\rangle + \beta^{(n)}|e_M\rangle + \sum_{m=1}^{n}\lambda_m^{(n)}|e_m\rangle\,, \tag{234}$$

where, in analogy to Section 8.4, $|e_i\rangle$ with $i = \mathcal{S}, M, m$ is the state where subsystem $i$ is in the excited state $|1\rangle$ and all the others in $|0\rangle$. Here, the subscript on each amplitude denotes the time step.

Using Eq. (21) with the replacements $g_z = 0$ and $S \to M$, the effective representation of unitary $\hat{U}_{\mathcal{S}M}$ in the present dynamics reads

$$\hat{U}_{\mathcal{S}M} = |00\rangle_{\mathcal{S}M}\langle 00| + \cos(G\Delta t)(|10\rangle_{\mathcal{S}M}\langle 10| + |01\rangle_{\mathcal{S}M}\langle 01|) - i\sin(G\Delta t)(|01\rangle_{\mathcal{S}M}\langle 10| + |10\rangle_{\mathcal{S}M}\langle 01|)\,, \tag{235}$$

where we used that state $|11\rangle$ is never involved in the dynamics. The form of $\hat{U}_{Mn}$ is identical provided that $G$ is replaced by $g$ and $\mathcal{S}M \to Mn$.

Based on Eq. (234), applying $\hat{U}_{Mn}\hat{U}_{\mathcal{S}M}$ on $|\Psi^{(n-1)}\rangle$ yields for $\alpha^{(n)}$ and $\beta^{(n)}$ the recurrence relation (see Appendix K for details)

$$\begin{pmatrix}\alpha^{(n)}\\ \beta^{(n)}\end{pmatrix} = \mathbf{D}\,.\begin{pmatrix}\alpha^{(n-1)}\\ \beta^{(n-1)}\end{pmatrix}\quad\text{with}\quad \mathbf{D} = \begin{pmatrix}C & -icS\\ -iS & c\,C\end{pmatrix}\,, \tag{236}$$

where for brevity we set $c = \cos(g\Delta t)$, $s = \sin(g\Delta t)$, $C = \cos(G\Delta t)$, $S = \sin(G\Delta t)$. The solution of this equation is simply given by

$$\begin{pmatrix}\alpha^{(n)}\\ \beta^{(n)}\end{pmatrix} = \mathbf{D}^n.\begin{pmatrix}\alpha^{(0)}\\ \beta^{(0)}\end{pmatrix} \tag{237}$$

with $\alpha^{(0)} = 1$ and $\beta^{(0)} = 0$.

59 We assume $\eta$ to be the same for all ancillas. If not, $\mathcal{M}$ simply becomes $n$-dependent.

60 One could define yet more general composite CMs featuring non-unitary collisions.

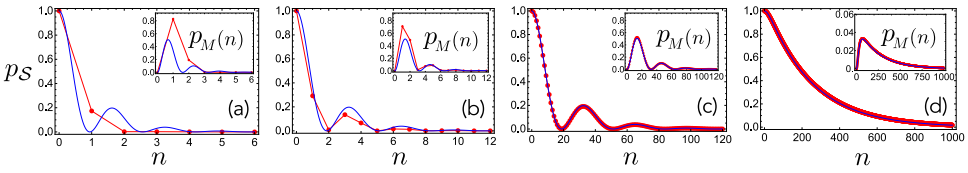


**Fig. 19.** *Dynamics of a composite collision model.* System $\mathcal{S}$, memory $M$ and all ancillas are qubits, while the collision unitaries have the form (232). Initially, $\mathcal{S}$ is in the excited state with $M$ and each ancilla in the ground state. Each panel shows $p_S = |\alpha^{(n)}|^2$ with the corresponding $p_M = |\beta^{(n)}|^2$ in the inset. Throughout we set $g = \sqrt{G/\Delta t}$. The first three panels [(a)–(c)] report the dynamics in the case $G = 1$ for $\Delta t = 2$ (a), $\Delta t = 1$ (b) and $\Delta t = 0.1$ (c), while in panel (d) we set $G = 0.1$, $\Delta t = 0.1$.

In Fig. 19, we plot the evolution of the excited-state population of $\mathcal{S}$ and $M$, respectively denoted with $p_S = |\alpha^{(n)}|^2$ and $p_M = |\beta^{(n)}|^2$, for $g = \sqrt{\gamma/\Delta t}$ and $G = 1$ [panels (a)–(c)], $G = 0.1$ (d), where energies are expressed in units of $\gamma = g^2\Delta t$. As $\Delta t$ decreases, the curves become more and more continuous as shown (for the case $G = 1$) by panels (a)–(c). We see that when $G$ is large [(a)–(c)], $\mathcal{S}$ and $M$ keep exchanging an excitation which eventually leaks out and gets dissipated into the bath of ancillas. In particular, $\mathcal{S}$ undergoes damped oscillations, exhibiting revivals which fade away for $n$ large enough. For $G$ small enough, however, the excitation of $\mathcal{S}$ monotonically decays and no revivals show up, while $p_M$ reaches a maximum and then decays. In the latter regime (small $G$), the interaction of $M$ with ancillas dominates over the $\mathcal{S}$-$M$ coupling so that as an excitation is transferred from $\mathcal{S}$ to $M$ this is immediately released into the bath before being reabsorbed by $\mathcal{S}$.

The above behavior is analogous to the dynamics of an atom coupled to a lossy cavity mode, a longstanding paradigm of non-Markovian dynamics [59]. Specifically, the regimes of damped oscillations [see Figs. 19(a)–(c)] and monotonic decay [see Fig. 19(d)] respectively correspond to the so called strong and weak coupling regimes of cavity QED. This link with cavity-QED dynamics can be formulated as an explicit mapping if we assume

$$G\Delta t \ll g\Delta t \ll 1 \tag{238}$$

and expand accordingly the overall unitary for short $\Delta t$ as [cf. Eqs. (232)–(233)]

$$\hat{U}_{\mathcal{S}M}\hat{U}_{Mn} \simeq \mathbb{I} - i(\hat{V}_{\mathcal{S}M} + \hat{V}_{Mn})\Delta t - \tfrac{1}{2}\hat{V}_{Mn}^2\Delta t^2\,. \tag{239}$$

This expression is now identical to Eq. (47) of Section 5.1 with $\hat{H}_0 = \hat{V}_{\mathcal{S}M}$ and $\hat{V}_n = \hat{V}_{Mn}$. It follows that the coarse-grained ME of the composite $\mathcal{S}$-$M$ system is given by [cf. Eqs. (64) and (65)]

$$\dot{\rho}_{\mathcal{S}M} = -i\,[G(\hat{\sigma}_+\hat{\sigma}_{M-} + \hat{\sigma}_-\hat{\sigma}_{M+}), \rho_{\mathcal{S}M}] + \gamma\left(\hat{\sigma}_{M-}\rho_{\mathcal{S}M}\hat{\sigma}_{M+} - \tfrac{1}{2}\,[\hat{\sigma}_{M+}\hat{\sigma}_{M-}, \rho_{\mathcal{S}M}]_+\right)\,, \tag{240}$$

where as usual $\gamma = g^2\Delta t$.[61] This is the bipartite ME of a two-level atom coupled to a leaky cavity mode initially in the vacuum state.[62] Now, if $\alpha(t)$ [$\beta(t)$] is the excited-state amplitude of $\mathcal{S}$ ($M$) at time $t$, it can be shown (see Appendix L) that ME (240) is equivalent to the pair of coupled equations

$$\dot{\alpha} = -iG\beta\,,\quad \dot{\beta} = -iG\alpha - \tfrac{\gamma}{2}\beta\,. \tag{241}$$

Solving the latter equation for $\beta(t)$[63] and replacing in the former yields the integro-differential equation

$$\dot{\alpha} = -\,G^2\int_0^t \mathrm{d}t'\, e^{-\frac{\gamma}{2}(t-t')}\alpha(t')\,, \tag{242}$$

whose solution is

$$\alpha(t) = e^{-\frac{\gamma}{4}t}\left[\cos\left(\tfrac{\delta t}{2}\right) + \tfrac{\gamma}{2\delta}\sin\left(\tfrac{\delta t}{2}\right)\right] \quad \text{with}\ \ \delta = \sqrt{4G^2 - \tfrac{1}{4}\gamma^2} \tag{243}$$

### 8.6. Mapping ancilla–ancilla collisions into a composite collision model

In Section 8.1, we saw that the open dynamics of a CM with fully-swapping ancilla–ancilla (AA) collisions reduces to a continuous interaction between $S$ and the same ancilla. Note that this can be seen as a special case of a composite CM with the memory trivially decoupled from the bath. Accordingly, one could guess that, when it comes to *arbitrary* AA

61 Given the approximations made, $\hat{U}_{\mathcal{S}M}$ and $\hat{U}_{Mn}$ commute. Hence, we can replace $\hat{U}_{\mathcal{S}M}\hat{U}_{Mn} \simeq e^{-i(\hat{V}_{\mathcal{S}M}+\hat{V}_{Mn})\Delta t}$, which can now be effectively thought as a single collision of duration $\Delta t$.

62 As no Fock states with more than one photon are involved in such dynamics, the bosonic ladder operators of the cavity can be equivalently replaced with ladder spin operators (here denoted as $\hat{\sigma}_{M\pm}$).

63 Specifically, this yields $\beta(t) = -i\,G\int_0^t \mathrm{d}t'\,\exp[-\frac{\gamma}{2}(t-t')]\alpha(t')$.

collisions, the open dynamics is effectively described by a suitably defined composite CM. We will show next that this is indeed the case and, remarkably, it is true no matter the form of AA unitaries.[64]

Let $\hat{R}_n = \hat{W}_{n+1,n}\hat{U}_{Sn}\cdots\hat{W}_{3,2}\hat{U}_{S2}\hat{W}_{2,1}\hat{U}_{S1}$ be the unitary describing the joint dynamics at the $n$th step.[65] Unitaries $\hat{R}_n$ then fulfill

$$\hat{R}_n = \hat{W}_{n+1,n}\hat{U}_{Sn}\,\hat{R}_{n-1}\,. \tag{244}$$

Let us also define for convenience a pairwise unitary on ancillas $n$ and $n-1$ as

$$\hat{W}'_{n,n-1} = \hat{S}_{n,n-1}\hat{W}_{n,n-1} \tag{245}$$

with $\hat{S}_{n,n-1}$ the usual swap operator.

At step $n=2$, we can arrange the total unitary as

$$\hat{R}_2 = \hat{W}_{3,2}\hat{U}_{S2}\hat{W}_{2,1}\hat{U}_{S1} = \hat{W}_{3,2}(\hat{S}_{2,1}\hat{U}_{S1}\hat{S}_{2,1})\hat{W}_{2,1}\hat{U}_{S1} = \hat{W}_{3,2}\hat{S}_{2,1}\hat{U}_{S1}\hat{W}'_{2,1}\hat{U}_{S1}\,, \tag{246}$$

where we expressed $\hat{U}_{S2}$ in terms of $\hat{U}_{S1}$ via (195) and used definition (245).

At step $n=3$, using (244) and (246), we get

$$\hat{R}_3 = \hat{W}_{4,3}\hat{U}_{S3}\hat{W}_{3,2}\hat{S}_{2,1}\hat{U}_{S1}\hat{W}'_{2,1}\hat{U}_{S1} = \hat{W}_{4,3}(\hat{S}_{3,2}\hat{U}_{S2}\hat{S}_{3,2})\hat{W}_{3,2}\hat{S}_{2,1}\hat{U}_{S1}\hat{W}'_{2,1}\hat{U}_{S1} = \hat{W}_{4,3}\hat{S}_{3,2}\hat{U}_{S2}\hat{W}'_{3,2}\hat{S}_{2,1}\hat{U}_{S1}\hat{W}'_{2,1}\hat{U}_{S1}. \tag{247}$$

Now, recalling that $\hat{O}_n\hat{S}_{n,n-1} = \hat{S}_{n,n-1}\hat{O}_{n-1}$, we move swap $\hat{S}_{2,1}$ to the left until it is placed to the right of $\hat{S}_{3,2}$. This turns $\hat{U}_{S2}\hat{W}'_{3,2}$ into $\hat{U}_{S1}\hat{W}'_{3,1}$, hence we get

$$\hat{R}_3 = \hat{W}_{4,3}\hat{S}_{3,2}\hat{S}_{2,1}\hat{U}_{S1}\hat{W}'_{3,1}\hat{U}_{S1}\hat{W}'_{2,1}\hat{U}_{S1} = \hat{W}_{4,3}(\hat{S}_{3,2}\hat{S}_{2,1})\hat{U}_{S1}\hat{W}'_{3,1}\hat{U}_{S1}\hat{W}'_{2,1}\hat{U}_{S1}\,. \tag{248}$$

By induction, at step $n$

$$\hat{R}_n = \hat{W}_{n+1,n}(\hat{S}_{n,n-1}\hat{S}_{n-1,n-2}\,\ldots\,\hat{S}_{2,1})\,\hat{U}_{S1}\hat{W}'_{n,1}\hat{U}_{S1}\hat{W}'_{n-1,1}\,\ldots\,\hat{U}_{S1}\hat{W}'_{2,1}\hat{U}_{S1}\,. \tag{249}$$

To get the reduced dynamics of $S$, we evolve the initial state via unitary $\hat{R}_n$ and trace off the ancillas as usual. In doing so, we add a further $\hat{S}_{n+1,n}$ to get another $\hat{W}'$ operator and move all the swaps to the left. Due to the partial trace, the sequence of swaps is eventually eliminated[66] so that we end up with

$$\rho_n = \mathrm{Tr}_{1,2,\ldots,n}\{\hat{R}_n\,\rho_0\otimes\eta_n\,\hat{R}_n^\dagger\} = \mathcal{T}_1\mathcal{T}_2\,\ldots\,\mathcal{T}_n\,\mathcal{W}'_{n+1,1}\mathcal{U}_{S1}\mathcal{W}'_{n,1}\mathcal{U}_{S1}\mathcal{W}'_{n-1,1}\,\ldots\,\mathcal{U}_{S1}\mathcal{W}'_{2,1}\mathcal{U}_{S1}[\rho_0\otimes_m\eta_m] \tag{250}$$

where as usual $\mathcal{U}_{S1}$ and $\mathcal{W}'_{n,1}$ are respectively the unitary maps associated with $\hat{U}_{S1}$ and $\hat{W}'_{n,1}$ [cf. Eq. (201)]. This open dynamics is identical to that of a composite CM as can be seen more explicitly by introducing a collision map on ancilla 1 as $\mathcal{M} = \mathcal{T}_n\mathcal{W}'_{n,1}$ so that Eq. (250) can be written as

$$\rho_n = \mathcal{T}_1\,(\mathcal{M}\,\mathcal{U}_{S1})^n\,[\rho_0\otimes\eta_1]. \tag{251}$$

Upon comparison with Eq. (231), we see that the open dynamics is indeed that of a composite CM where ancilla 1 embodies the memory. In this equivalent picture, the original SA collision unitary turns into the unitary describing the collision internal to the composite $S$-1 system, while the original AA unitary now embodies the collision describing memory–ancilla collisions.

The fact that it is enough to consider a single ancilla in order to get a composite system jointly undergoing Markovian dynamics clearly follows from the pairwise nature of each AA collision. For instance, if between two next SA collisions there occurred AA collisions overall involving *three* ancillas, then the composite Markovian system would comprise *two* ancillas (besides $S$). Thus the size of the effective composite system somehow measures how big is the portion of bath which we have to keep track in detail in order to describe our non-Markovian open dynamics. This effectively illustrates a distinctive feature of many non-Markovian dynamics, namely the impossibility to trace off the entire bath dynamics even if one is interested solely in the open dynamics.[67]

### 8.7. Non-Markovian collision models: state of the art

Non-Markovian CMs with ancilla–ancilla collisions (see Sections 8.1 and 8.2) were first introduced in Refs. [30,155] in the form of incoherent partial swaps [cf. (204)] alongside ME (209). CMs of the same class but with unitary ancilla–ancilla collisions, typically in the form of partial swaps [cf. Eq. (193)], were considered in Refs. [156–159] mostly

64 We will consider unitary AA collisions, yet the property can be extended to non-unitary collisions (as those in Section 8.2).

65 Note that the definition of step adopted here is slightly different from Eqs. (191) and (192). This yet has no effect on the open dynamics, which is our focus. Also, at variance with Section 8.1, here we explicitly show the $S$-dependence of SA collision unitaries, which facilitates establishing the connection with the notation used for introducing composite CMs.

66 This is because, if $\{|k_1,k_2,\ldots,k_n\rangle\}$ is an ancillas' basis, any given sequence of two-ancilla unitaries applied to all basis states $|k_1,k_2,\ldots,k_n\rangle$ yields another valid basis for computing the partial trace over the ancillas.

67 In this respect, the collisional dynamics in Section 8.2 is a remarkable exception which relies crucially on the non-unitary nature of AA collisions [cf. Eq. (204)].

with the goal of investigating the relationship between non-Markovianity and system–environment correlations (and changes in the bath state). Notably, this type of CMs are a convenient tool to introduce non-Markovian effects in quantum thermodynamics studies (see Section 7), which was applied in particular to investigate the Landauer principle of Section 7.12 in the presence of baths with memory [160–162], the temperature dependence of non-Markovianity [163], quantum engine performances [164,165] and a non-Markovian generalization of quantum homogenization (see Section Section 4.7) [166]. Remarkably, collisional dynamics with ancilla–ancilla collisions can be experimentally implemented in all-optical setups [167,168]. While most of these works considered qubits, continuous-variable versions of CMs with ancilla–ancilla collisions were proposed and studied in Ref. [169], featuring multipartite ancillas (environmental blocks), and Ref. [170], where both beam-splitter-like and two-mode-squeezing ancilla–ancilla interactions were investigated. It is also worth mentioning that ME (209) stimulated the study of a corresponding class of well-defined memory-kernel MEs [171–177].

A CM with initially-correlated ancillas (see Section 8.3) was introduced in Ref. [29]. The authors showed that any CPT map on a qubit $S$ can be simulated by a CM where $S$ collides with qutrits (i.e., three-level ancillas) initially prepared in a suitable, generally correlated, state. This includes the so called indivisible quantum channels [178], namely CPT maps that cannot be decomposed into infinitesimal CPT maps, thus violating in particular Eq. (16). The link discussed in Section 8.3 between correlated ancillas and mixtures of dynamical maps was extensively studied in Ref. [179] within a broader framework connected with concepts such as eternal CP indivisibility [180] and pictorially illustrated through Pauli maps (see also Ref. [181]). Note that in a condensed-matter scenario it is natural to consider ancillas as coupled spins described by a many-body Hamiltonian and, as such, initially correlated [182]. While one might expect that for growing inter-ancillary correlations the dynamics becomes more and more non-Markovian, correlations alone are yet insufficient to ensure non-Markovian behavior which indeed depends as well on the specific features of system–ancilla interaction. This was shown by Bernardes et al. [183] in terms of the non-Markovianity measure of Ref. [43] and then experimentally tested in all-optical [184] and NMR settings [185]. The CM in Ref. [183] was used as well to investigate the relationship between coarse-graining time and correlation time [186]. A collisional dynamics with initially-correlated ancillas was also experimentally implemented through the IBM Q Experience processors [187]. We also quote the use of such class of CMs in Ref. [188] investigating the relationship between CP divisibility and non-Markovianity.

CMs with multiple collisions (see Section 8.4) were proposed as a paradigm of non-Markovian quantum chain [189] (see also Ref. [190]) and recently applied in the study of quantum Markov order [191] and quantum cooling [192].

The derivation of Eq. (227) follows Ref. [193]. The equation is usually derived without resorting to the collisional approach, see e.g. Refs. [194,195]. Note that the phase $\phi$ which we included for completeness in the coupling Hamiltonian (221) significantly affects the emission.

This class of CMs with multiple, non-local, collisions were introduced in quantum optics by Refs. [56,196] which considered quantum emitters under a continuous drive [a dynamics considerably more involved than Eq. (227)]. Ref. [56] showed that the problem can be efficiently solved numerically using Matrix Product States (MPS), while Ref. [196] proposed an elegant diagrammatic technique mapping the non-Markovian dynamics of the emitter into the Markovian dynamics of a cascade of fictitious emitters. An algorithm for describing non-Markovian quantum trajectories based on such CMs was proposed in Ref. [197], while a thorough comparison between the collisional and MPS approach to time-delayed quantum optics dynamics was recently carried out in Ref. [57]. We note that this class of CMs with non-local collisions describe the dynamics of so called giant atoms [198] (a new paradigm of quantum optics) in the regime of non-negligible time delays [199].

Another type of CMs with multiple collisions was considered in Ref. [200] (see also [201]) considering an open system $S$ undergoing random collisions with a two-ancilla bath. At each step, both the ancilla colliding with $S$ and the collision unitary are selected randomly. It was found that the purity of $S$ as well as bipartite and tripartite entanglement reach time averaged equilibrium values characterized by large fluctuations.

Composite collision models of Section 8.5, whose theory was formulated in Ref. [202], are used as a versatile tractable model for investigating non-Markovian problems [58,138,162,163,203,204], including generalized versions where each subsystem is in contact with a different bath of ancillas [109]. The descriptive power of composite CMs (generalized to multiple baths) was studied in Ref. [205], where it was shown that they can simulate efficiently the Markovian dynamics of any multipartite open quantum system, i.e. with an error and resources (in terms of size and number of memory systems $M$) that scale polynomially with the size of $S$ and simulation time.

The mapping of a CM with ancilla–ancilla collisions into a composite CM (see Section 8.6) was introduced in Ref. [206]. In Ref. [158], the mapping was further developed and used for defining the concept of “memory depth". These works consider unitary ancilla–ancilla collisions, yet even when these are incoherent partial swaps (as in Section 8.2) a mapping into a suitably-defined composite CM is still possible as shown in Ref. [207].

## 9. Collision models from conventional models

We saw in Section 5.7 that the micromaser is naturally described by a CM. The micromaser is an instance of engineered, intrinsically discrete dynamics. In the present section, we discuss another major scenario (common in quantum optics) that admits a CM description. The paradigmatic model is a system $S$ – in typical cases a cavity mode or atom(s) – coupled to a white-noise bosonic field (we clarify later what “white-noise" means).

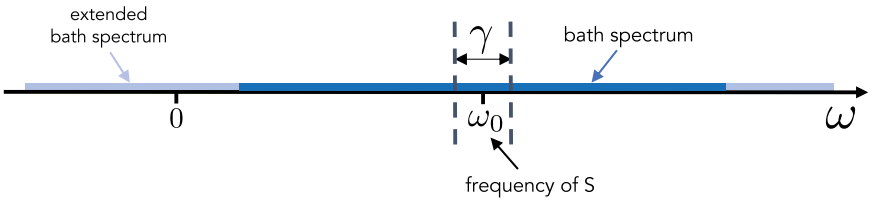


**Fig. 20.** *Sketch of involved frequencies.* Here, $\omega_0$ is the frequency of $S$ while the blue strip represents the spectrum of normal frequencies of the bath (i.e. the field $f$; we consider a single frequency band for simplicity). The open system $S$ significantly couples only to field modes with frequency lying within a narrow window of width $\gamma$ centered at $\omega_0$. Accordingly, once can extend the field spectrum to the entire $\omega$-axis (light blue strip) by introducing fictitious modes (including in particular frequencies $\omega < 0$).

The present section is conceptually important in that it shows how CMs are related to conventional system–bath microscopic models. The latter ones typically describe the bath as a continuum of modes which interact with $S$, in general, *all at the same time* [see Fig. 1(b)]. This is in stark contrast with (memoryless) CMs [see Fig. 1(a)], where $S$ interacts with the bath units (ancillas) *one at a time* (a major reason why CMs are an advantageous theoretical tool). Another key difference between the two frameworks is that, while in a CM the total Hamiltonian of $S$ and all the ancillas is intrinsically time-dependent (as we discussed in particular in Sections 7.5 and 7.8), conventional microscopic models usually feature a *time-independent* total Hamiltonian. The latter case matches the physical expectation that, since $S$ and the bath form a closed system, no intrinsic time-dependence is expected to arise in the total Hamiltonian. These issues (in particular) will be clarified in what follows, from which the CM will emerge as an effective *picture* to study a dynamics originally formulated in a conventional microscopic model. Notably, this will provide physical intuition about a number of properties of CMs postulated on a rather abstract ground in Sections 4.1 and 5.1.

### 9.1. White-noise bosonic bath and weak-coupling approximation

Let $S$ be a quantum system of frequency $\omega_0$ coupled to a continuum of bosonic modes $f$ (field), whose normal-mode ladder operators $\hat{b}_\omega$ and $\hat{b}^\dagger_\omega$ fulfill the commutation rules $[\hat{b}_\omega, \hat{b}^\dagger_{\omega'}] = \delta(\omega-\omega')$, $[\hat{b}_\omega, \hat{b}_{\omega'}] = [\hat{b}^\dagger_\omega, \hat{b}^\dagger_{\omega'}] = 0$. The total Hamiltonian reads

$$\hat{H} = \hat{H}_S + \hat{H}_f + \hat{V} \tag{252}$$

with

$$\hat{H}_S = \omega_0 \hat{A}^\dagger \hat{A}\,, \quad \hat{H}_f = \int_{-\infty}^{\infty} d\omega\, (\omega_0+\omega)\, \hat{b}^\dagger_\omega \hat{b}_\omega\,, \quad \hat{V} = \sqrt{\tfrac{\gamma}{2\pi}} \int_{-\infty}^{\infty} d\omega \left(\hat{A}^\dagger \hat{b}_\omega + \hat{A}\, \hat{b}^\dagger_\omega\right)\,. \tag{253}$$

The $S$ operators $\hat{A}$ and $\hat{A}^\dagger$ could be fermionic or bosonic, the essential requirement being only that $\hat{A}$ is an eigenoperator of $\hat{H}_S$, i.e. $[\hat{H}_S, \hat{A}] = -\omega_0 \hat{A}$ [cf. Eq. (151)]. Three major features of the Hamiltonian model (252) stand out:

(a) The coupling strength is $\omega$-independent (white coupling);
(b) $\hat{V}$ does not contain counter-rotating terms $\sim \hat{A}\hat{b}_\omega$, $\hat{A}^\dagger \hat{b}^\dagger_\omega$;
(c) Frequency $\omega$ takes values on the entire real axis.

These are all idealizations: in reality, the coupling depends on $\omega$, counter-rotating terms are present and $\omega$ is lower-bounded. The validity of (a)–(c) relies on the *weak coupling* approximation, namely the weakness of $S$-$B$ interaction (a usual situation, e.g. in quantum optics).[68] Because of it, $S$ undergoes a significant energy exchange only with field modes whose frequency $\omega$ lies within a narrow window around $\omega_0$ of width $\sim \gamma$ such that $\gamma \ll \omega_0$ (see Fig. 20). Accordingly, it makes no difference if the coupling rate at any frequency $\omega$ is replaced with its value at $\omega_0$, which we called $\sqrt{\gamma/2\pi}$ in Eq. (253), at the same time extending integrals over $\omega$ to the entire real axis (see Fig. 20) by introducing in particular negative-frequency fictitious modes (these remain uncoupled to $S$ in fact). Moreover, counter-rotating terms rotate fast compared to the time scale $\gamma^{-1}$ and are thus discarded (rotating wave approximation or RWA). Note that, for self-consistency, introduction of negative frequencies and RWA must be performed *together*: without the latter, an unphysical resonance at $\omega = -\omega_0$ would arise.

### 9.2. Time modes

Instead of normal modes (ladder operators $\hat{b}_\omega$), the bosonic bath can be equivalently represented in terms of *time modes* (henceforth all integrals are intended to run from $-\infty$ to $\infty$)

$$\hat{b}_s = \tfrac{1}{\sqrt{2\pi}} \int d\omega\, \hat{b}_\omega e^{-i\omega s}\,, \tag{254}$$

[68] For a derivation of Hamiltonian (252)–(253) through the weak-coupling approximation see e.g. Appendix A of Ref. [199].

which are thus related to $\hat{b}_\omega$ through Fourier transform. As is easily checked, time modes fulfill bosonic commutation rules

$$[\hat{b}_s, \hat{b}_{s'}^\dagger] = \delta(s-s')\,, \quad [\hat{b}_s, \hat{b}_{s'}] = [\hat{b}_s^\dagger, \hat{b}_{s'}^\dagger] = 0\,. \tag{255}$$

Despite having dimensions of time, $s$ should be regarded for now as just a label and time modes as an alternative way to represent the field (the connection with true time $t$ will become clear shortly).

### 9.3. Interaction picture

In the interaction picture with respect to $\hat{H}_0 = \hat{H}_S + \hat{H}_f$, ladder operators transform as $\hat{A} \to \hat{A}e^{-i\omega_0 t}$ and $\hat{b}_\omega \to \hat{b}_\omega e^{-i(\omega_0+\omega)t}$ so that the joint $S$-field state $\sigma$ evolves as $\dot{\sigma} = -i\,[\hat{V}_t, \sigma]$ with

$$\hat{V}_t = \sqrt{\gamma}\,\hat{A}^\dagger\,\hat{b}_{s=t} + \text{H.c.}\,, \tag{256}$$

hence, in the interaction picture: (i) time modes are non-interacting with each other,[69] (ii) at time $t$, $S$ only couples to the time mode $\hat{b}_{s=t} \equiv \hat{b}_t$. Note that (i) and (ii) strongly recall, respectively, assumptions (1) and (3) of Section 4.1.1, representing in fact a continuous version of these.

A consequence of the interaction picture is that $\hat{V}_t$ becomes *time-dependent*, hence the time evolution operator (propagator) is given by

$$\hat{\mathcal{U}}_t = \hat{\mathcal{T}}\, e^{-i\int_{t_0}^t ds\,\hat{V}(s)} \tag{257}$$

with $\hat{\mathcal{T}}$ the time-ordering operator.

### 9.4. Time discretization and coarse graining

Let us next consider a mesh of the time axis defined by $t_n = n\Delta t$ with $n$ an integer and $t_0 = 0$. In terms of this mesh, the propagator (257) can be split as[70]

$$\hat{\mathcal{U}}_t = \hat{U}_{t/\Delta t}\cdots\hat{U}_2\,\hat{U}_1 \qquad \text{with} \quad \hat{U}_n = \hat{\mathcal{T}}\, e^{-i\int_{t_{n-1}}^{t_n} ds\,\hat{V}_s}\,. \tag{258}$$

We take a time step much shorter than the characteristic interaction time, i.e., $\Delta t \ll \gamma^{-1}$. This allows us to expand each $\hat{U}_n$ to second order in $\Delta t$, which yields[71]

$$\hat{U}_n \simeq \mathbb{I} - i(\hat{V}_n + \hat{V}_n')\,\Delta t - \tfrac{1}{2}\hat{V}_n^2\,\Delta t^2 \tag{259}$$

with

$$\hat{V}_n = \tfrac{1}{\Delta t}\int_{t_{n-1}}^{t_n} ds\,\hat{V}_s\,, \quad \hat{V}_n' = \tfrac{i}{2\Delta t}\int_{t_{n-1}}^{t_n} ds \int_{t_{n-1}}^{s} ds'\,[\hat{V}_{s'}, \hat{V}_s]\,. \tag{260}$$

### 9.5. Emergence of the collision model

It can be shown (see Appendix B of Ref. [199]) that term $\hat{V}_n'$ gives negligible contribution for $\Delta t$ short enough. Thus each elementary unitary (259) reduces to

$$\hat{U}_n = \mathbb{I} - i\,\hat{V}_n\,\Delta t - \tfrac{1}{2}\hat{V}_n^2\,\Delta t^2\,, \tag{261}$$

where, using Eq. (256), $\hat{V}_n$ has the explicit form

$$\hat{V}_n = \sqrt{\tfrac{\gamma}{\Delta t}}\left(\hat{A}^\dagger\hat{b}_n + \hat{A}\,\hat{b}_n^\dagger\right)\,, \tag{262}$$

where we defined

$$\hat{b}_n = \tfrac{1}{\sqrt{\Delta t}}\int_{t_{n-1}}^{t_n} dt\;\hat{b}_t\,. \tag{263}$$

It is easily verified that $\hat{b}_n$ fulfill standard bosonic commutation rules

$$[\hat{b}_n, \hat{b}_{n'}^\dagger] = \delta_{n,n'}\,, \quad [\hat{b}_n, \hat{b}_{n'}] = [\hat{b}_n^\dagger, \hat{b}_{n'}^\dagger] = 0\,. \tag{264}$$

This is precisely the basic CM of Section 4.1 in the case that each ancilla is a quantum harmonic oscillator of frequency $\omega_0$. A number of comments follow.

---

[69] In the Schrödinger picture, time modes do couple to one another since $\hat{H}_f$ clearly cannot have a diagonal form when expressed in terms of time modes (note that these are *not* normal modes).

[70] We assume that $t/\Delta t$ is an integer. If not, the error committed becomes negligible for vanishing $\Delta t$.

[71] This perturbative expansion of the propagator is known as Magnus expansion [208].

(1) Note how the characteristic $1/\sqrt{\Delta t}$ dependence of the coupling strength – which we assumed repeatedly in this paper (see e.g. Section 5.8) – here in fact results from the model's white coupling [cf. Eq. (253)] combined with the need for well-defined bosonic commutation rules of the $\hat{b}_n$'s.[72]
(2) The CM arises in the interaction picture [recall Eq. (256)], which explains the time-dependent nature of the collisional Hamiltonian.
(3) The interaction picture is key in order for $S$ to collide with a new ancilla $\hat{b}_n$ at each time step and for the ancillas to be mutually non-interacting. In the Schrödinger picture, $S$ would be interacting all the time with the same ancilla and the ancillas would be coupled to one another (reflecting an analogous properties of continuous time modes).
(4) Among the three hypotheses in Section 4.1 which ensure lack of memory, the CM that we derived fulfills (1) and (3). Whether or not (2) holds (initially-uncorrelated ancillas) depends on the field initial state, as shown next.

### 9.6. Initial state of ancillas and condition for Markovian dynamics

We assume throughout that $S$ and the bosonic bath are initially uncorrelated, that is $\sigma_0 = \rho_0 \otimes \rho_f$. The field initial state $\rho_f$ is usually expressed in terms of the continuous normal modes (frequency domain) or through the time modes (time domain). Thus, in order to derive the corresponding initial state of ancillas, one first needs to express $\rho_f$ in terms of modes $\hat{b}_n$. At this point, we observe that, for an unspecified $\Delta t$, modes $\hat{b}_n$ in Eq. (263) clearly embody only part of the field degrees of freedom. This can be formally seen by Fourier-expanding $\hat{b}_t$ can in each time interval $[t_{n-1}, t_n[$ as

$$\hat{b}_t = \sum_{n=-\infty}^{\infty} \sum_{k=-\infty}^{\infty} \Theta_n(t) \, \tfrac{1}{\sqrt{\Delta t}} \, e^{-i\frac{2\pi k}{\Delta t}t} \, \hat{b}_{n,k} \quad \text{with} \quad \hat{b}_{n,k} = \tfrac{1}{\sqrt{\Delta t}} \int_{t_{n-1}}^{t_n} dt \; e^{i\frac{2\pi k}{\Delta t}t} \hat{b}_t \tag{265}$$

[recall that $\Theta_n(t) = 1$ inside interval $t_{n-1} \leq t < t_n$ while $\Theta_n(t) = 0$ elsewhere]. Here, ladder operators $\hat{b}_{n,k}$ are defined so as to obey bosonic commutation rules, $[\hat{b}_{n,k}, \hat{b}^\dagger_{n'k'}] = \delta_{n,n'}\delta_{k,k'}$, $[\hat{b}_{n,k}, \hat{b}_{n'k'}] = 0$. Note that for $k = 0$ we retrieve ancillas' modes (263), that is $\hat{b}_n \equiv \hat{b}_{n.0}$. It is easily shown that modes $\hat{b}_{n,k\neq 0}$ contain only field frequencies $\omega$ that diverge in the limit $\Delta t \to 0$ [38]. Accordingly, it is reasonable to assume that for all practical purposes these modes remain always unexcited, that is one in fact always deals with field initial states of the form

$$\rho_f = \rho_B \bigotimes_n \bigotimes_{k\neq 0} |0\rangle_{n,k}\langle 0| \; , \tag{266}$$

where $\rho_B$ stands for the state of modes $\hat{b}_n = \hat{b}_{n,0}$ (our *ancillas*) while $|0\rangle_{n,k}$ is the vacuum state of each mode $\hat{b}_{n,k}$.[73]

Based on the above, the initial state of ancillas (modes $\hat{b}_n$) is generally inferred from $\rho_f$ (initial state of the bosonic bath) by decomposing the field into modes $\hat{b}_{n,k}$ through the inverse of transform (254) followed by (265) (or only the latter when $\rho_f$ is already expressed in terms of time modes).

Notably, besides properties (1) and (3) of Section 4.1.1 (always matched as discussed before), property (2) will be fulfilled whenever $\rho_f$ is such that

$$\rho_B = \bigotimes_n \eta_n \quad \text{(condition for Markovian dynamics)} \tag{267}$$

with $\eta_n$ the initial state of mode $\hat{b}_n$. In this case, the emerging CM is memoryless (see Sections 4.1 and 4.5).

It turns out that condition (267) is fulfilled by a number of relevant classes of field states, some of which are illustrated next.

### 9.7. Vacuum state

The field vacuum state $|\text{vac}\rangle$ is defined as the state such that $\hat{b}_\omega|\text{vac}\rangle = 0$ for any $\omega$. Since the analogous statement clearly holds for time modes, Eq. (265) entails that $\hat{b}_{n,k}|\text{vac}\rangle = 0$ for any $n$, $k$. Hence, $\rho_B$ is of the form (267) – meaning that the dynamics is Markovian – with

$$\eta_n = |0\rangle_n\langle 0| \, . \tag{268}$$

In the case that $S$ is a qubit, namely $\hat{A} = \hat{\sigma}_-$ [cf. Eq. (253)], conservation of the total number of excitations $\hat{\sigma}_+\hat{\sigma}_- + \sum_n \hat{b}^\dagger_n \hat{b}_n$ entails that the state of each ancilla must lie in the subspace spanned by the pair of Fock states $|0\rangle_n$ and $|1\rangle_n$ with $|1\rangle_n = \hat{b}^\dagger_n|\text{vac}\rangle$. Thus ancillas behave as effective qubits.[74] We thus recover the all-qubit CM of Section 4.6 (when $g_z = 0$ and each ancilla is prepared in $|0\rangle$), which we used in particular to derive the spontaneous-emission ME (81).

[72] Commutation rules (264) crucially rely on having incorporated a factor $1/\sqrt{\Delta t}$ in the definition of $\hat{b}_n$ [cf. Eq. (263)].

[73] Note that the approximation according to which modes $\hat{b}_{n,k\neq 0}$ remain unexcited all the time is consistent with Eqs. (261) and (262) where only modes $\hat{b}_n \equiv \hat{b}_{n.0}$ appear.

[74] In passing, this justifies the convention to define $|1\rangle$ such that $\hat{\sigma}_z|1\rangle = |1\rangle$, which we followed throughout the paper.

### 9.8. Thermal states

Formally, a thermal state of the bosonic bath at inverse temperature $\beta = (KT)^{-1}$ would read

$$\rho_f = Z^{-1} e^{-\beta \hat{H}_f} \tag{269}$$

with $Z = \mathrm{Tr}_f\{e^{-\beta \hat{H}_f}\}$ the field partition function. In our case, replacing $\hat{H}_f$ with the expression in Eq. (253) would yield an unphysical thermal state due to the absence of a lower bound of the field spectrum. To get around this difficulty, it is customary to make the brute-force approximation consisting in replacing $\hat{H}_f$ in (269) with

$$\hat{H}_f \simeq \omega_0 \int_{-\infty}^{\infty} d\omega\, \hat{b}_\omega^\dagger \hat{b}_\omega \,. \tag{270}$$

Upon comparison with $\hat{H}_f$ in Eq. (253), we see that this is equivalent to stating that the field normal modes are perfectly resonant with $S$ (neglecting the dispersion). This again relies on weak coupling according to which only field normal modes within a narrow bandwidth around $\omega_0$ (cf. Fig. 20) exchange a significant amount of energy with $S$. Under approximation (270), by noting that $\int d\omega\, \hat{b}_\omega^\dagger \hat{b}_\omega$ is the total number of bosonic excitations, which can be equivalently expressed as $= \int dt\, \hat{b}_t^\dagger \hat{b}_t = \sum_{n,k} \hat{b}_{n,k}^\dagger \hat{b}_{n,k}$ [cf. Eq. (265)], we have

$$\rho_f \simeq Z^{-1} e^{-\beta\omega_0 \int d\omega\, \hat{b}_\omega^\dagger \hat{b}_\omega} = Z^{-1} e^{-\beta\omega_0 \int dt\, \hat{b}_t^\dagger \hat{b}_t} = Z^{-1} e^{-\beta\omega_0 \sum_{n,k} \hat{b}_{n,k}^\dagger \hat{b}_{n,k}} = \bigotimes_{n,k} Z_{n,k}^{-1}\, e^{-\beta\omega_0 \hat{b}_{n,k}^\dagger \hat{b}_{n,k}} \,. \tag{271}$$

with $Z_{n,k} = \mathrm{Tr}_{n,k}\{e^{-\beta\omega_0 \hat{b}_{n,k}^\dagger \hat{b}_{n,k}}\}$. Thereby, Eq. (267) holds with

$$\eta_n = Z_{n,0}^{-1}\, e^{-\beta\omega_0 \hat{b}_n^\dagger \hat{b}_n} \,. \tag{272}$$

It follows that $S$ is governed by the same finite-temperature master equation that we obtained in Section 7.1 to describe thermalization.[75]

### 9.9. Coherent states

A generic coherent state of the bosonic bath field has the form $\rho_f = |\alpha\rangle\langle\alpha|$ with[76]

$$|\alpha\rangle = e^{\int d\omega \left(\alpha_\omega \hat{b}_\omega^\dagger - \alpha_\omega^* \hat{b}_\omega\right)} |\mathrm{vac}\rangle \tag{273}$$

with $\alpha_\omega$ the pulse shape in the frequency domain. The standard continuous-wave case occurs for $\alpha_\omega \propto \delta(\omega - \omega_d)$ with $\omega_d$ the drive frequency. The state can be equivalently expressed in terms of time modes as

$$|\alpha\rangle = e^{\int dt \left(\alpha_t \hat{b}_t^\dagger - \alpha_t^* \hat{b}_t\right)} |\mathrm{vac}\rangle \,, \tag{274}$$

where $\alpha_t = 1/\sqrt{2\pi} \int d\omega\, \alpha_\omega e^{-i\omega t}$ encodes the pulse shape in the time domain. By decomposing $\hat{b}_t$ through (265), the exponent of (273) becomes

$$\int dt\, \left(\alpha_t \hat{b}_t^\dagger - \mathrm{H.c.}\right) = \sum_{n,k} \tfrac{1}{\sqrt{\Delta t}} \left( \int_{t_{n-1}}^{t_n} dt\, \alpha_t\, e^{i\frac{2\pi k}{\Delta t} t} \right) \hat{b}_{n,k}^\dagger - \mathrm{H.c.} \,. \tag{275}$$

Accordingly, condition (267) for Markovian dynamics is matched for $\eta_n = |\alpha_n\rangle_n \langle\alpha_n|$, where

$$|\alpha_n\rangle = e^{\alpha_n \sqrt{\Delta t}\, \hat{b}_n^\dagger - \alpha_n^* \sqrt{\Delta t}\, \hat{b}_n} |0_n\rangle \quad \text{with} \quad \alpha_n = \tfrac{1}{\Delta t} \int_{t_{n-1}}^{t_n} dt\, \alpha_t \tag{276}$$

($\alpha_n$ is the mean value of $\alpha_t$ on interval $[t_{n-1}, t_n]$).

Thus each ancilla is initially in a (single-mode) coherent state of amplitude $\alpha_n \sqrt{\Delta t}$ (note the $\sqrt{\Delta t}$-proportionality). For $\Delta t$ small enough this can be approximated to the lowest order as

$$|\alpha_n\rangle = e^{-\frac{1}{2}|\alpha_n|^2 \Delta t} \sum_{k=0}^{\infty} \frac{(\alpha_n \sqrt{\Delta t})^k}{\sqrt{k!}} |k_n\rangle \simeq \frac{1}{1 + |\alpha_n|^2 \Delta t} \left( |0\rangle_n + \alpha_n \sqrt{\Delta t}\, |1\rangle_n \right) \,, \tag{277}$$

75 Unlike Section 7.1, here ancillas do not have a free Hamiltonian since in the interaction picture chosen above the only Hamiltonian term is that describing the $S$-field interaction. Yet, the reduced dynamics of $S$ is the same as in Section 7.1 because the $S$-ancilla coupling and the ancilla initial state are identical.

76 For a discrete bosonic field, a multimode coherent state has the form $\bigotimes_j \exp(\alpha_j \hat{b}_j^\dagger - \alpha_j^* \hat{b}_j) |\mathrm{vac}\rangle = \exp[\sum_j (\alpha_j \hat{b}_j^\dagger - \alpha_j^* \hat{b}_j)] |\mathrm{vac}\rangle$, whose Eq. (273) represents the continuous version [86].

which is normalized to the first order in $\Delta t$ (here $|k_n\rangle = (\hat{b}_n^\dagger)^k/\sqrt{k!}\,|\text{vac}\rangle$). We thus retrieve state (82), which we considered in Section 5.8 for the all-qubit CM showing that it leads to optical Bloch Eqs. (84).[77]

### 9.10. General white-noise Gaussian state

By definition, a *Gaussian* state of the field is fully specified by the knowledge of first and second moments $\langle \hat{b}_t \rangle$ and $\langle \hat{b}_t^\dagger \hat{b}_{t'} \rangle$, $\langle \hat{b}_t \hat{b}_{t'} \rangle$ with $\langle \ldots \rangle = \text{Tr}_f\{\ldots \rho_f\}$. For $\delta$-correlated second moments, namely e.g. $\langle \hat{b}_t \hat{b}_{t'} \rangle \propto \delta(t-t')$, $\rho_f$ is a so called *white-noise* Gaussian state. The standard way to express its general form is [10]

$$\langle d\hat{B}_t \rangle = \beta_t\, dt\,, \quad \langle d\hat{B}_t^\dagger\, d\hat{B}_t \rangle = N\, dt\,, \quad \langle d\hat{B}_t\, d\hat{B}_t \rangle = M\, dt\,. \tag{278}$$

with $N \geq 0$ and where $\beta_t$ and $M$ are complex coefficients subject to the constraint $|M|^2 \leq N(N+1)$. Here, $M$ measures the amount of *squeezing* of the field, while $d\hat{B}_t = \int_t^{t+dt} ds\, \hat{b}_s$ is the so called quantum noise increment fulfilling the commutation rule $[d\hat{B}_t, d\hat{B}_t^\dagger] = dt$ [following from $[\hat{b}_t, \hat{b}_{t'}^\dagger] = \delta(t-t')$]. Thus Eq. (278) gives first and second moments of noise increments at the same time, while those at different times vanish (meaning, in particular, that time modes are initially uncorrelated). Using (263) this entails that first and second moments of ancillas are given by

$$\langle \hat{b}_n \rangle = \beta_n \sqrt{\Delta t}\,, \quad \langle \hat{b}_n^\dagger\, \hat{b}_{n'} \rangle = \delta_{n,n'}\, N\,, \quad \langle \hat{b}_n\, \hat{b}_{n'} \rangle = \delta_{n,n'}\, M \tag{279}$$

with $\beta_n$ the mean value of $\beta_t$ on the $n$th interval. Second moments vanish for $n \neq n'$, guaranteeing that condition (267) holds.[78] Corresponding to the continuous field state [cf. Eq. (278)], here $N$ is the average number of excitations of each ancilla while $M$ measures its squeezing.

The states discussed in the previous sections are special cases of (279): $\beta_n = N = M = 0$ (vacuum), $\beta_n = M = 0$ and $N = \bar{n}_{\omega_0}$ (thermal state), $\beta_n = \alpha_n$, $N = |\alpha_n|^2$ and $M = 0$ (coherent state) [recall definition (141)].

In light of Eqs. (64) and (65), the above in fact provides the most general master equation of $S$ for an arbitrary white-noise Gaussian state of the field. Note that the continuous-time limit [cf. Section 5.8] is always well-defined since $\langle \hat{b}_n \rangle \propto \sqrt{\Delta t}$ [cf. Eq. (279)].

### 9.11. Initially-correlated ancillas

There are a variety of field states such that condition (267) does not hold, which makes the dynamics non-Markovian. The simplest instance is probably a single-photon state like

$$|\Psi\rangle_f = \int dt\, \Psi_t\, \hat{b}_t^\dagger |\text{vac}\rangle\,, \tag{280}$$

where $\Psi_t$ is a photonic wavepacket. Using (265), the corresponding initial state of the ancillas reads $\rho_B = |\psi\rangle_B\langle\psi|$ with

$$|\psi\rangle_B = \sum_n c_n |1_n\rangle \quad \text{with} \quad c_n = \tfrac{1}{\sqrt{\Delta t}} \int_{t_{n-1}}^{t_n} dt\, \Psi_t\,, \tag{281}$$

which is a generally entangled, thus *correlated*, state [cf. Section 8.3].

### 9.12. Connection with input–output formalism

The collisional picture of the dynamics (see Section 9.5) was defined above in terms of evolution of *states*. Yet, one can let equivalently evolve operators so that each collision is governed by the operatorial equation[79]

$$\frac{d}{dt}\hat{b}_n(t) = i\,[\hat{V}_n, \hat{b}_n(t)] = -i\sqrt{\tfrac{\gamma}{\Delta t}}\,\hat{A}(t)\,. \tag{282}$$

where we used Eq. (262). Since $\Delta t$ is very short we can replace the derivative with $\Delta\hat{b}_n/\Delta t$, where $\Delta\hat{b}_n = \hat{b}_n(t_n) - \hat{b}_n(t_{n-1})$ (recall that the $n$th collision occurs in the time interval $t_{n-1} \leq t < t_n$). This yields

$$\hat{b}_n(t_n) = \hat{b}_n(t_{n-1}) - i\sqrt{\gamma\,\Delta t}\;\hat{A}(t_{n-1})\,. \tag{283}$$

---

[77] Strictly speaking, when $S$ is a qubit each ancilla behaves as an effective three-level system (with Hilbert space spanned by $\{|0_n\rangle, |1_n\rangle, |2_n\rangle\}$) due to the possible transition $|1_S\rangle|1_n\rangle \to |0_S\rangle|2_n\rangle$. Yet, in the limit of short $\Delta t$, this has negligible probability compared to $|0_S\rangle|1_n\rangle \to |1_S\rangle|1_n\rangle$ since the $|1_n\rangle$'s component of state (277) is of order $\sim\sqrt{\Delta t}$ so that the all-qubit CM is effectively retrieved (as usual, $|0_S\rangle$ and $|1_S\rangle$ are respectively the ground and excited states of $S$).

[78] Any two-mode Gaussian state $\rho_{12}$ such that $\langle \hat{b}_1^\dagger \hat{b}_2 \rangle = \langle \hat{b}_1 \hat{b}_2 \rangle = 0$ is necessarily a product state, i.e., $\rho_{12} = \rho_1 \otimes \rho_2$ (third- or higher-order correlation functions are zero since Gaussian states are by definition fully specified by first and second moments). This is naturally generalized to more than two modes.

[79] In the present subsection, time arguments appear in the standard form (not as subscripts or superscripts).

This equation can be understood by interpreting $\hat{b}_n(t_{n-1})$ as an *input* discrete field, whose interaction with $S$ produces an *output* field $\hat{b}_n(t_n)$. Indeed, (283) can be seen as the discrete version of the central equation underpinning the so called input–output formalism of quantum optics (see e.g. Ref. [10])

$$\hat{b}^{(\mathrm{out})}(t) = \hat{b}^{(\mathrm{in})}(t) - i\sqrt{\gamma}\,\hat{A}(t) \tag{284}$$

with $\hat{b}^{(\mathrm{in})}(t)$ and $\hat{b}^{(\mathrm{out})}(t)$ being the continuous limits of $\hat{b}_n(t_{n-1})/\sqrt{\Delta t}$ and $\hat{b}_n(t_n)/\sqrt{\Delta t}$, respectively.

### 9.13. Collision models from conventional models: state of the art

The above derivation of the CM from the microscopic bosonic model is largely based on Refs. [37,38,199] (see also Ref. [209]). In particular, Ref. [199] encompasses the extension to a multipartite system $S$ that can couple to the field non-locally. This brings about a new feature in that, relaxing the hypothesis that $S$ is point-like (as assumed throughout in the above), term $\hat{V}'_n$ in the elementary unitary (259) has a contribution due to vacuum fluctuations that yields an effective (second-order) induced Hamiltonian for $S$ [199]. In the case of systems each interacting with a waveguide field at multiple coupling points (such as "giant atoms" [198] or oscillators in looped geometries [210]), this effective Hamiltonian can be made decoherence-free [211]. This phenomenon was predicted in Ref. [212] (through methods not based on CMs) and then experimentally observed in a circuit-QED setup [213]. Mapping the dynamics into an effective CM allows for a full-fledged interpretation of the physical mechanism underlying such class of decoherence-free Hamiltonians, which was shown in Ref. [211].

Note that, while for vacuum and coherent states (Sections 9.7 and 9.9) the field time bins naturally behave as effective qubits, this is generally not the case (for instance for thermal or squeezed states). However, as shown in Ref. [38], one can always replace the time bins with suitably defined qubits yielding the same open dynamics of $S$.

In the model we considered, $\hat{H}_S$ is time-independent. One can yet extend the framework so as to account for an external drive on $S$, an approach that was successful in studying directional emission into a waveguide from a quantum emitter subject to a pulsed laser [214].

Relying on its tight link with the input–output formalism (see Section 9.12), the CM mapping was recently exploited to infer equations of motion and input–output relations of cavity-waveguide systems [215,216], carry out quantum simulations of coherent light–matter interactions [217,218], design qubit-oscillator circuits for implementing quantum error correction codes [219] and investigate non-equilibrium thermodynamics (see Section 7) in waveguide QED [220].

The CM mapping discussed here can be extended to a system $S$ coupled to the field at many points in the regime of non-negligible *delays*. This results in non-Markovian CMs with multiple *non-local* collisions (see Section 8.4), which were applied in Refs. [56,193,196].

Due to the natural connection of CMs with quantum trajectories (see Section 6), another promising application of the collisional mapping are non-Markovian extensions of photon counting and quantum trajectories (usually formulated for Markovian dynamics [10,78]). Examples are non-Markovian dynamics induced by single-photon states (see Section 9.11) [221–223], superposition of coherent states [224] and delayed coherent feedback [57,197].

We finally mention that, formally, even in the case of micromaser (cf. Section 5.7) one can define an effective quantum field whose the two-level atoms are the corresponding quanta [225].

## 10. Conclusions

In this paper, by adopting a pedagogical approach we presented the theory of quantum collisions models (CMs), reviewing at the same time the related state of the art. In line with Fig. 2, our discussion analyzed first the basic properties of CMs in Sections 4 and 5 and then considered the major areas of application of CMs to date: quantum trajectories/weak measurements (Section 6), non-equilibrium quantum thermodynamics (Section 7), non-Markovian extensions of CMs 8 and white-noise microscopic models (Section 9), the latter being recurrent in quantum optics.

Besides those featured in the previous state-of-the-art sections, there exist further interesting applications of CMs (and new ones keep being proposed). One of these is *quantum Darwinism* [226–230], where a CM description allows for a dynamical study of information spreading across the bath. Very recently, CMs started being applied to *quantum biology* problems, mostly as a versatile tool for modeling decoherence including non-Markovian effects (see Section 8). In particular, Ref. [231] investigated quantum transport across a Fenna–Matthews–Olson complex, while Ref. [232] studied decoherence of an avian-inspired quantum magnetic sensor. Other recent applications include: quantum classifiers [233] simulation of the Unruh effect [234], quantum friction [235], information scrambling [236], quantum batteries [237] and quantum metrology [238].

Needless to say, while the paper dealt with well-established theory, there are a number of problems which are still open some of which are mentioned next.

Section 8 introduced various classes of non-Markovian CMs. The relationships between these classes are still unexplored, e.g. whether or not it is possible to map one class into another, which was proven only for ancilla–ancilla collisions and composite CMs (see Section 8.6). This is an interesting question also from a fundamental viewpoint since it would help clarifying the relationship between seemingly different memory mechanisms corresponding to the relaxation of one of assumptions (1)–(3) in Section 4.1.1.

Another open issue concerns the derivation of CMs from conventional microscopic models, which was carried out in Section 9 only for bosonic baths. The procedure we followed there does depend on the bosonic commutation rules of the field, allowing to define in a relatively natural way independent ancillas (in the sense that operators of different ancillas are mutually commuting). A strictly analogous procedure for fermionic fields would lead to non-commuting ancillas, hence a suitable non-trivial extension is demanded. It appears reasonable to expect that a CM mapping exists also in this case since Markovian dynamics and Lindblad master equations occur for fermionic baths as well. This problem is arguably related to the definition of input–output formalism for fermionic fields [239].

While writing this paper, the interest in CMs keeps growing as e.g. witnessed by regular submissions of preprints to the Los Alamos archive. A natural question is to what extent the field of application of CMs could be enlarged. Should one envisage such approach becomes one day the conventional methodology? This is a non-trivial question to answer. One of the key points is the ability of CMs to describe non-Markovian dynamics. While research along this line is still in the early stages, one can expect (see e.g. Sections 8.1 and 8.6) that the higher is the degree of non-Markovianity the larger will be the number of (effective) bath ancillas one has to keep track with the same level of detail as the open system $S$ (see also Ref. [58]). Aside from the obvious difficulty to account for many degrees of freedom, we note that at some point this might even question the very nature of the collisional approach whose spirit is reducing complex dynamics to a sequence of simple interactions. This is well-illustrated by the instance in Fig. 17 to describe which we needed to cope somehow with all ancillas at each step (which was possible only because a single excitation was involved in the problem).

What appears by now well-assessed is that the collisional approach performs extremely well in a number of problems such as derivation of well-defined master equations, both Markovian and non-Markovian, the calculation of thermodynamic rates in non-equilibrium processes (where handling conventional microscopic models is often beyond reach), the physical interpretation of complex dynamics, the study of non-Markovianity.

An interesting future direction would be to synergically combine CMs or CM-inspired methods with other techniques (such as tensor network), as recently done in Ref. [240].

On a merely pedagogical ground, we envisage that CMs could become a standard strategy for introducing students to the basics of open quantum systems theory. In this respect, note that our discussion dealt with most main concepts of this field such as quantum maps, Lindblad master equation, steady states, POVMs, quantum trajectories, stochastic Schrödinger equation, Stinespring dilation theorem. The required background is in fact some familiarity with elementary quantum mechanics. Moreover, developing a physical intuition of the various topics (e.g. the conditions for the Lindblad master equation to hold) is facilitated compared to conventional microscopic models (cf. Appendix F).

We hope that the systematic settlement of the CMs theory that we tried to carry out here could spur an increasing use of CMs among students and researchers or at least stimulate a “collisional thinking" of open quantum systems problems in addition to, or possibly in combination with, other methods.

## Declaration of competing interest

The authors declare that they have no known competing financial interests or personal relationships that could have appeared to influence the work reported in this paper.

## Acknowledgments

What we learned about collision models over these years greatly benefited from discussions and collaborations with a number of valuable people to whom we are deeply grateful. Among these are (in alphabetical order) D. Burgarth, G. Benenti, S. Campbell, A. Carollo, D. Chisholm, D. Cilluffo, G. De Chiara, A. Grimsmo, J. A. Gross, G. T. Landi, S. Maniscalco, R. McCloskey, M. Paternostro, T. Tufarelli and B. Vacchini.

We gratefully acknowledge D. Cilluffo, S. Campbell, G. T. Landi, B. Vacchini, G. De Chiara and G. Manzano for the critical reading of the manuscript. We are indebted to D. Cilluffo for the help offered in the preparation of Section 4.9.

We acknowledge financial support from MUR through project PRIN (Project No. 2017SRN-BRK QUSHIP).

## Appendix A. Density matrices

The most general state of a quantum system $S$ is described by a *density operator* $\rho$ (often referred to as density matrix). This is a Hermitian, positive semi-definite operator of trace one. As such, it can always be expanded (“spectrally decomposed") as

$$\rho = \sum_{\nu} p_{\nu} |\nu\rangle\langle\nu| \tag{A.1}$$

with $p_{\nu} \geq 0$ (positivity[80]) and $\mathrm{Tr}\rho = \sum_{\nu} p_{\nu} = 1$ (normalization). Here, $\{|\nu\rangle\}$ are the eigenstates of $\rho$, i.e. $\rho|\nu\rangle = p_{\nu}|\nu\rangle$ for all $\nu$, which form an orthonormal basis of the Hilbert space of $S$. When all probability $p_{\nu}$ vanish but one, $\rho$ reduces to a simple projector, in which case we say that the state is *pure*. In all other cases, we deal with a mixed state. While

[80] Rigorously speaking, this expresses non-negativity, but we will refer to this property as “positivity" to simplify the language.

the usual description through kets is always possible for pure states, the density–matrix language is indispensable for representing *mixed* states.

Spectral decomposition (A.1) expresses $\rho$ as a mixture of *orthogonal* (pure) states. A density matrix can however be alternatively expressed as a mixture of non-orthogonal states, for instance a legitimate state for a qubit is $\rho = 1/2|0\rangle\langle 0| + 1/2|+\rangle\langle +|$ with $|\pm\rangle = \frac{1}{\sqrt{2}}(|0\rangle + |1\rangle)$, where $|0\rangle$ and $|+\rangle$ are non-orthogonal.

The density–matrix language is essential for describing subsystems. Assume that $S$ is part of a larger bipartite system, the other subsystem being $E$ (no matter how big). Then, if $\sigma$ is the joint $S-E$ state, the state of $S$ is given by the partial trace over $E$

$$\rho = \mathrm{Tr}_E\,\sigma = \sum_{\mu} {}_E\langle \mu|\sigma|\mu\rangle_E\,, \tag{A.2}$$

where $\{|\mu\rangle_E\}$ is an arbitrary orthonormal basis of $E$ (it is easily checked that this satisfies the definition of density operator).

## Appendix B. Von Neumann entropy, mutual information and relative entropy

Given a (generally mixed) state $\rho$ the *Von Neumann entropy* is defined as [21]

$$\mathcal{S}(\rho) = -\mathrm{Tr}\{\rho\log\rho\}\,. \tag{B.1}$$

This is the natural quantum analogue of the Shannon entropy occurring in classical information theory. This can be seen by spectrally decomposing $\rho$ as in Eq. (A.1), which entails

$$\mathcal{S}(\rho) = -\sum_{\nu} p_\nu \log p_\nu\,. \tag{B.2}$$

Also, this shows that $\mathcal{S}(\rho)\geq 0$ for any $\rho$. Specifically, entropy vanishes for pure states and is non-zero for mixed states. This matches the picture of a mixed state as a statistical mixture of pure states. For instance, consider the qubit state $\rho = 1/2|0\rangle\langle 0| + 1/2|1\rangle\langle 1| = \frac{1}{2}\mathbb{I}$. This can be interpreted by saying that we are fully ignorant about whether $S$ is in $|0\rangle$ or $|1\rangle$. Entropy is a measure of such *ignorance*. Indeed, in the considered instance, it takes its maximum value $\mathcal{S} = \log 2$.[81] In contrast, $\mathcal{S}(|0\rangle\langle 0|) = 0$ as we are fully sure that $S$ is in the pure state $|0\rangle$. An important property of the Von Neumann entropy is that it does not change under a unitary transformation, i.e.

$$\mathcal{S}(\rho) = \mathcal{S}(\hat{U}\rho\hat{U}^\dagger) \tag{B.3}$$

for any state $\rho$ and unitary $\hat{U}$. This is immediately seen from (A.1) by noting that $\hat{U}\rho\,\hat{U}^\dagger$ has the same spectral decomposition as $\rho$ under the change of basis $\{|\nu\rangle\}\to\{\hat{U}|\nu\rangle\}$.

The Von Neumann entropy underpins the definition of two useful quantities, quantum relative entropy and quantum mutual information.

Unlike Von Neumann entropy which is associated with a single state, the quantum *relative entropy* depends on a pair of states, say $\rho$ and $\rho'$. It is defined as

$$\mathcal{S}(\rho\parallel\rho') = -\mathrm{Tr}\{\rho\,\log\rho'\} - \mathcal{S}(\rho) = \mathrm{Tr}\{\rho\,(\log\rho - \log\rho')\}\,. \tag{B.4}$$

It can be shown that $\mathcal{S}(\rho\parallel\rho')\geq 0$ (non-negativity) with $\mathcal{S}(\rho\parallel\rho') = 0$ if and only if $\rho=\rho'$. Relative entropy is useful because it is a measure of the *distinguishability* between two quantum states. Notably, it is not symmetric under swap of states, i.e. $\mathcal{S}(\rho\parallel\rho')\neq\mathcal{S}(\rho'\parallel\rho)$.[82]

Another entropic quantity is quantum *mutual information*, the quantum version of mutual information (a longstanding measure of correlations). Given a pair of systems $S$ and $E$, it is defined as

$$\mathcal{I}_{SE} = \mathcal{S}(\rho_S) + \mathcal{S}(\rho_E) - \mathcal{S}(\rho_{SE}) \tag{B.5}$$

with $\rho_{SE}$ the joint state and $\rho_{S(E)} = \mathrm{Tr}_{E(S)}\{\rho_{SE}\}$ the reduced states. Mutual information fulfills $\mathcal{I}_{SE}\geq 0$ with

$$\mathcal{I}_{SE} = 0 \;\Leftrightarrow\; \rho_{SE} = \rho_S\otimes\rho_E\,. \tag{B.6}$$

Thus $\mathcal{I}_{SE} > 0$ witnesses the existence of $S$-$E$ correlations.

81 This is the maximum value for a qubit. In general, for a system with Hilbert space dimension $d$, the maximum entropy is $S = \log d$ (for a qubit, $d = 2$)

82 This is a reason why relative entropy cannot be used to define a metric in the Hilbert space.

## Appendix C. Quantum maps

Transformations of density matrices are described by *quantum maps*. A quantum map transforms a state $\rho$ into another state $\rho'$, which is expressed as $\rho' = \mathcal{M}[\rho]$. A major class of quantum maps is that defined by

$$\rho' = \mathcal{M}[\rho] = \sum_m \hat{K}_m \, \rho \, \hat{K}_m^\dagger \quad \text{with} \quad \sum_m \hat{K}_m^\dagger \hat{K}_m = \mathbb{I} \, . \tag{C.1}$$

These are called *completely positive and trace-preserving (CPT) maps*.[83]

The rightmost expansion in (C.1) is called *Kraus decomposition* and $\hat{K}_m$ the Kraus operators. The Kraus decomposition (demonstrably) ensures that, if $\rho$ is a well-defined density matrix, then so is $\rho'$. The importance of CPT maps indeed relies on the fact that they describe physically-legitimate transformations, e.g. due to a dynamical evolution or measurement, i.e. they map physical states into physical states.

Note that, like any operator, a unitary transformation transforms a density matrix as $\rho' = \hat{U} \rho \, \hat{U}^\dagger$ subject to $\hat{U}^\dagger \hat{U} = \mathbb{I}$, which is a special case of quantum map (C.1) having only one Kraus operator $\hat{U}$. Actually, a unitary transformation fulfills $\hat{U}\hat{U}^\dagger = \mathbb{I}$ as well, while in general $\sum_m \hat{K}_m \hat{K}_m^\dagger \neq \mathbb{I}$ this expressing the fact that a quantum map is generally *non-unitary*.

Non-unitarity most notably entails that the scalar product of two states is not invariant under a quantum map. The best instance to see this is probably the decay of a two-level atom: the excited state $|e\rangle$ eventually evolves into the ground state $|g\rangle$, while the ground state is unaffected. Thus $|e\rangle$ and $|g\rangle$ (which are orthogonal states) are both mapped into the same state $|g\rangle$, with the scalar product thereby changing from zero to one.

## Appendix D. Dynamical map

If $S$ is closed (decoupled from anything else) its state $\rho$ evolves in time according to the Von Neumann (or quantum Liouville) equation (recall that we set $\hbar = 1$) $\dot{\rho} = -i[\hat{H}_S, \rho]$. This is in fact just the Schrödinger equation expressed in the density–matrix formalism. Accordingly, the time evolution of $\rho$ is *unitary*, $\rho_t = \hat{U}_{St} \rho_0 \hat{U}_{St}^\dagger$, with $\hat{U}_{St} = e^{-i\hat{H}_S t}$ the time-evolution operator.

If $S$ is open then its time evolution is generally *non-unitary*. This can be seen in the case that $S$ and $E$ overall form a closed system so that they jointly evolve unitarily as $\sigma_t = \hat{U}_t \, \sigma_0 \, \hat{U}_t^\dagger$. Hence, tracing off $E$, the state of $S$ at time $t$ is given by

$$\rho_t = \sum_\mu {}_E\langle \mu | \, \hat{U}_t \, \rho_0 \otimes \rho_E \, \hat{U}_t^\dagger \, | \mu \rangle_E \, , \tag{D.1}$$

where we assumed that $S$ and $E$ start in the *uncorrelated* state $\sigma_0 = \rho_0 \otimes \rho_E$. Replacing now $\rho_E$ with its spectral decomposition $\rho_E = \sum_\lambda p_\lambda |\lambda\rangle_E \langle\lambda|$, $\rho$ can be arranged in the form

$$\rho_t = \Lambda_t[\rho_0] = \sum_{\nu\lambda} \left( \sqrt{p_\lambda} \, {}_E\langle \mu | \, \hat{U}_t \, | \lambda \rangle_E \right) \rho_0 \left( \sqrt{p_\lambda} \, {}_E\langle \mu | \, \hat{U}_t \, | \lambda \rangle_E \right)^\dagger \, . \tag{D.2}$$

Eq. (D.2) defines the so called *dynamical map*: for any given initial state of $S$, $\rho_0$, $\Lambda_t$ returns the dynamically evolved state at time $t$, $\rho_t$. The dynamical map $\Lambda_t$ can be seen as the open-system counterpart of the time-evolution operator. Remarkably, by comparing Eq. (D.2) with (C.1), we see that $\Lambda_t$ is a CPT map whose generic Kraus operator, labeled by the double index $(\nu, \lambda)$, reads

$$\hat{K}_{\nu\lambda} = \sqrt{p_\lambda} \, {}_E\langle \mu | \, \hat{U}_t \, | \lambda \rangle_E \, . \tag{D.3}$$

## Appendix E. Stinespring dilation theorem

We have just seen in Appendix D that, starting from an uncorrelated $S$-$E$ state, a global unitary dynamics results upon partial trace in a CPT map on $S$. According to the Stinespring dilation theorem, the converse property holds as well: given a CPT map $\mathcal{M}$ [cf. Eq. (C.1)] one can always find an ancillary system $A$, an initial state of $A$, $\rho_A$, and a global unitary $\hat{U}_{SA}$ (acting on $S$ and $A$) such that

$$\rho' = \mathcal{M}[\rho] = \mathrm{Tr}_A \left\{ \hat{U}_{SA} \, \rho \otimes \rho_A \, \hat{U}_{SA}^\dagger \right\} \, . \tag{E.1}$$

Note that in general there are infinite pairs $(\rho_A, \hat{U}_{SA})$ producing the same CPT map $\mathcal{M}$ through (E.1). We stress that the lack of initial correlations between $S$ and $A$ in Eq. (E.1) is essential for a CPT map to emerge.

For more detailed treatments of the topics from Appendix A to Appendix E see e.g. Refs. [21,241].

[83] We do not discuss here the concept of *complete* positivity, using (C.1) as the definition of a CPT map.

## Appendix F. Lindblad master equation

Consider the class of dynamical maps such that

$$\Lambda_t = \Lambda_{t-t'}\,\Lambda_{t'}\,. \tag{F.1}$$

for any $t$ and $t'$ such that $0 \le t' \le t$. Eq. (F.1) is called *semigroup property* and can be regarded as a formal definition of a Markovian, i.e. memoryless, dynamics.

It can be shown [7] that, if (F.1) holds, then $\rho = \Lambda_t[\rho_0]$ is the solution of a master equation (ME) having the general form

$$\frac{d\rho}{dt} = -i\,[\hat{\mathcal{H}},\rho] + \sum_\nu \gamma_\nu \left(\hat{L}_\nu \rho \hat{L}_\nu^\dagger - \tfrac{1}{2}[\hat{L}_\nu^\dagger \hat{L}_\nu,\rho]_+\right) \tag{F.2}$$

with $\hat{\mathcal{H}}$ a Hermitian operator and $\gamma_\nu \ge 0$ for each $\nu$. Here, $\hat{L}_\nu$ are a set of operators on $S$ called *jump operators*. Eq. (F.2) is the so called Gorini–Kossakowski–Sudarshan–Lindblad equation, more often referred to simply as *Lindblad ME* (or ME in Lindblad form).

### F.1. Microscopic derivation from a conventional system–bath model

We ask under what physical conditions the Lindblad ME correctly describes the open dynamics. Thus consider the generic system–bath Hamiltonian

$$\hat{H} = \hat{H}_S + \hat{H}_B + \hat{V}\,. \tag{F.3}$$

In the interaction picture with respect to $\hat{H}_0 = \hat{H}_S + \hat{H}_B$, the joint $S$-$B$ state evolves according to the Von-Neumann equation $\dot{\sigma} = -i\,[\hat{V}_t,\sigma]$. Solving it formally yields

$$\sigma_t = \sigma_0 - i\int_0^t dt'\,[\hat{V}_{t'},\hat{\sigma}_{t'}]\,. \tag{F.4}$$

. Plugging this back into the Von-Neumann equation one gets

$$\frac{d\sigma}{dt} = -i\,[\hat{V}_t,\sigma_0] - \int_0^t dt'\,[\hat{V}_t,[\hat{V}_{t'},\sigma_{t'}]]\,. \tag{F.5}$$

We assume no initial correlations between system and environment, i.e. $\sigma_0 = \rho_0 \otimes \rho_B$, where $\rho_0$ and $\rho_B$ are respectively the initial reduced density operators of $S$ and $B$. Also, we assume $\mathrm{Tr}_B[\hat{V}_t,\sigma_0] = 0$, which is the case e.g. when $\rho_B$ is such that $[\hat{H}_B,\rho_B] = 0$ (e.g. in the case of a thermal state). Using these and tracing off the bath $B$ in Eq. (F.5) yields

$$\frac{d\rho}{dt} = -\int_0^t dt'\,\mathrm{Tr}_B\left\{[\hat{V}_t,[\hat{V}_{t'},\sigma_{t'}]]\right\}\,. \tag{F.6}$$

Although system and bath start in a product state, as a consequence of their interaction, mutual correlations between the two will build up. However if $B$ is a reservoir (very large number of degrees of freedom), one intuitively expects its reduced state to be little modified by the interaction with the system. Accordingly, in Eq. (F.6) one can approximate

$$\sigma_t \simeq \rho_t \otimes \rho_B\,, \tag{F.7}$$

which is known as *Born approximation*.[84] At the same time, we expand the interaction Hamiltonian as $\hat{V}_t = \sum_\nu g_\nu \hat{A}_{\nu t}\hat{B}_{\nu t}$ (always possible), where $\hat{A}_{\nu t} = e^{i\hat{H}_S t}\hat{A}_\nu e^{-i\hat{H}_S t}$ and $\hat{B}_{\nu t} = e^{i\hat{H}_B t}\hat{B}_\nu e^{-i\hat{H}_B t}$ are a set of operators on respectively $S$ and $B$ in the interaction picture ($\hat{A}_\nu$ and $\hat{B}_\nu$ are Hermitian). With these replacements and the Born approximation (F.7), (F.6) takes the form

$$\begin{aligned}\frac{d\rho}{dt} &= -\sum_{\mu,\nu} g_\mu g_\nu \int_0^t dt'\,\mathrm{Tr}_B\left\{\left[\hat{A}_{\mu t}\hat{B}_{\mu t},[\hat{A}_{\nu t'}\hat{B}_{\nu t'},\rho_{t'}\rho_B]\right]\right\} = \\ &= -\sum_{\mu,\nu} g_\mu g_\nu \int_0^t dt'\left(\langle\hat{A}_{\mu t}\hat{A}_{\nu t'}\rho_{t'} - \hat{A}_{\nu t'}\hat{\rho}_{t'}\hat{A}_{\mu t})\langle\hat{B}_{\mu t}\hat{B}_{\nu t'}\rangle + (\rho_{t'}\hat{A}_{\nu t'}\hat{A}_{\mu t} - \hat{A}_{\mu t}\hat{\rho}_{t'}\hat{A}_{\nu t'})\langle\hat{B}_{\nu t'}\hat{B}_{\mu t}\rangle\right)\,,\end{aligned} \tag{F.8}$$

where we defined

$$\langle\hat{B}_{\nu t'}\hat{B}_{\mu t}\rangle = \mathrm{Tr}_B\{\hat{B}_{\nu t'}\hat{B}_{\mu t}\rho_B\}.$$

For a large reservoir $B$, each two-time correlation function $\langle\hat{B}_{\mu t}\hat{B}_{\nu t'}\rangle$ is strongly peaked around $t - t' \simeq \tau_c$ with $\tau_c$ usually referred to as the *correlation time*. This entails that any fluctuation in the bath state due to its interaction with the

[84] We point out that approximation (F.7) is made only in Eq. (F.6) determining the reduced dynamics of $S$.

environment dies out on a time scale of the order $\sim \tau_c$. This time is typically very short, in particular when compared to the evolution timescale of $S$. Accordingly, in each integral over $t'$ appearing in Eq. (F.8), we can approximate

$$\rho_{t'} \simeq \rho_t \,, \tag{F.9}$$

which is known as the *Markov approximation*.

### F.2. Secular approximation

For each $\hat{A}_\nu$, we now conveniently define $\hat{A}_{\nu\omega} = \sum'_{E,E'} \hat{\Pi}_E \hat{A}_\nu \hat{\Pi}_{E'}$ with $\hat{\Pi}_E$ the projector onto the eigenspace of $\hat{H}_S$ of energy $E$ and where the sum runs over all pairs $(E, E')$ such that $E' - E = \omega$. It is then easily checked that $\hat{A}_\nu = \sum_\omega \hat{A}_{\nu\omega}$ and, moreover, $[\hat{H}_S, \hat{A}_{\nu\omega}] = -\omega \hat{A}_{\nu\omega}$. It follows that, in the interaction picture, $\hat{A}_{\nu t} = \sum_\omega e^{-i\omega t} \hat{A}_{\nu\omega}$. Replacing this and (F.9) in Eq. (F.8) this can be arranged in the form

$$\frac{d\rho}{dt} = \sum_{\omega,\omega'} \sum_{\nu,\mu} e^{i(\omega'-\omega)t}\, \gamma_{\nu\mu}(\omega) \left( \hat{A}_{\mu\omega} \rho \hat{A}^\dagger_{\nu\omega'} - \hat{A}^\dagger_{\nu\omega'} \hat{A}_{\mu\omega} \rho \right) + \text{H.c.} \tag{F.10}$$

with

$$\gamma_{\nu\mu}(\omega) = \int_0^\infty ds e^{i\omega s} \langle \hat{B}^\dagger_{\nu t} \hat{B}_{\mu(t-s)} \rangle \,, \tag{F.11}$$

where in the last integral we approximated the upper limit of integration with $+\infty$ since the integrand function (see above) decays with a characteristic time $\tau_c$. For $\rho_B$ such that $[\hat{H}_B, \rho_B] = 0$ (e.g. a thermal state), the above two-time correlation function actually depends only on the time difference $s$ and thus can be replaced with $\hat{B}^\dagger_{\nu s} \hat{B}_{\mu 0}$.

The secular approximation consists in throwing away all counter-rotating terms in Eq. (F.10), i.e. those corresponding to $\omega \neq \omega'$. This results in an equation with time-independent coefficients, which reads

$$\frac{d\rho}{dt} = \sum_{\omega} \sum_{\nu,\nu'} \gamma_{\nu\nu'}(\omega) \left( \hat{A}_{\nu'\omega} \rho \hat{A}^\dagger_{\nu\omega} - \hat{A}^\dagger_{\nu\omega} \hat{A}_{\nu'\omega} \rho \right) + \text{H.c.} \tag{F.12}$$

### F.3. Master equation in Lindblad form

Defining next

$$S_{\nu\nu'}(\omega) = \tfrac{1}{2i} \left( \gamma_{\nu\nu'}(\omega) - \gamma^*_{\nu'\nu}(\omega) \right) \,, \quad \gamma_{\nu\nu'}(\omega) = \gamma_{\nu\nu'}(\omega) + \gamma^*_{\nu'\nu}(\omega) = \int_{-\infty}^{\infty} ds\, e^{i\omega s}\, \text{Tr}_B\{ \hat{B}^\dagger_\nu(s) \hat{B}_{\nu'}(0) \} \,, \tag{F.13}$$

Eq. (F.8) takes the form

$$\frac{d\rho}{dt} = -i[\hat{\mathcal{H}}, \rho] + \mathcal{D}[\rho] \tag{F.14}$$

with

$$\hat{\mathcal{H}} = \sum_{\omega} \sum_{\nu,\nu'} S_{\nu\nu'}(\omega) \hat{A}^\dagger_\nu(\omega) \hat{A}_{\nu'}(\omega) \,, \quad \mathcal{D}[\rho] = \sum_{\omega} \sum_{\nu,\nu'} \gamma_{\nu\nu'}(\omega) \left( \hat{A}_{\nu'\omega} \rho \hat{A}^\dagger_{\nu\omega} - \tfrac{1}{2} [\hat{A}^\dagger_{\nu\omega} \hat{A}_{\nu'\omega}, \rho]_+ \right) . \tag{F.15}$$

This master equation can be put in the standard Lindblad form (F.2) upon diagonalization of each matrix $\gamma_{\nu\nu'}(\omega)$.

The above derivation of the Lindblad master equation from the Hamiltonian model (F.3) follows standard textbooks, in particular Refs. [7,78], to which the reader is referred for further details. In the context of the present paper, it serves the purpose of illustrating that the derivation of the Lindblad ME from a standard microscopic model is a relatively involved procedure which requires a number of non-trivial approximations.

## Appendix G. Lindblad master equation from the stochastic schrödinger equation

Using Eqs. (122) and (123), the three terms in Eq. (126) are worked out as

$$\begin{aligned} (d|\psi\rangle)\,\langle\psi| &= -\tfrac{1}{2}\gamma\, (\hat{\sigma}_+\hat{\sigma}_- - \langle\hat{\sigma}_+\hat{\sigma}_-\rangle)|\psi\rangle\langle\psi|\, dt + \left( \frac{\hat{\sigma}_-}{\sqrt{\langle\hat{\sigma}_+\hat{\sigma}_-\rangle}} - \mathbb{I} \right) |\psi\rangle\langle\psi|\, \overline{dN} \\ &= -\tfrac{\gamma}{2}\, \hat{\sigma}_+\hat{\sigma}_-\rho\, dt + \tfrac{\gamma}{2} \langle\hat{\sigma}_+\,\hat{\sigma}_-\rangle\, \rho\, dt + \frac{\gamma}{\sqrt{\langle\hat{\sigma}_+\,\hat{\sigma}_-\rangle}}\, \hat{\sigma}_-\, \rho\; dt - \gamma\, \langle\hat{\sigma}_+\,\hat{\sigma}_-\rangle\, \rho\, dt \,, \end{aligned} \tag{G.1}$$

$$\begin{aligned} |\psi\rangle\, (d\langle\psi|) &= -\tfrac{1}{2}\gamma |\psi\rangle\langle\psi| (\hat{\sigma}_+\hat{\sigma}_- - \langle\hat{\sigma}_+\hat{\sigma}_-\rangle)\, dt + |\psi\rangle\langle\psi| \left( \frac{\hat{\sigma}_+}{\sqrt{\langle\hat{\sigma}_+\hat{\sigma}_-\rangle}} - \mathbb{I} \right) \overline{dN} \\ &= -\tfrac{\gamma}{2}\, \rho\, \hat{\sigma}_+\hat{\sigma}_-\, dt + \tfrac{\gamma}{2} \langle\hat{\sigma}_+\,\hat{\sigma}_-\rangle\, \rho\, dt + \frac{\gamma}{\sqrt{\langle\hat{\sigma}_+\,\hat{\sigma}_-\rangle}}\, \rho\, \hat{\sigma}_+\; dt - \gamma\, \langle\hat{\sigma}_+\,\hat{\sigma}_-\rangle\, \rho\, dt \,, \end{aligned} \tag{G.2}$$

$$d|\psi\rangle d\langle\psi| = \left(\frac{\hat\sigma_-}{\sqrt{\langle\hat\sigma_+\hat\sigma_-\rangle}} - \mathbb{I}\right)|\psi\rangle\langle\psi|\left(\frac{\hat\sigma_+}{\sqrt{\langle\hat\sigma_+\hat\sigma_-\rangle}} - \mathbb{I}\right)\overline{dN^2}$$
$$= \gamma\,\hat\sigma_-\rho\,\hat\sigma_+\,dt - \frac{\gamma}{\sqrt{\langle\hat\sigma_+\hat\sigma_-\rangle}}\,\hat\sigma_-\,\rho\;dt - \frac{\gamma}{\sqrt{\langle\hat\sigma_+\hat\sigma_-\rangle}}\,\rho\,\hat\sigma_+\;\;dt + \gamma\langle\hat\sigma_+\hat\sigma_-\rangle\,\rho\,dt\,, \tag{G.3}$$

where in the second line of Eqs. (G.1) and (G.3) we replaced $\rho = |\psi\rangle\langle\psi|$ and neglected terms $\sim dt^2$ and $\sim dt\,\overline{dN}$ [note that instead $\overline{(\mathrm{d}N)^2} \sim dt$]. Summing the three increments, it can be seen that many terms cancel out in a way that we are left with $d\rho = \gamma\left(\hat\sigma_-\rho\,\hat\sigma_+ - \frac{1}{2}\left[\hat\sigma_+\hat\sigma_-,\rho\right]_+\right)dt$.

## Appendix H. Equivalence between Eqs. (150) and (153)

For simplicity, we assume here that both $S$ and ancilla $n$ are finite-dimensional systems (the derivation can yet be easily extended to infinite dimension). Let us introduce the spectral decompositions of $\hat H_S$ and $\hat H_n$ as

$$\hat H_S = \sum_j E_j\hat\Pi_S^j\,, \qquad \sum_j \hat\Pi_S^j = \mathbb{I}_S\,, \tag{H.1}$$
$$\hat H_n = \sum_i e_i\hat\Pi_n^i\,, \qquad \sum_i \hat\Pi_n^i = \mathbb{I}_n\,, \tag{H.2}$$

where $E_j$ ($e_i$) is the generic eigenvalue of $\hat H_S$ ($\hat H_n$) and $\hat\Pi_S^j$ ($\hat\Pi_n^i$) the projector on the corresponding eigenspace. Projectors associated with different energies are orthogonal, i.e.

$$\hat\Pi_S^j\hat\Pi_S^{j'} = \delta(E_j - E_{j'})\hat\Pi_S^j\,, \quad \hat\Pi_n^i\hat\Pi_n^{i'} = \delta(E_i - E_{i'})\hat\Pi_n^i\,. \tag{H.3}$$

Here, we conveniently defined $\delta(x)$ as a function taking value 1 for $x = 0$ and 0 otherwise.

Accordingly, by denoting with $\bar E_\ell$ the eigenvalues of $\hat H_S + \hat H_n$ this can be spectrally-decomposed as

$$\hat H_S + \hat H_n = \sum_\ell \bar E_\ell\;\hat\Pi_{Sn}^\ell\,, \tag{H.4}$$

where $\hat\Pi_{Sn}^\ell$ are the (complete) orthonormal projectors on the system–ancilla Hilbert space defined by

$$\hat\Pi_{Sn}^\ell = \sum_{j,i}\delta(E_j + e_i - \bar E_\ell)\;\hat\Pi_S^j\otimes\hat\Pi_n^i\,. \tag{H.5}$$

Now, we observe that the commutation between $\hat V_n$ and $\hat H_S + \hat H_n$ [cf. Eq. (150)] is equivalent to stating that $\hat V_n$ can be spectrally decomposed in the same basis of projectors $\{\hat\Pi_{Sn}^\ell\}$ as $\hat H_S + \hat H_n$ [cf. Eq. (H.4)], i.e.

$$\hat V_n = \sum_\ell v_\ell\;\hat\Pi_{Sn}^\ell = \sum_{j,i}\sum_\ell v_\ell\;\delta(E_j + e_i - \bar E_\ell)\,\hat\Pi_S^j\otimes\hat\Pi_n^i\,. \tag{H.6}$$

Here, in the last step we replaced $\hat\Pi_{Sn}^\ell$ with (H.5).

Consider now the operator defined by

$$\sum_{j'',j',i'',i'}\delta(E_{j''} + e_{i''} - (E_{j'} + e_{i'}))\hat\Pi_S^{j''}\otimes\hat\Pi_n^{i''}\;\hat V_n\;\hat\Pi_S^{j'}\otimes\hat\Pi_n^{i'} =$$
$$\sum_{j,i}\sum_\ell v_\ell\;\delta(E_j + e_i - \bar E_\ell)\sum_{j'',j',i'',i'}\delta(E_{j''} + e_{i''} - (E_{j'} + e_{i'}))\,\hat\Pi_S^{j''}\otimes\hat\Pi_n^{i''}\,(\hat\Pi_S^j\otimes\hat\Pi_n^i)\,\hat\Pi_S^{j'}\otimes\hat\Pi_n^{i'}\,,$$

where in the last step we replaced $\hat V_n$ with (H.6). This operator coincides just with $\hat V_n$. Indeed, using the orthogonality relations (H.3), the last expression can be arranged as

$$\sum_{j,i}\sum_\ell v_\ell\;\delta(E_j + e_i - \bar E_\ell)$$
$$\times\sum_{j'',j',i'',i'}\delta(E_{j''} + e_{i''} - (E_{j'} + e_{i'}))\delta(E_{j''} - E_j)\delta(e_{i''} - e_i)\delta(E_j - E_{j'})\delta(e_i - e_{i'})\,\hat\Pi_S^j\otimes\hat\Pi_n^i$$
$$= \sum_{j,i}\sum_\ell \Delta_\ell\;\delta(E_j + e_i - \bar E_\ell)\,\hat\Pi_S^j\otimes\hat\Pi_n^i = \hat V_n\,. \tag{H.7}$$

Thereby,

$$\hat V_n = \sum_{j,j',i,i'}\delta(E_j + e_i - (E_{j'} + e_{i'}))\,\hat\Pi_S^j\otimes\hat\Pi_n^i\;\hat V_n\;\hat\Pi_S^{j'}\otimes\hat\Pi_n^{i'}\,. \tag{H.8}$$

Plugging now $\hat{V}_n = \sum_\nu g_\nu \hat{A}'_\nu \hat{B}'_\nu$ [cf. Eq. (60)] on the right-hand side yields

$$\hat{V}_n = \sum_\nu g_\nu \sum_{j,j',i,i'} \delta(E_j - E_{j'} + e_i - e_{i'})\ \hat{\Pi}_S^j \hat{A}'_\nu \hat{\Pi}_S^{j'} \otimes \hat{\Pi}_n^i \hat{B}'_\nu \hat{\Pi}_n^{i'} . \tag{H.9}$$

By defining $\hat{A}_\nu = \hat{\Pi}_S^j \hat{A}'_\nu \hat{\Pi}_S^{j'}$ for $j < j'$, we note that it is an eigenoperator of $\hat{H}_S$ with eigenvalue $\omega_\nu = E_j - E_{j'}$ [cf. Eq. (151)]. Likewise, $\hat{B}_\nu = \hat{\Pi}_n^i \hat{B}'_\nu \hat{\Pi}_n^{i'}$ with $i < i'$ is an eigenoperator of $\hat{H}_n$ with eigenvalue $w_\nu = e_i - e_{i'}$ [cf. Eq. (152)]. Therefore (H.9) is exactly of the same form as (153), which completes the proof.

## Appendix I. Fully swapping ancilla–ancilla collisions: proof of Eq. (198)

Using Eq. (197), the reduced state of $S$ at the $n$th step is given by

$$\rho_n = \mathrm{Tr}_{1,2,\ldots,n}\{(\hat{S}_{2,1}\cdots\hat{S}_{n-1,n-2}\hat{S}_{n,n-1})\ \hat{U}_1^n\ \rho_0 \otimes_{m=1}^n \eta_m\ \hat{U}_1^{\dagger n}\ (\hat{S}_{n,n-1}\hat{S}_{n-1,n-2}\ \ldots\hat{S}_{2,1})\} . \tag{I.1}$$

Taking now advantage of the homogeneity of $\eta_n$, we can write

$$(\hat{S}_{3,2}\cdots\hat{S}_{n-1,n-2}\hat{S}_{n,n-1})\,\eta_2\otimes\eta_3\otimes\cdots\otimes\eta_n\,(\hat{S}_{3,2}\cdots\hat{S}_{n-1,n-2}\hat{S}_{n,n-1})^\dagger = \eta_2\otimes\eta_3\otimes\cdots\otimes\eta_n . \tag{I.2}$$

Replacing back in (I.1), this reduces to (we refer to a basis $|k_1,k_2\rangle_{12}$ for computing the partial trace)

$$\begin{aligned}\rho_n &= \mathrm{Tr}_{1,2}\,\{\hat{S}_{2,1}\hat{U}_1^n\rho_0\,\eta_1\,\eta_2\,\hat{U}_1^{n\dagger}\hat{S}_{2,1}\} = \sum_{k_1,k_2}\langle k_1,k_2|\hat{S}_{2,1}^\dagger\,\hat{U}_1^n\rho_0\,\eta_1\,\eta_2\,\hat{U}_1^{n\dagger}\hat{S}_{2,1}|k_1,k_2\rangle \\ &= \sum_{k_1,k_2}\langle k_1,k_2|\hat{U}_1^n\rho_0\,\eta_1\,\eta_2\,\hat{U}_1^{n\dagger}|k_1,k_2\rangle = \sum_{k_1}\langle k_1|\hat{U}_1^n\rho_0\,\eta_1\,\hat{U}_1^{n\dagger}|k_1\rangle = \mathrm{Tr}_1\{\hat{U}_1^n\rho_0\,\eta_1\,\hat{U}_1^{n\dagger}\} ,\end{aligned} \tag{I.3}$$

where we used that $\hat{S}_{2,1}|k_1,k_2\rangle$ is another valid basis for computing the *partial trace* (this being invariant under a change of basis). This completes the proof of Eq. (198).

## Appendix J. Ancilla–ancilla collisions: derivation of master equation (209)

By subtracting from Eq. (208) the analogous equation for $\rho_{n-1}$ we get

$$\Delta\rho_n = (1-p)\sum_{j=1}^{n-2} p^{j-1}\mathcal{F}_j[\Delta\rho_{n-j}] + (1-p)p^{n-1}\mathcal{F}_{n-1}[\rho_1] + \quad \Delta\left(p^{n-1}\mathcal{F}_n\right)[\rho_0] , \tag{J.1}$$

where, as usual, $\Delta A_n = A_n - A_{n-1}$ with $A$ a map or state. By expressing each power of $p$ in the form of an exponential as $p^j = e^{-\Gamma(\Delta t j)} = e^{-\Gamma t'}$ with $t' = j\Delta t$ and likewise $p^n = e^{-\Gamma t}$, in the limit $\Delta t \ll \Gamma$ the three terms on the right hand side of Eq. (J.1) become

$$\begin{aligned}&\frac{(1-p)\sum_{j=1}^{n-2} p^{(j-1)}\mathcal{E}_j\left[\rho_{n-j}-\rho_{n-1-j}\right]}{\Delta t} \simeq \Gamma\int_0^t dt' e^{-\Gamma t'}\mathcal{E}(t')\left[\frac{d\rho(t-t')}{d(t-t')}\right] , \\ &\frac{(1-p)p^{n-1}\mathcal{E}_{n-1}}{\Delta t}[\rho_1] \simeq \Gamma e^{-\Gamma t}\mathcal{E}(t)[\rho_0] , \\ &\frac{\Delta(p^{n-1}\mathcal{E}_n)}{\Delta t} = \frac{p^{n-1}\mathcal{E}_n - p^{n-2}\mathcal{E}_{n-1}}{\Delta t} \simeq \frac{e^{-\Gamma(t+2\Delta t)}\mathcal{E}(t+\Delta t) - e^{-\Gamma(t+\Delta t)}\mathcal{E}(t)}{\Delta t} = \frac{d}{dt}\left(e^{-\Gamma t}\mathcal{E}(t)\right) .\end{aligned}$$

Thus in the continuous-time limit, Eq. (J.1) reduces to Eq. (209).

## Appendix K. Composite CMs: derivation of the recurrence relation (236)

From Eqs. (234) (for $n \to n-1$) and (235) it follows

$$\hat{U}_{Mn} = |00\rangle_{Mn}\langle 00| + \cos(g\Delta t)(|10\rangle_{Mn}\langle 10| + |01\rangle_{Mn}\langle 01|) - i\sin(g\Delta t)(|01\rangle_{Mn}\langle 10| + |10\rangle_{Mn}\langle 01|) , \tag{K.1}$$

$$\begin{aligned}\hat{U}_{Mn}\hat{U}_{\mathcal{S}M}|\Psi^{(n-1)}\rangle &= \hat{U}_{Mn}\left((C\alpha^{(n-1)} - iS\beta^{(n-1)})|e_{\mathcal{S}}\rangle + (C\beta^{(n-1)} - iS\alpha^{(n-1)})|e_M\rangle + \sum_{m=1}^{n}\lambda_m^{(n-1)}|e_m\rangle\right) \\ &= (C\alpha^{(n-1)} - iS\beta^{(n-1)})|e_{\mathcal{S}}\rangle + (c\,C\beta^{(n-1)} - icS\alpha^{(n-1)})|e_M\rangle \\ &\quad + \sum_{m=1}^{n-1}\lambda_m^{(n-1)}|e_m\rangle - is(C\beta^{(n-1)} - iS\alpha^{(n-1)})|e_n\rangle .\end{aligned} \tag{K.2}$$

Comparing with Eq. (234), we get the recurrence relation (236) for the excitation amplitudes of $\mathcal{S}$ and $M$.

## Appendix L. Composite CMs: derivation of linear system (241)

By looking at Eq. (234) we see that, upon trace over the bath, the joint state of $\mathcal{S}$ and $M$ has the form

$$\rho_{SM} = |\alpha_n|^2|10\rangle\langle 10| + |\beta_n|^2|01\rangle\langle 01| + (\alpha_n\beta_n^*|10\rangle\langle 01| + \text{H.c.}) + (1 - |\alpha_n|^2 - |\beta_n|^2)|00\rangle\langle 00| \,. \tag{L.1}$$

This remains true when $\alpha_n \to \alpha(t)$ and $\beta_n \to \beta(t)$. Replacing $\rho_{SM}(t)$ into master equation (240) this is turned into the coupled differential equations

$$\tfrac{\mathrm{d}}{\mathrm{d}t}|\alpha|^2 = iG(\alpha\beta^* - \alpha^*\beta)\,,\ \ \tfrac{\mathrm{d}}{\mathrm{d}t}|\beta|^2 = -iG(\alpha\beta^* - \alpha^*\beta) - \gamma|\beta|^2\,,\ \ \tfrac{\mathrm{d}}{\mathrm{d}t}\left(\alpha\beta^*\right) = -\tfrac{\gamma}{2}\alpha\beta^* + i\left[G(|\alpha|^2 - |\beta|^2)\right]\,. \tag{L.2}$$

It is easily checked that these are indeed equivalent to (241) (e.g. $\frac{\mathrm{d}}{\mathrm{d}t}|\alpha|^2$ is obtained from $\alpha^*\dot{\alpha} = -iG\alpha^*\beta$ by adding to either side the respective c.c.). This completes the proof.

## References


[1] J.P. Dowling, G.J. Milburn, Quantum technology: the second quantum revolution, Philos. Trans. R. Soc. Lond. Series A: Math. Phys. Eng. Sci. 361 (1809) (2003) 1655–1674.
[2] R. Kosloff, Quantum thermodynamics: A dynamical viewpoint, Entropy 15 (6) (2013) 2100–2128, http://dx.doi.org/10.3390/e15062100, URL https://www.mdpi.com/1099-4300/15/6/2100.
[3] J. Goold, M. Huber, A. Riera, L.d. Rio, P. Skrzypczyk, The role of quantum information in thermodynamics—a topical review, J. Phys. A 49 (14) (2016) 143001, http://dx.doi.org/10.1088/1751-8113/49/14/143001, URL http://stacks.iop.org/1751-8121/49/i=14/a=143001.
[4] S. Vinjanampathy, J. Anders, Quantum thermodynamics, Contemp. Phys. 57 (4) (2016) 545–579, http://dx.doi.org/10.1080/00107514.2016.1201896.
[5] F. Binder, L.A. Correa, C. Gogolin, J. Anders, G. Adesso, Thermodynamics in the quantum regime Fundamental Theories of Physics, Berlin: Springer, 2018.
[6] S. Deffner, S. Campbell, Quantum Thermodynamics: An Introduction to The Thermodynamics Of Quantum Information, Morgan & Claypool Publishers, 2019.
[7] H.-P. Breuer, F. Petruccione, et al., The Theory Of Open Quantum Systems, Oxford University Press, 2002.
[8] C. Gardiner, P. Zoller, P. Zoller, Quantum Noise: A Handbook Of Markovian And Non-Markovian Quantum Stochastic Methods With Applications to Quantum Optics, Springer Science & Business Media, 2004.
[9] A. Rivas, S.F. Huelga, Open Quantum Systems: An Introduction, in: SpringerBriefs in Physics, Springer-Verlag, Berlin Heidelberg, 2012, URL www.springer.com/gp/book/9783642233531.
[10] H.M. Wiseman, G.J. Milburn, Quantum Measurement And Control, Cambridge University Press, 2009.
[11] K. Jacobs, Quantum Measurement Theory And Its Applications, Cambridge University Press, 2014.
[12] K. Modi, C.A. Rodríguez-Rosario, A. Aspuru-Guzik, Positivity in the presence of initial system-environment correlation, Phys. Rev. A 86 (6) (2012) 064102, http://dx.doi.org/10.1103/PhysRevA.86.064102, URL https://link.aps.org/doi/10.1103/PhysRevA.86.064102.
[13] H.R. Brown, W. Myrvold, Boltzmann's H-theorem, its limitations, and the birth of (fully) statistical mechanics, 2008, arXiv preprint arXiv:0809.1304.
[14] J. Rau, Relaxation phenomena in spin and harmonic oscillator systems, Phys. Rev. 129 (4) (1963) 1880–1888, http://dx.doi.org/10.1103/PhysRev.129.1880, URL https://link.aps.org/doi/10.1103/PhysRev.129.1880.
[15] C.M. Caves, Quantum mechanics of measurements distributed in time. a path-integral formulation, Phys. Rev. D 33 (6) (1986) 1643–1665, http://dx.doi.org/10.1103/PhysRevD.33.1643, URL https://link.aps.org/doi/10.1103/PhysRevD.33.1643.
[16] C.M. Caves, Quantum mechanics of measurements distributed in time. II. connections among formulations, Phys. Rev. D 35 (6) (1987) 1815–1830, http://dx.doi.org/10.1103/PhysRevD.35.1815, URL https://link.aps.org/doi/10.1103/PhysRevD.35.1815.
[17] C.M. Caves, G.J. Milburn, Quantum-mechanical model for continuous position measurements, Phys. Rev. A 36 (12) (1987) 5543–5555, http://dx.doi.org/10.1103/PhysRevA.36.5543, URL https://link.aps.org/doi/10.1103/PhysRevA.36.5543.
[18] P. Filipowicz, J. Javanainen, P. Meystre, Theory of a microscopic maser, Phys. Rev. A 34 (4) (1986) 3077–3087, http://dx.doi.org/10.1103/PhysRevA.34.3077, URL https://link.aps.org/doi/10.1103/PhysRevA.34.3077.
[19] P. Filipowicz, J. Javanainen, P. Meystre, Quantum and semiclassical steady states of a kicked cavity mode, J. Opt. Soc. Amer. B 3 (6) (1986) 906–910.
[20] P. Filipowicz, J. Javanainen, P. Meystre, The microscopic maser, Opt. Commun. 58 (5) (1986) 327–330.
[21] M.A. Nielsen, I. Chuang, Quantum computation and quantum information, American Association of Physics Teachers, 2002.
[22] M. Ziman, P. Štelmachovič, V. Bužek, M, V. Scarani, N. Gisin, Diluting quantum information: An analysis of information transfer in system-reservoir interactions, Phys. Rev. A 65 (4) (2002) 042105, http://dx.doi.org/10.1103/PhysRevA.65.042105, URL https://link.aps.org/doi/10.1103/PhysRevA.65.042105.
[23] V. Scarani, M. Ziman, P. Štelmachovič, N. Gisin, V. Bužek, Thermalizing quantum machines: dissipation and entanglement, Phys. Rev. Lett. 88 (9) (2002) 097905, http://dx.doi.org/10.1103/PhysRevLett.88.097905, URL https://link.aps.org/doi/10.1103/PhysRevLett.88.097905.
[24] T.A. Brun, A simple model of quantum trajectories, Am. J. Phys. 70 (7) (2002) 719–737, http://dx.doi.org/10.1119/1.1475328, URL https://aapt.scitation.org/doi/10.1119/1.1475328.
[25] H.-P. Breuer, Foundations and measures of quantum non-Markovianity, J. Phys. B: At. Mol. Opt. Phys. 45 (15) (2012) 154001, http://dx.doi.org/10.1088/0953-4075/45/15/154001, URL http://stacks.iop.org/0953-4075/45/i=15/a=154001.
[26] H.-P. Breuer, E.-M. Laine, J. Piilo, B. Vacchini, Colloquium: Non-Markovian dynamics in open quantum systems, Rev. Modern Phys. 88 (2) (2016) 021002, http://dx.doi.org/10.1103/RevModPhys.88.021002, URL https://link.aps.org/doi/10.1103/RevModPhys.88.021002.
[27] I. de Vega, D. Alonso, Dynamics of non-Markovian open quantum systems, Rev. Modern Phys. 89 (1) (2017) 015001, http://dx.doi.org/10.1103/RevModPhys.89.015001, URL https://link.aps.org/doi/10.1103/RevModPhys.89.015001.
[28] L. Li, M.J. Hall, H.M. Wiseman, Concepts of quantum non-Markovianity: A hierarchy, Phys. Rep. 759 (2018) 1–51.
[29] T. Rybár, S.N. Filippov, M. Ziman, V. Bužek, Simulation of indivisible qubit channels in collision models, J. Phys. B: At. Mol. Opt. Phys. 45 (15) (2012) 154006, http://dx.doi.org/10.1088/0953-4075/45/15/154006, URL http://stacks.iop.org/0953-4075/45/i=15/a=154006.
[30] F. Ciccarello, G.M. Palma, V. Giovannetti, Collision-model-based approach to non-Markovian quantum dynamics, Phys. Rev. A 87 (4) (2013) 040103, http://dx.doi.org/10.1103/PhysRevA.87.040103, URL https://link.aps.org/doi/10.1103/PhysRevA.87.040103.
[31] P. Strasberg, G. Schaller, T. Brandes, M. Esposito, Quantum and information thermodynamics: A unifying framework based on repeated interactions, Phys. Rev. X 7 (2017) 021003, http://dx.doi.org/10.1103/PhysRevX.7.021003, URL https://link.aps.org/doi/10.1103/PhysRevX.7.021003.

[32] M.O. Scully, M.S. Zubairy, G.S. Agarwal, H. Walther, Extracting work from a single heat bath via vanishing quantum coherence, Science 299 (5608) (2003) 862–864.
[33] C.A. Rodriguez, The theory of non-Markovian open quantum systems, (Ph.D. thesis), 2008, URL https://repositories.lib.utexas.edu/handle/2152/3929.
[34] M. Ziman, V. Bu?ek, Open system dynamics of simple collision models, in: Quantum Dynamics And Information, WORLD SCIENTIFIC, 2010, pp. 199–227, http://dx.doi.org/10.1142/9789814317443_0011, URL https://www.worldscientific.com/doi/10.1142/9789814317443_0011.
[35] D. Layden, Indirect Quantum Control: An Implementation-Independent Scheme, University of Waterloo, 2016.
[36] N. Altamirano, P. Corona-Ugalde, R.B. Mann, M. Zych, Unitarity, feedback, interactions—dynamics emergent from repeated measurements, New J. Phys. 19 (1) (2017) 013035, http://dx.doi.org/10.1088/1367-2630/aa551b, URL http://stacks.iop.org/1367-2630/19/i=1/a=013035.
[37] F. Ciccarello, Collision models in quantum optics, Quantum Meas. Quantum Metrol. 4 (1) (2017) http://dx.doi.org/10.1515/qmetro-2017-0007, URL http://www.degruyter.com/view/j/qmetro.2017.4.issue-1/qmetro-2017-0007/qmetro-2017-0007.xml.
[38] J.A. Gross, C.M. Caves, G.J. Milburn, J. Combes, Qubit models of weak continuous measurements: markovian conditional and open-system dynamics, Quantum Sci. Technol. 3 (2) (2018) 024005, http://dx.doi.org/10.1088/2058-9565/aaa39f, URL http://stacks.iop.org/2058-9565/3/i=2/a=024005.
[39] D. Grimmer, Interpolated collision model formalism, 2020, arXiv preprint arXiv:2009.10472.
[40] G.T. Landi, M. Paternostro, Irreversible entropy production, from quantum to classical, 2020, http://dx.doi.org/10.1103/RevModPhys.93.035008.
[41] S. Campbell, B. Vacchini, Collision models in open system dynamics: A versatile tool for deeper insights? 2021, http://dx.doi.org/10.1209/0295-5075/133/60001.
[42] L. Bruneau, A. Joye, M. Merkli, Repeated interactions in open quantum systems, J. Math. Phys. 55 (7) (2014) 075204.
[43] A. Rivas, S.F. Huelga, M.B. Plenio, Entanglement and non-Markovianity of quantum evolutions, Phys. Rev. Lett. 105 (2010) 050403, http://dx.doi.org/10.1103/PhysRevLett.105.050403, URL https://link.aps.org/doi/10.1103/PhysRevLett.105.050403.
[44] R. Orús, A practical introduction to tensor networks: Matrix product states and projected entangled pair states, Ann. Phys. 349 (2014) 117–158.
[45] R. Gawatz, Matrix product state based algorithms, 2017, URL https://www.nbi.ku.dk/english/theses/masters-theses/raffael-gawatz/RGawatz_Msc.pdf.
[46] J. Biamonte, V. Bergholm, Tensor networks in a nutshell, 2017, arXiv preprint arXiv:1708.00006URL https://arxiv.org/abs/1708.00006.
[47] G. Gennaro, G. Benenti, G.M. Palma, Relaxation due to random collisions with a many-qudit environment, Phys. Rev. A 79 (2) (2009) 022105, http://dx.doi.org/10.1103/PhysRevA.79.022105, URL https://link.aps.org/doi/10.1103/PhysRevA.79.022105.
[48] F. Caruso, V. Giovannetti, C. Lupo, S. Mancini, Quantum channels and memory effects, Rev. Mod. Phys. 86 (4) (2014) 1203.
[49] A. Rivas, S.F. Huelga, M.B. Plenio, Quantum non-Markovianity: characterization, quantification and detection, Rep. Progr. Phys. 77 (9) (2014) 094001, http://dx.doi.org/10.1088/0034-4885/77/9/094001, URL http://stacks.iop.org/0034-4885/77/i=9/a=094001.
[50] D. Burgarth, G. Chiribella, V. Giovannetti, P. Perinotti, K. Yuasa, Ergodic and mixing quantum channels in finite dimensions, New J. Phys. 15 (7) (2013) 073045, http://dx.doi.org/10.1088/1367-2630/15/7/073045, URL http://stacks.iop.org/1367-2630/15/i=7/a=073045.
[51] D. Kretschmann, R.F. Werner, Quantum channels with memory, Phys. Rev. A 72 (2005) 062323, http://dx.doi.org/10.1103/PhysRevA.72.062323, URL https://link.aps.org/doi/10.1103/PhysRevA.72.062323.
[52] M. Ziman, P. Stelmachovic, V. Buzek, Saturation of Coffman–Kundu–Wootters inequalities via quantum homogenization, J. Opt. B: Quantum Semiclass. Opt 5 (3) (2003) S439, http://dx.doi.org/10.1088/1464-4266/5/3/383, URL http://stacks.iop.org/1464-4266/5/i=3/a=383.
[53] D. Burgarth, V. Giovannetti, Mediated homogenization, Phys. Rev. A 76 (2007) 062307, http://dx.doi.org/10.1103/PhysRevA.76.062307, URL https://link.aps.org/doi/10.1103/PhysRevA.76.062307.
[54] V. Giovannetti, G.M. Palma, Master equations for correlated quantum channels, Phys. Rev. Lett. 108 (4) (2012) 040401, http://dx.doi.org/10.1103/PhysRevLett.108.040401, URL https://link.aps.org/doi/10.1103/PhysRevLett.108.040401.
[55] V. Giovannetti, G.M. Palma, Master equation for cascade quantum channels: a collisional approach, J. Phys. B: At. Mol. Opt. Phys. 45 (15) (2012) 154003, http://dx.doi.org/10.1088/0953-4075/45/15/154003, URL http://stacks.iop.org/0953-4075/45/i=15/a=154003.
[56] H. Pichler, P. Zoller, Photonic circuits with time delays and quantum feedback, Phys. Rev. Lett. 116 (9) (2016) 093601, http://dx.doi.org/10.1103/PhysRevLett.116.093601, URL https://link.aps.org/doi/10.1103/PhysRevLett.116.093601.
[57] S. Arranz Regidor, G. Crowder, H. Carmichael, S. Hughes, Modeling quantum light-matter interactions in waveguide QED with retardation, nonlinear interactions, and a time-delayed feedback: Matrix product states versus a space-discretized waveguide model, Phys. Rev. Res. 3 (2021) 023030, http://dx.doi.org/10.1103/PhysRevResearch.3.023030, URL https://link.aps.org/doi/10.1103/PhysRevResearch.3.023030.
[58] I.A. Luchnikov, S.V. Vintskevich, H. Ouerdane, S.N. Filippov, Simulation complexity of open quantum dynamics: Connection with tensor networks, Phys. Rev. Lett. 122 (2019) 160401, http://dx.doi.org/10.1103/PhysRevLett.122.160401, URL https://link.aps.org/doi/10.1103/PhysRevLett.122.160401.
[59] S. Haroche, J.-M. Raimond, Exploring The Quantum: Atoms, Cavities, And Photons, Oxford University Press, 2006, URL http://www.oxfordscholarship.com/view/10.1093/acprof:oso/9780198509141.001.0001/acprof-9780198509141.
[60] B.-G. Englert, G. Morigi, Five lectures on dissipative master equations, in: Coherent Evolution In Noisy Environments, Springer, 2002, pp. 55–106.
[61] P. Meystre, M. Sargent, Elements Of Quantum Optics, Springer Science & Business Media, 2007.
[62] M. Ziman, P. Štelmachovič, V. Bužek, Description of quantum dynamics of open systems based on collision-like models, Open Syst. Inf. Dyn. 12 (01) (2005) 81–91, http://dx.doi.org/10.1007/s11080-005-0488-0, URL https://www.worldscientific.com/doi/abs/10.1007/s11080-005-0488-0.
[63] M. Ziman, V. Bužek, All (qubit) decoherences: Complete characterization and physical implementation, Phys. Rev. A 72 (2) (2005) 022110, http://dx.doi.org/10.1103/PhysRevA.72.022110, URL https://link.aps.org/doi/10.1103/PhysRevA.72.022110.
[64] S. Seah, S. Nimmrichter, V. Scarani, Nonequilibrium dynamics with finite-time repeated interactions, Phys. Rev. E 99 (2019) 042103, http://dx.doi.org/10.1103/PhysRevE.99.042103, URL https://link.aps.org/doi/10.1103/PhysRevE.99.042103.
[65] J.B. Brask, G. Haack, N. Brunner, M. Huber, Autonomous quantum thermal machine for generating steady-state entanglement, New J. Phys. 17 (11) (2015) 113029, http://dx.doi.org/10.1088/1367-2630/17/11/113029.
[66] S.N. Filippov, G.N. Semin, A.N. Pechen, Quantum master equations for a system interacting with a quantum gas in the low-density limit and for the semiclassical collision model, Phys. Rev. A 101 (2020) 012114, http://dx.doi.org/10.1103/PhysRevA.101.012114, URL https://link.aps.org/doi/10.1103/PhysRevA.101.012114.
[67] J. Bergou, L. Davidovich, M. Orszag, C. Benkert, M. Hillery, M.O. Scully, Role of pumping statistics in maser and laser dynamics: Density-matrix approach, Phys. Rev. A 40 (1989) 5073–5080, http://dx.doi.org/10.1103/PhysRevA.40.5073, URL https://link.aps.org/doi/10.1103/PhysRevA.40.5073.
[68] H.-J. Briegel, B.-G. Englert, Macroscopic dynamics of a maser with non-Poissonian injection statistics, Phys. Rev. A 52 (1995) 2361–2375, http://dx.doi.org/10.1103/PhysRevA.52.2361, URL https://link.aps.org/doi/10.1103/PhysRevA.52.2361.
[69] D. Grimmer, D. Layden, R.B. Mann, E. Martín-Martínez, Open dynamics under rapid repeated interaction, Phys. Rev. A 94 (2016) 032126, http://dx.doi.org/10.1103/PhysRevA.94.032126, URL https://link.aps.org/doi/10.1103/PhysRevA.94.032126.
[70] G. Milburn, Decoherence and the conditions for the classical control of quantum systems, Philos. Trans. R. Soc. A: Math. Phys. Eng. Sci. 370 (1975) (2012) 4469–4486.

[71] D. Layden, E. Martín-Martínez, A. Kempf, Universal scheme for indirect quantum control, Phys. Rev. A 93 (2016) 040301, http://dx.doi.org/10.1103/PhysRevA.93.040301, URL https://link.aps.org/doi/10.1103/PhysRevA.93.040301.
[72] B. Sutton, S. Datta, Manipulating quantum information with spin torque, Sci. Rep. 5 (1) (2015) 1–12.
[73] H.J. Carmichael, Quantum trajectory theory for cascaded open systems, Phys. Rev. Lett. 70 (15) (1993) 2273–2276, http://dx.doi.org/10.1103/PhysRevLett.70.2273.
[74] C.W. Gardiner, Driving a quantum system with the output field from another driven quantum system, Phys. Rev. Lett. 70 (1993) 2269–2272, http://dx.doi.org/10.1103/PhysRevLett.70.2269.
[75] S. Cusumano, A. Mari, V. Giovannetti, Interferometric quantum cascade systems, Phys. Rev. A 95 (5) (2017) 053838, http://dx.doi.org/10.1103/PhysRevA.95.053838, URL https://link.aps.org/doi/10.1103/PhysRevA.95.053838.
[76] S. Cusumano, A. Mari, V. Giovannetti, Interferometric modulation of quantum cascade interactions, Phys. Rev. A 97 (5) (2018) 053811, http://dx.doi.org/10.1103/PhysRevA.97.053811, URL https://link.aps.org/doi/10.1103/PhysRevA.97.053811.
[77] P. Lodahl, S. Mahmoodian, S. Stobbe, A. Rauschenbeutel, P. Schneeweiss, J. Volz, H. Pichler, P. Zoller, Chiral quantum optics, Nature 541 (7638) (2017) 473–480, http://dx.doi.org/10.1038/nature21037.
[78] H. Carmichael, An Open Systems Approach to Quantum Optics: Lectures Presented At The UniversitÉ Libre De Bruxelles, October 28 To November 4, 1991, Vol. 18, Springer Science & Business Media, 2009.
[79] K. Mølmer, Y. Castin, J. Dalibard, Monte Carlo wave-function method in quantum optics, J. Opt. Soc. Amer. B 10 (3) (1993) 524–538.
[80] M.B. Plenio, P.L. Knight, The quantum-jump approach to dissipative dynamics in quantum optics, Rev. Modern Phys. 70 (1998) 101–144, http://dx.doi.org/10.1103/RevModPhys.70.101, URL https://link.aps.org/doi/10.1103/RevModPhys.70.101.
[81] D. Kafri, J. Taylor, A noise inequality for classical forces, 2013, arXiv preprint arXiv:1311.4558.
[82] D. Kafri, J. Taylor, G. Milburn, A classical channel model for gravitational decoherence, New J. Phys. 16 (6) (2014) 065020.
[83] H.-J. Briegel, B.-G. Englert, N. Sterpi, H. Walther, One-atom maser: Statistics of detector clicks, Phys. Rev. A 49 (1994) 2962–2985, http://dx.doi.org/10.1103/PhysRevA.49.2962, URL https://link.aps.org/doi/10.1103/PhysRevA.49.2962.
[84] K. Beyer, K. Luoma, W.T. Strunz, Collision-model approach to steering of an open driven qubit, Phys. Rev. A 97 (3) (2018) 032113, http://dx.doi.org/10.1103/PhysRevA.97.032113, URL https://link.aps.org/doi/10.1103/PhysRevA.97.032113.
[85] D. Cilluffo, I. Lesanovsky, G. Buonaiuto, A. Carollo, S. Lorenzo, G.M. Palma, F. Ciccarello, F. Carollo, Microscopic biasing of discrete-time quantum trajectories, 2020, http://dx.doi.org/10.1088/2058-9565/ac15e2.
[86] R. Loudon, The Quantum Theory Of Light, OUP Oxford, 2000.
[87] R. Landauer, Irreversibility and heat generation in the computing process, IBM J. Res. Dev. 5 (3) (1961) 183–191, http://dx.doi.org/10.1147/rd.53.0183.
[88] F. Barra, The thermodynamic cost of driving quantum systems by their boundaries, Sci. Rep. 5 (2015) 14873, http://dx.doi.org/10.1038/srep14873, URL https://www.nature.com/articles/srep14873.
[89] G.D. Chiara, G. Landi, A. Hewgill, B. Reid, A. Ferraro, A.J. Roncaglia, M. Antezza, Reconciliation of quantum local master equations with thermodynamics, New J. Phys. 20 (11) (2018) 113024, http://dx.doi.org/10.1088/1367-2630/aaecee.
[90] R. Kosloff, Quantum thermodynamics and open-systems modeling, J. Chem. Phys. 150 (20) (2019) 204105.
[91] M. Esposito, K. Lindenberg, C.V. den Broeck, Entropy production as correlation between system and reservoir, New J. Phys. 12 (1) (2010) 013013, http://dx.doi.org/10.1088/1367-2630/12/1/013013.
[92] G. Manzano, J.M. Horowitz, J.M.R. Parrondo, Quantum fluctuation theorems for arbitrary environments: Adiabatic and nonadiabatic entropy production, Phys. Rev. X 8 (2018) 031037, http://dx.doi.org/10.1103/PhysRevX.8.031037, URL https://link.aps.org/doi/10.1103/PhysRevX.8.031037.
[93] L.D. Landau, E.M. Lifšic, E.M. Lifshitz, L. Pitaevskii, Statistical physics: theory of the condensed state, Vol. 9, Butterworth-Heinemann, 1980.
[94] V. Scarani, Entanglement and irreversibility in the approach to thermal equilibrium, Eur. Phys. J. Spec. Top. 151 (1) (2007) 41–49, http://dx.doi.org/10.1140/epjst/e2007-00360-y, URL https://link.springer.com/article/10.1140/epjst/e2007-00360-y.
[95] L. Diósi, T. Feldmann, R. Kosloff, On the exact identity between thermodynamic and informatic entropies in a unitary model of friction, Int. J. Quantum Inform. 04 (01) (2006) 99–104, http://dx.doi.org/10.1142/S0219749906001645, URL https://www.worldscientific.com/doi/abs/10.1142/S0219749906001645.
[96] A. Chimonidou, E.C.G. Sudarshan, Relaxation phenomena in a system of two harmonic oscillators, Phys. Rev. A 77 (3) (2008) 032121, http://dx.doi.org/10.1103/PhysRevA.77.032121, URL https://link.aps.org/doi/10.1103/PhysRevA.77.032121.
[97] D. Grimmer, E. Brown, A. Kempf, R.B. Mann, E. Martín-Martínez, Gaussian ancillary bombardment, Phys. Rev. A 97 (2018) 052120, http://dx.doi.org/10.1103/PhysRevA.97.052120, URL https://link.aps.org/doi/10.1103/PhysRevA.97.052120.
[98] D. Grimmer, R.B. Mann, E. Martín-Martínez, Thermal contact: mischief and time scales, J. Phys. A: Math. Theor. 52 (39) (2019) 395305, http://dx.doi.org/10.1088/1751-8121/ab3a19.
[99] M. Lostaglio, A.M. Alhambra, C. Perry, Elementary thermal operations, Quantum 2 (2018) 52, http://dx.doi.org/10.22331/q-2018-02-08-52.
[100] A. Shu, Y. Cai, S. Seah, S. Nimmrichter, V. Scarani, Almost thermal operations: Inhomogeneous reservoirs, Phys. Rev. A 100 (2019) 042107, http://dx.doi.org/10.1103/PhysRevA.100.042107, URL https://link.aps.org/doi/10.1103/PhysRevA.100.042107.
[101] S. Cusumano, V. Cavina, M. Keck, A. De Pasquale, V. Giovannetti, Entropy production and asymptotic factorization via thermalization: A collisional model approach, Phys. Rev. A 98 (2018) 032119, http://dx.doi.org/10.1103/PhysRevA.98.032119, URL https://link.aps.org/doi/10.1103/PhysRevA.98.032119.
[102] S. Seah, S. Nimmrichter, D. Grimmer, J.P. Santos, V. Scarani, G.T. Landi, Collisional quantum thermometry, Phys. Rev. Lett. 123 (2019) 180602, http://dx.doi.org/10.1103/PhysRevLett.123.180602, URL https://link.aps.org/doi/10.1103/PhysRevLett.123.180602.
[103] A. Shu, S. Seah, V. Scarani, Surpassing the thermal cramér-rao bound with collisional thermometry, Phys. Rev. A 102 (2020) 042417, http://dx.doi.org/10.1103/PhysRevA.102.042417, URL https://link.aps.org/doi/10.1103/PhysRevA.102.042417.
[104] E. O'Connor, B. Vacchini, S. Campbell, Stochastic collisional quantum thermometry, Entropy 23 (12) (2021) 1634.
[105] D. Karevski, T. Platini, Quantum nonequilibrium steady states induced by repeated interactions, Phys. Rev. Lett. 102 (2009) 207207, http://dx.doi.org/10.1103/PhysRevLett.102.207207, URL https://link.aps.org/doi/10.1103/PhysRevLett.102.207207.
[106] G.T. Landi, E. Novais, M.J. de Oliveira, D. Karevski, Flux rectification in the quantum XXZ chain, Phys. Rev. E 90 (2014) 042142, http://dx.doi.org/10.1103/PhysRevE.90.042142, URL https://link.aps.org/doi/10.1103/PhysRevE.90.042142.
[107] E. Pereira, Heat, work, and energy currents in the boundary-driven XXZ spin chain, Phys. Rev. E 97 (2018) 022115, http://dx.doi.org/10.1103/PhysRevE.97.022115, URL https://link.aps.org/doi/10.1103/PhysRevE.97.022115.
[108] D. Heineken, K. Beyer, K. Luoma, W.T. Strunz, Quantum memory enhanced dissipative entanglement creation in non-equilibrium steady states, 2020, http://dx.doi.org/10.1103/PhysRevA.104.052426.
[109] L. Li, J. Zou, H. Li, B.-M. Xu, Y.-M. Wang, B. Shao, Effect of coherence of nonthermal reservoirs on heat transport in a microscopic collision model, Phys. Rev. E 97 (2018) 022111, http://dx.doi.org/10.1103/PhysRevE.97.022111, URL https://link.aps.org/doi/10.1103/PhysRevE.97.022111.
[110] A. Levy, R. Kosloff, The local approach to quantum transport may violate the second law of thermodynamics, EPL (Europhys. Lett.) 107 (2) (2014) 20004, http://dx.doi.org/10.1209/0295-5075/107/20004.

[111] G. De Chiara, M. Antezza, Quantum machines powered by correlated baths, Phys. Rev. Research 2 (2020) 033315, http://dx.doi.org/10.1103/PhysRevResearch.2.033315, URL https://link.aps.org/doi/10.1103/PhysRevResearch.2.033315.
[112] S. Daryanoosh, B.Q. Baragiola, T. Guff, A. Gilchrist, Quantum master equations for entangled qubit environments, Phys. Rev. A 98 (2018) 062104, http://dx.doi.org/10.1103/PhysRevA.98.062104, URL https://link.aps.org/doi/10.1103/PhysRevA.98.062104.
[113] O. Pusuluk, O.E. Müstecaplogğlu, Quantum Rayleigh problem and thermocoherent onsager relations, Phys. Rev. Res. 3 (2021) 023235, http://dx.doi.org/10.1103/PhysRevResearch.3.023235, URL https://link.aps.org/doi/10.1103/PhysRevResearch.3.023235.
[114] H.T. Quan, P. Zhang, C.P. Sun, Quantum-classical transition of photon-carnot engine induced by quantum decoherence, Phys. Rev. E 73 (2006) 036122, http://dx.doi.org/10.1103/PhysRevE.73.036122, URL https://link.aps.org/doi/10.1103/PhysRevE.73.036122.
[115] H. Li, J. Zou, W.-L. Yu, B.-M. Xu, J.-G. Li, B. Shao, Quantum coherence rather than quantum correlations reflect the effects of a reservoir on a system's work capability, Phys. Rev. E 89 (2014) 052132, http://dx.doi.org/10.1103/PhysRevE.89.052132, URL https://link.aps.org/doi/10.1103/PhysRevE.89.052132.
[116] C.B. Dağ, W. Niedenzu, Ö.E. Müstecaplıoğlu, G. Kurizki, Multiatom quantum coherences in micromasers as fuel for thermal and nonthermal machines, Entropy 18 (7) (2016) 244.
[117] D. Türkpençe, O.E. Müstecaploğlu, Quantum fuel with multilevel atomic coherence for ultrahigh specific work in a photonic carnot engine, Phys. Rev. E 93 (2016) 012145, http://dx.doi.org/10.1103/PhysRevE.93.012145, URL https://link.aps.org/doi/10.1103/PhysRevE.93.012145.
[118] T. Guff, S. Daryanoosh, B.Q. Baragiola, A. Gilchrist, Power and efficiency of a thermal engine with a coherent bath, Phys. Rev. E 100 (2019) 032129, http://dx.doi.org/10.1103/PhysRevE.100.032129, URL https://link.aps.org/doi/10.1103/PhysRevE.100.032129.
[119] R. Dillenschneider, E. Lutz, Energetics of quantum correlations, EPL (Europhys. Lett.) 88 (5) (2009) 50003, http://dx.doi.org/10.1209/0295-5075/88/50003.
[120] C.B. Dagg, W. Niedenzu, F. Ozaydin, O.E. Mustecaplioglu, G. Kurizki, Temperature control in dissipative cavities by entangled dimers, J. Phys. Chem. C 123 (7) (2019) 4035–4043.
[121] A.Ü. Hardal, Ö.E. Müstecaplıoğlu, Superradiant quantum heat engine, Sci. Rep. 5 (1) (2015) 1–9.
[122] R. Uzdin, R. Kosloff, The multilevel four-stroke swap engine and its environment, New J. Phys. 16 (9) (2014) 095003, http://dx.doi.org/10.1088/1367-2630/16/9/095003.
[123] K. Beyer, K. Luoma, W.T. Strunz, Steering heat engines: A truly quantum maxwell demon, Phys. Rev. Lett. 123 (2019) 250606, http://dx.doi.org/10.1103/PhysRevLett.123.250606, URL https://link.aps.org/doi/10.1103/PhysRevLett.123.250606.
[124] G. Manzano, R. Silva, J.M.R. Parrondo, Autonomous thermal machine for amplification and control of energetic coherence, Phys. Rev. E 99 (2019) 042135, http://dx.doi.org/10.1103/PhysRevE.99.042135, URL https://link.aps.org/doi/10.1103/PhysRevE.99.042135.
[125] F. Barra, Dissipative charging of a quantum battery, Phys. Rev. Lett. 122 (2019) 210601, http://dx.doi.org/10.1103/PhysRevLett.122.210601, URL https://link.aps.org/doi/10.1103/PhysRevLett.122.210601.
[126] A. Hewgill, J.O. González, J.P. Palao, D. Alonso, A. Ferraro, G. De Chiara, Three-qubit refrigerator with two-body interactions, Phys. Rev. E 101 (2020) 012109, http://dx.doi.org/10.1103/PhysRevE.101.012109, URL https://link.aps.org/doi/10.1103/PhysRevE.101.012109.
[127] N. Piccione, G. De Chiara, B. Bellomo, Power maximization of two-stroke quantum thermal machines, Phys. Rev. A 103 (2021) 032211, http://dx.doi.org/10.1103/PhysRevA.103.032211, URL https://link.aps.org/doi/10.1103/PhysRevA.103.032211.
[128] E. Bäumer, M. Perarnau-Llobet, P. Kammerlander, H. Wilming, R. Renner, Imperfect thermalizations allow for optimal thermodynamic processes, Quantum 3 (2019) 153, http://dx.doi.org/10.22331/q-2019-06-24-153.
[129] M. Quadeer, K. Korzekwa, M. Tomamichel, Work fluctuations due to partial thermalizations in two-level systems, Phys. Rev. E 103 (2021) 042141, http://dx.doi.org/10.1103/PhysRevE.103.042141, URL https://link.aps.org/doi/10.1103/PhysRevE.103.042141.
[130] O.A.D. Molitor, G.T. Landi, Stroboscopic two-stroke quantum heat engines, Phys. Rev. A 102 (2020) 042217, http://dx.doi.org/10.1103/PhysRevA.102.042217, URL https://link.aps.org/doi/10.1103/PhysRevA.102.042217.
[131] F.L.S. Rodrigues, G. De Chiara, M. Paternostro, G.T. Landi, Thermodynamics of weakly coherent collisional models, Phys. Rev. Lett. 123 (2019) 140601, http://dx.doi.org/10.1103/PhysRevLett.123.140601, URL https://link.aps.org/doi/10.1103/PhysRevLett.123.140601.
[132] K. Hammam, Y. Hassouni, R. Fazio, G. Manzano, Optimizing autonomous thermal machines powered by energetic coherence, New J. Phys. (2021) URL http://iopscience.iop.org/article/10.1088/1367-2630/abeb47.
[133] R. Román-Ancheyta, B. Çakmak, O.E. Müstecaplıoğlu, Spectral signatures of non-thermal baths in quantum thermalization, Quantum Sci. Technol. 5 (1) (2019) 015003, http://dx.doi.org/10.1088/2058-9565/ab5e4f.
[134] M.S. Kim, N. Imoto, Phase-sensitive reservoir modeled by beam splitters, Phys. Rev. A 52 (1995) 2401–2410, http://dx.doi.org/10.1103/PhysRevA.52.2401, URL https://link.aps.org/doi/10.1103/PhysRevA.52.2401.
[135] G. Manzano, F. Galve, R. Zambrini, J.M.R. Parrondo, Entropy production and thermodynamic power of the squeezed thermal reservoir, Phys. Rev. E 93 (2016) 052120, http://dx.doi.org/10.1103/PhysRevE.93.052120, URL https://link.aps.org/doi/10.1103/PhysRevE.93.052120.
[136] G. Manzano, Squeezed thermal reservoir as a generalized equilibrium reservoir, Phys. Rev. E 98 (2018) 042123, http://dx.doi.org/10.1103/PhysRevE.98.042123, URL https://link.aps.org/doi/10.1103/PhysRevE.98.042123.
[137] G. Manzano, J.M. Parrondo, G.T. Landi, Non-abelian quantum transport and thermosqueezing effects, 2020, ArXiv:2011.04560.
[138] S. Lorenzo, R. McCloskey, F. Ciccarello, M. Paternostro, G.M. Palma, Landauer's principle in multipartite open quantum system dynamics, Phys. Rev. Lett. 115 (2015) 120403, http://dx.doi.org/10.1103/PhysRevLett.115.120403, URL https://link.aps.org/doi/10.1103/PhysRevLett.115.120403.
[139] S. Lorenzo, A. Farace, F. Ciccarello, G.M. Palma, V. Giovannetti, Heat flux and quantum correlations in dissipative cascaded systems, Phys. Rev. A 91 (2015) 022121, http://dx.doi.org/10.1103/PhysRevA.91.022121, URL https://link.aps.org/doi/10.1103/PhysRevA.91.022121.
[140] D. Reeb, M.M. Wolf, An improved Landauer principle with finite-size corrections, New J. Phys. 16 (10) (2014) 103011, http://dx.doi.org/10.1088/1367-2630/16/10/103011.
[141] G. Manzano, R. Zambrini, Quantum thermodynamics under continuous monitoring: a general framework, 2021, http://dx.doi.org/10.1103/PRXQuantum.3.010304.
[142] J.M. Horowitz, Quantum-trajectory approach to the stochastic thermodynamics of a forced harmonic oscillator, Phys. Rev. E 85 (2012) 031110, http://dx.doi.org/10.1103/PhysRevE.85.031110, URL https://link.aps.org/doi/10.1103/PhysRevE.85.031110.
[143] J.M. Horowitz, J.M.R. Parrondo, Entropy production along nonequilibrium quantum jump trajectories, New J. Phys. 15 (8) (2013) 085028, http://dx.doi.org/10.1088/1367-2630/15/8/085028.
[144] F. Barra, C. Ledó, Stochastic thermodynamics of quantum maps with and without equilibrium, Phys. Rev. E 96 (2017) 052114, http://dx.doi.org/10.1103/PhysRevE.96.052114, URL https://link.aps.org/doi/10.1103/PhysRevE.96.052114.
[145] P. Strasberg, Operational approach to quantum stochastic thermodynamics, Phys. Rev. E 100 (2019) 022127, http://dx.doi.org/10.1103/PhysRevE.100.022127, URL https://link.aps.org/doi/10.1103/PhysRevE.100.022127.
[146] P. Strasberg, Repeated interactions and quantum stochastic thermodynamics at strong coupling, Phys. Rev. Lett. 123 (2019) 180604, http://dx.doi.org/10.1103/PhysRevLett.123.180604, URL https://link.aps.org/doi/10.1103/PhysRevLett.123.180604.
[147] J.D. Cresser, Time-reversed quantum trajectory analysis of micromaser correlation properties and fluctuation relations, Phys. Scr. 94 (3) (2019) 034005, http://dx.doi.org/10.1088/1402-4896/aaf902.
[148] G.T. Landi, M. Paternostro, A. Belenchia, Informational steady-states and conditional entropy production in continuously monitored systems, 2021, arXiv preprint arXiv:2103.06247.

[149] G. Benenti, G. Strini, Dynamical casimir effect and minimal temperature in quantum thermodynamics, Phys. Rev. A 91 (2015) 020502, http://dx.doi.org/10.1103/PhysRevA.91.020502, URL https://link.aps.org/doi/10.1103/PhysRevA.91.020502.
[150] G. Guarnieri, D. Morrone, B. Çakmak, F. Plastina, S. Campbell, Non-equilibrium steady-states of memoryless quantum collision models, Phys. Lett. A 384 (24) (2020) 126576, http://dx.doi.org/10.1016/j.physleta.2020.126576, URL https://www.sciencedirect.com/science/article/pii/S0375960120304436.
[151] R. Román-Ancheyta, M. Kolář, G. Guarnieri, R. Filip, Enhanced steady-state coherences via repeated system-bath interactions, 2020, http://dx.doi.org/10.1103/PhysRevA.104.062209.
[152] A. Smith, Y. Lu, S. An, X. Zhang, J.-N. Zhang, Z. Gong, H.T. Quan, C. Jarzynski, K. Kim, Verification of the quantum nonequilibrium work relation in the presence of decoherence, New J. Phys. 20 (1) (2018) 013008, http://dx.doi.org/10.1088/1367-2630/aa9cd6.
[153] K. Beyer, K. Luoma, W.T. Strunz, Work as an external quantum observable and an operational quantum work fluctuation theorem, Phys. Rev. Res. 2 (2020) 033508, http://dx.doi.org/10.1103/PhysRevResearch.2.033508, URL https://link.aps.org/doi/10.1103/PhysRevResearch.2.033508.
[154] K. Modi, A. Brodutch, H. Cable, T. Paterek, V. Vedral, The classical-quantum boundary for correlations: Discord and related measures, Rev. Modern Phys. 84 (4) (2012) 1655–1707, http://dx.doi.org/10.1103/RevModPhys.84.1655, URL https://link.aps.org/doi/10.1103/RevModPhys.84.1655.
[155] F. Ciccarello, V. Giovannetti, A quantum non-Markovian collision model: incoherent swap case, Phys. Scr. 2013 (T153) (2013) 014010, http://dx.doi.org/10.1088/0031-8949/2013/T153/014010, URL http://stacks.iop.org/1402-4896/2013/i=T153/a=014010.
[156] R. McCloskey, M. Paternostro, Non-Markovianity and system-environment correlations in a microscopic collision model, Phys. Rev. A 89 (5) (2014) 052120, http://dx.doi.org/10.1103/PhysRevA.89.052120, URL https://link.aps.org/doi/10.1103/PhysRevA.89.052120.
[157] B. Çakmak, M. Pezzutto, M. Paternostro, Ö.E. Müstecaplıoğlu, Non-Markovianity, coherence and system-environment correlations in a long-range collision model, Phys. Rev. A 96 (2) (2017) http://dx.doi.org/10.1103/PhysRevA.96.022109.
[158] S. Campbell, F. Ciccarello, G.M. Palma, B. Vacchini, System-environment correlations and Markovian embedding of quantum non-Markovian dynamics, Phys. Rev. A 98 (2018) 012142, http://dx.doi.org/10.1103/PhysRevA.98.012142, URL https://link.aps.org/doi/10.1103/PhysRevA.98.012142.
[159] S. Campbell, M. Popovic, D. Tamascelli, B. Vacchini, Precursors of non-Markovianity, New J. Phys. 21 (5) (2019) 053036, http://dx.doi.org/10.1088/1367-2630/ab1ed6.
[160] M. Pezzutto, M. Paternostro, Y. Omar, Implications of non-Markovian quantum dynamics for the Landauer bound, New J. Phys. 18 (12) (2016) 123018.
[161] Z.-X. Man, Y.-J. Xia, R.L. Franco, Validity of the Landauer principle and quantum memory effects via collisional models, Phys. Rev. A 99 (4) (2019) 042106.
[162] Q. Zhang, Z.-X. Man, Y.-J. Xia, Non-Markovianity and the Landauer principle in composite thermal environments, Phys. Rev. A 103 (2021) 032201, http://dx.doi.org/10.1103/PhysRevA.103.032201, URL https://link.aps.org/doi/10.1103/PhysRevA.103.032201.
[163] Z.-X. Man, Y.-J. Xia, R. Lo Franco, Temperature effects on quantum non-Markovianity via collision models, Phys. Rev. A 97 (2018) 062104, http://dx.doi.org/10.1103/PhysRevA.97.062104, URL https://link.aps.org/doi/10.1103/PhysRevA.97.062104.
[164] M. Pezzutto, M. Paternostro, Y. Omar, An out-of-equilibrium non-Markovian quantum heat engine, Quantum Sci. Technol. 4 (2) (2019) 025002.
[165] O.C. Abah, M. Paternostro, Implications of non-Markovian dynamics on information-driven engine, J. Phys. Commun. (2020).
[166] T. Saha, A. Das, S. Ghosh, Quantum homogenization in non-markovian collisional model, arXiv preprint arXiv:2201.08412 (2022).
[167] J. Jin, V. Giovannetti, R. Fazio, F. Sciarrino, P. Mataloni, A. Crespi, R. Osellame, All-optical non-Markovian stroboscopic quantum simulator, Phys. Rev. A 91 (2015) 012122, http://dx.doi.org/10.1103/PhysRevA.91.012122, URL https://link.aps.org/doi/10.1103/PhysRevA.91.012122.
[168] Á. Cuevas, A. Geraldi, C. Liorni, L.D. Bonavena, A. De Pasquale, F. Sciarrino, V. Giovannetti, P. Mataloni, All-optical implementation of collision-based evolutions of open quantum systems, Sci. Rep. 9 (1) (2019) 1–8.
[169] J. Jin, C.-s. Yu, Non-Markovianity in the collision model with environmental block, New J. Phys. 20 (5) (2018) 053026, http://dx.doi.org/10.1088/1367-2630/aac0cb, URL http://stacks.iop.org/1367-2630/20/i=5/a=053026.
[170] R.R. Camasca, G.T. Landi, Memory kernel and divisibility of Gaussian collisional models, Phys. Rev. A 103 (2021) 022202, http://dx.doi.org/10.1103/PhysRevA.103.022202, URL https://link.aps.org/doi/10.1103/PhysRevA.103.022202.
[171] B. Vacchini, Non-Markovian master equations from piecewise dynamics, Phys. Rev. A 87 (3) (2013) 030101, http://dx.doi.org/10.1103/PhysRevA.87.030101, URL https://link.aps.org/doi/10.1103/PhysRevA.87.030101.
[172] B. Vacchini, General structure of quantum collisional models, Int. J. Quantum Inform. 12 (02) (2014) 1461011, http://dx.doi.org/10.1142/S0219749914610115, URL https://www.worldscientific.com/doi/abs/10.1142/S0219749914610115.
[173] B. Vacchini, Generalized master equations leading to completely positive dynamics, Phys. Rev. Lett. 117 (23) (2016) 230401, http://dx.doi.org/10.1103/PhysRevLett.117.230401, URL https://link.aps.org/doi/10.1103/PhysRevLett.117.230401.
[174] B. Vacchini, Quantum renewal processes, Sci. Rep. 10 (1) (2020) 1–13.
[175] D. Chruściński, A. Kossakowski, Sufficient conditions for a memory-kernel master equation, Phys. Rev. A 94 (2) (2016) 020103, http://dx.doi.org/10.1103/PhysRevA.94.020103, URL https://link.aps.org/doi/10.1103/PhysRevA.94.020103.
[176] D. Chruściński, A. Kossakowski, Generalized semi-Markov quantum evolution, Phys. Rev. A 95 (4) (2017) 042131, http://dx.doi.org/10.1103/PhysRevA.95.042131, URL https://link.aps.org/doi/10.1103/PhysRevA.95.042131.
[177] K. Siudzińska, D. Chruściński, Memory kernel approach to generalized Pauli channels: Markovian, semi-Markov, and beyond, Phys. Rev. A 96 (2) (2017) 022129, http://dx.doi.org/10.1103/PhysRevA.96.022129, URL https://link.aps.org/doi/10.1103/PhysRevA.96.022129.
[178] M.M. Wolf, J.I. Cirac, Dividing quantum channels, Commun. Math. Phys. 279 (1) (2008) 147–168.
[179] S.N. Filippov, J. Piilo, S. Maniscalco, M. Ziman, Divisibility of quantum dynamical maps and collision models, Phys. Rev. A 96 (3) (2017) 032111, http://dx.doi.org/10.1103/PhysRevA.96.032111, URL https://link.aps.org/doi/10.1103/PhysRevA.96.032111.
[180] N. Megier, D. Chruściński, J. Piilo, W.T. Strunz, Eternal non-Markovianity: from random unitary to Markov chain realisations, Sci. Rep. 7 (1) (2017) 1–11.
[181] V. Pathak, A. Shaji, Non-markovian open dynamics from collision models, Open Systems & Information Dynamics 26 (04) (2019) 1950018.
[182] E. Mascarenhas, I. de Vega, Quantum critical probing and simulation of colored quantum noise, Phys. Rev. A 96 (6) (2017) 062117, http://dx.doi.org/10.1103/PhysRevA.96.062117, URL https://link.aps.org/doi/10.1103/PhysRevA.96.062117.
[183] N.K. Bernardes, A.R.R. Carvalho, C.H. Monken, M.F. Santos, Environmental correlations and Markovian to non-Markovian transitions in collisional models, Phys. Rev. A 90 (3) (2014) 032111, http://dx.doi.org/10.1103/PhysRevA.90.032111, URL https://link.aps.org/doi/10.1103/PhysRevA.90.032111.
[184] N.K. Bernardes, A. Cuevas, A. Orieux, C.H. Monken, P. Mataloni, F. Sciarrino, M.F. Santos, Experimental observation of weak non-Markovianity, Sci. Rep. 5 (2015) 17520, http://dx.doi.org/10.1038/srep17520, URL https://www.nature.com/articles/srep17520.
[185] N.K. Bernardes, J.P.S. Peterson, R.S. Sarthour, A.M. Souza, C.H. Monken, I. Roditi, I.S. Oliveira, M.F. Santos, High resolution non-Markovianity in NMR, Sci. Rep. 6 (2016) 33945, http://dx.doi.org/10.1038/srep33945, URL https://www.nature.com/articles/srep33945.
[186] N.K. Bernardes, A.R.R. Carvalho, C.H. Monken, M.F. Santos, Coarse graining a non-Markovian collisional model, Phys. Rev. A 95 (3) (2017) 032117, http://dx.doi.org/10.1103/PhysRevA.95.032117, URL https://link.aps.org/doi/10.1103/PhysRevA.95.032117.

[187] G. García-Pérez, M.A. Rossi, S. Maniscalco, IBM Q experience as a versatile experimental testbed for simulating open quantum systems, Npj Quantum Inform. 6 (1) (2020) 1–10.
[188] S. Milz, M.S. Kim, F.A. Pollock, K. Modi, Completely positive divisibility does not mean Markovianity, Phys. Rev. Lett. 123 (2019) 040401, http://dx.doi.org/10.1103/PhysRevLett.123.040401, URL https://link.aps.org/doi/10.1103/PhysRevLett.123.040401.
[189] A. Bodor, L. Diósi, Z. Kallus, T. Konrad, Structural features of non-Markovian open quantum systems using quantum chains, Phys. Rev. A 87 (5) (2013) 052113, http://dx.doi.org/10.1103/PhysRevA.87.052113, URL https://link.aps.org/doi/10.1103/PhysRevA.87.052113.
[190] C. Pellegrini, F. Petruccione, Non-Markovian quantum repeated interactions and measurements, J. Phys. A: Math. Theor. 42 (42) (2009) 425304.
[191] P. Taranto, S. Milz, F.A. Pollock, K. Modi, Structure of quantum stochastic processes with finite Markov order, Phys. Rev. A 99 (2019) 042108, http://dx.doi.org/10.1103/PhysRevA.99.042108, URL https://link.aps.org/doi/10.1103/PhysRevA.99.042108.
[192] P. Taranto, F. Bakhshinezhad, P. Schüttelkopf, M. Huber, Exponential improvement for quantum cooling through finite memory effects, 2020, http://dx.doi.org/10.1103/PhysRevApplied.14.054005.
[193] D. Cilluffo, F. Ciccarello, Quantum non-Markovian collision models from colored-noise baths, in: Advances In Open Systems And Fundamental Tests Of Quantum Mechanics, Springer, 2019, pp. 29–40.
[194] U. Dorner, P. Zoller, Laser-driven atoms in half-cavities, Phys. Rev. A 66 (2002) 023816, http://dx.doi.org/10.1103/PhysRevA.66.023816, URL https://link.aps.org/doi/10.1103/PhysRevA.66.023816.
[195] T. Tufarelli, F. Ciccarello, M.S. Kim, Dynamics of spontaneous emission in a single-end photonic waveguide, Phys. Rev. A 87 (2013) 013820, http://dx.doi.org/10.1103/PhysRevA.87.013820, URL https://link.aps.org/doi/10.1103/PhysRevA.87.013820.
[196] A.L. Grimsmo, Time-delayed quantum feedback control, Phys. Rev. Lett. 115 (6) (2015) 060402, http://dx.doi.org/10.1103/PhysRevLett.115.060402, URL https://link.aps.org/doi/10.1103/PhysRevLett.115.060402.
[197] S.J. Whalen, Collision model for non-Markovian quantum trajectories, Phys. Rev. A 100 (2019) 052113, http://dx.doi.org/10.1103/PhysRevA.100.052113, URL https://link.aps.org/doi/10.1103/PhysRevA.100.052113.
[198] A.F. Kockum, Quantum optics with giant atoms—the first five years, in: International Symposium On Mathematics, Quantum Theory, And Cryptography, Springer, Singapore, 2021, pp. 125–146.
[199] D. Cilluffo, A. Carollo, S. Lorenzo, J.A. Gross, G.M. Palma, F. Ciccarello, Collisional picture of quantum optics with giant emitters, Phys. Rev. Res. 2 (2020) 043070, http://dx.doi.org/10.1103/PhysRevResearch.2.043070, URL https://link.aps.org/doi/10.1103/PhysRevResearch.2.043070.
[200] G. Gennaro, G. Benenti, G.M. Palma, Entanglement dynamics and relaxation in a few-qubit system interacting with random collisions, Europhys. Lett. 82 (2) (2008) 20006, http://dx.doi.org/10.1209/0295-5075/82/20006, URL http://stacks.iop.org/0295-5075/82/i=2/a=20006.
[201] G. Gennaro, S. Campbell, M. Paternostro, G.M. Palma, Structural change in multipartite entanglement sharing: A random matrix approach, Phys. Rev. A 80 (6) (2009) 062315, http://dx.doi.org/10.1103/PhysRevA.80.062315, URL https://link.aps.org/doi/10.1103/PhysRevA.80.062315.
[202] S. Lorenzo, F. Ciccarello, G.M. Palma, Composite quantum collision models, Phys. Rev. A 96 (3) (2017) 032107, http://dx.doi.org/10.1103/PhysRevA.96.032107, URL https://link.aps.org/doi/10.1103/PhysRevA.96.032107.
[203] I.A. Luchnikov, S.V. Vintskevich, D.A. Grigoriev, S.N. Filippov, Machine learning non-Markovian quantum dynamics, Phys. Rev. Lett. 124 (2020) 140502, http://dx.doi.org/10.1103/PhysRevLett.124.140502, URL https://link.aps.org/doi/10.1103/PhysRevLett.124.140502.
[204] G. Karpat, I. Yalçınkaya, B. Çakmak, G.L. Giorgi, R. Zambrini, Synchronization and non-Markovianity in open quantum systems, 2020, http://dx.doi.org/10.1103/PhysRevA.103.062217.
[205] M. Cattaneo, G. De Chiara, S. Maniscalco, R. Zambrini, G.L. Giorgi, Collision models can efficiently simulate any multipartite Markovian quantum dynamics, Phys. Rev. Lett. 126 (2021) 130403, http://dx.doi.org/10.1103/PhysRevLett.126.130403, URL https://link.aps.org/doi/10.1103/PhysRevLett.126.130403.
[206] S. Kretschmer, K. Luoma, W.T. Strunz, Collision model for non-Markovian quantum dynamics, Phys. Rev. A 94 (1) (2016) 012106, http://dx.doi.org/10.1103/PhysRevA.94.012106, URL https://link.aps.org/doi/10.1103/PhysRevA.94.012106.
[207] S. Lorenzo, F. Ciccarello, G.M. Palma, Class of exact memory-kernel master equations, Phys. Rev. A 93 (5) (2016) 052111, http://dx.doi.org/10.1103/PhysRevA.93.052111, URL https://link.aps.org/doi/10.1103/PhysRevA.93.052111.
[208] W. Magnus, On the exponential solution of differential equations for a linear operator, Commun. Pure Appl. Math. 7 (4) (1954) 649–673.
[209] K. Fischer, Derivation of the quantum-optical master equation based on coarse-graining of time, J. Phys. Commun. 2 (9) (2018) 091001.
[210] T.M. Karg, B. Gouraud, P. Treutlein, K. Hammerer, Remote Hamiltonian interactions mediated by light, Phys. Rev. A 99 (6) (2019) 063829.
[211] A. Carollo, D. Cilluffo, F. Ciccarello, Mechanism of decoherence-free coupling between giant atoms, Phys. Rev. Res. 2 (4) (2020) 043184.
[212] A.F. Kockum, G. Johansson, F. Nori, Decoherence-free interaction between giant atoms in waveguide quantum electrodynamics, Phys. Rev. Lett. 120 (2018) 140404.
[213] B. Kannan, M.J. Ruckriegel, D.L. Campbell, A.F. Kockum, J. Braumüller, D.K. Kim, M. Kjaergaard, P. Krantz, A. Melville, B.M. Niedzielski, et al., Waveguide quantum electrodynamics with superconducting artificial giant atoms, Nature 583 (7818) (2020) 775–779.
[214] K.A. Fischer, R. Trivedi, V. Ramasesh, I. Siddiqi, J. Vučković, Scattering into one-dimensional waveguides from a coherently-driven quantum-optical system, Quantum 2 (2018) 69, http://dx.doi.org/10.22331/q-2018-05-28-69, URL https://quantum-journal.org/papers/q-2018-05-28-69/.
[215] M. Heuck, K. Jacobs, D.R. Englund, Photon-photon interactions in dynamically coupled cavities, Phys. Rev. A 101 (2020) 042322, http://dx.doi.org/10.1103/PhysRevA.101.042322, URL https://link.aps.org/doi/10.1103/PhysRevA.101.042322.
[216] M. Heuck, K. Jacobs, D.R. Englund, Controlled-phase gate using dynamically coupled cavities and optical nonlinearities, Phys. Rev. Lett. 124 (2020) 160501, http://dx.doi.org/10.1103/PhysRevLett.124.160501, URL https://link.aps.org/doi/10.1103/PhysRevLett.124.160501.
[217] G. Vissers, L. Bouten, Implementing quantum stochastic differential equations on a quantum computer, Quantum Inf. Process. 18 (5) (2019) 152.
[218] L. Bouten, G. Vissers, F. Schmidt-Kaler, Quantum algorithm for simulating an experiment: Light interference from single ions and their mirror images, Phys. Rev. A 100 (2019) 022323, http://dx.doi.org/10.1103/PhysRevA.100.022323, URL https://link.aps.org/doi/10.1103/PhysRevA.100.022323.
[219] B. Royer, S. Singh, S.M. Girvin, Stabilization of finite-energy Gottesman-Kitaev-Preskill states, Phys. Rev. Lett. 125 (2020) 260509, http://dx.doi.org/10.1103/PhysRevLett.125.260509, URL https://link.aps.org/doi/10.1103/PhysRevLett.125.260509.
[220] M. Maffei, P.A. Camati, A. Auffèves, Probing nonclassical light fields with energetic witnesses in waveguide quantum electrodynamics, Phys. Rev. Research 3 (2021) L032073, http://dx.doi.org/10.1103/PhysRevResearch.3.L032073, https://link.aps.org/doi/10.1103/PhysRevResearch.3.L032073.
[221] A. Dabrowska, G. Sarbicki, D. Chruściński, Quantum trajectories for a system interacting with environment in a single-photon state: Counting and diffusive processes, Phys. Rev. A 96 (2017) 053819, http://dx.doi.org/10.1103/PhysRevA.96.053819, URL https://link.aps.org/doi/10.1103/PhysRevA.96.053819.
[222] A. Dabrowska, G. Sarbicki, D. Chruściński, Quantum trajectories for a system interacting with environment in N-photon state, J. Phys A: Math. Theor. 52 (10) (2019) 105303.
[223] A.M. Dabrowska, From a posteriori to a priori solutions for a two-level system interacting with a single-photon wavepacket, J. Opt. Soc. Amer. B 37 (4) (2020) 1240–1248.
[224] A.M. Dabrowska, Quantum trajectories for environment in superposition of coherent states, Quantum Inf. Process. 18 (7) (2019) 1–22.

[225] J.D. Cresser, Quantum-field model of the injected atomic beam in the micromaser, Phys. Rev. A 46 (1992) 5913–5931, http://dx.doi.org/10.1103/PhysRevA.46.5913, URL https://link.aps.org/doi/10.1103/PhysRevA.46.5913.
[226] S. Campbell, B. Çakmak, O.E. Müstecaploğlu, M. Paternostro, B. Vacchini, Collisional unfolding of quantum darwinism, Phys. Rev. A 99 (2019) 042103, http://dx.doi.org/10.1103/PhysRevA.99.042103, URL https://link.aps.org/doi/10.1103/PhysRevA.99.042103.
[227] G. García-Pérez, D.A. Chisholm, M.A.C. Rossi, G.M. Palma, S. Maniscalco, Decoherence without entanglement and quantum darwinism, Phys. Rev. Res. 2 (2020) 012061, http://dx.doi.org/10.1103/PhysRevResearch.2.012061, URL https://link.aps.org/doi/10.1103/PhysRevResearch.2.012061.
[228] S. Lorenzo, M. Paternostro, G.M. Palma, Anti-Zeno-based dynamical control of the unfolding of quantum darwinism, Phys. Rev. Res. 2 (2020) 013164, http://dx.doi.org/10.1103/PhysRevResearch.2.013164, URL https://link.aps.org/doi/10.1103/PhysRevResearch.2.013164.
[229] S. Lorenzo, M. Paternostro, G.M. Palma, Reading a qubit quantum state with a quantum meter: time unfolding of quantum darwinism and quantum information flux, Open Syst. Inform. Dyn. 26 (04) (2019) 1950023.
[230] B. Çakmak, Ö.E. Müstecaplıoğlu, M. Paternostro, B. Vacchini, S. Campbell, Quantum darwinism in a composite system: Objectivity versus classicality, Entropy 23 (8) (2021) 995.
[231] D.A. Chisholm, G. García-Pérez, M.A.C. Rossi, G.M. Palma, S. Maniscalco, Stochastic collision model approach to transport phenomena in quantum networks, New J. Phys. 23 (3) (2021) 033031, http://dx.doi.org/10.1088/1367-2630/abd57d.
[232] T.P. Le, A. Olaya-Castro, Basis-independent system-environment coherence is necessary to detect magnetic field direction in an avian-inspired quantum magnetic sensor, 2020, arXiv preprint arXiv:2011.15016.
[233] D. Türkpençe, T.Ç. Akıncı, S. Şeker, A steady state quantum classifier, Phys. Lett. A 383 (13) (2019) 1410–1418.
[234] S. Vriend, D. Grimmer, E. Martín-Martínez, The Unruh effect in slow motion, 2020, http://dx.doi.org/10.3390/sym13111977.
[235] D. Grimmer, A. Kempf, R.B. Mann, E. Martín-Martínez, Zeno friction and antifriction from quantum collision models, Phys. Rev. A 100 (2019) 042702, http://dx.doi.org/10.1103/PhysRevA.100.042702, URL https://link.aps.org/doi/10.1103/PhysRevA.100.042702.
[236] Y. Li, X. Li, J. Jin, Information scrambling in a collision model, Phys. Rev. A 101 (2020) 042324, http://dx.doi.org/10.1103/PhysRevA.101.042324, URL https://link.aps.org/doi/10.1103/PhysRevA.101.042324.
[237] G.T. Landi, Battery charging in collision models with Bayesian risk strategies, Entropy 23 (12) (2021) 1627.
[238] A. Altherr, Y. Yang, Quantum metrology for non-markovian processes, Phys. Rev. Lett. 127 (2021) 060501, http://dx.doi.org/10.1103/PhysRevLett.127.060501, https://link.aps.org/doi/10.1103/PhysRevLett.127.060501.
[239] C. Gardiner, Input and output in damped quantum systems III: Formulation of damped systems driven by Fermion fields, Opt. Commun. 243 (1–6) (2004) 57–80.
[240] A. Purkayastha, G. Guarnieri, S. Campbell, J. Prior, J. Goold, Periodically refreshed baths to simulate open quantum many-body dynamics, Phys. Rev. B 104 (2021) 045417, http://dx.doi.org/10.1103/PhysRevB.104.045417, URL https://link.aps.org/doi/10.1103/PhysRevB.104.045417.
[241] J. Preskill, Lecture notes for physics 229: Quantum information and computation, Calif. Inst. Technol. 16 (1998) 10.